

ISSN 1881-7815    Online ISSN 1881-7823

# **BST**

## **BioScience Trends**

**Volume 19, Number 3**  
**June 2025**



[www.biosciencetrends.com](http://www.biosciencetrends.com)



**BioScience Trends** is one of a series of peer-reviewed journals of the International Research and Cooperation Association for Bio & Socio-Sciences Advancement (IRCA-BSSA) Group. It is published bimonthly by the International Advancement Center for Medicine & Health Research Co., Ltd. (IACMHR Co., Ltd.) and supported by the IRCA-BSSA.

**BioScience Trends** devotes to publishing the latest and most exciting advances in scientific research. Articles cover fields of life science such as biochemistry, molecular biology, clinical research, public health, medical care system, and social science in order to encourage cooperation and exchange among scientists and clinical researchers.

**BioScience Trends** publishes Original Articles, Brief Reports, Reviews, Policy Forum articles, Communications, Editorials, News, and Letters on all aspects of the field of life science. All contributions should seek to promote international collaboration.

## Editorial Board

### Editor-in-Chief:

Norihiro KOKUDO  
*Japan Institute for Health Security, Tokyo, Japan*

### Co-Editors-in-Chief:

Xishan HAO  
*Tianjin Medical University, Tianjin, China*  
Takashi KARAKO  
*Japan Institute for Health Security, Tokyo, Japan*  
John J. ROSSI  
*Beckman Research Institute of City of Hope, Duarte, CA, USA*

Hongen LIAO  
*Tsinghua University, Beijing, China*  
Misao MATSUSHITA  
*Tokai University, Hiratsuka, Japan*  
Fanghua QI  
*Shandong Provincial Hospital, Ji'nan, China*  
Ri SHO  
*Yamagata University, Yamagata, Japan*  
Yasuhiko SUGAWARA  
*Kumamoto University, Kumamoto, Japan*  
Ling WANG  
*Fudan University, Shanghai, China*

### Senior Editors:

Tetsuya ASAKAWA  
*The Third People's Hospital of Shenzhen, Shenzhen, China*  
Yu CHEN  
*The University of Tokyo, Tokyo, Japan*  
Xunjia CHENG  
*Fudan University, Shanghai, China*  
Yoko FUJITA-YAMAGUCHI  
*Beckman Research Institute of the City of Hope, Duarte, CA, USA*  
Jianjun GAO  
*Qingdao University, Qingdao, China*  
Na HE  
*Fudan University, Shanghai, China*

### Proofreaders:

Curtis BENTLEY  
*Roswell, GA, USA*  
Thomas R. LEBON  
*Los Angeles, CA, USA*

### Editorial and Head Office

Pearl City Koishikawa 603,  
2-4-5 Kasuga, Bunkyo-ku, Tokyo 112-0003, Japan  
E-mail: [office@biosciencetrends.com](mailto:office@biosciencetrends.com)

# BioScience Trends

## Editorial and Head Office

Pearl City Koishikawa 603, 2-4-5 Kasuga, Bunkyo-ku,  
Tokyo 112-0003, Japan

E-mail: [office@biosciencetrends.com](mailto:office@biosciencetrends.com)  
URL: [www.biosciencetrends.com](http://www.biosciencetrends.com)

## Editorial Board Members

Girdhar G. AGARWAL

(Lucknow, India)

Hirotsugu AIGA

(Geneva, Switzerland)

Hidechika AKASHI

(Tokyo, Japan)

Moazzam ALI

(Geneva, Switzerland)

Ping AO

(Shanghai, China)

Hisao ASAMURA

(Tokyo, Japan)

Michael E. BARISH

(Duarte, CA, USA)

Boon-Huat BAY

(Singapore, Singapore)

Yasumasa BESSHO

(Nara, Japan)

Generoso BEVILACQUA

(Pisa, Italy)

Shiuan CHEN

(Duarte, CA, USA)

Yi-Li CHEN

(Yiwu, China)

Yue CHEN

(Ottawa, Ontario, Canada)

Naoshi DOHMAE

(Wako, Japan)

Zhen FAN

(Houston, TX, USA)

Ding-Zhi FANG

(Chengdu, China)

Xiao-Bin FENG

(Beijing, China)

Yoshiharu FUKUDA

(Ube, Japan)

Rajiv GARG

(Lucknow, India)

Ravindra K. GARG

(Lucknow, India)

Makoto GOTO

(Tokyo, Japan)

Demin HAN

(Beijing, China)

David M. HELFMAN

(Daejeon, Korea)

Takahiro HIGASHI

(Tokyo, Japan)

De-Fei HONG

(Hangzhou, China)

De-Xing HOU

(Kagoshima, Japan)

Sheng-Tao HOU

(Guanzhou, China)

Xiaoyang HU

(Southampton, UK)

Yong HUANG

(Ji'ning, China)

Hirofumi INAGAKI

(Tokyo, Japan)

Masamine JIMBA

(Tokyo, Japan)

Chun-Lin JIN

(Shanghai, China)

Kimitaka KAGA

(Tokyo, Japan)

Michael Kahn

(Duarte, CA, USA)

Kazuhiro KAKIMOTO

(Osaka, Japan)

Kiyoko KAMIBEPPU

(Tokyo, Japan)

Haidong KAN

(Shanghai, China)

Kenji KARAKO

(Tokyo, Japan)

Bok-Luel LEE

(Busan, Korea)

Chuan LI

(Chengdu, China)

Mingjie LI

(St. Louis, MO, USA)

Shixue LI

(Ji'nan, China)

Ren-Jang LIN

(Duarte, CA, USA)

Chuan-Ju LIU

(New York, NY, USA)

Lianxin LIU

(Hefei, China)

Xinqi LIU

(Tianjin, China)

Daru LU

(Shanghai, China)

Hongzhou LU

(Guanzhou, China)

Duan MA

(Shanghai, China)

Masatoshi MAKUUCHI

(Tokyo, Japan)

Francesco MAROTTA

(Milano, Italy)

Yutaka MATSUYAMA

(Tokyo, Japan)

Qingyue MENG

(Beijing, China)

Mark MEUTH

(Sheffield, UK)

Michihiro Nakamura

(Yamaguchi, Japan)

Munehiro NAKATA

(Hiratsuka, Japan)

Satoko NAGATA

(Tokyo, Japan)

Miho OBA

(Odawara, Japan)

Xianjun QU

(Beijing, China)

Carlos SAINZ-FERNANDEZ

(Santander, Spain)

Yoshihiro SAKAMOTO

(Tokyo, Japan)

Erin SATO

(Shizuoka, Japan)

Takehito SATO

(Isehara, Japan)

Akihito SHIMAZU

(Tokyo, Japan)

Zhifeng SHAO

(Shanghai, China)

Xiao-Ou SHU

(Nashville, TN, USA)

Sarah Shuck

(Duarte, CA, USA)

Judith SINGER-SAM

(Duarte, CA, USA)

Raj K. SINGH

(Dehradun, India)

Peipei SONG

(Tokyo, Japan)

Junko SUGAMA

(Kanazawa, Japan)

Zhipeng SUN

(Beijing, China)

Hiroshi TACHIBANA

(Isehara, Japan)

Tomoko TAKAMURA

(Tokyo, Japan)

Tadatoshi TAKAYAMA

(Tokyo, Japan)

Shin'ichi TAKEDA

(Tokyo, Japan)

Sumihito TAMURA

(Tokyo, Japan)

Puay Hoon TAN

(Singapore, Singapore)

Koji TANAKA

(Tsu, Japan)

John TERMINI

(Duarte, CA, USA)

Usa C. THISYAKORN

(Bangkok, Thailand)

Toshifumi TSUKAHARA

(Nomi, Japan)

Mudit Tyagi

(Philadelphia, PA, USA)

Kohjiro UEKI

(Tokyo, Japan)

Masahiro UMEZAKI

(Tokyo, Japan)

Junming WANG

(Jackson, MS, USA)

Qing Kenneth WANG

(Wuhan, China)

Xiang-Dong WANG

(Boston, MA, USA)

Hisashi WATANABE

(Tokyo, Japan)

Jufeng XIA

(Tokyo, Japan)

Feng XIE

(Hamilton, Ontario, Canada)

Jinfu XU

(Shanghai, China)

Lingzhong XU

(Ji'nan, China)

Masatake YAMAUCHI

(Chiba, Japan)

Aitian YIN

(Ji'nan, China)

George W-C. YIP

(Singapore, Singapore)

Xue-Jie YU

(Galveston, TX, USA)

Rongfa YUAN

(Nanchang, China)

Benny C-Y ZEE

(Hong Kong, China)

Yong ZENG

(Chengdu, China)

Wei ZHANG

(Shanghai, China)

Wei ZHANG

(Tianjin, China)

Chengchao ZHOU

(Ji'nan, China)

Xiaomei ZHU

(Seattle, WA, USA)

(as of April 2025)



**Review**

- 243-251**      **Integrative neurorehabilitation using brain-computer interface: From motor function to mental health after stroke.**  
*Ya-nan Ma, Kenji Karako, Peipei Song, Xiqi Hu, Ying Xia*
- 252-265**      **Promoting active health with AI technologies: Current status and prospects of high-altitude therapy, simulated hypoxia, and LLM-driven lifestyle rehabilitation approaches.**  
*Mingyu Liu, Wenli Zhang, Junyu Wang, Kehan Bao, Ziyi Fu, Boyuan Wang*
- 266-280**      **Current status and perspectives of molecular mechanisms of gender difference in hepatocellular carcinoma: The tip of the iceberg?**  
*Zhi-Quan Xu, Shi-Qiao Luo, Zhong-Jun Wu, Rui Liao*
- 281-295**      **Traditional Chinese medicine modulates hypothalamic neuropeptides for appetite regulation: A comprehensive review.**  
*Yuqi Wang, Fanghua Qi, Min Li, Yuan Xu, Li Dong, Pingping Cai*
- 296-308**      **Advancing precision medicine in immune checkpoint blockade for HIV/AIDS: Current strategies and future directions.**  
*Xiangyi Tang, Cheng Wang, Xiling Zhang, Qibin Liao, Hongzhou Lu*
- 309-327**      **Multimodal treatment of colorectal liver metastases: Where are we? Current strategies and future perspectives.**  
*Caterina Accardo, Ivan Vella, Fabrizio di Francesco, Sergio Rizzo, Sergio Calamia, Alessandro Tropea, Pasquale Bonsignore, Sergio Li Petri, Salvatore Gruttadauria*

**Original Article**

- 328-336**      **Advancing hepatobiliary diagnosis and treatment using shortwave-infrared fluorescence imaging with ICG-C9.**  
*Kosuke Hatta, Ryota Tanaka, Kenjiro Kimura, Naoki Yamashita, Jie Li, Terufusa Kunisada, Takeaki Ishizawa*
- 337-350**      **SNRPA promotes hepatocellular carcinoma proliferation and lenvatinib resistance via B7-H6-STAT3/AKT axis by facilitating B7-H6 pre-mRNA maturation.**  
*Jiejun Hu, Junhua Gong, Xia Shu, Xin Dai, Dong Cai, Zhibo Zhao, Jinhao Li, Guochao Zhong, Jianping Gong*

- 
- 351-360**      **Platelet count as a double-edged sword: The impact of thrombocytosis and thrombocytopenia on long-term outcomes after hepatic resection for hepatocellular carcinoma.**  
*Xuedong Wang, Pengfei Wang, Bingjun Tang, Jiahao Xu, Baidong Wang, Lihui Gu, Yingjian Liang, Hongwei Guo, Han Liu, Yifan Wu, Hong Wang, Yahao Zhou, Yongyi Zeng, Yongkang Diao, Lanqing Yao, Mingda Wang, Chao Li, Timothy M. Pawlik, Feng Shen, Lei Cai, Tian Yang*
- 361-367**      **Liver exposure during laparoscopic right-sided hepatectomy *via* stretching of the ligamentum teres hepatis: A propensity score matching analysis.**  
*Keda Song, Yang Xu, Zhongyu Li, Mingyuan Wang, Dong Chen, Yongzhi Zhou, Guangchao Yang, Yong Ma*

# Integrative neurorehabilitation using brain-computer interface: From motor function to mental health after stroke

Ya-nan Ma<sup>1,§</sup>, Kenji Karako<sup>2,§</sup>, Peipei Song<sup>3,4</sup>, Xiqi Hu<sup>5,\*</sup>, Ying Xia<sup>1,5,\*</sup>

<sup>1</sup> Department of Neurosurgery, Haikou Affiliated Hospital of Central South University Xiangya School of Medicine, Haikou, China;

<sup>2</sup> Department of Surgery, Graduate School of Medicine, The University of Tokyo, Tokyo, Japan;

<sup>3</sup> Center for Clinical Sciences, Japan institute for Health Security, Tokyo, Japan;

<sup>4</sup> National College of Nursing Japan, Tokyo, Japan;

<sup>5</sup> Integrated Neuroscience Center, Geriatric Hospital of Hainan, Haikou, China.

**SUMMARY:** Stroke remains a leading cause of mortality and long-term disability worldwide, frequently resulting in impairments in motor control, cognition, and emotional regulation. Conventional rehabilitation approaches, while partially effective, often lack individualization and yield suboptimal outcomes. In recent years, brain-computer interface (BCI) technology has emerged as a promising neurorehabilitation tool by decoding neural signals and providing real-time feedback to enhance neuroplasticity. This review systematically explores the use of BCI systems in post-stroke rehabilitation, focusing on three core domains: motor function, cognitive capacity, and emotional regulation. This review outlines the neurophysiological principles underpinning BCI-based motor rehabilitation, including neurofeedback training, Hebbian plasticity, and multimodal feedback strategies. It then examines recent advances in upper limb and gait recovery using BCI integrated with functional electrical stimulation (FES), robotics, and virtual reality (VR). Moreover, it highlights BCI's potential in cognitive and language rehabilitation through EEG-based neurofeedback and the integration of artificial intelligence (AI) and immersive VR environments. In addition, it discusses the role of BCI in monitoring and regulating post-stroke emotional disorders *via* closed-loop systems. While promising, BCI technologies face challenges related to signal accuracy, device portability, and clinical validation. Future research should prioritize multimodal integration, AI-driven personalization, and large-scale randomized trials to establish long-term efficacy. This review underscores BCI's transformative potential in delivering intelligent, personalized, and cross-domain rehabilitation solutions for stroke survivors.

**Keywords:** neurorehabilitation, neural plasticity, motor dysfunction, cognitive reconstruction, neurofeedback, post-stroke depression

## 1. Introduction

Stroke is one of the leading causes of mortality and long-term disability worldwide, with its high incidence and associated impairments imposing a substantial burden on individuals, families, and society. According to 2021 statistics, more than 16 million people globally suffer from stroke, and approximately one-third of these patients experience permanent disability (1). As a neurovascular emergency, stroke commonly results in motor deficits, cognitive dysfunction, and emotional disturbances. Chronic motor dysfunction, and particularly hemiplegia, affects nearly 30% of stroke survivors, making it one of the most disabling outcomes (2). Moreover, post-stroke cognitive impairment (PSCI) is reported in 25% to 80% of patients (3), and a study in a Chinese cohort showed that 57.8% of 963 stroke

patients exhibited depressive symptoms (4). Although conventional rehabilitation approaches, including physical therapy, occupational therapy, and speech therapy, have demonstrated certain benefits, their efficacy is often limited by insufficient individualization, suboptimal therapeutic outcomes, and prolonged recovery periods. Research indicates that approximately 20% to 30% of stroke patients are unsuitable candidates for therapies such as constraint-induced movement therapy (CIMT) and other conventional rehabilitation strategies (5).

In recent years, advances in neuroscience and engineering have led to the emergence of brain-computer interface (BCI) technology, which offers novel therapeutic avenues for stroke rehabilitation. BCIs decode neural signals and either translate them into commands for external devices or use them directly

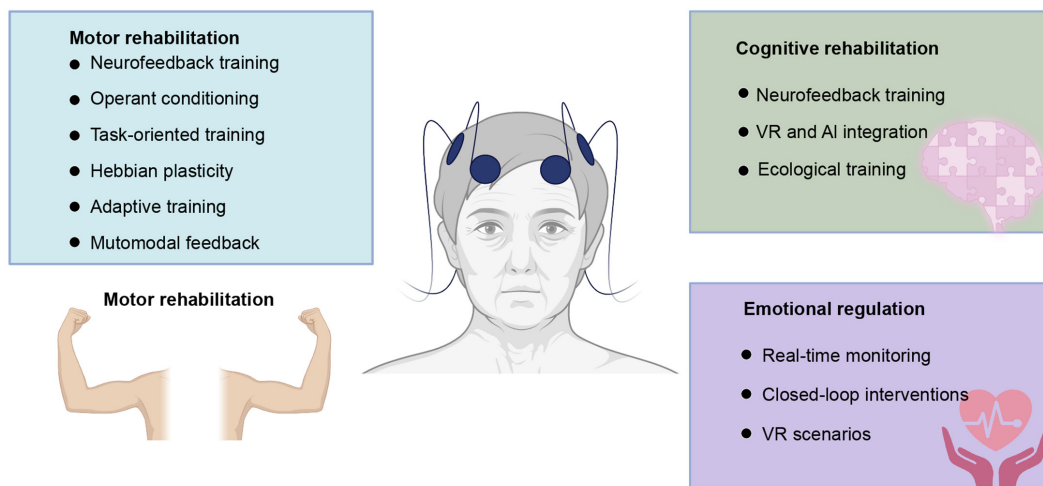


**Figure 1. Mechanisms of brain-computer interface applications across motor, cognitive, and emotional domains in stroke rehabilitation.**

for neurofeedback, thereby enhancing neuroplasticity and functional recovery (6). BCI applications have displayed considerable potential in motor recovery, cognitive training, and emotional regulation. The rehabilitation needs of stroke patients are complex and multidimensional, encompassing motor function restoration, cognitive reorganization, and emotional stabilization (7). These domains are highly interrelated. For instance, cognitive impairments may reduce the motivation for motor training, while emotional disturbances can exacerbate functional limitations. Consequently, the development of interdisciplinary and personalized rehabilitation strategies based on BCI technology has become a critical focus of contemporary research.

This review investigates the role of BCI in stroke rehabilitation by examining its applications across motor, cognitive, and emotional domains (Figure 1). Specifically, it explores BCI-driven motor rehabilitation mechanisms and techniques, assesses cognitive and emotional training potentials, and discusses the integration of artificial intelligence (AI) and virtual reality (VR) into BCI-based interventions. Finally, it outlines the technical and clinical challenges that remain and proposes future research directions aimed at advancing this promising field.

## 2. BCI-based motor function rehabilitation

### 2.1. Principles of BCI rehabilitation for motor dysfunction

Motor dysfunction is one of the most common and debilitating sequelae of stroke, severely compromising patients independence in daily living. BCI-based rehabilitation systems offer innovative and effective approaches to restoring motor function by enhancing neural plasticity through real-time brain signal interaction.

#### 2.1.1. Neurofeedback training

Neurofeedback training is a foundational mechanism in BCI-based motor rehabilitation, allowing patients to self-regulate brain activity by observing real-time neural signals (8). By visualizing the activation of motor-related cortical regions on a screen, patients can reinforce motor-related brain activity through motor imagery (9). This technique enhances motor intention and promotes functional reorganization of cortical networks (10). Repeated neurofeedback sessions have been shown to reactivate impaired motor areas, leading to measurable improvements in motor performance (11).

#### 2.1.2. Operant conditioning

Operant conditioning utilizes a reward-based mechanism to reinforce desired neural patterns (12). In the BCI context, when patients successfully generate motor intention, such as imagining raising of the arm, the system delivers visual, tactile, or electrical feedback as reinforcement (13). This positive feedback not only boosts patient confidence but also reinforces motor circuit reorganization through reinforcement learning principles (14).

#### 2.1.3. Repetitive participation and task-oriented training

The principle of "use it or lose it" underscores the necessity of repeated motor activity to enhance neural circuits. BCI systems enable patients to repeatedly engage in task-oriented training, such as controlling a virtual arm to perform grasping tasks using brain signals (15). Such task-oriented practice facilitates the remodeling of key motor pathways, including the corticospinal tract and corpus callosum, ultimately improving motor coordination and accuracy (16).

#### 2.1.4. Hebbian plasticity

Hebbian plasticity, commonly summarized as "neurons that fire together, wire together," is another core concept in BCI motor rehabilitation (17). Stroke survivors often experience a disconnect between motor intention and actual movement, resulting in diminished sensory feedback to the motor cortex (18). BCI systems restore this feedback loop *via* robotic or tactile stimulation, re-establishing the association between intention and feedback, thereby promoting cortical disinhibition and functional recovery (17,19).

#### 2.1.5. Personalized and adaptive training

Due to individual differences in stroke lesion location and severity, rehabilitation protocols must be highly individualized. Modern BCI platforms employ machine learning algorithms to dynamically adjust training difficulty and feedback modalities. Patients with more severe impairments may receive simplified tasks with intensive feedback, whereas those with better residual function can be challenged with more complex tasks to further enhance recovery potential.

#### 2.1.6. Multimodal feedback integration

Conventional BCI systems often rely solely on visual feedback. However, integrating multimodal stimuli, including tactile, auditory, and VR-based feedback, has been shown to significantly enhance therapeutic outcomes (20,21). VR technologies, in particular, offer immersive environments that increase training engagement and perceived agency (22). This multisensory feedback fosters deeper neural engagement and promotes more effective reorganization of motor networks.

### 2.2. Advances in BCI-based motor rehabilitation

Stroke-related motor dysfunction significantly limits activities of daily living and social participation. Upper limb impairments are particularly prevalent, affecting approximately 80% of survivors (23). Recent innovations in BCI motor rehabilitation have incorporated neurofeedback, functional electrical stimulation (FES), robotic systems, and VR, expanding therapeutic possibilities.

#### 2.2.1. BCI in upper limb rehabilitation: Clinical applications

Initial BCI research primarily focused on recovery of upper limb function, exploring how decoding brain activity could restore voluntary motor control. Buch *et al.* were among the pioneers utilizing magnetoencephalography (MEG) to assess sensorimotor rhythm (SMR) training in chronic stroke patients, who displayed increased motor cortex activation

following BCI training (24). Later, Ang *et al.* integrated electroencephalography (EEG)-based BCI with the MIT-Manus robotic system, and they reported a 4.9-point average improvement in Fugl-Meyer Assessment (FMA) scores after 12 sessions (25). However, a meta-analysis revealed that training of a shorter duration (< 12 hours) was associated with greater functional gains, suggesting an optimal training window (26).

#### 2.2.2. Motor recovery with FES

FES complements BCI-based rehabilitation by executing movements corresponding to decoded motor intentions. Chung *et al.* found that BCI-triggered FES improved postural stability and gait coordination in chronic hemiplegic patients, as evinced by improved timed up and go (TUG) test scores (27). FES also enhances Hebbian plasticity *via* closed-loop feedback, facilitating cortical reorganization (28). A randomized controlled trial (RCT) by Jiang *et al.* further confirmed that BCI-FES training significantly improved hand grip strength and enhanced alpha wave activity in the motor cortex, indicating that this combined approach facilitates motor network reorganization (29).

#### 2.2.3. Integration of robotic assistance and VR

Robotic devices are increasingly being integrated into BCI systems to provide precise mechanical support and stimulate neuroplasticity (30). Ramos-Murguialday *et al.* developed a BCI-controlled robotic arm, resulting in notable improvements in hand strength and movement precision (31). Functional magnetic resonance imaging (fMRI) results confirmed increased activation in motor-related brain areas post-training (32). VR-enhanced BCI systems further improve user engagement and realism. For instance, Pichiorri *et al.* combined VR with motor imagery (MI) tasks, which improved both MI success rates and motor function (33). Immersive VR enhances the realism of imagined movements, thereby optimizing training outcomes (22).

#### 2.2.4. Gait rehabilitation and locomotion training

Gait impairment is a common post-stroke functional deficit, characterized by reduced step length, decreased gait speed, and poor balance control, severely affecting independent ambulation (34). BCI-based gait rehabilitation has emerged as a key research focus. Tang *et al.* explored a BCI gait rehabilitation system combining MI with visual feedback. After six weeks of training, significant improvements were observed in TUG test performance and gait stability and were correlated with increased corticospinal activity in the contralateral primary motor cortex (M1) (34,35). Kim *et al.* further developed a BCI-integrated exoskeleton-based lower limb training platform, allowing patients to control



the exoskeleton for gait training, which led to significant improvements in gait accuracy and stability (36).

#### 2.2.5. Multimodal integration and personalized rehabilitation approaches

Recent developments emphasize multimodal integration and personalized training protocols. Dual-modality BCI systems combining EEG and functional near-infrared spectroscopy (fNIRS) significantly improve the accuracy of motor intention decoding. For example, Kwak *et al.* proposed an fNIRS-guided attention network (FGANet) system that improved MI task accuracy by 4.0% and mental arithmetic performance by 2.7% compared to conventional models (37). Moreover, adaptive BCI systems utilizing AI can tailor task difficulty and feedback in real time. Zhang *et al.* found that such systems improved training efficiency and patient outcomes (38), highlighting the advantages of individualized rehabilitation.

#### 2.2.6. Clinical validation and long-term outcomes

Despite promising results in laboratory settings, clinical evidence remains limited. A meta-analysis by Cervera *et al.* found that BCI interventions produced a standardized mean difference (SMD) of 0.79 in FMA for upper extremity (FMA-UE) scores, a result comparable to conventional therapies such as mirror therapy and CIMT (39). However, small sample sizes and a lack of long-term follow-up limit generalizability. To address this gap, Wang *et al.* conducted a multicenter RCT involving 296 stroke patients, comparing a BCI rehabilitation group with a conventional rehabilitation group (40). After one month, the BCI group showed significantly greater improvements in FMA-UE scores (13.17 vs. 9.83; between-group difference: 3.35; 95% CI: 1.05–5.65;  $P = 0.0045$ ).

### 3. BCI-based cognitive and language rehabilitation

#### 3.1. Mechanisms and applications in cognitive rehabilitation

Cognitive rehabilitation is a vital aspect of post-stroke recovery, and yet conventional methods often lack precision and have limited efficacy. In contrast, BCI technology offers the significant potential to enhance cognitive function in stroke patients, particularly through neurofeedback-based cognitive assessment and memory training (41). Studies suggest that BCI systems utilizing theta and alpha waves — key neural oscillations tied to memory encoding — can precisely control the timing of item presentation in memory tasks, leading to substantial improvements in memory performance (42,43).

##### 3.1.1. Neural features of PSCI and EEG-based targeting

PSCI typically affects domains such as attention, memory, executive function, and language processing (44). These deficits typically arise from disrupted neural networks or functional impairments caused by brain damage. For example, dysfunction in the frontal and parietal lobes often leads to attention deficits and executive dysfunction, while hippocampal atrophy is strongly associated with memory decline.

BCI systems offer dynamic assessment of these impairments by decoding EEG patterns and other neural markers. Research has shown that variations in beta/theta power correlate with attentional control, while alpha wave activity is linked to memory performance (45,46). By modulating these EEG patterns, BCI systems can target specific cognitive impairments, offering tailored therapeutic interventions that enhance recovery.

##### 3.1.2. Neurofeedback and modulation strategies

Neurofeedback training serves as a cornerstone of BCI-based cognitive rehabilitation, providing real-time feedback that allows patients to consciously regulate abnormal neural activity. Evidence suggests that this approach can improve attention and memory function in stroke populations (47). For example, neurofeedback interventions have resulted in measurable improvements in both short-term and long-term verbal memory in patients and healthy controls (48). A case study by Mroczkowska *et al.* demonstrated that adjusting the beta/theta ratio in the C3 cortical region significantly enhanced attentional control and information processing efficiency (43). Moreover, neurofeedback strategies targeting specific cognitive domains have yielded promising results. In one study, patients trained to increase beta power in the prefrontal cortex *via* neurofeedback showed significant improvements in executive function task performance (49). These findings highlight the promise of BCI-based neurofeedback in restoring cognitive function.

##### 3.1.3. Role of VR and AI in adaptive cognitive training

The incorporation of VR into BCI-based cognitive rehabilitation enables the creation of immersive environments for ecologically valid cognitive training. By simulating real-world scenarios such as virtual shopping, navigation, and social interactions, VR enables patients to engage in practical cognitive exercises (50). A recent study found that a BCI-VR system significantly improved multitasking abilities and spatial memory (51). Pichiorri *et al.* further developed VR-based cognitive tasks within a BCI system, leading to enhanced attention control and working memory performance in stroke patients (33).

In addition, integrating AI into BCI systems allows for dynamic adjustments to training protocols based on real-time patient feedback. Machine learning

algorithms can detect cognitive fatigue or plateau states by analyzing EEG patterns and dynamically modulate training intensity, thereby maximizing training efficiency (52). Despite these promising results, large-scale clinical trials need to be conducted to validate these technologies and expand their clinical applications.

### 3.2. Exploration of BCI-based language rehabilitation

Language impairment, a frequent and complex consequence of stroke, affects approximately 30% of patients during the acute phase, with many experiencing persistent deficits in comprehension or expression during long-term recovery (53-55). While conventional approaches such as speech-language therapy (SLT) and computer-assisted language training (CALT) offer some benefits, their effectiveness is often limited by low patient adherence, insufficient personalization, and marginal improvements (56). BCI technology offers a novel, targeted approach to address these challenges.

#### 3.2.1. Characteristics of aphasia and BCIs applicability

Aphasia, a multifaceted neurological language disorder, impairs both expressive abilities (*e.g.*, word retrieval and articulation) and comprehension (*e.g.*, semantics and syntax). Its manifestations vary depending on the location of brain damage, with lesions in Brocas area typically linked to expressive aphasia and damage to Wernickes area associated with comprehension difficulties (57).

BCI technology enhances rehabilitation by capturing and decoding neural signals related to language processing, providing real-time feedback to strengthen neural activity and connectivity. Both EEG and fNIRS have proven effective in detecting changes in neural activity within Brocas and Wernickes areas, providing a basis for designing individualized neurofeedback interventions (58).

#### 3.2.2. Neurofeedback-based language rehabilitation

Neurofeedback training is a pivotal technique in BCI-based language rehabilitation, enabling patients to monitor and regulate brain activity associated with language processing. For example, Mroczkowska *et al.* showed that modulating beta wave activity at the C3 electrode site significantly improved word selection and generation in patients with expressive aphasia (43). Moreover, neurofeedback targeting relative alpha wave power in the occipital lobe yielded moderate improvements in naming, image and color recognition, sentence completion, and language fluency (59). In a 10-session intervention, training to enhance the beta/theta ratio at the C3 EEG electrode site significantly improved speech fluency, word retrieval speed and accuracy, and comprehension of complex syntactic structures (43). However, the generalizability of these findings remains

limited by small sample sizes and lack of a long-term follow-up.

## 4. BCI-based emotional regulation and mental health interventions

### 4.1. Impact of post-stroke emotional disorders

Emotional disturbances such as post-stroke depression (PSD) and anxiety significantly affect rehabilitation outcomes by reducing motivation, adherence, and overall quality of life. Studies estimate that 25% to 50% of patients experience depression during the acute phase, with approximately 30% continuing to suffer in the chronic phase (60,61). Depression often manifests as negative thought patterns, diminished motivation, and social withdrawal, all of which indirectly impede the progress of rehabilitation.

Similarly, post-stroke anxiety (PSA) affects 18% to 34% of survivors within the first year, with rates remaining stable up to five years post-stroke (62-66). Patients with PSA frequently exhibit excessive worry about their prognosis, including fears of recurrence, returning to work, falling, or losing independence. This anxiety can exacerbate depression and cognitive impairment, further worsening outcomes (63).

### 4.2. Real-time emotional monitoring and closed-loop regulation techniques

BCI technology enables real-time monitoring of emotional states by decoding key brain activity features. EEG signals, and particularly alpha and beta waves, are widely studied in emotional regulation. Low alpha-wave activity is typically linked to anxiety and tension, while high alpha-wave activity indicates relaxation and stability. Increased frontal midline theta power, conversely, correlates with positive emotions (67).

To improve emotion detection accuracy, recent BCI models have integrated multimodal signals such as EEG, heart rate variability (HRV), and electrodermal activity (EDA). Reduced HRV is often indicative of psychological distress, while heightened EDA is associated with anxiety (68). This integrative approach provides a more comprehensive assessment of emotional dynamics. In addition to monitoring, BCI systems with affective closed-loop interactions show promise in emotional regulation. For example, participants have successfully modulated musical feedback by recalling emotionally salient memories, illustrating the potential of BCI-assisted emotional self-regulation (69). Closed-loop systems can also detect negative emotions and trigger real-time interventions — such as mood-regulating music, VR-based meditation environments, or neurofeedback training — to adjust EEG activity and restore emotional balance (70). Recent advances in AI and machine learning have significantly enhanced

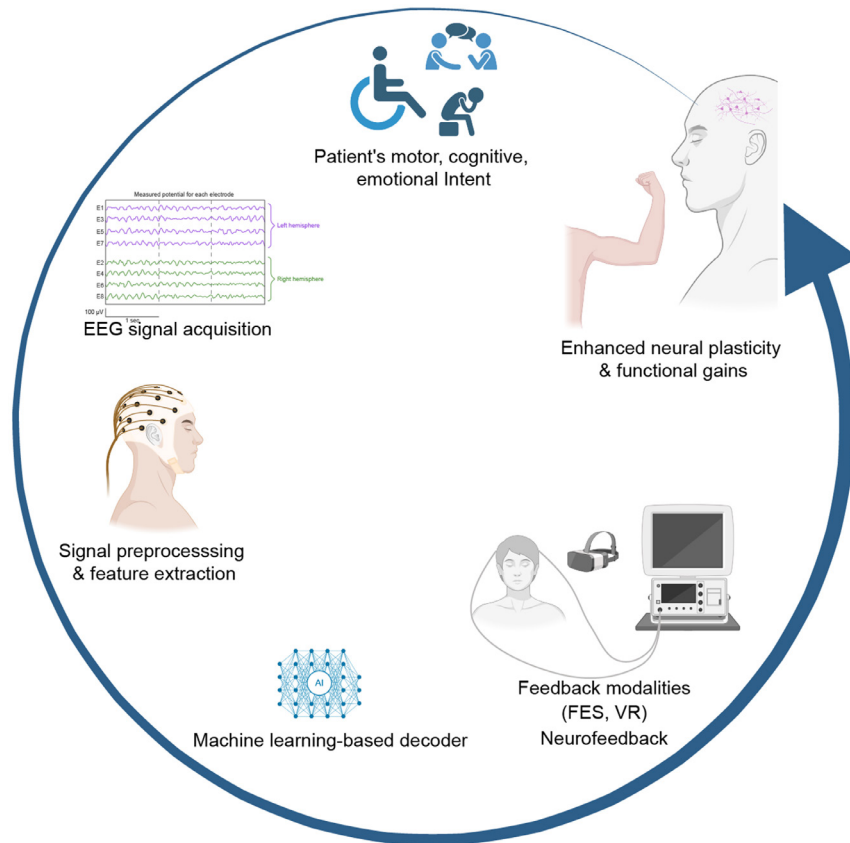


**Figure 2.** A conceptual framework of brain-computer interface-driven neurorehabilitation in stroke.

the accuracy and efficiency of real-time EEG-based emotion recognition within BCI systems. Self-supervised learning models, which reduce the need for large labeled datasets, have shown promise in decoding affective states by learning internal signal representations through signal transformation tasks prior to fine-tuning for emotion classification (71). Similarly, deep 3D convolutional neural networks with multiscale kernels have demonstrated a high level of accuracy — up to 95.67% on the DEAP dataset — by capturing complex spatiotemporal EEG patterns (72). Transformer-based architectures, known for their sequence modeling capabilities, have also emerged as powerful tools for EEG-based decoding of emotion, enabling more scalable and generalizable models for real-time applications (73).

One proof-of-concept study integrated real-time fMRI-based neurofeedback (rtfMRI-NFB) with both musical stimuli and immersive virtual environments, demonstrating the feasibility of such multimodal closed-loop systems. This interface employed both localized (region of interest, or ROI) and distributed (support vector machine, or SVM) neural activity analyses, enabling more precise detection and modulation of emotion-related brain states (70). The combination of BCI and VR technology offers particular advantages in managing emotional dysregulation. Through BCI-mediated neurocognitive training, both the patient and the system help to modify neuronal activity, which

can lead to significant reductions in anxiety-related symptoms (74). In one study, a VR scenario displaying calming landscapes (*e.g.*, forests or oceans) was activated when anxiety was detected, significantly reducing anxiety scores and enhancing well-being (75). Similarly, SMR-BCI systems, which decode motor-related alpha and beta waves to control external devices like robots or exoskeletons, suggest broader applications in emotional rehabilitation (76). These findings highlight BCIs potential to deliver integrated, interactive, and patient-centered mental health interventions post-stroke.

## 5. Discussion

In recent years, BCI technology has made remarkable progress in enhancing motor, cognitive, and emotional recovery following stroke. As an interdisciplinary tool integrating neuroscience, engineering, and AI, BCI has shown significant potential to reshape conventional neurorehabilitation paradigms (as illustrated in Figure 2). By enabling real-time decoding of neural activity and providing personalized feedback, BCI-based interventions offer novel and precise rehabilitation strategies across multiple functional domains. Despite these promising developments, several technical and clinical challenges must be addressed to fully realize the clinical potential of BCI systems. One of the primary limitations is the accuracy and stability of signal



decoding. EEG-based motor intention signals are highly susceptible to noise and artifacts, which can compromise decoding reliability and reduce system responsiveness. Future research should prioritize the integration of multimodal data sources, such as EEG combined with fNIRS or fMRI, to enhance signal fidelity and improve the precision of motor intention and emotional state recognition.

Another critical area where advances are needed is the personalization of rehabilitation protocols. Current BCI interventions often employ static, one-size-fits-all task models, which limit adaptability to individual patient profiles. The integration of AI and machine learning can address this issue by enabling real-time adaptation of training difficulty, feedback type, and task complexity based on patient performance and cognitive-emotional states. This approach can significantly improve training efficiency and patient engagement. In addition, the clinical translation of BCI systems remains hindered by practical limitations. Most current systems are confined to research or laboratory settings due to their complexity, bulkiness, and cost. To increase accessibility and facilitate home-based, long-term rehabilitation, wireless, lightweight, and cost-effective BCI devices need to be developed. Advances in wearable sensor technology and mobile computing may facilitate the design of portable, user-friendly BCI platforms suitable for continuous at-home use.

A major gap in the field is the lack of large-scale, multicenter RCTs to establish the long-term efficacy and safety of BCI interventions. Existing studies are often limited by small sample sizes, heterogeneous methodologies, and follow-up of an insufficient duration. Future research should focus on conducting well-designed clinical trials to evaluate both short- and long-term outcomes across diverse patient populations. Additionally, the development of standardized clinical guidelines and training protocols will be essential to the widespread adoption of BCI technology in routine rehabilitation practice.

## 6. Conclusion

In summary, BCI technology represents a transformative innovation in stroke rehabilitation, offering integrated and adaptive solutions for motor function recovery, cognitive enhancement, and emotional regulation. BCI technology currently has limitations, but ongoing advances in neuroscience, AI, VR, and wearable systems should help to further refine BCI platforms. In the future, BCI is poised to become a cornerstone of personalized, intelligent neurorehabilitation, providing stroke survivors with more effective, accessible, and holistic recovery pathways.

**Funding:** This work was supported by grants from the National Natural Science Foundation of China

(82460268), the Hainan Province Clinical Medical Research Center (No. LCYX202309), the Hainan Province Postdoctoral Research Project (403254), and Grants-in-Aid from the Ministry of Education, Science, Sports, and Culture of Japan (24K14216).

**Conflict of Interest:** The authors have no conflicts of interest to disclose.

## References

1. Diseases GBD, Injuries C. Global incidence, prevalence, years lived with disability (YLDs), disability-adjusted life-years (DALYs), and healthy life expectancy (HALE) for 371 diseases and injuries in 204 countries and territories and 811 subnational locations, 1990-2021: A systematic analysis for the global burden of disease study 2021. *Lancet*. 2024; 403:2133-2161.
2. Hachinski V, Donnan GA, Gorelick PB, *et al*. Stroke: Working toward a prioritized world agenda. *Stroke*. 2010; 41:1084-1099.
3. Li J, You SJ, Xu YN, Yuan W, Shen Y, Huang JY, Xiong KP, Liu CF. Cognitive impairment and sleep disturbances after minor ischemic stroke. *Sleep Breath*. 2019; 23:455-462.
4. Xiao W, Liu Y, Huang J, Huang LA, Bian Y, Zou G. Analysis of factors associated with depressive symptoms in stroke patients based on a national cross-sectional study. *Sci Rep*. 2024; 14:9268.
5. Taub E, Uswatte G, Pidikiti R. Constraint-induced movement therapy: A new family of techniques with broad application to physical rehabilitation--A clinical review. *J Rehabil Res Dev*. 1999; 36:237-251.
6. Wolpaw JR, Birbaumer N, McFarland DJ, Pfurtscheller G, Vaughan TM. Brain-computer interfaces for communication and control. *Clin Neurophysiol*. 2002; 113:767-791.
7. Cramer SC. Treatments to promote neural repair after stroke. *J Stroke*. 2018; 20:57-70.
8. Ang KK, Guan C. Brain-computer interface in stroke rehabilitation. *J Comput Sci Eng*. 2013; 7:139-146.
9. Ono T, Tomita Y, Inose M, Ota T, Kimura A, Liu M, Ushiba J. Multimodal sensory feedback associated with motor attempts alters BOLD responses to paralyzed hand movement in chronic stroke patients. *Brain Topogr*. 2015; 28:340-351.
10. Young BM, Stamm JM, Song J, Remsik AB, Nair VA, Tyler ME, Edwards DF, Caldera K, Sattin JA, Williams JC, Prabhakaran V. Brain-computer interface training after stroke affects patterns of brain-behavior relationships in corticospinal motor fibers. *Front Hum Neurosci*. 2016; 10:457.
11. Sulzer J, Papageorgiou TD, Goebel R, Hendler T. Neurofeedback: New territories and neurocognitive mechanisms of endogenous neuromodulation. *Philos Trans R Soc Lond B Biol Sci*. 2024; 379:20230081.
12. Meng F, Tong K-y, Chan S-t, Wong W-w, Lui K-h, Tang K-w, Gao X, Gao S. BCI-FES training system design and implementation for rehabilitation of stroke patients. In: 2008 IEEE International Joint Conference on Neural Networks (IEEE World Congress on Computational Intelligence) (IEEE, 2008; pp. 4103-4106).
13. Remsik AB, Dodd K, Williams L, Jr., *et al*. Behavioral outcomes following brain-computer interface intervention

- for upper extremity rehabilitation in stroke: A randomized controlled trial. *Front Neurosci.* 2018; 12:752.
14. Nojima I, Sugata H, Takeuchi H, Mima T. Brain-computer interface training based on brain activity can induce motor recovery in patients with stroke: A meta-analysis. *Neurorehabil Neural Repair.* 2022; 36:83-96.
15. Hong X, Lu ZK, Teh I, Nasrallah FA, Teo WP, Ang KK, Phua KS, Guan C, Chew E, Chuang KH. Brain plasticity following MI-BCI training combined with tDCS in a randomized trial in chronic subcortical stroke subjects: A preliminary study. *Sci Rep.* 2017; 7:9222.
16. Varkuti B, Guan C, Pan Y, Phua KS, Ang KK, Kuah CW, Chua K, Ang BT, Birbaumer N, Sitaram R. Resting state changes in functional connectivity correlate with movement recovery for BCI and robot-assisted upper-extremity training after stroke. *Neurorehabil Neural Repair.* 2013; 27:53-62.
17. Krueger J, Krauth R, Reichert C, *et al.* Hebbian plasticity induced by temporally coincident BCI enhances post-stroke motor recovery. *Sci Rep.* 2024; 14:18700.
18. Kukkar KK, Rao N, Huynh D, Shah S, Contreras-Vidal JL, Parikh PJ. Context-dependent reduction in corticomuscular coupling for balance control in chronic stroke survivors. *Exp Brain Res.* 2024; 242:2093-2112.
19. Dobkin BH. Brain-computer interface technology as a tool to augment plasticity and outcomes for neurological rehabilitation. *J Physiol.* 2007; 579:637-642.
20. Zhao CG, Ju F, Sun W, Jiang S, Xi X, Wang H, Sun XL, Li M, Xie J, Zhang K, Xu GH, Zhang SC, Mou X, Yuan H. Effects of training with a brain-computer interface-controlled robot on rehabilitation outcome in patients with subacute stroke: A randomized controlled trial. *Neurol Ther.* 2022; 11:679-695.
21. Yoo IG. Electroencephalogram-based neurofeedback training in persons with stroke: A scoping review in occupational therapy. *NeuroRehabilitation.* 2021; 48:9-18.
22. Vourvopoulos A, Bermudez IBS. Motor priming in virtual reality can augment motor-imagery training efficacy in restorative brain-computer interaction: A within-subject analysis. *J Neuroeng Rehabil.* 2016; 13:69.
23. Langhorne P, Coupar F, Pollock A. Motor recovery after stroke: A systematic review. *Lancet Neurol.* 2009; 8:741-754.
24. Buch E, Weber C, Cohen LG, Braun C, Dimyan MA, Ard T, Mellinger J, Caria A, Soekadar S, Fourkas A, Birbaumer N. Think to move: A neuromagnetic brain-computer interface (BCI) system for chronic stroke. *Stroke.* 2008; 39:910-917.
25. Ang KK, Guan C, Chua KS, Ang BT, Kuah C, Wang C, Phua KS, Chin ZY, Zhang H. Clinical study of neurorehabilitation in stroke using EEG-based motor imagery brain-computer interface with robotic feedback. *Annu Int Conf IEEE Eng Med Biol Soc.* 2010; 2010:5549-5552.
26. Zhang M, Zhu F, Jia F, Wu Y, Wang B, Gao L, Chu F, Tang W. Efficacy of brain-computer interfaces on upper extremity motor function rehabilitation after stroke: A systematic review and meta-analysis. *NeuroRehabilitation.* 2024; 54:199-212.
27. Chung E, Lee BH, Hwang S. Therapeutic effects of brain-computer interface-controlled functional electrical stimulation training on balance and gait performance for stroke: A pilot randomized controlled trial. *Medicine (Baltimore).* 2020; 99:e22612.
28. Cho W, Sabathiel N, Ortner R, Lechner A, Irimia DC, Allison BZ, Edlinger G, Guger C. Paired associative stimulation using brain-computer interfaces for stroke rehabilitation: A pilot study. *Eur J Transl Myol.* 2016; 26:6132.
29. Jang YY, Kim TH, Lee BH. Effects of brain-computer interface-controlled functional electrical stimulation training on shoulder subluxation for patients with stroke: A randomized controlled trial. *Occup Ther Int.* 2016; 23:175-185.
30. Mehrholz J, Pohl M, Platz T, Kugler J, Elsner B. Electromechanical and robot-assisted arm training for improving activities of daily living, arm function, and arm muscle strength after stroke. *Cochrane Database Syst Rev.* 2018; 9:CD006876.
31. Ramos-Murguialday A, Broetz D, Rea M, *et al.* Brain-machine interface in chronic stroke rehabilitation: A controlled study. *Ann Neurol.* 2013; 74:100-108.
32. Baniqued PDE, Stanyer EC, Awais M, Alazmani A, Jackson AE, Mon-Williams MA, Mushtaq F, Holt RJ. Brain-computer interface robotics for hand rehabilitation after stroke: A systematic review. *J Neuroeng Rehabil.* 2021; 18:15.
33. Pichiorri F, Morone G, Petti M, Toppi J, Pisotta I, Molinari M, Paolucci S, Inghilleri M, Astolfi L, Cincotti F, Mattia D. Brain-computer interface boosts motor imagery practice during stroke recovery. *Ann Neurol.* 2015; 77:851-865.
34. Khatkova SE, Kostenko EV, Akulov MA, Diagileva VP, Nikolaev EA, Orlova AS. Modern aspects of the pathophysiology of walking disorders and their rehabilitation in post-stroke patients. *Zh Nevrol Psikhiatr Im S S Korsakova.* 2019; 119:43-50. (in Russian)
35. Tang N, Guan C, Ang K, Phua K, Chew E. Motor imagery-assisted brain-computer interface for gait retraining in neurorehabilitation in chronic stroke. *Ann Phys Rehabil Med.* 2018; 61:e188.
36. Kim J, Kim DY, Chun MH, Kim SW, Jeon HR, Hwang CH, Choi JK, Bae S. Effects of robot-(Morning Walk(R)) assisted gait training for patients after stroke: A randomized controlled trial. *Clin Rehabil.* 2019; 33:516-523.
37. Kwak Y, Song WJ, Kim SE. FGANet: fNIRS-guided attention network for hybrid EEG-fNIRS brain-computer interfaces. *IEEE Trans Neural Syst Rehabil Eng.* 2022; 30:329-339.
38. Zhang R, Wang C, He S, Zhao C, Zhang K, Wang X, Li Y. An adaptive brain-computer interface to enhance motor recovery after stroke. *IEEE Trans Neural Syst Rehabil Eng.* 2023; 31:2268-2278.
39. Cervera MA, Soekadar SR, Ushiba J, Millan JDR, Liu M, Birbaumer N, Garipelli G. Brain-computer interfaces for post-stroke motor rehabilitation: A meta-analysis. *Ann Clin Transl Neurol.* 2018; 5:651-663.
40. Wang A, Tian X, Jiang D, *et al.* Rehabilitation with brain-computer interface and upper limb motor function in ischemic stroke: A randomized controlled trial. *Med.* 2024; 5:559-569 e554.
41. Ali JJ, Viczko J, Smart CM. Efficacy of neurofeedback interventions for cognitive rehabilitation following brain injury: Systematic review and recommendations for future research. *J Int Neuropsychol Soc.* 2020; 26:31-46.
42. Cannon KB, Sherlin L, Lyle RR. Neurofeedback efficacy in the treatment of a 43-year-old female stroke victim: A case study. *J Neurother.* 2010; 14:107-121.
43. Mroczkowska D, Białkowska J, Rakowska A. Neurofeedback as supportive therapy after stroke. Case report. *Postep Psychiatr Neurol.* 2014; 23:190-201.
44. Park SH, Sohn MK, Jee S, Yang SS. The characteristics

- of cognitive impairment and their effects on functional outcome after inpatient rehabilitation in subacute stroke patients. *Ann Rehabil Med*. 2017; 41:734-742.
45. Klimesch W. alpha-band oscillations, attention, and controlled access to stored information. *Trends Cogn Sci*. 2012; 16:606-617.
46. Bazanova OM, Vernon D. Interpreting EEG alpha activity. *Neurosci Biobehav Rev*. 2014; 44:94-110.
47. Mane R, Chouhan T, Guan C. BCI for stroke rehabilitation: Motor and beyond. *J Neural Eng*. 2020; 17:041001.
48. Kober SE, Schweiger D, Witte M, Reichert JL, Grieshofer P, Neuper C, Wood G. Specific effects of EEG based neurofeedback training on memory functions in post-stroke victims. *J Neuroeng Rehabil*. 2015; 12:107.
49. Van Doren J, Arns M, Heinrich H, Vollebregt MA, Strehl U, S KL. Sustained effects of neurofeedback in ADHD: A systematic review and meta-analysis. *Eur Child Adolesc Psychiatry*. 2019; 28:293-305.
50. Pengcheng C, Nuo G. Research of VR-BCI and its application in hand soft rehabilitation system. In: 2021 IEEE 7th International Conference on Virtual Reality (ICVR) IEEE, 2021; pp. 254-261.
51. Drigas A, Sideraki A. Brain neuroplasticity leveraging virtual reality and brain-computer interface technologies. *Sensors (Basel)*. 2024; 24:5725.
52. Silva GA. A New Frontier: The convergence of nanotechnology, brain machine interfaces, and artificial intelligence. *Front Neurosci*. 2018; 12:843.
53. Berthier ML. Poststroke aphasia: Epidemiology, pathophysiology and treatment. *Drugs Aging*. 2005; 22:163-182.
54. Dickey L, Kagan A, Lindsay MP, Fang J, Rowland A, Black S. Incidence and profile of inpatient stroke-induced aphasia in Ontario, Canada. *Arch Phys Med Rehabil*. 2010; 91:196-202.
55. Mingming Y, Bolun Z, Zhijian L, Yingli W, Lanshu Z. Effectiveness of computer-based training on post-stroke cognitive rehabilitation: A systematic review and meta-analysis. *Neuropsychol Rehabil*. 2022; 32:481-497.
56. Mane R, Wu Z, Wang D. Poststroke motor, cognitive and speech rehabilitation with brain-computer interface: A perspective review. *Stroke Vasc Neurol*. 2022; 7:541-549.
57. Ardila A. A proposed reinterpretation and reclassification of aphasic syndromes. *Aphasiology*. 2010; 24:363-394.
58. Abibullaev B, An J, Moon J-I. Neural network classification of brain hemodynamic responses from four mental tasks. *Int J Optomechatronics*. 2011; 5:340-359.
59. Nan W, Dias APB, Rosa AC. Neurofeedback training for cognitive and motor function rehabilitation in chronic stroke: Two case reports. *Front Neurol*. 2019; 10:800.
60. Berg A, Palomäki H, Lehtihalmes M, Lönnqvist J, Kaste M. Poststroke depression: An 18-month follow-up. *Stroke*. 2003; 34:138-143.
61. Sun N, Li Q-J, Lv D-M, Man J, Liu X-S, Sun M-L. A survey on 465 patients with post-stroke depression in China. *Arch Psychiatr Nurs*. 2014; 28:368-371.
62. Chun HY, Whiteley WN, Dennis MS, Mead GE, Carson AJ. Anxiety after stroke: The importance of subtyping. *Stroke*. 2018; 49:556-564.
63. Lincoln NB, Brinkmann N, Cunningham S, Dejaeger E, De Weerd W, Jenni W, Mahdzir A, Putman K, Schupp W, Schuback B, De Wit L. Anxiety and depression after stroke: A 5 year follow-up. *Disabil Rehabil*. 2013; 35:140-145.
64. Ojagbemi A, Akinyemi J, Owolabi M, Akinyemi R, Arulogun O, Gebregziabher M, Akpa O, Olaniyan O, Salako B, Ovbiagele B. Predictors and prognoses of new onset post-stroke anxiety at one year in black Africans. *J Stroke Cerebrovasc Dis*. 2020; 29:105082.
65. Wang J, Zhao D, Lin M, Huang X, Shang X. Post-stroke anxiety analysis via machine learning methods. *Front Aging Neurosci*. 2021; 13:657937.
66. Rafsten L, Danielsson A, Sunnerhagen KS. Anxiety after stroke: A systematic review and meta-analysis. *J Rehabil Med*. 2018; 50:769-778.
67. Torres PE, Torres EA, Hernandez-Alvarez M, Yoo SG. EEG-based BCI emotion recognition: A survey. *Sensors (Basel)*. 2020; 20:5083.
68. Yasemin M, Sarikaya MA, Ince G. Emotional state estimation using sensor fusion of EEG and EDA. *Annu Int Conf IEEE Eng Med Biol Soc*. 2019; 2019:5609-5612.
69. Ehrlich SK, Agres KR, Guan C, Cheng G. A closed-loop, music-based brain-computer interface for emotion mediation. *PLoS One*. 2019; 14:e0213516.
70. Lorenzetti V, Melo B, Basilio R, Suo C, Yucel M, Tierra-Criollo CJ, Moll J. Emotion regulation using virtual environments and real-time fMRI neurofeedback. *Front Neurol*. 2018; 9:390.
71. Wang X, Ma Y, Cammon J, Fang F, Gao Y, Zhang Y. Self-supervised EEG emotion recognition models based on CNN. *IEEE Trans Neural Syst Rehabil Eng*. 2023; 31:1952-1962.
72. Su Y, Zhang Z, Li X, Zhang B, Ma H. The multiscale 3D convolutional network for emotion recognition based on electroencephalogram. *Front Neurosci*. 2022; 16:872311.
73. Vafaei E, Hosseini M. Transformers in EEG Analysis: A review of architectures and applications in motor imagery, seizure, and emotion classification. *Sensors (Basel)*. 2025; 25:1293.
74. Micoulaud-Franchi JA, Jeunet C, Pelissolo A, Ros T. EEG neurofeedback for anxiety disorders and post-traumatic stress disorders: A blueprint for a promising brain-based therapy. *Curr Psychiatry Rep*. 2021; 23:84.
75. Parsons TD. Virtual reality for enhanced ecological validity and experimental control in the clinical, affective and social neurosciences. *Front Hum Neurosci*. 2015; 9:660.
76. Edelman BJ, Meng J, Suma D, Zurn C, Nagarajan E, Baxter BS, Cline CC, He B. Noninvasive neuroimaging enhances continuous neural tracking for robotic device control. *Sci Robot*. 2019; 4:eaaw6844.

Received March 7, 2025; Revised April 10, 2025; Accepted April 15, 2025.

\*These authors contributed equally to this work.

\*Address correspondence to:

Xiqi Hu, Integrated Neuroscience Center, Geriatric Hospital of Hainan, Haikou 571100, China.

E-mail: 218302048@csu.edu.cn

Ying Xia, Department of Neurosurgery, Haikou Hospital Affiliated with the Central South University Xiangya School of Medicine, Haikou 570208, China; Integrated Neuroscience Center, Geriatric Hospital of Hainan, Haikou 571100, China.

E-mail: xiaying008@163.com

Released online in J-STAGE as advance publication April 17, 2025.

# Promoting active health with AI technologies: Current status and prospects of high-altitude therapy, simulated hypoxia, and LLM-driven lifestyle rehabilitation approaches

Mingyu Liu<sup>1</sup>, Wenli Zhang<sup>2,\*</sup>, Junyu Wang<sup>3</sup>, Kehan Bao<sup>4</sup>, Ziyi Fu<sup>5</sup>, Boyuan Wang<sup>6,7,8,\*</sup>

<sup>1</sup> College of International Tourism and Public Administration, Hainan University, Haikou, China;

<sup>2</sup> School of Information Science and Technology, Beijing University of Technology, Beijing, China;

<sup>3</sup> State Key Laboratory of Integrated Chip and Systems, School of Microelectronics, Fudan University, Shanghai, China;

<sup>4</sup> Business Department, Mediva inc, Tokyo, Japan;

<sup>5</sup> Business Development of Particle Accelerator in China, Hitachi Particle Engineering & Services, Inc. Pleasanton, USA;

<sup>6</sup> Beijing Xiaotangshan Hospital, Beijing, China;

<sup>7</sup> Department of Biomedical Sciences, City University of Hong Kong, Hong Kong;

<sup>8</sup> Zhuhai Fudan Innovation Institute, Fudan University, Zhuhai, China.

**SUMMARY:** In the context of the rising global prevalence of obesity, traditional intervention measures have proven insufficient to meet the demands of personalized and sustainable health management, necessitating the exploration of innovative solutions through innovative technologies. This study explores how advanced digital technologies, including Internet of Things (IoT) and Artificial Intelligence (AI), can manage weight and enhance full-lifecycle health in individuals with obesity under simulated high-altitude hypoxic conditions (HC). The findings suggest that integrating simulated HC with digital health technologies offers a novel and safe approach to obesity rehabilitation. By leveraging environmental stimuli, real-time monitoring through wearable devices, and intelligent evaluation using large language models (LLMs), this method enables more scientific weight loss, prevents rebound weight gain, and fosters proactive healthy lifestyles, significantly improving weight control outcomes for individuals with obesity. Future research should evaluate the efficacy of simulated HC in weight management and its long-term impact on obesity control. Establishing an integrated framework that combines simulated HC, lifestyle interventions, and smart health ecosystems is crucial for advancing rehabilitative healthcare and addressing the global burden of obesity through digital innovation.

**Keywords:** personalized weight management, digital health innovation, lifestyle intervention, obesity rehabilitation, sustainable health improvement, public health management, plateau innovation industry

## 1. Introduction

With societal development, lifestyle changes have led to increased obesity globally. GBD projections warn that without strict interventions, by 2050, 38 billion adults — over half the global adult population — will be overweight or obese. Besides, one-third (746 million) of children and adolescents will be overweight or obese, with about 360 million suffering from obesity (1). These trends underscore the urgent need for effective obesity interventions.

Globally, obesity has been identified as the fifth leading risk factor for mortality (3), primarily due to complications like type 2 diabetes, cardiovascular diseases, osteoarthritis, sleep apnea, and cancer (4). By 2025, over 1.31 billion people are projected to have diabetes due to rising obesity rates (5), while

cardiovascular events may double in some countries within a decade (6). According to a prediction, by 2070, obesity is predicted to cause over 2 million new cancer cases annually, accounting for 7% of all cancers (7).

Beyond health risks, obesity strains global public health systems and socioeconomic resources. In high-income countries, it adds pressure to aging populations and healthcare costs, while in low- and middle-income countries, it worsens child malnutrition and overburdens limited resources (8). In 2019, obesity-related costs ranged from 3.19 billion in low – income countries to 1.33 trillion in high-income countries (9). By 2035, the obesity epidemic could reduce global GDP by 2.9%, equivalent to a \$4 trillion loss (10), underscoring its critical impact on modern public health.

The evolving understanding of obesity as a complex chronic disease has spurred advancements in its



treatment (4), including oral medications to bariatric surgery (BS). Oral medications can cause gastrointestinal side effects despite better weight loss than placebos (11), while BS effectively achieves rapid, sustained weight loss but comes with significant complications (early complications require specialized center care, while later complications are managed locally) (12,13).

Therefore, multiple countries are now prioritizing lifestyle-based interventions such as health management for obesity. For instance, on March 9, 2025, China's National Health Commission promoted a "Weight Management Year" three-year action, declaring "healthy weight as the core indicator of national health," and integrating weight management into chronic disease prevention and treatment strategies. Since 2024, in collaboration with other departments, they've launched campaigns to boost public awareness and skills in weight management, aiming to control overweight, obesity, and prevent chronic diseases. This initiative not only covers all age groups but also emphasizes the family as the smallest unit of health management, which needs to take primary responsibility (92).

Current research on weight management utilizing health management approaches includes lifestyle interventions (14), commercial weight management programs such as the CSIRO Total Wellbeing Diet Online (15), online exercise programs (16), and dietary interventions (17), all of which have been shown to significantly improve obesity. Recently, hypobaric hypoxia environments have gained attention for their role in weight management. Studies show high altitudes positively correlate with metabolic health and a non-obese phenotype, while negatively associating with unhealthy metabolic states (18). Multiple studies confirm altitude's beneficial impact on weight loss (19-21),

positioning high-altitude environment as a promising intervention. Recently, HC has been applied to both acute (single exposure) and chronic (repeated exposure over several weeks) sessions for overweight and obese individuals. The aim is to enhance cardiac metabolic health and promote weight loss (2). Encouraging obese individuals to engage in diet or physical activities in simulated high altitude environment promotes weight management, while combining HC with exercise offers therapeutic potential (22). This approach supports weight loss and enhances metabolic health, making simulated high-altitude environment an innovative obesity solution. An integrated scenario for weight intervention is illustrated in Figure 1.

Modern technologies like IoT, AI, and 5G are revolutionizing weight management by effectively intervening in the lifestyles of obese individuals. Johanna *et al.* studied wearable IoT devices for lifestyle changes in obese pregnant women (23). Sharareh *et al.* used AI to predict obesity, showing that AI algorithms can accurately forecast obesity (3). These digital innovations have proven effective in addressing obesity. However, research on integrating HC with AI, IoT, and 5G for enhanced weight management is scarce.

This study investigates the integration of IoT, AI, and 5G with HC (via simulated high altitude environment in laboratory) for weight management in obese patients. By promoting lifestyle interventions and supporting the entire life cycle, it offers theoretical support for simulated high-altitude environment as a weight management strategy, improving patient quality of life and reducing public health burdens. The contributions of this study:

1). Highlights the effectiveness of combining lifestyle interventions, physical exercise, and hypobaric hypoxic therapy in simulated high-altitude environment as an

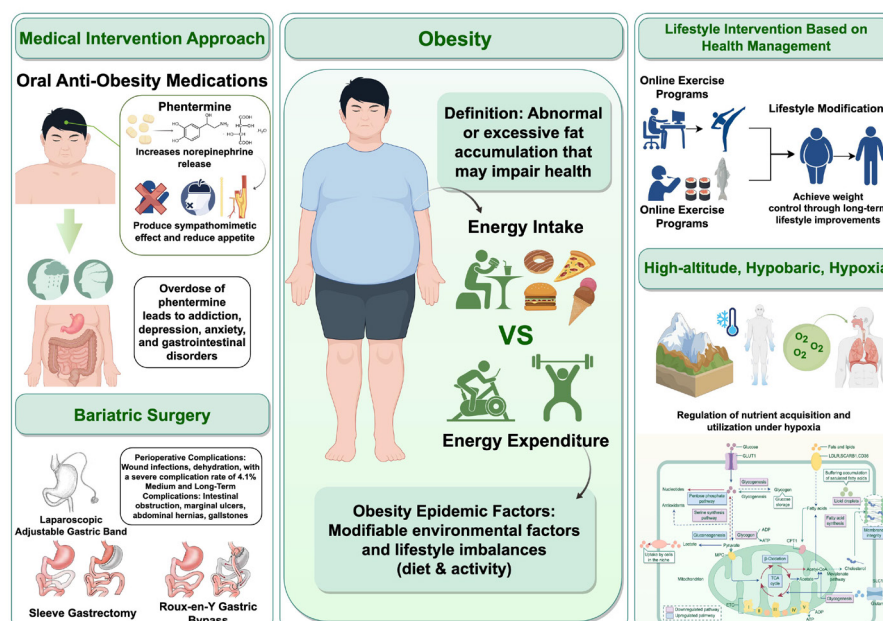


Figure 1. Scenario diagram of four obesity management approaches.

emerging weight management approach.

2). Integrates innovative technologies (IoT, AI, 5G) with traditional methods to offer personalized solutions. Utilizes wearable health monitoring devices and AI-driven predictions for obesity and related diseases.

3). Identifies research gaps in technology integration and hypobaric hypoxic applications, proposing further exploration of simulated high-altitude environment's long-term effects on weight management, offering valuable insights for researchers and global public health innovation.

## 2. Fundamental theory

### 2.1. Obesity and weight management

The WHO defines obesity as "an abnormal or excessive fat accumulation that may impair health," pointing out that the fundamental cause of obesity is an energy imbalance between calories consumed and calories expended (3,24). Research indicates that genetic factors only account for obesity in a very small segment of the population, with the widespread prevalence of obesity mainly attributed to modifiable environmental factors and individual lifestyle choices (25). In other words, overeating and insufficient physical activity are the primary causes of obesity. This is because diet is the form through which humans consume calories, while physical activity is the main pathway through which humans expend calories.

Jeffrey emphasized that obesity should be viewed as a biological disease akin to other chronic conditions like heart disease, hypercholesterolemia, diabetes, or hypertension (26). The adverse effects of obesity extend beyond its complications to the challenges in its treatment. Stella highlighted the difficulty overweight or obese individuals face in returning to a normal or healthy weight once classified as such (27). Although weight loss can improve complications and quality of life, maintaining that weight loss remains a significant challenge (4).

The primary goal of obesity management has shifted from merely achieving weight loss to improving health at a broader level (28), encompassing lifestyle changes, weight-loss medications, and bariatric surgery (16). Lifestyle interventions, mainly including dietary modifications, tailored exercise plans, and personalized behavioral counseling, have been shown to significantly improve weight outcomes and are now widely used in weight management.

Moreover, comprehensive behavioral weight management programs that combine physical activity with dietary restrictions have proven more effective for both short-term and long-term weight loss compared to interventions based solely on diet or physical activity (29). On one hand, creating a calorie deficit through prescribed caloric intake and appropriate physical

activity is aimed at sustained weight loss (16); on the other hand, personalized weight loss behavioral counseling serves to motivate obese patients by adjusting and optimizing weight loss strategies in real time (14). This approach provides a gentle yet effective pathway for weight loss among obese patients, emphasizing gradual and sustainable improvements in lifestyle.

### 2.2. The efficacy of HC in simulated high-altitude environment

High-altitude environment refers to elevated areas above 2,500 meters (30,31). HC is defined as exposure to systemic and/or local hypoxia at rest (passive) or combined with exercise training (active) (2). With advancements in technology, the ability to simulate high-altitude environments has become more accessible, leading to a surge in its popularity. This trend has attracted numerous researchers to investigate the effects and applications of simulated HC. Such environments offer promising avenues for studying weight management, cardio-metabolic health, and other physiological impacts on obese populations, spurring innovation and exploration in both research and practical applications.

Simulated high-altitude environments, characterized by low atmospheric pressure, reduced oxygen partial pressure, long daylight hours, and low humidity, create unique physiological effects on the human body. Exposure to hypobaric hypoxia condition often leads to weight loss (19), driven by multiple factors: decreased oxygen levels at higher altitudes reduce blood and tissue oxygen partial pressure, triggering compensatory responses such as increased ventilation and sympathetic nervous system activation, which elevate metabolic demands (32,33). Additionally, reduced appetite (20) or impaired gut function (34) decreases energy intake, creating a negative energy balance. Cold environments further increase energy expenditure for thermoregulation, depleting fat stores (35), while extra exercises amplify this effect through increased energy expend, altering body composition (22). Combining hypobaric hypoxia conditioning with dietary or exercise interventions has been proposed as an effective weight management strategy. Kayser noted that intermittent hypoxic exposure during rest or exercise improves body composition, exercise tolerance, metabolism, and arterial pressure (36). Quintero *et al.* highlighted oxygen availability as a key regulator of body weight and energy homeostasis (37), showcasing promising potential for obesity treatment. The mechanisms underlying weight reduction in simulated high-altitude hypobaric hypoxia environments are illustrated in Figure 2.

Rapid adaptation training in a simulated hypobaric and hypoxic environment may challenge the body's ability to acclimatize to acute hypoxia, but it offers a unique opportunity for weight management and health improvement. This environment can effectively promote

weight loss, but it is also important to take precautions against acute mountain sickness (AMS), commonly caused by hypoxia. Zhou *et al.* found that weight loss at high altitudes correlates with the severity of AMS, particularly due to fatigue(38), while Ge *et al.* noted that higher body weight increases susceptibility to AMS under hypoxic conditions(21). Therefore, while simulated HC provide potential for weight management, attention must also be paid to preventing and managing AMS, especially in obese individuals.

### 2.3. The integrated application of digital innovation technologies such as IoT, 5G, and AI

The Internet of Things (IoT), defined as an open network of intelligent objects capable of self-organizing, sharing data, and reacting to environmental changes, enables previously impossible connectivity and communication (39). IoT devices, including sensors and actuators, gather and store data locally or in the cloud, supporting applications like smart homes, smart health, and smart cities (40,41). Integrating IoT with machine learning (ML) or deep learning (DL) architectures tailored to specific needs has revolutionized healthcare, enabling innovative solutions for disease detection and health monitoring (40).

AI, particularly ML and DL, has proven effective in predicting obesity risks. Faria Ferdowsy achieved 97.09% accuracy in obesity risk prediction using ML techniques (42), while Sharareh Rostam demonstrated AI's potential for early detection, enabling timely interventions to prevent related diseases like type 2 diabetes and cardiovascular conditions (3). Similarly, Mahmood Safaei and Elankovan validated the efficacy of ML methods, such as neural networks, decision trees, random forests, and DL, in managing obesity (43).

The advent of 5G, with its high bandwidth, low latency, reliability, and massive connectivity, is a key driver of IoT growth (44). In healthcare, 5G-enabled IoT expands device connectivity and enhances wireless services. For instance, Chen *et al.* developed a personalized emotion-aware healthcare system using 5G, targeting emotional care for children, psychiatric patients, and the elderly (45). This integration highlights the transformative potential of combining digital innovations, as illustrated in Figure 3.

This study synthesizes a comprehensive strategy through an integrative review of the literature, combining lifestyle interventions with simulated high-altitude hypoxia, enhanced by digital innovations. It supports weight management for obese individuals, monitors hypoxia-related risks, and ensures holistic health protection. The approach benefits personal health and provides solutions to global public health challenges associated with obesity. Additionally, it enhances safety for obese patients in simulated high-altitude environments, ensuring comprehensive health protection.

### 3. Methodology

This study adheres to the PRISMA framework (46), conducting a systematic review of literature on weight management, high-altitude environment (hypobaric hypoxia intervention), AMS, and the application of 5G-IoT and AI (ML/DL) technologies in healthcare. Through four stages—identification, screening, eligibility assessment, and inclusion—a conceptual model was developed to explore the potential of high-altitude environment in improving obesity symptoms and its integration with digital innovations. From January to March 2025, searches were conducted in Web of Science, PubMed, and IEEE databases, targeting high-quality journals. Inclusion criteria focused on English peer-reviewed articles published after 1990 at SJR Q1 level (47). The search strategy revolved around several themes:

Related to weight management: "obesity" OR "overweight" OR "obesity management" OR "weight management"

Related to high-altitude environment (hypobaric hypoxia intervention): "high altitude" OR "low pressure" OR "low oxygen" OR "hypobaric" OR "hypoxia"

Related to digital innovation technologies: "5G-IoT" OR "AI" OR "ML" OR "DL"

Related to AMS: "acute mountain sickness" OR "AMS"

The specific classifications and results analysis are as follows:

A systematic search was conducted using the keywords "obesity" OR "overweight" OR "obesity management" OR "weight management," yielding 1,400,452 articles, of which 126,079 met the inclusion criteria. Among these, 88 studies explored the application of AI (ML/DL) in weight management. A combined search using the keywords ("high altitude" OR "low pressure" OR "low oxygen" OR "hypobaric" OR "hypoxia") AND ("obesity" OR "overweight" OR "obesity management" OR "weight management") generated 1,101 publications, with 122 selected to demonstrate the effects of hypobaric hypoxia on body composition. Additionally, a search combining terms ("5G" OR "IoT" OR "AI" OR "ML" OR "DL") with high-altitude-related keywords retrieved 2,658 articles, of which 119 were retained; 15 studies focused on digital interventions for treating respiratory diseases and chronic kidney disease, which are closely associated with obesity. Also, we noted that 13 papers highlighted the significant role of technologies in the early detection and prevention of AMS.

Based on the above literature search and screening results, the study ultimately included 181 articles for in-depth review. Existing research highlights high-altitude environment, simulated or real hypobaric hypoxia, weight management, and digital technologies as key areas. However, interdisciplinary research remains scarce, particularly integrating high-altitude environment



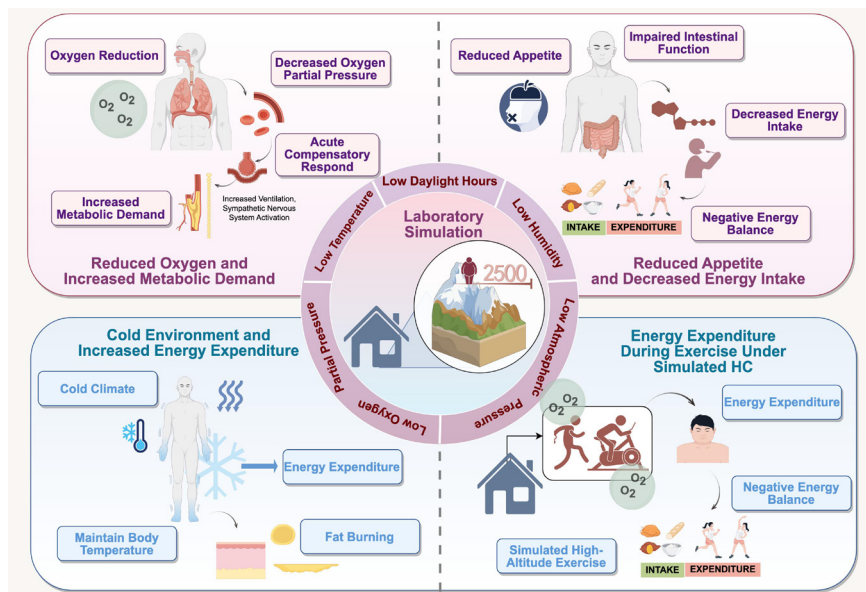


Figure 2. Schematic diagram of weight management in simulated high-altitude hypobaric & hypoxic environments.

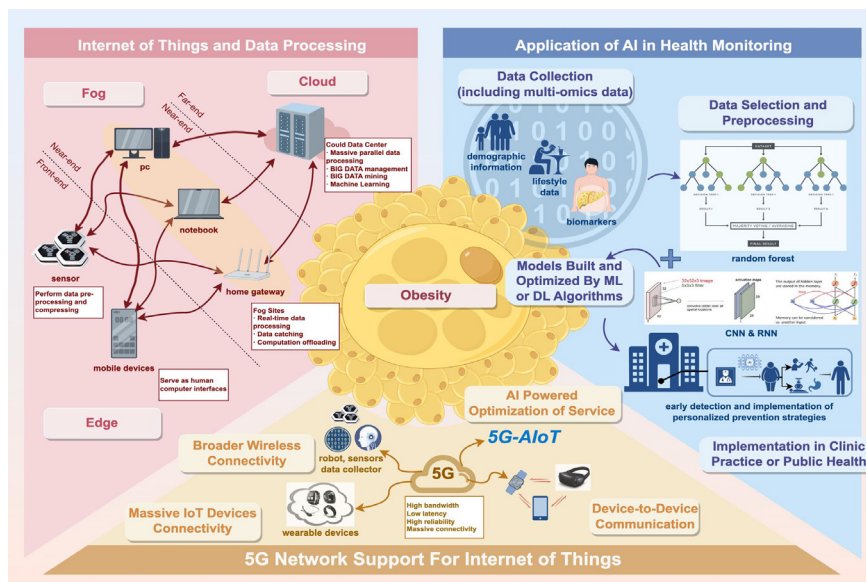


Figure 3. Integrated application scenarios of digital innovation technologies.

with digital innovations. This gap underscores the need for further exploration in this field. The search process and criteria are illustrated in Figure 4.

#### 4. 5G-IoT and AI Synergy for Weight Management and Safety in Hypobaric Conditions

This study reviews an integrated health management strategy, merging simulated high-altitude environment's hypobaric hypoxia (combine with diet and exercise) with digital innovations. This approach supports weight management for obese individuals, relevant health risks, and ensures comprehensive health protection. It benefits personal health and provides innovative solutions and technical support for global public health systems facing rising obesity rates among various age groups.

##### 4.1. Data-driven obesity management and safety rescue

AI (ML, DL) can describe, classify, and predict obesity-related risks and outcomes using data from sensors, smartphone apps, electronic health records, and insurance data. Besides, ML and DL analyze causes and risks of dietary plan failures, such as alcohol consumption and self-efficacy. Additionally, IoT wearable devices monitor physiological indicators in real time for tailored diet and exercise plans. By applying AI, we can comprehensively analyze data from obese patients engaging in simulated high-altitude environment, assessing and predicting their obesity risks and severity. Combining exercise habits, dietary risks, and environmental conditions at laboratory, personalized hypobaric hypoxia weight management plans can be developed for each patient.



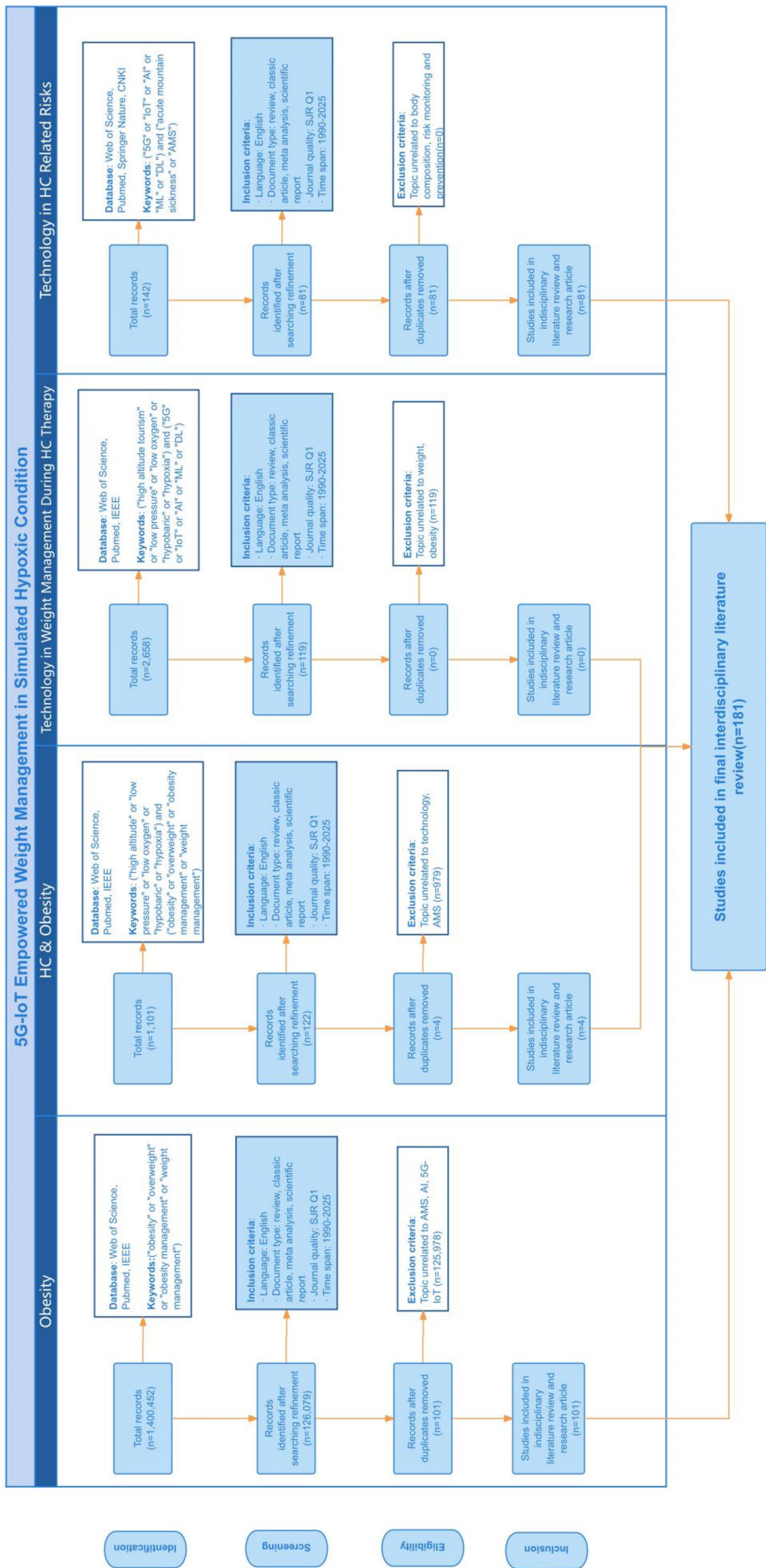


Figure 4. Literature review process and screening criteria.

For example, DeGregory *et al.* reviewed ML methods (*e.g.*, regression, neural networks, decision trees) applied to health survey data, demonstrating their potential for large-scale obesity analysis (48). Chatterjee *et al.* developed an intelligent eCoach system using ML to predict risks and provide personalized recommendations for obesity and related conditions (49). Sala *et al.* created an ML model predicting dietary lapses, identifying alcohol and low self-efficacy as key risk factors (50). Greco *et al.* highlighted AI's role in accurately segmenting adipose tissue in CT/MR images, aiding weight change tracking (51). Varun *et al.* assessed wearable-EHR integration for remote obesity monitoring, finding positive patient attitudes toward sharing activity data with healthcare teams (52). Please see Table 1 for details of the study and the proof process.

#### 4.2. Real-time health monitoring and adverse health event prevention – Under simulated hypobaric hypoxia conditions

IoT wearables monitor hydration, respiratory conditions, and other physiological indicators in real time. AI algorithms analyze these data to predict relevant risks and recommend preventive measures. Continuous tracking of weight, oxygen levels, exercise, and nutrition enables early health warnings and timely adjustments to weight management plans, enhancing safety and precision in obesity treatment.

Nicholas *et al.* showed obese individuals lost more weight in simulated hypoxia than in normoxic conditions, marking the first trial of hypoxia-induced weight loss and highlighting normobaric hypoxia's potential for non-dietary weight management (53). Hobbins *et al.* reviewed passive and active hypoxic conditioning (HC), finding passive HC increased energy expenditure and altered fuel use, while active HC reduced weight and blood pressure, though results were inconsistent for triglycerides, cholesterol, and fitness.

These studies fully confirm the effectiveness and feasibility of weight loss in simulated high-altitude environments. With the widespread adoption of technologies like IoT and AI, wearable devices' health monitoring capabilities and smart healthcare ecosystems based on digital innovation now provide strong support for such weight loss programs. Real-time monitoring of patients' physiological indicators *via* IoT devices, combined with data sharing through 5G cloud platforms, enables healthcare providers to better understand patient conditions, enhance doctor-patient communication, and optimize weight management strategies.

Many studies have indicated that fluid retention, obesity, and obesity-related symptoms (such as respiratory impairments) are major factors contributing to the risk of AMS among obese patients at high altitudes (54-57). With the effective promotion of weight management for obese patients in simulated HC, the

**Table 1. Analysis of the role of AI and IoT in weight management**

| Method   | Region  | Participant   | Way  | Result  | Ref. |
|--|---------|---|--|---|------|
| ML Methods                                     | America | A nationally representative sample of US adults                 | The study compared logistic regression, decision trees, neural networks, and deep learning for predicting hypertension and body fat percentage   | Innovative mathematical methods in ML are needed to analyze new data sources in obesity, meeting the demand for advanced predictions and descriptions.  | (48) |
| ML Methods - Digital eCoaching System          | Norway  | Targeting men and women in age groups >20 and <60,              | Statistical analysis was performed on public datasets from "Kaggle" and "UCI" using ML models, evaluating their classification and regression performance                                | The digital eCoaching system will collect data on obesity/overweight risk factors from male and female trials in southern Norway, using this for regression and prediction to provide automated, personalized advice to participants. | (49) |
| EMA and ML Analysis Methods                    | America | One sample had 58 overweight/obese individuals; another had 29. | The first group received Weight Watchers (WW) or WW + Just-In-Time Adaptive Interventions (JITAIs). The second group followed the WW Freestyle diet and completed six EMA surveys daily. | Alcohol consumption and self-efficacy influenced dietary lapses, enhancing JITAIs for personalized interventions.   | (50) |
| AI Algorithms                                  | Italy   | /   | Utilizing AI algorithms to extract quantitative data from computed tomography (CT) and magnetic resonance (MR) images.   | AI effectively quantifies visceral (VAT) and subcutaneous adipose tissue (SAT) in CT images and shows promise for analyzing abdominal fat in MR images.   | (51) |
| RPM plan integrated wearable devices with EHR. | America | Recruited 10 PCPs and 8 obese patients from UMass clinics.      | Wearable data were uploaded to EHR, followed by interviews with PCPs and patients.   | Patients wanted to share PA data via EHR for more specific consultations. Providers were open to PA-focused RPM solutions that fit their workflow and supported health equity.  | (52) |

application of innovation technologies to help obese patients avoid the risk of AMS under this condition. For instance, Pablo *et al.*'s wearable system monitors vital signs and environmental conditions for workers, providing real-time cardiac and respiratory analysis *via* Bluetooth (58). Wei *et al.* used ML algorithms for an AMS risk model, demonstrating higher accuracy with multivariate analysis (59).

Table 2 shows details of the main research methods and results.

#### 4.3. Personalized lifestyle support – Prognosis

During and after high-altitude environment therapy, the big data analytics powered by AI and IoT technologies, along with personal health data tracking, can not only provide each participant with customized daily health meal plans and appropriate regular exercise programs but also monitor for post-travel physical discomfort. This helps in the prognosis of obese patients. Such personalized health management strategies contribute to long-term weight management and overall health maintenance, supporting healthy living while preventing weight regain.

Woo *et al.* demonstrated that AI-IoT technology improves elderly healthcare by enhancing medication habits, managing hypertension, frailty, diabetes, and promoting physical activity and nutrition (60). Ying *et al.* showcased how AI dietitians improve food recognition, dietary recording, nutritional assessment, and recipe suggestions, significantly boosting efficiency (61). Rafael *et al.* highlighted wearable devices for personalized medicine in ketosis and diabetic ketoacidosis (DKA) management, emphasizing their role in early diagnosis and timely interventions (62).

Renu *et al.* explored an Ambient Assisted Living (AAL) system using a DNN-based IoMT architecture to accelerate data collection and processing, enabling effective healthcare predictions (63). Saeed *et al.* proposed an IoT framework with an ML activity classification system to monitor surgical and overweight patients, facilitating accurate patient profiles and automated data analysis (64). Chioma *et al.*'s review underscored the effectiveness of ML and DL algorithms in analyzing sensor data for various health issues, including activity monitoring and sleep disorder detection (65). Alireza *et al.* found that integrating IoT and AI in smart fitness equipment enhances user self-awareness and motivation during workouts (66). Table 3 shows the specific details of these studies.

#### 4.4. 5G-enabled comprehensive health management services – Empowering VR/AR, IoT, and AI technologies to build a digital healthcare ecosystem

By integrating the advantages of 5G networks (high speed, low latency, and massive connectivity), IoT, AI algorithms,

**Table 2. The simulated HC strategy in weight management**

| Method  | Region  | Participant  | Way   | Result   | Ref. |
|---|---------|--|---|--|------|
| Low intense physical exercise in normobaric hypoxia | Germany | 32 obese participants (mean age: 47.6 years; mean BMI: 33.1; 16 males, 4 females)  | 8-week intervention with low-intensity exercise (3 sessions/week, 90 minutes/session).<br>No dietary interventions applied.   | The hypoxia group lost more weight than the placebo. BMI trended down, but HbA1c didn't change. Eight weeks of mild exercise in 15% O <sub>2</sub> led to greater weight loss than the placebo for obese individuals.                            | (53) |
| Normobaric hypoxic conditioning                     | Chile   | Human participants aged 21 to 51, including those with obesity, overweight, and sedentary lifestyles, as well as animal participants | Animals underwent intermittent hypoxia and continuous hypoxia training, while humans engaged in exercise training under passive hypoxia exposure, active hypoxia exposure, or a combination of both | Passive HC increases energy expenditure and alters fuel utilization, while active HC leads to weight loss and reduced blood pressure. However, the effects on lipid profiles, cholesterol levels, and physical fitness remain inconsistent       | (2)  |
| Wearable Oximeter - Maxim Oximeter                  | America | Volunteers provided informed consent for participation.  | Data collection involved using Maxim oximeters worn at different positions (wrist, sternum, forehead, ear).   | The forehead provided excellent signal quality, while the sternum required more power and motion artifact mitigation. The wearable oximeter monitors hypoxemia at high altitudes and shock during trauma, aiding safety in extreme environments. | (91) |
| 25 ML Algorithms                                    | China   | 32 participants (25 males and 7 females) were involved.  | Participants hiked from Cui Fengshan Forest Park (2300m) to Wuling (3275m). ML analyses on physiological, environmental data, and LLS established AMS risk algorithms.                              | 25 ML algorithms analyzed the data, showing improved sensitivity, specificity, and accuracy over previous studies, aiding AMS risk assessment model development.   | (59) |

**Table 3. A global analysis of smart health technology applications**

| Method   | Region       | Participant  | Way   | Result  | Ref. |
|--|--------------|--|---|---|------|
| AI-IoT in Healthcare   | Korea        | Utilizing this service, 21,966 smartphone users              | Provided non-face-to-face health consultations and customized services to health experts, categorized into healthy, formerly weak, and disadvantaged groups.  | Over 97% controlled hypertension and diabetes, with improvements up to 50.4% and 34.8%. Physical activity and diet improved by over 50%. Frailty scores decreased by 41% to 65%.  | (60) |
| AI Nutritionist  | China        | 177 AI dietitians  | AI dietitians use algorithms to assess personalized nutrition at the molecular level, matching genotypes and phenotypes with diets, and provide detailed analyses via self-monitoring.              | With a comprehensive understanding of food and habits, they improve dietary assessment accuracy and efficiency for broader populations.   | (61) |
| Mobile and Wearable Sensing Devices                              | America      | DKA patients   | Wearable sensing technology and alternative body fluids enable quick, non-invasive measurement of beta-hydroxybutyrate, a key ketone for DKA diagnosis.   | This platform allows painless home monitoring with faster analysis, lower cost, and higher sensitivity, improving diagnostic reliability without relying on clinics or professionals.   | (62) |
| IoMT-AAL Architecture  | India        | Used for healthcare monitoring in 10 patients                | IoMT-AAL collects and analyzes sensor data to identify behavioral patterns, habits, and living difficulties, enabling preventive measures for smarter daily environments.                           | Compared to PHD-HBD, ERPS-MLT-MA, and DDRU, IoMT-AAL achieves 94.3% transmission speed and 90.1% accuracy, validated through experimental analysis.   | (63) |
| IoT Framework Benefiting from ML Activity Classification Systems | Saudi Arabia | Obesity patients   | The IoT infrastructure gathers wearables data on vital signs and activities, using machine learning to classify movements. It supports health and nutrition, especially for postoperative patients. | The proposed IoT framework further extends by including a calorie intake analysis system based on ML and activity-based calorie burning, which can help create precise weight prediction factors, having a better impact on patients. | (64) |
| Mobile and Wearable Sensors for Health Monitoring                | British      | /  | Mobile and wearable devices monitor health in areas like contact tracing, activity recognition, fall detection, Parkinson's detection, and disease diagnosis.                                       | These sensor-based systems enable real-time diagnosis, management, and prevention of diseases, along with treatment suggestions.  | (65) |
| IoT-Based Smart Fitness  | France       | Users of fitness trackers, motion analysis, and fitness apps | Users interact with a four-layer system: Observation, Contextualization, Decision, and Action.  | Fitness trackers and smartwatches help users gain self-awareness and motivate casual runners to achieve their goals and improve training experiences.   | (66) |



and VR/AR, it is possible to achieve full-process health management supervision and remote hyper-realistic assistance for obese patients. This applies whether patients are undergoing HC in simulated high-altitude environment or managing their health independently at home after completing their treatment programs.

Specifically, 5G will enhance telemedicine by enabling remote precision medicine through seamless connectivity of medical devices to cloud platforms, avoiding network congestion. This supports immersive VR, real-time AR, and latency-free interactions, providing doctors with accurate diagnostic tools and improving training quality (67). By integrating 5G with IoT, wearable devices monitor patient health data, analyzed *via* cloud, fog, and edge computing, creating a "smart network" ecosystem that optimizes health plans and visualizes outcomes. Furthermore, 5G-enabled emotion recognition, with up to 99.87% accuracy (68), provides real-time emotional feedback for obese patients in HC, facilitating timely treatment adjustments and remote psychological counseling.

It is evident that the application of cutting-edge technologies such as 5G in healthcare not only enhances the quality of health management services but also ensures comprehensive weight management from the short term to the long term, ultimately achieving the goal of full lifecycle health assurance.

Machorro-Cano *et al.*'s PISIoT platform effectively aids weight loss and reduces myocardial infarction risk in elderly obese patients (69). Mohanta *et al.* describe Healthcare 5.0, which uses AI, IoT, and 5G for swift transmission of large medical files, enhancing remote monitoring (70). Singh highlights gamified 5G wearable interventions for childhood obesity, proving effective through engaging strategies and motivational challenges (71). Venkatachalam *et al.* demonstrate diabetes management in obese patients using IoT devices integrated with 5G networks (72). Dong *et al.*'s smart physical education system improves college student fitness through 5G and VR technology (73). Chen *et al.*'s 5GCS-Health-Sys focuses on emotional interaction, benefiting children, psychiatric patients, and the elderly (45). Specific details of the relevant studies can be viewed in Table 4.

These technologies optimize weight management strategies for obese patients in HC, enhance safety during simulated high-altitude therapy, and support full lifecycle health management. They offer new solutions to public health challenges posed by rising global obesity rates, improving service quality and addressing critical health issues (as summarized in Table 4 and illustrated in Figure 5).

## 5. Limitations and future prospects of current research

Despite the potential of 5G and IoT in healthcare,

**Table 4. Next-gen weight care: Harnessing AI and IoT for effective obesity treatment**

| Method  | Region  | Participant  | Way   | Result   | Ref. |
|---|---------|--|---|--|------|
| PISIoT  | Mexico  | 40 obese elderly aged 60–80 with myocardial infarction symptoms or history participated in a weight loss study | PISIoT, a user-centric IoT solution, integrates data from various devices, analyzes it using ML, and provides real-time monitoring, alerts, and medical advice.   | By phase three, 40% achieved weight loss (1–7 kg) and lower BMI. PISIoT reduced myocardial infarction risk, improved health, and enhanced quality of life. | (69) |
| Healthcare 5.0  | India   | Open access  | Components include IIoT controllers, smart IoT devices, smart blood banks, automated pathology labs, smart waste management, and 5G services covering over 2000 users.                                      | Monitoring sensory data enables early disease prediction, promoting healthier lives.   | (70) |
| Gamified 5G Wearable Device Interventions                                       | America | Child obesity patients.  | Gamified 5G wearables use engaging games, challenges, and education to help obese children lose weight through exercise, motivating them to take initiative and build daily weight management habits.       | These devices make weight loss fun and effective for children.   | (71) |
| Diabetes Vehicle System (Involving IoT and 5G)                                  | China   | Potential patients with diabetes caused by obesity.  | IoT devices monitor health metrics such as blood glucose and blood pressure. The data is processed and analyzed at 5G edge nodes, and diagnostic results are shared with patients.                          | The system supports self-care, lifestyle analysis, and real-time monitoring to prevent and manage diabetes caused by obesity.                              | (72) |
| Smart Physical Education Program System Platform                                | China   | 8352 university graduates from 2020 and 2021   | Students use tablets and VR glasses to access 3D videos for learning in class and during leisure time, fostering exercise awareness. Peer discussions and extracurricular talks improve fitness and health. | This 5G and VR-enhanced PE led to better physical performance and greater interest in sports compared to traditional methods.                              | (73) |
| A New Healthcare System Based on 5G Cognitive Systems (5G-Csys)—5GCS-Health-Sys | China   | 24 participants recorded in the dataset; 13 males and 11 females aged 20 to 30.                                | 5GCS-Health-Sys recognizes voice emotions, categorizes them into six types, and sends results to smart terminals via the cloud. These terminals generate commands for EPIC-Robot to execute.                | 5GCS-Health-Sys accurately identifies user emotions and responds accordingly to improve negative emotions, enhancing healthcare outcomes.                  | (45) |

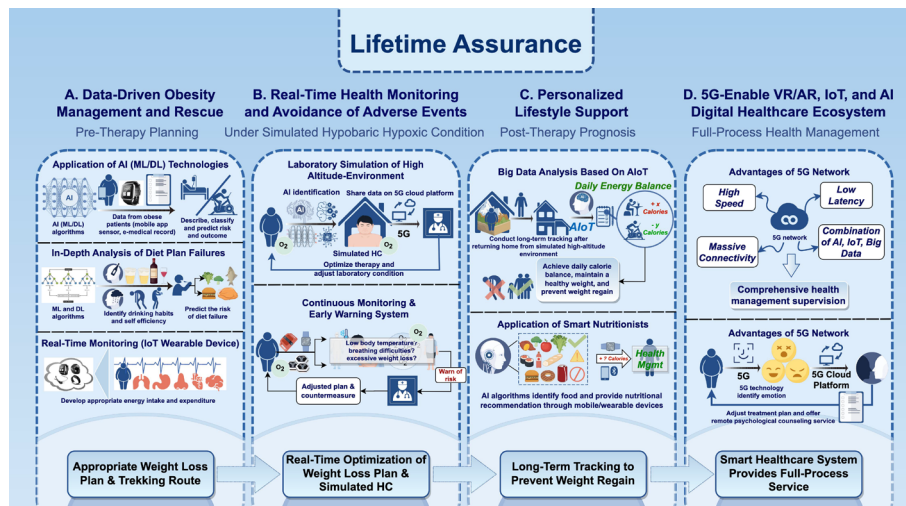


Figure 5. Schematic diagram of 5G-IoT-driven full-lifecycle weight management in HC.

their application in weight management for obese patients in simulated high-altitude (hypobaric hypoxia) environments remains limited. Most studies focus on isolated domains rather than integrating these technologies for comprehensive HC interventions. While 5G offers superior security, reliability, and mobility compared to Wi-Fi, making it ideal for monitoring patients and providing real-time feedback during simulated hypoxia, empirical research is scarce (74-78). Peralta *et al.*'s review reveals that only 15.91% of studied cases involve operational 5G-based smart healthcare systems, indicating a lack of large-scale implementation (79-82). This gap extends to obesity management in HC, where cross-domain technological integration is crucial. Managing sensitive health data in 5G-IoT systems is challenging, especially for resource-constrained devices (83). AI-driven authentication mechanisms, such as radio frequency fingerprinting, are essential to protect privacy and build trust (84,85).

Empirical evidence on hypoxia's impact in simulated high-altitude environments is also limited, with only 0.87% of studies addressing this topic, notably Gutwenger *et al.*'s low-altitude control study (86). Findings suggest improvements in BMI, cardiovascular health, and metabolism in HC and the integration of digital innovations like 5G-IoT remain understudied. Lippl *et al.* demonstrated weight loss driven by increased metabolic rates and reduced food intake, though their study relied on traditional methods (87). Similarly, Marlatt *et al.* and Mackenzie *et al.* confirmed metabolic benefits but did not incorporate modern technologies (88,89). Kayser *et al.* noted that systematic implementation of hypoxia-induced weight loss is premature due to insufficient evidence (90). Current efforts focus on theoretical frameworks and short-term outcomes, emphasizing the need for empirical validation of 5G-IoT applications to ensure safe deployment. These advancements aim to improve health outcomes and foster inclusive healthcare solutions.

## 6. Conclusion

This study addresses the gap in systematically reviewing IoT and AI technologies for laboratory-simulated high-altitude (hypobaric hypoxia) weight management. It highlights their potential in personalized weight management, real-time health monitoring, mitigating risks, and supporting long-term health. Integrating IoT and AI with laboratory-simulated hypobaric hypoxia weight management leverages synergies in HC, reducing chronic disease risks and global health burdens. This approach opens new frontiers in weight management and builds comprehensive health systems, improving global health outcomes.

## Acknowledgements

We thank Hainan University faculty for their instruction in public administration, which enhanced my expertise in public health management. We also acknowledge using Figdraw for Figures 1, 2, 3, and 5.

**Funding:** This research was funded by the National Key R&D Program 'Prevention and Treatment Research for Cancer, Cardiovascular, Respiratory, and Metabolic Diseases' under the Science and Technology Innovation 2030 initiative, Project 'Key Technology and Intervention Strategy Research for Plateau Holistic Health Security Based on Multi-center Population Cohorts', grant number 2023ZD0505300/2023ZD0505303 and Medical Scientific Research Foundation of Guangdong Province of China, grant number A2023159.

**Conflict of Interest:** The authors have no conflicts of interest to disclose.

## References

1. GBD 2021 Adolescent BMI Collaborators. Global,

- regional, and national prevalence of child and adolescent overweight and obesity, 1990–2021, with forecasts to 2050: a forecasting study for the Global Burden of Disease Study 2021. *Lancet*. 2025; 405:785-812.
2. Hobbins L, Hunter S, Gaoua N, Girard O. Normobaric hypoxic conditioning to maximize weight loss and ameliorate cardio-metabolic health in obese populations: A systematic review. *Am J Physiol Regul Integr Comp Physiol*. 2017; 313:R251-R264.
3. Rostam S, Najafi F, Hasannejadasl H, Soroush H. Artificial intelligence-enabled obesity prediction: a systematic review of cohort data analysis. *Int J Med Inform*. 2025; 196:105804.
4. Perdomo CM, Cohen RV, Sumithran P, Clément K, Frühbeck G. Contemporary medical, device, and surgical therapies for obesity in adults. *Lancet*. 2023; 401:1116-1130.
5. Ong KL, Lauryn K. Global, regional, and national burden of diabetes from 1990 to 2021, with projections of prevalence to 2050: a systematic analysis for the Global Burden of Disease Study 2021. *Lancet*. 2023; 402:203-234.
6. Mohebi R, Chen C, Nasrien E. Cardiovascular disease projections in the United States based on the 2020 census estimates. *J Am Coll Cardiol*. 2022; 80:565-578.
7. Soerjomataram I, Bray F. Planning for tomorrow: global cancer incidence and the role of prevention 2020-2070. *Nat Rev Clin Oncol*. 2021; 18:663-672.
8. GBD 2021 Adult BMI Collaborators. Global, regional, and national prevalence of adult overweight and obesity, 1990-2021, with forecasts to 2050: a forecasting study for the Global Burden of Disease Study 2021. *Lancet*. 2025; 405:813-838.
9. Adeyemi O, Rachel N, Garrison S, Jaynaide P, Johanna R, John W. Economic impacts of overweight and obesity: current and future estimates for 161 countries. *BMJ Glob Health*. 2022; 7:e009773.
10. World Obesity Federation. World Obesity Atlas 2023. <https://data.worldobesity.org/publications/?cat=19> (accessed March 31, 2025).
11. Benedictus B, Pratama VK, Purnomo CW, Tan K, Puspita RF. Efficacy of oral medication in weight loss management: A systematic review and network meta-analysis. *Clin Ther*. 2025; 47:316-329.
12. Healy P, Clarke C, Reynolds I, Arumugasamy M, Deborah M. Complications of bariatric surgery: What the general surgeon needs to know. *Surgeon*. 2016; 14:91-98.
13. Agarwal N, Kavita S. Optimizing micro and macro nutrients: Navigating weight loss success and health risks in bariatric surgery for obesity management. *Endocrinol Metab Clin North Am*. 2025; 54:135-147.
14. Kumari A, Kaur D, Ranjan P, Malhotra A, Pandey S, Kumar A, Kaloija G, Mohanty A, Ahuja N, Vikram NK. Efficacy of a lifestyle intervention for weight management in postpartum women: A randomised controlled trial at a tertiary care centre in India. *Midwifery*. 2025;143:104312.
15. Hendrie G, Baird D, James-Martin G, Brindal E, Brooker P. Weight loss patterns and outcomes over 12 months on a commercial weight management program (CSIRO Total Wellbeing Diet Online): large-community cohort evaluation study. *J Med Internet Res*. 2025; 27:e65122.
16. Wichansawakun S, Srikhajonjit W, Srichan C, Jutamat T. Efficacy of an online exercise program to improve weight management outcomes in individuals with obesity: A randomised trial. *Clin Nutr ESPEN*. 2025; 66:202-207.
17. Tan LJ, Sangah S. Impact of eating duration on weight management, sleeping quality, and psychological stress: A pilot study. *J Nutr Biochem*. 2025; 137:109835.
18. Peng W, Shi L, Huang Q, Li T, Jian W, Zhao L, Xu R, Liu T, Zhang B, Wang H, Tong L, Tang H, Wang Y. Metabolite profiles of distinct obesity phenotypes integrating impacts of altitude and their association with diet and metabolic disorders in Tibetans. *Sci Total Environ*. 2024; 949:174754.
19. Tschöp M, Morrison KM. Weight loss at high altitude. In: Hypoxia: from genes to the bedside (Roach RC, Wagner PD, Hackett PH, eds.). Springer US, Boston, MA, USA, 2001; pp. 237-247.
20. Westerterp-Plantenga MS, Westerterp KR, Rubbens M, Verwegen CR, Richelet JP, Gardette B. Appetite at "high altitude" [Operation Everest III (Comex-97)]: a simulated ascent of Mount Everest. *J Appl Physiol*. 1999; 87:391-399.
21. Ge RL, Wood H, Yang HH, Liu YN, Wang XJ, Babb T. The body weight loss during acute exposure to high-altitude hypoxia in sea level residents. *Acta Physiol Sin*. 2010; 62:541-546.
22. Dünwald T, Gatterer H, Faulhaber M, Arvandi M, Schobersberger W. Body composition and body weight changes at different altitude levels: a systematic review and meta-analysis. *Front Physiol*. 2019; 10:430.
23. Saarikko J, Axelin A, Huvinen E, Rahmani AM, Kolari T, Niela-Vilén H. Effectiveness of supporting lifestyle change in pregnant mothers with obesity through the wearable internet-of-things (SLIM)-intervention on self-efficacy in weight management in pregnant women: a quasi-experimental trial. *Midwifery*. 2025; 140:104235.
24. Camacho S, Ruppel A. Is the calorie concept a real solution to the obesity epidemic? *Glob Health Action*. 2017; 10:1289650.
25. Karaoglan M, Karaoglan M. The evolution of obesity and the origin of adipose tissue. *Obes Med*. 2024; 52:100561.
26. Jeffrey MF. On the causes of obesity and its treatment: The end of the beginning. *Cell Metab*. 2025; 37:570-577.
27. Lartey ST, Si L, Otahal P, de Graaff B, Boateng GO, Biritwum RB, Minicuci N, Kowal P, Magnussen CG, Palmer AJ. Annual transition probabilities of overweight and obesity in older adults: evidence from World Health Organization Study on global AGEing and adult health. *Soc Sci Med*. 2020; 247:112821.
28. Piccinini-Vallis H, Evdaev V, Asaminew J, McCurdy T, Rogers M, Vallis M. Obesity management in primary care: are we adequately preparing the next generation of Canadian family physicians? *Obes Pillars*. 2024; 12:100151.
29. Chieh C, Stojic S, Boehl G, Wong S, Lüscher J, Bertolo A, Itodo OA, Mueller G, Stoyanov J, Gemperli A, Perret C, Eriks-Hoogland I, Glisic M. Can lifestyle and behavioral interventions improve weight management in individuals with spinal cord injury? A systematic review and meta-analysis. *Arch Phys Med Rehabil*. 2025; 106:580-589.
30. Grannemann JJ, Roper A. Travelling to high altitude destinations after recovery from COVID-19-infection: new aspects of medical advice in altitude medicine. *Pneumologie*. 2021; 75:214-220.
31. Tsao TM, Hwang JS, Tsai MJ, Lin ST, Wu C, Su TC. Seasonal effects of high-altitude forest travel on cardiovascular function: an overlooked cardiovascular risk of forest activity. *Int J Environ Res Public Health*. 2021;



- 18:9472.
32. Kara T, Narkiewicz K, Somers VK. Chemoreflexes — physiology and clinical implications. *Acta Physiol Scand*. 2003; 177:377-384.
33. Bagdish AL, Wolfel EE, Levine BD. Cardiovascular system. In: High altitude: human adaptation to hypoxia (Swenson ER, Bärtsch P, eds.). Springer New York, New York, US, 2014; pp. 103-139.
34. Hamad N, Travis SP. Weight loss at high altitude: pathophysiology and practical implications. *Eur J Gastroenterol Hepatol*. 2006; 18:5-10.
35. Burtcher M, Gatterer H, Burtcher J, Mairbäurl H. Extreme terrestrial environments: life in thermal stress and hypoxia. A narrative review. *Front Physiol*. 2018; 9:572.
36. Kayser B, Verges S. Hypoxia, energy balance and obesity: from pathophysiological mechanisms to new treatment strategies. *Obes Rev*. 2013; 14:579-592.
37. Quintero P, Milagro FI, Campión J, Martínez JA. Impact of oxygen availability on body weight management. *Med Hypotheses*. 2010; 74:901-907.
38. Zhou S, Dong H, Huang P, Li Y, Zhong Z, Xiao H, Xie J, Wu Y, Li P. Changes in body composition during acute exposure to high altitude is related to acute mountain sickness. *Travel Med Infect Dis*. 2025; 64:102815.
39. Madakam S, Ramaswamy R, Tripathi S. Internet of Things (IoT): a literature review. *J Comput Commun*. 2015; 3:164-173.
40. Rhmann W, Khan J, Khan GA, Ashraf Z, Pandey B, Khan MA, Ali A, Ishrat A, Alghamdi AA, Ahamad B, Shaik MK. Comparative study of IoT- and AI-based computing disease detection approaches. *Data Sci Manag*. 2025; 8:94-106.
41. Shafique K, Bilal KA, Sabir F, Qazi S, Mustaqim M. Internet of Things (IoT) for next-generation smart systems: a review of current challenges, future trends and prospects for emerging 5G-IoT scenarios. *IEEE Access*. 2020; 8:23022-23040.
42. Ferdowsy F, Rahi KSA, Jabiullah MI, Tarek HM. A machine learning approach for obesity risk prediction. *Curr Res Behav Sci*. 2021; 2:100053.
43. Safaei M, Sundararajan EA, Driss M, Boulila W, Shapi'i A. A systematic literature review on obesity: understanding the causes & consequences of obesity and reviewing various machine learning approaches used to predict obesity. *Comput Biol Med*. 2021; 136:104754.
44. Kar S, Mishra P, Wang KC. 5G-IoT architecture for next generation smart systems. *IEEE 5G World Forum*. 2021; 2021:241-246.
45. Chen M, Yang J, Hao Y, Mao S, Hwang K. A 5G cognitive system for healthcare. *Big Data Cogn Comput*. 2017; 1:2.
46. Liberati A, Altman DG, Tetzlaff J, Mulrow C, Gøtzsche PC, Ioannidis JP, Clarke M, Devereaux PJ, Kleijnen J, Moher D. The PRISMA statement for reporting systematic reviews and meta-analyses of studies that evaluate health care interventions: explanation and elaboration. *J Clin Epidemiol*. 2009; 62:e1-34.
47. Ritchie BW, Jiang Y. Risk, crisis and disaster management in hospitality and tourism: a comparative review. *Int J Contemp Hosp Manag*. 2021; 33:3465-3493.
48. DeGregory KW, Kuiper P, DeSilvio T, Pleuss JD, Miller R, Roginski JW, Fisher CB, Harness D, Viswanath S, Heymsfield SB, Dungan I, Thomas DM. A review of machine learning in obesity. *Obes Rev*. 2018; 19:668-685.
49. Chatterjee A, Gerdes MW, Martinez SG. Identification of risk factors associated with obesity and overweight: a machine learning overview. *Sensors (Basel)*. 2020; 20:2734.
50. Sala M, Taylor A, Crochiere RJ, Zhang F, Forman EM. Application of machine learning to discover interactions predictive of dietary lapses. *Appl Psychol Health Well Being*. 2023; 15:1166-1181.
51. Greco F, Mallio CA. Artificial intelligence and abdominal adipose tissue analysis: a literature review. *Quant Imaging Med Surg*. 2021; 11:4461-4474.
52. Ayyaswami V, Subramanian J, Nickerson J, Erban S, Rosano N, McManus DD, Gerber BS, Faro JM. A clinician and electronic health record wearable device intervention to increase physical activity in patients with obesity: formative qualitative study. *JMIR Form Res*. 2024; 8:e56962.
53. Netzer NC, Chytra R, Küpper T. Low intense physical exercise in normobaric hypoxia leads to more weight loss in obese people than low intense physical exercise in normobaric sham hypoxia. *Sleep Breath*. 2008; 12:129-134.
54. Hackett PH, Rennie D, Grover RF, Reeves JT. Acute mountain sickness and the edemas of high altitude: a common pathogenesis? *Respir Physiol*. 1981; 46:383-390.
55. Ge RL, Chase PJ, Witkowski S, Wyrick BL, Stone JA, Levine BD, Babb TG. Obesity: associations with acute mountain sickness. *Ann Intern Med*. 2003; 139:253-257.
56. Caravedo MA, Mozo K, Morales ML, Smiley H, Stuart J, Tilley DH, Cabada MM. Risk factors for acute mountain sickness in travellers to Cusco, Peru: coca leaves, obesity and sex. *J Travel Med*. 2022; 29:taab102.
57. Gatterer H, Wille M, Faulhaber M, Lukaski H, Melmer A, Ebenbichler C, Burtcher M. Association between body water status and acute mountain sickness. *PLoS One*. 2013; 8:e73185.
58. Aqueveque P, Gutiérrez C, Rodríguez FS, Pino EJ, Morales AS, Wiechmann EP. Monitoring physiological variables of mining workers at high altitude. *IEEE Trans Ind Appl*. 2017; 53:2628-2634.
59. Wei CY, Chen PN, Lin SS, Huang TW, Sun LC, Tseng CW, Lin KF. Using machine learning to determine the correlation between physiological and environmental parameters and the induction of acute mountain sickness. *BMC Bioinformatics*. 2022; 22:628.
60. Woo Y, Choi J, Kim D. Effectiveness analysis of AI-IoT based public health care service for elderly in Korea. *Arch Phys Med Rehabil*. 2024; 105:e14.
61. Liang Y, Xiao R, Huang F, Lin Q, Guo J, Zeng W, Dong J. AI nutritionist: intelligent software as the next generation pioneer of precision nutrition. *Comput Biol Med*. 2024; 178:108711.
62. Rafael, Saha T, Moonla C, Ernesto, Joseph W. Ketone bodies detection: wearable and mobile sensors for personalized medicine and nutrition. *Trends Analyt Chem*. 2023; 159:116938.
63. Yadav R, Pradeepa P, Srinivasan S, Rajora CS, Rajalakshmi R. A novel healthcare framework for ambient assisted living using the internet of medical things (IOMT) and deep neural network. *Meas Sens*. 2024; 33:101111.
64. Alsareii SA, Raza M, Alamri AM, AlAsmari MY, Irfan M, Raza H, Awais M. Artificial intelligence and Internet of Things enabled intelligent framework for active and healthy living. *Comput Mater Contin*. 2023; 75:3833-3848.
65. Anikwe CV, Nweke HF, Ikegwu AC, Ekwuonwu CA, Onu FU, Alo UR, Teh YW. Mobile and wearable sensors



- for data-driven health monitoring system: state-of-the-art and future prospect. *Expert Syst Appl.* 2022; 202:117362.
66. Farrokhi A, Farahbakhsh R, Rezazadeh J, Minerva R. Application of Internet of Things and artificial intelligence for smart fitness: a survey. *Comput Netw.* 2021; 189:107859.
67. Li D. 5G and intelligence medicine: How the next generation of wireless technology will reconstruct healthcare? *Precis Clin Med.* 2019; 2:205-208.
68. Hossain MS, Muhammad G. Emotion-aware connected healthcare big data towards 5G. *IEEE Internet Things J.* 2018; 5:2399-2406.
69. Machorro-Cano I, Alor-Hernández G, Paredes-Valverde MA, Ramos-Deonati U, Sánchez-Cervantes JL, Rodríguez-Mazahua L. PISIoT: A machine learning and IoT-based smart health platform for overweight and obesity control. *Appl Sci.* 2019; 9:3037.
70. Mohanta B, Das P, Patnaik S. Healthcare 5.0: A paradigm shift in digital healthcare system using artificial intelligence, IoT 5G Comm. 2019; 2019:191-196.
71. Singh P. Gamified wearables in childhood obesity therapy driven by 5G wireless communication system with special emphasis on Pacific Island countries. In: *5G Wireless Communication Systems in Healthcare Informatics*. CRC Press; 2023:113-132.
72. Venkatachalam K, Prabu P, Alluhaidan AS, Hubálovský S, Trojovský P. Deep belief neural network for 5G diabetes monitoring in big data on edge IoT. *Mob Netw Appl.* 2022; 27:106.
73. Dong Y. Analysis of intelligent physical education teaching scheme based on 5G communication and VR technology. *Mob Inf Syst.* 2022; 2022:8598077.
74. Ahad A, Tahir M, Yau K-LA. 5G-based smart healthcare network: Architecture, taxonomy, challenges and future research directions. *IEEE Access.* 2019; 7:100747-100762.
75. Ahad A, Tahir M, Sheikh MA, Ahmed KI, Mughees A. An intelligent clustering-based routing protocol (CRP-GR) for 5G-based smart healthcare using game theory and reinforcement learning. *Appl Sci.* 2021; 11:9993.
76. Pradhan B, Das S, Roy DS, Routray S, Benedetto F, Jhaveri RH. An AI-assisted smart healthcare system using 5G communication. *IEEE Access.* 2023; 11:108339-108355.
77. Gupta N, Juneja PK, Sharma S, Garg U. Future aspect of 5G-IoT architecture in smart healthcare system. *Int Conf Intell Comput Control Syst.* 2021; 2021:406-411.
78. Devi DH, Duraisamy K, Armghan A, Alsharari M, Aliqab K, Sorathiya V, Das S, Rashid N. 5G technology in healthcare and wearable devices: A review. *Sensors.* 2023; 23:2519.
79. Rocha NP, Dias A, Santinha G, Rodrigues M, Queirós A, Rodrigues C. Smart cities and public health: A systematic review. *Procedia Comput Sci.* 2019; 164:516-523.
80. Rocha NP, Bastardo R, Pavao J, Santinha G, Rodrigues M, Rodrigues C, Queiros A, Dias A. Smart cities' applications to facilitate the mobility of older adults: A systematic review of the literature. *Appl Sci.* 2021; 11:6395.
81. Pacheco Rocha N, Dias A, Santinha G, Rodrigues M, Queirós A, Rodrigues C. Smart cities and healthcare: A systematic review. *Technologies.* 2019; 7:58.
82. Peralta-Ochoa AM, Chaca-Asmal PA, Guerrero-Vásquez LF, Ordoñez-Ordoñez JO, Coronel-González EJ. Smart healthcare applications over 5G networks: A systematic review. *Appl Sci.* 2023; 13:1469.
83. Ghavimi F, Chen HH. M2M communications in 3GPP LTE/LTE-A networks: Architectures, service requirements, challenges, and applications. *IEEE Commun Surv Tutorials.* 2014; 17:525-549.
84. Sodhro AH, Awad AI, Beek JV, Nikolakopoulos G. Intelligent authentication of 5G healthcare devices: A survey. *Internet of Things.* 2022; 20:100610.
85. Ahmed S, Subah Z, Ali MZA. Cryptographic data security for IoT healthcare in 5G and beyond networks. *IEEE Sensor.* 2022; 2022:1-4.
86. Gutwenger I, Hofer G, Gutwenger AK, Sandri M, Wiedermann CJ. Pilot study on the effects of a 2-week hiking vacation at moderate versus low altitude on plasma parameters of carbohydrate and lipid metabolism in patients with metabolic syndrome. *BMC Res Notes.* 2015; 8:103.
87. Lippl FJ, Neubauer S, Schipfer S, Lichter N, Tufman A, Otto B, Fischer R. Hypobaric hypoxia causes body weight reduction in obese subjects. *Obesity.* 2010; 18:675-681.
88. Marlatt KL, Greenway FL, Schwab JK, Ravussin E. Two weeks of moderate hypoxia improves glucose tolerance in individuals with type 2 diabetes. *Int J Obes.* 2020; 44:744-747.
89. Mackenzie R, Maxwell N, Castle P, Brickley G, Watt P. Acute hypoxia and exercise improve insulin sensitivity ( $S_{I}^{2*}$ ) in individuals with type 2 diabetes. *Diabetes Metab Res Rev.* 2011; 27:94-101.
90. Kayser B, Verges S. Hypoxia, energy balance, and obesity: An update. *Obes Rev.* 2021; 22:e13192.
91. Telfer B, Reed H, Lacirignola J, Patel T, Siegel A, Swiston A, Singh N, Trebicka R, Weston C, Williamson J. Wearable Oxim for Harsh Env. 2017; 2017: 107-110.
92. Xinhuanet. Press conference on the theme of people's livelihood at the Third Session of the 14th National People's Congress. <https://www.cche.org.cn/portal/gzdt/xwtt/2025/3/97ab62ad2b18441fae9317fc6a58e9e8.htm> (accessed March 11, 2025).

Received April 7, 2025; Revised April 23, 2025; Accepted April 26, 2025.

*\*Address correspondence to:*

Wenli Zhang, School of Information Science and Technology, Beijing University of Technology, No. 100 Pingleyuan, Chaoyang District, Beijing, 100124, China.  
E-mail: zhangwenli@bjut.edu.cn

Boyuan Wang, Beijing Xiaotangshan Hospital, No. 390, Yinjie North Road, Xiaotangshan Town, Changping District, Beijing, 102211, China.  
E-mail: boyuanwang@fudan-zhuhai.org.cn

Released online in J-STAGE as advance publication April 29, 2025.

# Current status and perspectives of molecular mechanisms of gender difference in hepatocellular carcinoma: The tip of the iceberg?

Zhi-Quan Xu<sup>§</sup>, Shi-Qiao Luo<sup>§</sup>, Zhong-Jun Wu<sup>\*</sup>, Rui Liao<sup>\*</sup>

Department of Hepatobiliary Surgery, the First Affiliated Hospital of Chongqing Medical University, Chongqing, China.

**SUMMARY:** Hepatocellular carcinoma (HCC) risk factors and incidence vary globally, but men generally have higher incidence than women. Men also tend to have a worse prognosis in terms of survival period and pathological characteristics. Furthermore, there are notable gender differences in treatment strategies and drug responses. While traditional risk factors such as hepatitis B virus, hepatitis C virus, alcohol consumption, and metabolic syndrome contribute to these differences, the underlying molecular mechanisms remain partly understood. Recent research has focused on elucidating the roles of sex hormones, DNA damage and repair pathways, immune microenvironments, and genetic/epigenetic factors in driving gender-specific disparities. For instance, estrogen receptor signaling has been shown to suppress HCC progression, whereas androgen receptor signaling promotes tumor development. Additionally, immune cells such as tumor-associated macrophages and regulatory T cells exhibit gender-specific patterns, with males typically showing higher levels of immunosuppressive cells. Omics analyses, including genomics, transcriptomics, and proteomics, have further revealed sex-specific differences in gene expression, protein interactions, and metabolic pathways. Despite these advances, significant gaps remain in understanding the interplay between environmental, hormonal, and genetic factors in shaping gender disparities in HCC. Future research should prioritize the identification of novel molecular targets, the development of gender-specific therapeutic strategies, and the integration of multi-omics data to address these disparities. Addressing these challenges will be critical for improving diagnostic, prognostic, and therapeutic outcomes in HCC patients of both sexes.

**Keywords:** epidemiological characteristics, sex hormones, immune microenvironment, multi-omics analysis

## 1. Introduction

Gender differences significantly influence the incidence and mortality rates of tumors worldwide, spanning a wide range of ages and various cancer types. Research reveals that the incidence rates of hematological malignancies, as well as cancers of the bladder, colon, skin, liver, and brain, are notably higher in men than in women (1). Furthermore, these gender differences contribute to variations in prognoses, which are shaped not only by biological, environmental, and hormonal factors but also by differences in the immune system (2).

Hepatocellular carcinoma (HCC) ranks as the sixth most common tumor globally and is the third leading cause of cancer-related mortality, accounting for 865,269 new cases and 757,948 deaths annually (3). The primary risk factors for HCC include hepatitis B virus, hepatitis C virus, exposure to aflatoxins, alcohol consumption, smoking, obesity, and diabetes (4). The incidence of HCC is at least two to three times higher in men than in

women, with a worse prognosis observed in men (3). This gender disparity is attributed not only to differences in sex hormones but also to an unequal distribution of risk factors, such as alcohol use and smoking, which are more prevalent among men.

The pathogenesis of HCC involves intricate molecular and immune processes. Recent research has underscored the pivotal roles of various immune cells and signaling pathways within the tumor microenvironment of HCC. Tumor-associated macrophages (TAMs) display notable heterogeneity and plasticity, with M2-type TAMs driving tumor progression and immune suppression through the release of anti-inflammatory cytokines, such as IL-10 and TGF- $\beta$ . Similarly, regulatory T cells contribute to immune homeostasis by inhibiting T-cell activation, thereby dampening anti-tumor immune responses. Additionally, myeloid-derived suppressor cells amplify immune suppression by restraining the functional activities of T cells and natural killer cells (5,6).

The goal of this review is to explore the factors

influencing sex-based differences in the incidence and prognosis of HCC, delve into the current understanding and future perspectives of the molecular mechanisms underlying these differences, and discuss the clinical implications that contribute to this heterogeneity.

## 2. Epidemiological Sex Differences in HCC Incidence and Prognosis

### 2.1. Sex Differences in HCC Incidence

According to statistics from the International Agency for Research on Cancer, in recent years, the global incidence and mortality rates of HCC have consistently been significantly higher in males than in females. While the magnitude of this sex difference varies across regions and ethnic groups, the overall trend remains consistent (3).

In East and Southeast Asia, such as China and Japan, the incidence of HCC is 2 to 3 times higher in males than in females, which is primarily attributed to hepatitis B virus (HBV) infection (7,8). In West and North Africa, the male-to-female ratio of HCC incidence is 1 to 2 times higher, with hepatitis C virus (HCV) and HBV infections being the main etiologies (9,10). In North America and Europe, the primary etiologies are alcohol use and metabolic syndrome. In the United States, the incidence of HCC in males is 3.18 times higher than in females (11). In Europe, the male-to-female ratio of HCC incidence ranges from 2:1 to 5:1. Notably, in countries such as France and Malta, the male-to-female ratios are as high as 5.0 and 4.8, respectively (3). However, in Mexico, the sex difference in HCC incidence is smaller, with a male-to-female ratio of approximately 1.4, primarily attributed to alcoholic liver disease and HCV infection (12). The male-to-female ratios of HCC incidence across different regions and countries are summarized in Table 1.

### 2.2. Sex Differences in HCC Prognosis

Significant sex differences exist in the prognosis of HCC. Females are typically older at the time of HCC diagnosis. For instance, in a multi-ethnic Asian cohort study involving 1,716 patients, the median age at diagnosis

was 69 years for females, compared to 62 years for males (13). Another retrospective study of 1,110 patients also found that the mean age at diagnosis was 62.5 years for females, compared to 59.2 years for males (14).

Males have shorter overall and disease-free survival than females. In the aforementioned retrospective study of 1,110 patients, the median overall survival was 17.1 months for females versus 12.0 months for males<sup>19</sup>. Additionally, in a single-center study of patients with unresectable HCC, the median survival was 14 months for females and 9 months for males (15). Males also have higher HCC recurrence rates and shorter disease-free survival. One study showed that the median disease-free survival was 19.5 months for females versus 4.5 months for males (16).

Males with HCC exhibit higher malignancy than females. In the cohort of 1,716 patients, males presented with more advanced tumor stages at diagnosis, with 39.7% of females versus 28.4% of males in BCLC stage 0/A. Males had a higher incidence of distant metastasis (11% vs. 7.7% in females) and portal vein tumor thrombosis (33.4% vs. 19.4% in females). Additionally, males had a higher incidence of multifocal lesions (39.5% vs. 30% in females) (13).

Overall, males typically have a worse prognosis than females in HCC, with differences observed in age at onset, overall survival, recurrence rate, disease-free survival, and tumor characteristics (Table 2).

## 3. Sex differences in therapeutic strategy and drug response of HCC

### 3.1. Sex differences in therapeutic strategy

Sex differences exist in healthcare utilization and treatment adherence for HCC. Females are more proactive in utilizing healthcare resources, such as engaging in preventive services like liver cancer screening, which may be attributed to their generally higher health awareness and willingness to undergo medical check-ups. In contrast, males tend to seek medical care only when the disease progresses to more advanced stages (17). Additionally, females tend to show better adherence to medical advice during treatment, such as taking medications as prescribed and attending

**Table 1. Etiologies and male-to-female incidence ratios of HCC across different regions and countries**

| Region                | Country | Main etiology                             | Male-to-Female Incidence Ratio |
|-----------------------|---------|---|--------------------------------|
| Asia                  | China   | HBV                                       | 2.71                           |
|                       | Japan   | HBV                                       | 2.14                           |
| West and North Africa | Gambia  | HBV                                       | 1.56                           |
|                       | Egypt   | HCV                                       | 1.50                           |
| North America         | USA     | Alcohol and metabolic syndrome            | 3.18                           |
| Europe                | France  | Alcohol and metabolic syndrome            | 5.0                            |
|                       | Malta   | Alcohol and metabolic syndrome            | 4.8                            |
| South America         | Mexico  | Alcoholic liver disease and HCV infection | 1.4                            |

**Table 2. Gender Differences in the Prognosis of HCC**

| Prognosis Factor             |                                  | Male  | Female |
|------------------------------|----------------------------------|-------|--------|
| Survival time                | Median age at onset (years)      | 62    | 69     |
|                              | Median overall survival (months) | 12.0  | 17.1   |
|                              | Disease-free survival (months)   | 4.5   | 19.5   |
| Pathological characteristics | BCLC stage 0/A rate              | 28.4% | 39.7%  |
|                              | Distant metastasis rate          | 11%   | 7.7%   |
|                              | Vascular invasion rate           | 33.4% | 19.4%  |
|                              | multiple lesion rate             | 39.5% | 30%    |

regular follow-ups, which helps improve treatment outcomes and prognosis. In contrast, males may have poorer adherence due to reasons such as busy work schedules or insufficient emphasis on treatment (14).

Sex differences also exist in the selection of HCC treatment approaches. Multiple studies have indicated that females are more inclined to undergo surgical resection and ablation for HCC treatment (18). This may be related to females being diagnosed at earlier stages, making them more suitable for surgical treatment. Early access to effective treatment may be one reason why females have a better prognosis than males with HCC.

### 3.2. Sex differences in drug response

Females exhibit higher blood drug concentrations and longer drug elimination times in chemotherapeutic pharmacokinetics, which may be related to lower drug clearance capacity and higher drug exposure levels (19). A clinical trial with over 23,000 patients found that females had a 34% higher risk of severe toxicity when receiving immunotherapy, targeted therapy, or chemotherapy (2). Conversely, due to lower drug clearance rates in females, chemotherapeutic agents may remain in the body for a longer period, potentially leading to better therapeutic outcomes (19).

Estrogen-related drugs have been confirmed to have a protective effect on HCC. A study of over 3,000 HCC patients in China found that females and oral contraceptive use were associated with improved survival (20). Another case-control study of 234 female HCC patients found that hormone therapy was associated with improved survival (21). However, the use of estrogen-related drugs for HCC treatment has not yet been applied in clinical practice, and is a promising direction for future research.

## 4. Epidemiological risk factors in gender disparity of HCC

Gender disparities in HCC are influenced by several epidemiological risk factors, including sex hormones, alcohol consumption, smoking, metabolic states, diet, and HBV infection. These risk factors vary between genders, contributing to the observed differences in the incidence and progression of HCC (Figure 1).

### 4.1. Sex hormones

Recent studies indicate that sex hormones may play a pivotal role in the onset and progression of HCC (20,21). Furthermore, HBV-associated HCC appears to be more prevalent in men and postmenopausal women compared to premenopausal women, likely due to its close relationship with sex hormones. Broadly speaking, the androgen axis tends to promote tumor development in HCC, whereas the estrogen axis generally exerts a tumor-suppressing effect (22).

The estrogen pathway constitutes a signaling network involving estrogen and its related receptors, believed to have a protective role in the pathogenesis of HCC. These anti-tumor effects are thought to be mediated through various transduction pathways. Estrogen receptor  $\alpha$  appears to inhibit HCC cell invasion by transcriptionally regulating the expression of circRNA SMG1.72, achieved by directly binding to the 5' promoter region of its host gene, SMG1 (23). Protein tyrosine phosphatase receptor type O has been identified as an inhibitor of JAK- and PI3K-dependent dephosphorylation signaling, as well as STAT3 transcriptional activity, thereby suppressing tumorigenesis and progression. ER $\alpha$  functions as a transcription factor for Protein tyrosine phosphatase receptor type O, promoting its expression and enhancing its anti-tumor activity (24). Additionally, within the tumor microenvironment, estrogens may act as immunoregulatory agents. Estrogen-related genes have been shown to influence immune cell infiltration and modulate the response to immunotherapy in cases of HCC.

Phosphorylation of the androgen receptor by the mechanistic target of rapamycin complex 1 promotes hepatic steatosis as well as the development and progression of HCC, both independently and synergistically with androgen (25). Recent findings reveal that androgen receptor (AR) variant 7 amplifies c-MYC-driven hepatocarcinogenesis by enhancing its oncogenic functions while suppressing its anti-oncogenic roles (26). Transcriptionally active splice variants of the AR have been shown to accelerate the progression of HCC. Furthermore, the activation of Toll-like receptor 4 (TLR4) is essential for the progression of HCC. By interacting with TLR4, the AR facilitates the development, migration, and invasion of HCC cells (27).



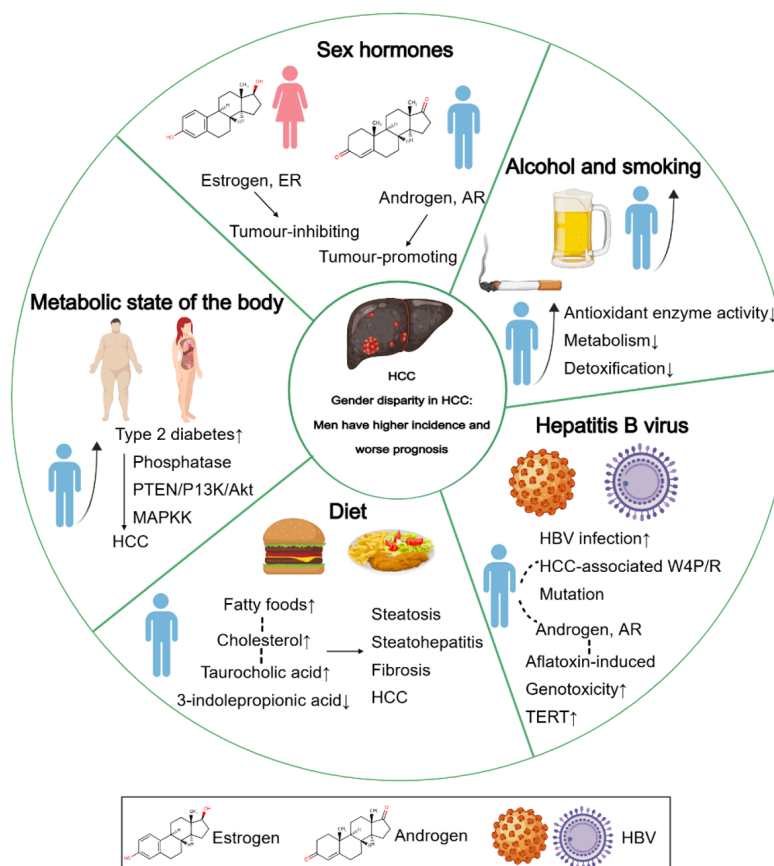


**Figure 1. Epidemiological risk factors in gender disparity of HCC.** Epidemiological risk factors in gender disparity of HCC include sex hormones, alcohol and smoking, metabolic state of the body, diet, and HBV. Estrogen and estrogen receptors (ER) have a tumor-inhibiting effect, while androgen and androgen receptors (AR) have a tumor-promoting effect. Men consume alcohol and smoke at higher rates than women. Among smokers, antioxidant enzyme activity in the liver of men is lower than that of women. Men's liver has weak ability to metabolize and detoxify smoking-related toxins. The incidence of type 2 diabetes in men is higher than that in women. Insulin resistance and hyperinsulinemia caused by type 2 diabetes affect the development of HCC through several molecular pathways, including phosphatase and tensin homolog (PTEN)/P13K/Akt and MAPK kinase (MAPKK). Men prefer fatty foods, which contain abundant cholesterol. Dietary cholesterol induces changes in gut bacterial metabolites, including increased taurocholic acid and decreased 3-indolepropionic acid, which can lead to the sequential progression of steatosis, steatohepatitis, fibrosis and ultimately HCC. Men are more likely to become infected with HBV. A novel HCC-associated W4P/R mutation in HBV genotype C large surface protein, found exclusively in male HCC patients. Androgen may enhance aflatoxin-induced genotoxicity and inflammation to HCC in male hepatitis B patients. HBV-integrated AR-induced telomerase reverse transcriptase gene (TERT) upregulation and point mutation in TERT promoter region identified as mechanism for male dominance of HBV-related HCC.

#### 4.2. Alcohol and smoking

Alcohol abuse has been established as a significant contributor to HCC. Among patients with alcohol-associated cirrhosis, the annual incidence of HCC ranges from 1.3% to 3%. In 2019, alcohol was responsible for approximately 20% of global HCC-related deaths (28). Alcohol can cause HCC through various mechanisms, including the mutagenic effects of acetaldehyde toxicity, which leads to the formation of proteins and DNA adducts. Additionally, excessive iron deposition in the liver can lead to alterations in reactive oxygen species, lipid peroxidation, and metabolism. Inflammatory and damaged immune responses, modifications to DNA methylation, and various signaling pathways, including the gut-liver axis, can also contribute to the progression of HCC (29). Women are generally more susceptible to the toxic effects of alcohol than men,

which may be attributed to the lower activity of alcohol dehydrogenase and aldehyde dehydrogenase in women. Women may develop severe alcoholic liver disease with comparatively lower alcohol consumption, and women are at an elevated risk of developing HCC due to alcoholic liver disease (30). Due to cultural, lifestyle, and economic differences, alcohol consumption patterns between genders differ across various countries and regions. Overall, men consume alcohol at significantly higher rates than women (31). Additionally, due to the anti-cancer effect of estrogen on HCC and the promoting effect of androgens on HCC, men are more likely to develop HCC.

Smoking is an independent risk factor for liver fibrosis and also contributes to the development of HCC. Smoking is more prevalent in men than in women in most countries (32). Female and male smokers exhibit distinct smoking-induced immune cell profiles in the

tumor microenvironment (33). Male livers have a reduced capacity to metabolize and detoxify smoking-related toxins, leading to a higher risk of HCC among male smokers. Smoking increases the risk of HCC through multiple molecular mechanisms, including DNA damage, oxidative stress, and inflammatory responses. Antioxidant enzyme activity in the liver of men is lower than in women, and DNA damage and oxidative stress caused by smoking are more significant in men (34). Moreover, the activities of T cells and NK cells are significantly lower in male smokers than in female smokers, resulting in decreased immune surveillance against HCC in men (33).

#### 4.3. Metabolic state of the body

Metabolic syndrome is a clinical syndrome characterized by obesity, dyslipidemia, hyperglycemia, and hypertension, and is associated with an increased risk of HCC (35). Metabolic comorbidities have been strongly correlated with higher all-cause mortality rates in HCC patients. Notably, the risk of all-cause mortality rises significantly in HCC patients who present with two or more metabolic risk factors, such as diabetes, hypertension, or high cholesterol (36).

Metabolic complications, such as obesity and diabetes, are cancer-promoting factors. Although women have higher rates of obesity, obese men face a higher risk of HCC. Furthermore, men are more prone than women to develop insulin resistance and hyperglycemia in response to nutritional challenges (37). Research indicates that many aspects of energy balance and glucose metabolism are regulated differently between sexes, influencing susceptibility to type 2 diabetes. Globally, the incidence of type 2 diabetes is higher in men than in women, particularly among young people (38). Recent studies have shown that type 2 diabetes increases the risk of HCC by 2.5- to 4-fold (39). Moreover, patients with long-standing and poorly controlled disease seem to face a higher risk. Insulin resistance and hyperinsulinemia caused by type 2 diabetes affect the development of HCC through several molecular pathways, including the PTEN/PI3K/Akt and MAPK pathways (40). Insulin resistance and the insulin-like growth factor-1 signaling pathways are major contributors to the development of HCC. Insulin resistance induces inflammation, oxidative stress, DNA damage, and activates cellular pathways that promote cell growth and proliferation, thereby contributing to HCC development (39).

#### 4.4. Diet

The liver plays a crucial role in the metabolism of carbohydrates, fats, and proteins. Consequently, diet has significant biological impacts on key pathways that are hypothesized to be involved in the risk of HCC. Research conducted by Peng Zhou *et al.* demonstrates that elevated

levels of uridine diphospho-N-acetylglucosamine and O-GlcNAcylation, resulting from high dietary fructose intake, contribute to the progression of HCC (41). Małgorzata Grzymisławska *et al.* found that dietary behavior, dietary styles, and dietary profiles are associated with gender. Men prefer high-fat foods with strong flavors, primarily driven by the pleasure of eating (42). However, fatty foods contain abundant cholesterol. Dietary cholesterol induces changes in gut bacterial metabolites, including increased taurocholic acid and decreased 3-indolepropionic acid, which can drive the sequential progression from steatosis to steatohepatitis, fibrosis, and ultimately HCC (43). Yanan Ma *et al.* found a positive association between the intake of meat-derived mutagenicity or heterocyclic amines and the risk of HCC. The intake of processed red meat may be associated with a higher risk, while the intake of poultry or fish may be associated with a lower risk of HCC (44). There is currently limited evidence to confirm the role of diet in gender differences in HCC, and further research in this area is warranted.

#### 4.5. Hepatitis B virus

Hepatitis B Virus (HBV) is a DNA-based virus, belonging to the Hepadnaviridae family, which can cause liver disease and increase the risk of developing HCC in infected individuals. Many epidemiological studies have reported that men are more likely to become infected with HBV and to develop HCC (45). The gender disparity in HBV-related liver disease has long been recognized and may be attributed to the effects of sex hormones and immune responses (4).

Seoung-Ae Lee recently reported a novel HCC-associated W4P/R mutation in the HBV genotype C large surface protein, found exclusively in male HCC patients, which may contribute to sex differences (46). HBV integration with androgen receptor-induced TERT upregulation and point mutations in the TERT promoter region have been identified as mechanisms underlying male prevalence in HBV-related HCC (47). Androgen may enhance aflatoxin-induced genotoxicity and inflammation, contributing to HCC development in male hepatitis B patients (47). The androgen pathway can increase HBV transcription by directly binding to the androgen-responsive element in viral enhancer I (27).

The molecular mechanisms of HCC associated with epidemiological risk factors contributing to gender disparity are summarized in Table 3.

### 5. Gender-biased molecular mechanisms of HCC

Significant differences exist between men and women in DNA damage and repair, X chromosome mutations, and immune system function, which may contribute to disparate incidences and prognosis of HCC. Analysis of these molecular mechanisms may elucidate the

underlying causes of gender disparities in HCC and offer novel insights for future clinical research and therapeutic strategies.

### 5.1. DNA damage and repair

DNA alterations are fundamental to carcinogenesis, and DNA damage repair (DDR) mechanisms may contribute to gender disparities in cancer incidence. The activation of DNA repair mechanisms following DNA damage is essential for suppressing carcinogenesis. Carcinogenic agents and metabolic processes can induce genetic changes that lead to genomic instability and malignant transformation (48). A recent study demonstrated that high DDR activity in HCC is significantly associated with high microsatellite instability (MSI) and high intratumor heterogeneity. Additionally, increased DDR activity correlates with enhanced cell proliferation and poorer survival outcomes in HCC patients (49).

DDR alterations in HCC patients have been categorized into two distinct subtypes with heterogeneous clinical and molecular profiles: activated and suppressed DDR. Moreover, DDR status has emerged as a potential biomarker for predicting clinical outcomes in HCC. Typically, men exhibit higher levels of DNA damage, whereas women demonstrate reduced DNA repair capacity (50). Following exposure to ionizing radiation, solid tumors occurred more frequently in male survivors of the Hiroshima and Nagasaki atomic bombings (93.7

and 86.9 per 104 person-years, respectively) compared with female survivors (63.7 and 48.8 per 104 person-years, respectively) (51). TP53, a key DDR gene, may influence HCC patient survival by modulating anti-tumor immunity (52). When exposed to UV-B, male and female vascular smooth muscle cells exhibit sex-specific differences in p53 localization and cell fate, with male cells more prone to apoptosis and female cells more likely to undergo senescence (53).

### 5.2. X chromosome mutation

In mammals, the X chromosome harbors genes that are present in one copy in males (XY) and two copies in females (XX). This dosage difference necessitates complex regulatory mechanisms to ensure proper gene expression, which can influence the severity of diseases caused by X-linked mutations. Tarek Mohamed Kamal Motawi *et al.* identified a promoter SNP (rs2267531) within the glypican-3 gene (GPC3) on the X chromosome, which is associated with HCC in Egyptians (54). Sital Singh and colleagues further demonstrated that GPC3 is an X-linked recessive trait, contributing to higher HCC incidence in men compared to women (55). Another study revealed that the Wilms tumor gene on the X chromosome is downregulated in HCC tissues, and WTX loss activates the TGF- $\beta$  pathway, promoting HCC cell proliferation, migration, invasion, and autophagy (56). S. H. Yeh showed that X chromosomal

**Table 3. The molecular mechanisms of HCC in relation to epidemiological risk factors and gender disparity**

| Epidemiological risk factors | The molecular mechanisms  |
|------------------------------|---|
| Diet                         | High-fructose diet intake causes increased levels of UDP-GlcNAc and O-GlcNAcylation, and high-cholesterol diet causes increased cholic acid and decreased 3-indolepropionic acid, leading to fatty liver, steatohepatitis, liver fibrosis, and ultimately HCC.  |
| Alcohol and smoking          | The mutagenic effect of acetaldehyde toxicity leads to the formation of proteins and DNA adducts. Excessive iron deposition in the liver can cause changes in reactive oxygen species, lipid peroxidation, and metabolism, leading to HCC.<br><br>Smoking causes liver fibrosis, causing DNA damage and oxidative stress. Male smokers have significantly lower T cell and NK cell activities than women, causing HCC.  |
| Metabolic state of the body  | Insulin resistance and hyperinsulinemia caused by type 2 diabetes affect the development of HCC through several molecular pathways, including PTEN/P13K/Akt and MAPKK. IR and IGF-1 signaling pathways are the main factors contributing to the development of HCC.   |
| Sex hormones                 | ER $\alpha$ may inhibit the invasion of HCC cells by transcriptionally regulating the expression of circRNA SMG1.72 by binding directly to the 5' promoter region of its host gene SMG145. PTPRO inhibits JAK and PI3K dephosphorylation-dependent signaling and STAT3 transcriptional activity, thereby suppressing tumorigenesis and development.<br><br>AR by mTORC1 drives hepatic steatosis and HCC development and progression with androgen. AR-V7 enhances c-MYC-driven hepatocellular carcinogenesis by potentiating its oncogenic and diminishing its anti-oncogenic functions. The interaction between TLR4 and AR promotes the development, migration, and invasion of HCC cells. |
| Hepatitis B virus            | A novel HCC-associated W4P/R mutation in HBV genotype C large surface protein, found exclusively in male HCC patients and can cause a sex difference. HBV-integrated AR-induced TERT upregulation and point mutation in TERT promoter region identified as mechanism for male dominance of HBV-related HCC.   |

allele imbalance contributes to the progression from liver cirrhosis to HCC (57). F. Liu *et al.* discovered that the long non-coding RNA FTX (lnc-FTX), an X-inactivation-specific transcript (XIST) regulator, is involved in HCC and may explain gender disparities in disease incidence. lnc-FTX acts as a tumor suppressor by binding to miR-374a and minichromosome maintenance protein 2 (MCM2), potentially contributing to the observed gender differences in HCC (58).

### 5.3. Immune system

The liver is an organ capable of suppressing its immune responses to prevent pathogen invasion and tumor formation. However, immune evasion is a hallmark of inflammation-associated tumorigenesis and can lead to the development of HCC. The HCC tumor microenvironment (TME) is a dynamic system comprising cancer cells, a complex cytokine milieu, the extracellular matrix, immune cell subsets, and other components (59). Tumor-associated macrophages (TAMs), neutrophils (TANs), and dendritic cells are key components of the TME and can promote tumor progression, including proliferation, metastasis, and invasion. Immune suppression, particularly of T cells, as observed in chronic liver disease, is associated with the development of HCC (60).

Male-dominated sex differences in antitumor immunity are driven by androgen receptor-mediated CD8<sup>+</sup> T cell stemness programs. Hyunwoo Kwon *et al.* found that androgens conspire with the CD8<sup>+</sup> T cell exhaustion program, contributing to sex bias in cancer (61). Additionally, the major circulating estrogens and each of the three estrogen receptors (ER $\alpha$ , ER $\beta$ , and G-protein-coupled receptor) regulate the activity of different immune cells, leading to females exhibiting more robust immune responses than males (62). Wei *et al.* demonstrated that estrogens can significantly upregulate the NLRP3 inflammasome *via* the E2/ER $\beta$ /MAPK pathway, which suppresses the development and progression of HCC (63). Moreover, interleukin-6 (IL-6) levels are significantly elevated in HCC patients and correlate with HCC incidence and prognosis (64). Naugler *et al.* found that IL-6 levels increase more in males than in females following DEN serum administration (65).

#### 5.3.1. Immune cell interactions in the immune microenvironment

The TME of HCC is a complex ecosystem that includes a diverse array of immune cells, such as tumor-associated macrophages (TAMs), regulatory T cells (Tregs), myeloid-derived suppressor cells (MDSCs), and natural killer (NK) cells, among others. These immune cells interact with one another and with cancer cells, thereby playing a crucial role in the progression and prognosis of

HCC (60).

The heterogeneity and dynamic plasticity of TAMs in HCC can influence the progression of the disease by altering their phenotypes in response to changes in the tumor microenvironment. TAMs are categorized into two major subtypes: pro-inflammatory M1 and anti-inflammatory M2 macrophages. M2-type TAMs promote tumor progression and immunosuppression by secreting anti-inflammatory cytokines, such as IL-10 and TGF- $\beta$ . These cytokines can inhibit the activation and function of T cells and NK cells, thereby suppressing the anti-tumor immune response (5). However, the phenotype and function of TAMs differ between cancer patients of different sexes. Multiple studies have demonstrated that men typically exhibit a higher proportion of M2-type TAMs in various tumors, including HCC, a distribution influenced by sex hormones (6). This may lead to gender differences in HCC.

Tregs are a subset of T cells with significant immunosuppressive properties that inhibit the proliferation and activation of effector T cells, such as CD8<sup>+</sup> T cells, by secreting inhibitory cytokines, including TGF- $\beta$  and IL-10. This inhibition can weaken the anti-tumor immune response, thereby promoting tumor immune escape and progression (61). In HCC, the expression of Tregs exhibits gender differences. Studies have shown that male patients have a higher number of Tregs, and activation of the androgen receptor can enhance the immunosuppressive function of Tregs. This enhancement leads to a weakened anti-tumor immune response, thereby promoting tumor immune escape and progression (66). This may be one of the reasons for the poor prognosis of HCC in men.

MDSCs are a group of immature myeloid cells with immunosuppressive functions. They can inhibit the activity of T cells and NK cells by producing reactive oxygen species (ROS) and arginase. In the TME of HCC, MDSCs can suppress the proliferation and activation of T cells and NK cells, resulting in immune tolerance and tumor progression (67). Androgens enhance the immunosuppressive function of MDSCs. Research indicates that, within a range of organs, the immune cells primarily consist of myeloid immune cells, such as neutrophils and macrophages, which are positively regulated by androgens (68). These findings offer significant insights into the gender differences in HCC.

#### 5.3.2. Molecular immune signaling networks in immune microenvironments

In the TME of HCC, a variety of complex molecular immune signaling networks are involved in modulating the functions of immune cells and their interactions with cancer cells, and these networks exhibit notable gender disparities.

The TGF- $\beta$  signaling pathway plays a crucial role



in the progression of HCC and exhibits distinct activity patterns between males and females. Male HCC patients often display higher expression levels of TGF- $\beta$ , which is associated with the promotional effect of androgens on the TGF- $\beta$  signaling pathway. Androgens can bind to their receptors and enhance the activity of the TGF- $\beta$  signaling pathway, thereby promoting the epithelial-mesenchymal transition (EMT), invasion, and metastasis of tumor cells, while also suppressing the activity of T cells and natural killer (NK) cells and enhancing the functions of immunosuppressive cells. In contrast, in females, estrogen may inhibit the activity of the TGF- $\beta$  signaling pathway, reducing its promotion of tumor progression and immunosuppression, thereby helping to maintain anti-tumor immune responses (65,69).

The IL-6/STAT3 signaling pathway is a crucial pro-inflammatory pathway that is frequently activated in the TME of HCC. IL-6 can bind to its receptors on immune cells, such as TAMs and Tregs, thereby activating the STAT3 signaling pathway. The activation of STAT3 promotes the production of anti-inflammatory cytokines, such as IL-10 and TGF- $\beta$ , leading to immune suppression and tumor progression (64). Studies have shown that IL-6 levels are significantly higher in male HCC patients, which may be one of the reasons for the faster progression of HCC in males (70).

The PI3K/AKT/mTOR signaling pathway is involved in modulating immune cell metabolism and function in the TME of HCC. The activation of this signaling pathway can promote the proliferation and activation of immune cells, such as T lymphocytes and

natural killer (NK) cells, and enhance their anti-tumor immune responses. However, the activation of this signaling pathway can also promote the production of immunosuppressive cells, such as TAMs and MDSCs, leading to immune suppression and tumor progression (71). Ren QN *et al.* found that the phosphorylation of the androgen receptor by mTORC1 promotes liver steatosis and tumorigenesis, with the PI3K/AKT/mTOR signaling pathway playing a significant role in this process (25). This leads to faster progression of HCC tumors in male.

The NLRP3 inflammasome is a multiprotein complex that plays a pivotal role in regulating immune responses within the TME of HCC. The activation of the NLRP3 inflammasome can facilitate the production of pro-inflammatory cytokines, such as IL-1 $\beta$  and IL-18, thereby inducing immune activation and tumor regression (72,73). A study conducted by Wei Q *et al.* revealed that estrogens can significantly upregulate the NLRP3 inflammasome *via* the E2/ER $\beta$ /MAPK pathway, thereby inhibiting the development and progression of HCC (63). Perhaps this is one of the reasons why HCC progresses more slowly in women than in men.

Gender disparity in the molecular mechanisms of HCC in relation with the immune system is summarized in Figure 2.

## 6. Gene and Epigenetic differences in HCC based on omics analysis

Current multi-omics studies, including genomics,

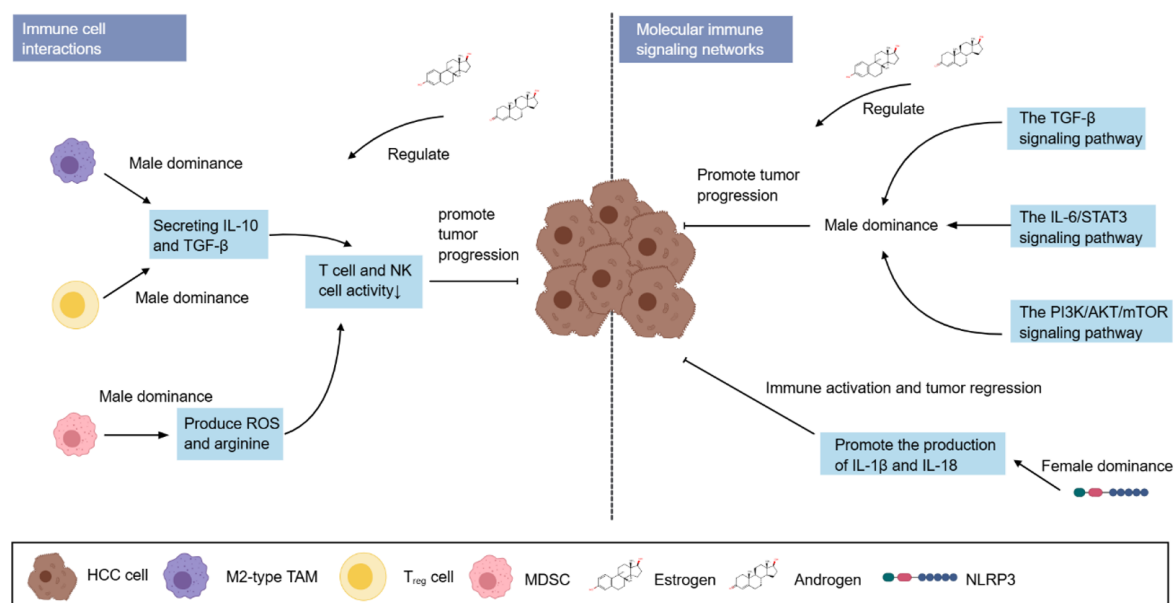


**Figure 2. The molecular mechanisms of HCC related with immune system in gender disparity.** The left side illustrates the roles of different immune cells in tumor progression. M2-type tumor-associated macrophages (TAMs) and regulatory T cells (Tregs) secrete IL-10 and TGF- $\beta$ , while myeloid-derived suppressor cells (MDSCs) produce reactive oxygen species (ROS) and arginine. Male-dominant M2-type TAMs, Tregs, and MDSCs can all decrease the activity of T cells and NK cells, thereby promoting tumor progression. The right side shows molecular immune signaling networks. Male-dominant TGF- $\beta$ , IL-8/STAT3, and PI3K/AKT/mTOR signaling pathways can promote tumor progression. Female-dominant NLRP3 inflammasome can promote the production of IL-1 $\beta$  and IL-18 to activate immune responses and tumor regression.

transcriptomics, proteomics, and metabolomics, have helped us gain a deeper understanding of the mechanisms underlying HCC and its gender differences. These studies have revealed gene mutations, transcriptional regulation, protein expression, and metabolic changes associated with HCC, providing a solid theoretical basis for the development of targeted therapeutic strategies (Figure 3).

### 6.1. Genomic analysis

Genomics is a cross-disciplinary field that involves the collective characterization, quantitative study, and comparative analysis of genomes across different organisms. It plays a crucial role in the study of HCC. By analyzing the genomes of patients with HCC, scientists can identify specific genetic changes and mutations associated with the pathogenesis and development of HCC. TERT promoter, CTNNB1 and TP53 mutations are the most common alterations identified to date (74). A study identified 26 genes that were significantly mutated in HCC. These genes included TP53 (31%), AXIN1 (8%), and RB1 (4%), which were inactivated by mutation, as well as CTNNB1 (27%), an oncogene in the WNT pathway, and the chromatin remodeling genes ARID1A (7%), ARID2 (5%), and BAP1 (5%) (75). Another

study showed that CTNNB1 was found in only 14% of Taiwanese patients, whereas ALDH2 and KMT2C were mutated at much higher frequencies in this cohort than in TCGA (76).

Many studies have found that  $kras^{V12}$ ,  $xmrk$  and  $Myc$  oncogenes induce HCC in zebrafish and cause males to develop faster and more severe hepatocellular carcinoma than females (77). An examination of HCC patients in Qidong showed that men expressed higher levels of aflatoxin metabolism genes, including AHR and CYP1A1, and lower levels of non-homologous DNA end joining factors, including XRCC4, LIG4 and MRE11, than women, which increased the incidence of HCC (78). Bioinformatics analysis showed that compared with female HCC patients, CDK1 and CCNB1 genes were downregulated in males, which is associated with reduced male survival. CYP3A4 and SERPINA4 genes were downregulated in males, which may serve as markers of poor male prognosis (79).

### 6.2. Transcriptomic analysis

Transcriptomics is the study of gene transcription and transcriptional regulation in cells at the whole cell level, and gene expression at the RNA level. A transcriptome

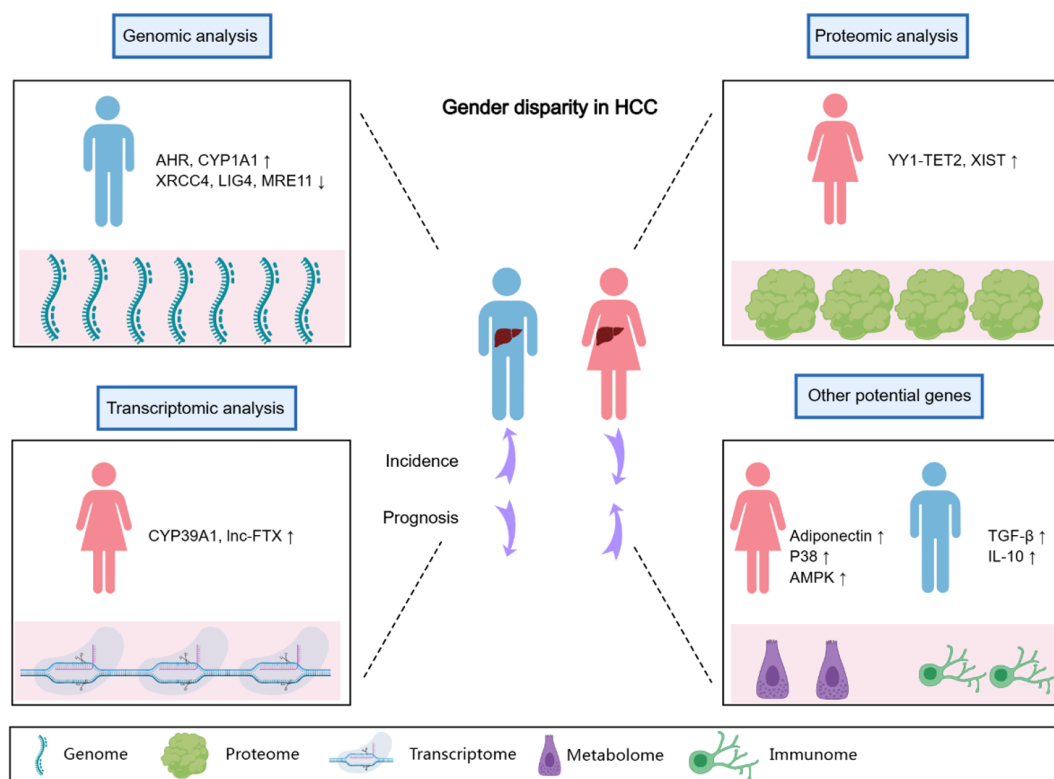


**Figure 3. Gene and Epigenetic differences in HCC based on omics analysis.** Genome analysis shows that AHR and CYP1A1 gene expression is upregulated in males, while XRCC4, LIG4, and MRE11 gene expression is downregulated. Transcriptome analysis shows that CYP38A1 and Inc-FTX gene expression is upregulated in females. Proteomics analysis shows that the YY1-TET2 protein complex and XIST gene expression are upregulated in females. Metabolomics analysis shows that adiponectin, p38, and AMPK protein expression is upregulated in females. Immunomics analysis shows high expression of TGF-β and IL-10 cytokines in males. The results of these omics analyses explain the gender differences in HCC from different perspectives: males have a higher incidence and worse prognosis.

is the sum of all RNA transcribed by a given tissue or cell at a given stage of development or functional state, including mainly messenger RNA and non-coding RNA. Using single-cell RNA sequencing analysis, Jialu Liang *et al.* identified a cluster of proliferative cancer cells (HCC C4) with significant levels of KI67, TOP2A, and CENPF (80). KI-67 expression in HCC is related to differentiation grading, TOP2A is up-regulated in HCC, CENPF is related to the centrosome kinetochore complex and affects cell proliferation and metastasis in HCC (81). Complementary to scRNA-seq sequencing, Yue-Fan Wang *et al.* used spatial transcriptome sequencing (ST) analysis to reveal the spatial expression patterns in specific regions of some key molecules, including CCL15, CCL19, and CCL21, which affect the infiltration and recruitment of various immune cells and collectively contribute to the intratumoral heterogeneity of the HCC microenvironment, thereby affecting the prognosis of HCC patients (82).

CYP39A1, which is highly expressed in females, blocks the transcriptional activation activity of c-Myc and suppresses the development of HCC through its C-terminal region (83). Long non-coding RNA FTX, a regulatory factor highly expressed in females, inhibits HCC proliferation and metastasis. The androgen receptor enhances HBV transcription and replication, which significantly increases the risk of HCC; estrogen suppresses HBV transcription by increasing the hepatic expression of estrogen receptor alpha, which may reduce the risk of HCC (4). MiRNA-23a and p53 are activated by estradiol and induce cell apoptosis, conferring a protective role, thereby reducing the risk of HCC in women (84). These transcriptomics related studies collectively indicate the reasons for gender differences in HCC, but the specific molecular mechanisms still need further investigation.

### 6.3. Proteomic analysis

In 1994, Marc Wilkins defined and coined the concept of the proteome. Proteomics, the study of the proteome - how different proteins interact and what role they play in the living organism - provides unique insights into disease biology beyond the genomic and transcriptomic (85). Traditionally, HCC has been broadly classified into two major classes based on transcriptomic characteristics, the proliferative class and the non-proliferative class, each comprising ~50% of HCC patients (86). Jiang Ying and colleagues classified HCC into subtypes S-I, S-II, and S-III, each of which has a different clinical outcome. The S-III subtype was associated with the lowest overall survival and the highest recurrence rate after first-line surgery and was characterized by proliferation, immune infiltration, and disrupted cholesterol homeostasis (87). Based on the proteome molecular classification data of early HCC, Zhiwen Gu *et al.* showed that LYZ levels were significantly increased in the most malignant HCC

subgroup (88).

Proteomics analysis has also contributed to insights into gender differences in HCC. Zhihui Dai *et al.* found that YY1 and TET2 could interact to form protein complexes that bind to the promoter region of XIST and regulate the methylation level of XIST, and female patients with higher XIST in HCC had a higher overall survival (OS) and longer recurrence-free survival (RFS) (89). By high-throughput comparative proteomic analysis, Huiling Li *et al.* identified 1344 differentially expressed proteins (DEPs) in Hras<sup>12V</sup> transgenic male and female HCC mice, with significantly higher DEPs in males than in females, providing insight into the mechanism of ras oncogene-induced HCC and male-biased HCC (90). Another proteomic analysis of Hras12V transgenic mice also showed that 5 pathways in males but only 1 in females were significantly altered in terms of up-regulated proteins in tumor tissues compared with normal liver tissues (91). These data indicate that female hepatocytes are more difficult to be disturbed by oncogenes.

### 6.4. Other potential genes

Besides genomics, proteomics and transcriptomics, omics also includes metabolomics, immunomics, *etc.*, which are related and together explain the gender differences of HCC.

Cancer cells have metabolic dysregulation to support the demands of uncontrolled proliferation. Metabolomics is the global analysis of small-molecule metabolites, providing critical information about how cancer and cancer treatment interact with metabolism at the cellular and systemic level (92). Non-targeted metabolomics and stable isotope tracing revealed that high levels of dietary fructose promote the progression of HCC through the enhancement of O-GlcNAcylation *via* microbiota-derived acetate (41). Loss of the metabolic regulator Sirt5 leads to abnormal bile acid levels and the immunosuppressive microenvironment favoring the development of HCC (93). The decrease in propionyl-CoA metabolism mediated by ALDH6A1 contributes to metabolic remodeling and facilitates hepatocarcinogenesis (94). Specific diacylglycerols enriched by hepatic lipogenesis increase the transcriptional activity of hepatic AR and increase the risk of HCC, a novel mechanism underlying the higher risk of HCC in obese/NAFLD men (95). Adiponectin is a hormone secreted by fat cells, with higher levels in women. It can inhibit HCC proliferation and damage its growth through activation of p38 and AMPK proteins in liver cells (96). Research has shown that although women's fasting triacylglycerol levels are higher, they can more effectively take advantage of the protective effects of N<sup>6</sup>-methyladenosine (m<sup>6</sup>A) modification and achieve greater health benefits under a high-fat diet, explaining the sex differences in liver metabolism from

the perspective of RNA modification (97).

Immunomics technology has also provided a new perspective for studying gender differences in HCC. By analyzing the composition of immune cells, immune signaling pathways, and the regulatory effects of sex hormones on immune responses, studies have revealed significant differences between genders in the occurrence, progression, and immune treatment responses of HCC. For example, activation of the androgen receptor can modulate the function of immune cells and affect the expansion of regulatory T cells, thereby inhibiting antitumor immune responses (98). In addition, targeting the androgen receptor signaling pathway can enhance the efficacy of immunotherapy, offering new strategies for personalized treatment of HCC. Males have a higher proportion of M2 (anti-inflammatory) macrophages. M2-type tumor-associated macrophages (TAMs) promote tumor progression and immune suppression by secreting anti-inflammatory cytokines (such as IL - 10 and TGF -  $\beta$ ), resulting in a worse prognosis for male HCC (99). These findings indicate that immunomics plays a significant role in elucidating the underlying mechanisms of gender differences in HCC.

The detailed gene and epigenetic differences in HCC based on omics analysis are summarized in Table 4.

## 7. Conclusions and perspectives

HCC exhibits striking gender disparities in incidence and prognosis, with males generally experiencing higher rates of occurrence and worse outcomes compared to females. These disparities are shaped by a complex interplay of epidemiological, molecular, and genetic

factors. While traditional risk factors such as hepatitis B virus (HBV), hepatitis C virus (HCV), alcohol consumption, and metabolic syndrome contribute to these differences, recent advances in molecular biology and multi-omics analysis have provided deeper insights into the underlying mechanisms.

Sex hormones, such as estrogen and androgen, play pivotal roles in modulating HCC progression. Estrogen receptor (ER) signaling is generally protective, suppressing tumor development, while androgen receptor (AR) signaling promotes tumorigenesis. Additionally, gender-specific differences in DNA damage repair, immune microenvironments, and genetic/epigenetic factors further contribute to the observed disparities. For instance, males typically exhibit higher levels of immunosuppressive cells such as M2-type tumor-associated macrophages (TAMs) and regulatory T cells (Tregs), which dampen anti-tumor immune responses. Multi-omics analyses, including genomics, transcriptomics, and proteomics, have revealed sex-specific differences in gene expression, protein interactions, and metabolic pathways, providing a foundation for developing targeted therapeutic strategies.

Despite these advances, significant gaps remain in understanding the precise mechanisms driving gender disparities in HCC. Future research should prioritize the following directions:

i) Identification of Novel Molecular Targets: Further exploration of gender-specific molecular pathways, particularly those involving sex hormones, immune microenvironments, and epigenetic modifications, is critical. For example, elucidating how estrogen and androgen signaling interact with metabolic pathways and

**Table 4. The detailed gene and epigenetic differences in HCC based on omics analysis**

| Category        | Name                      | Gender Differences  |
|-----------------|---------------------------|---|
| Genes           | <i>krasV12, xmrk, Myc</i> | Induces faster and more severe HCC in males compared to females.  |
|                 | <i>AHR, CYP1A1</i>        | Higher expression in males, associated with increased HCC incidence.  |
|                 | <i>XRCC4, LIG4, MRE11</i> | Lower expression in males, associated with increased HCC incidence.   |
|                 | <i>CDK1, CCNB1</i>        | Downregulated in males, associated with reduced male survival.  |
|                 | <i>CYP3A4, SERPINA4</i>   | Downregulated in males, may serve as a marker of poor male prognosis.   |
|                 | <i>CYP3A1</i>             | Highly expressed in females, inhibits HCC development by blocking c-Myc activity.   |
|                 | <i>lnc-FTX</i>            | Highly expressed in females, inhibits HCC proliferation and metastasis.   |
|                 | <i>AR</i>                 | Enhances HBV transcription and replication, increasing HCC risk, more impactful in males.                                 |
|                 | <i>ERa</i>                | Suppresses HBV transcription in females, reducing HCC risk.   |
|                 | <i>XIST</i>               | Higher expression in female HCC patients, associated with better overall survival and recurrence-free survival.           |
| Proteins        | <i>ALDH6A1</i>            | Mediates decreased propionyl-CoA metabolism in males, facilitating hepatocarcinogenesis.                                  |
|                 | YY1                       | Forms complexes with TET2 to regulate XIST methylation, influencing survival in female HCC patients.                      |
|                 | TET2                      | Forms complexes with YY1 to regulate XIST methylation, influencing survival in female HCC patients.                       |
| Metabolites     | p38, AMPK                 | Activated by adiponectin in females, inhibits HCC proliferation.  |
|                 | Propionyl-CoA             | Decreased metabolism in males, promoting hepatocarcinogenesis.  |
| Other Molecules | Specific diacylglycerols  | Increased in obese/NAFLD males, activates AR and increases HCC risk.  |
|                 | m6A modification          | More effectively utilized by females for protection under high-fat diets, explaining sex differences in liver metabolism. |
| Cytokines       | Adiponectin               | Higher levels in females, inhibits HCC proliferation through activation of p38 and AMPK.                                  |
|                 | IL - 10, TGF - $\beta$    | Higher expression in males, associated with increased HCC incidence.  |



immune cells could reveal new therapeutic targets.

ii) Integration of Multi-Omics Data: Combining genomics, transcriptomics, proteomics, and metabolomics data will help uncover the complex interplay between genetic, epigenetic, and environmental factors in shaping gender disparities. This integrative approach may identify biomarkers for early diagnosis and personalized treatment.

iii) Development of Gender-Specific Therapies: Given the distinct molecular and immunological profiles between males and females, therapeutic strategies tailored to gender-specific mechanisms should be explored. For instance, estrogen-related drugs or AR-targeted therapies may offer promising avenues for improving outcomes in HCC patients.

iv) Longitudinal and Population-Based Studies: Large-scale, longitudinal studies are needed to better understand how gender differences in HCC evolve over time and across diverse populations. These studies should account for regional, ethnic, and socioeconomic variations in risk factors and outcomes.

v) Prevention and Public Health Interventions: Targeted public health initiatives aimed at reducing gender-specific risk factors, such as alcohol consumption, smoking, and metabolic syndrome, could help mitigate gender disparities in HCC incidence and prognosis.

In conclusion, addressing the challenges of gender disparities in HCC requires a multidisciplinary approach that integrates epidemiological, molecular, and clinical insights. By prioritizing research into the underlying mechanisms and translating these findings into clinical practice, we can improve diagnostic, prognostic, and therapeutic outcomes for both male and female patients. Future studies should continue to explore the interactions between environmental, hormonal, and genetic factors to develop personalized therapeutic strategies for HCC in different sexes.

**Funding:** This research was supported by the National Natural Science Foundation of China (No. 82170666); Natural Science Foundation of Chongqing (No. CSTB2022NSCQ-MSX0112); Program for Youth Innovation in Future Medicine, Chongqing Medical University (W0087).

**Conflict of Interest:** The authors have no conflicts of interest to disclose.

## References

1. Dong M, Cioffi G, Wang J, Waite KA, Ostrom QT, Kruchko C, Lathia JD, Rubin JB, Berens ME, Connor J, Barnholtz-Sloan JS. Sex Differences in Cancer Incidence and Survival: A Pan-Cancer Analysis. *Cancer Epidemiol Biomarkers Prev.* 2020; 29:1389-1397.
2. Unger JM, Vaidya R, Albain KS, LeBlanc M, Minasian LM, Gotay CC, Henry NL, Fisch MJ, Lee SM, Blanke CD, Hershman DL. Sex Differences in Risk of Severe Adverse Events in Patients Receiving Immunotherapy,

Targeted Therapy, or Chemotherapy in Cancer Clinical Trials. *J Clin Oncol.* 2022; 40:1474-1486.

3. Bray F, Laversanne M, Sung H, Ferlay J, Siegel RL, Soerjomataram I, Jemal A. Global cancer statistics 2022: GLOBOCAN estimates of incidence and mortality worldwide for 36 cancers in 185 countries. *CA Cancer J Clin.* 2024; 74:229-263.
4. Ruggieri A, Gagliardi MC, Anticoli S. Sex-Dependent Outcome of Hepatitis B and C Viruses Infections: Synergy of Sex Hormones and Immune Responses? *Front Immunol.* 2018; 9:2302.
5. Wang S, Wang J, Chen Z, Luo J, Guo W, Sun L, Lin L. Targeting M2-like tumor-associated macrophages is a potential therapeutic approach to overcome antitumor drug resistance. *NPJ Precis Oncol.* 2024; 8:31.
6. Yan C, Yang Q, Gong Z. Tumor-Associated Neutrophils and Macrophages Promote Gender Disparity in Hepatocellular Carcinoma in Zebrafish. *Cancer Res.* 2017; 77:1395-1407.
7. Long J, Cui K, Wang D, Qin S, Li Z. Burden of Hepatocellular Carcinoma and Its Underlying Etiologies in China, 1990-2021: Findings From the Global Burden of Disease Study 2021. *Cancer Control.* 2024; 31:10732748241310573.
8. Nakano M, Yatsushashi H, Bekki S, *et al.* Trends in hepatocellular carcinoma incident cases in Japan between 1996 and 2019. *Sci Rep.* 2022; 12:1517.
9. Kirk GD, Lesi OA, Mendy M, Akano AO, Sam O, Goedert JJ, Hainaut P, Hall AJ, Whittle H, Montesano R. The Gambia Liver Cancer Study: Infection with hepatitis B and C and the risk of hepatocellular carcinoma in West Africa. *Hepatology.* 2004; 39:211-219.
10. Boukaira S, Madihi S, Bouafi H, Rchiad Z, Belkadi B, Benani A. Hepatitis C in North Africa: A Comprehensive Review of Epidemiology, Genotypic Diversity, and Hepatocellular Carcinoma. *Adv Virol.* 2025; 2025:9927410.
11. Abboud Y, Ismail M, Khan H, Medina-Morales E, Alsakarneh S, Jaber F, Pysopoulou NT. Hepatocellular Carcinoma Incidence and Mortality in the USA by Sex, Age, and Race: A Nationwide Analysis of Two Decades. *J Clin Transl Hepatol.* 2024; 12:172-181.
12. Melchor-Ruan J, Santiago-Ruiz L, Murillo-Ortiz BO, *et al.* Characteristics of Hepatocellular Carcinoma by Sex in Mexico: A Multi-Institutional Collaboration. *Diseases.* 2024; 12:262.
13. Liou W-L, Tan TJ-Y, Chen K, Goh GB-B, Chang JP-E, Tan C-K. Gender survival differences in hepatocellular carcinoma: Is it all due to adherence to surveillance? A study of 1716 patients over three decades. *JGH Open.* 2023; 7:377-386.
14. Rich NE, Murphy CC, Yopp AC, Tiro J, Marrero JA, Singal AG. Sex disparities in presentation and prognosis of 1110 patients with hepatocellular carcinoma. *Aliment Pharmacol Ther.* 2020; 52:701-709.
15. Buch SC, Kondragunta V, Branch RA, Carr BI. Gender-based outcomes differences in unresectable hepatocellular carcinoma. *Hepatol Int.* 2008; 2:95-101.
16. Ng IO, Ng MM, Lai EC, Fan ST. Better survival in female patients with hepatocellular carcinoma. Possible causes from a pathologic approach. *Cancer.* 1995; 75:18-22.
17. Lai M-W, Chu Y-D, Lin C-L, Chien R-N, Yeh T-S, Pan T-L, Ke P-Y, Lin K-H, Yeh C-T. Is there a sex difference in postoperative prognosis of hepatocellular carcinoma? *BMC cancer.* 2019; 19:250.

18. Cauble S, Abbas A, Balart L, Bazzano L, Medvedev S, Shores N. United States women receive more curative treatment for hepatocellular carcinoma than men. *Dig Dis Sci*. 2013; 58:2817-2825.
19. Özdemir BC, Gerard CL, Espinosa da Silva C. Sex and Gender Differences in Anticancer Treatment Toxicity: A Call for Revisiting Drug Dosing in Oncology. *Endocrinology*. 2022; 163:bqac058.
20. Lam CM, Yong JL, Chan AO, Ng KK, Poon RT, Liu CL, Lo CM, Fan ST. Better survival in female patients with hepatocellular carcinoma: oral contraceptive pills related? *J Clin Gastroenterol*. 2005; 39:533-539.
21. Hassan MM, Botrus G, Abdel-Wahab R, *et al*. Estrogen Replacement Reduces Risk and Increases Survival Times of Women With Hepatocellular Carcinoma. *Clin Gastroenterol Hepatol*. 2017; 15:1791-1799.
22. Zheng B, Zhu Y-J, Wang H-Y, Chen L. Gender disparity in hepatocellular carcinoma (HCC): multiple underlying mechanisms. *Sci China Life Sci*. 2017; 60:575-584.
23. Xiao Y, Liu G, Sun Y, Gao Y, Ouyang X, Chang C, Gong L, Yeh S. Targeting the estrogen receptor alpha (ER $\alpha$ )-mediated circ-SMG1.72/miR-141-3p/Gelsolin signaling to better suppress the HCC cell invasion. *Oncogene*. 2020; 39:2493-2508.
24. Hou J, Xu J, Jiang R, Wang Y, Chen C, Deng L, Huang X, Wang X, Sun B. Estrogen-sensitive PTPRO expression represses hepatocellular carcinoma progression by control of STAT3. *Hepatology*. 2013; 57:678-688.
25. Ren Q-N, Zhang H, Sun C-Y, Zhou Y-F, Yang X-F, Long J-W, Li X-X, Mai S-J, Zhang M-Y, Zhang H-Z, Mai H-Q, Chen M-S, Zheng XFS, Wang H-Y. Phosphorylation of androgen receptor by mTORC1 promotes liver steatosis and tumorigenesis. *Hepatology*. 2022; 75:1123-1138.
26. Kido T, Lau Y-FC. Androgen receptor variant 7 exacerbates hepatocarcinogenesis in a c-MYC-driven mouse HCC model. *Oncogenesis*. 2023; 12:4.
27. Han Q, Yang D, Yin C, Zhang J. Androgen Receptor (AR)-TLR4 Crosstalk Mediates Gender Disparities in Hepatocellular Carcinoma Incidence and Progression. *J Cancer*. 2020; 11:1094-1103.
28. Huang DQ, Mathurin P, Cortez-Pinto H, Loomba R. Global epidemiology of alcohol-associated cirrhosis and HCC: trends, projections and risk factors. *Nat Rev Gastroenterol Hepatol*. 2023; 20:37-49.
29. Taniai M. Alcohol and hepatocarcinogenesis. *Clin Mol Hepatol*. 2020; 26:736-741.
30. Bizzaro D, Becchetti C, Trapani S, Lavezzo B, Zanetto A, D'Arcangelo F, Merli M, Lapenna L, Invernizzi F, Taliani G, Burra P, Hepatology ASIGoGi. Influence of sex in alcohol-related liver disease: Pre-clinical and clinical settings. *United European Gastroenterol J*. 2023; 11:218-227.
31. Collaborators GA. Population-level risks of alcohol consumption by amount, geography, age, sex, and year: a systematic analysis for the Global Burden of Disease Study 2020. *Lancet*. 2022; 400:185-235.
32. Giovino GA, Mirza SA, Samet JM, Gupta PC, Jarvis MJ, Bhala N, Peto R, Zatonski W, Hsia J, Morton J, Palipudi KM, Asma S, Group GC. Tobacco use in 3 billion individuals from 16 countries: an analysis of nationally representative cross-sectional household surveys. *Lancet*. 2012; 380:668-679.
33. Alisoltani A, Qiu X, Jaroszewski L, Sedova M, Iyer M, Godzik A. Gender differences in smoking-induced changes in the tumor immune microenvironment. *Arch Biochem Biophys*. 2023; 739:109579.
34. Li C-L, Lin Y-K, Chen H-A, Huang C-Y, Huang M-T, Chang Y-J. Smoking as an Independent Risk Factor for Hepatocellular Carcinoma Due to the  $\alpha$ 7-Nachr Modulating the JAK2/STAT3 Signaling Axis. *J Clin Med*. 2019; 8:1391.
35. Yuan C, Shu X, Wang X, Chen W, Li X, Pei W, Su X, Hu Z, Jie Z. The impact of metabolic syndrome on hepatocellular carcinoma: a mendelian randomization study. *Sci Rep*. 2025; 15:1941.
36. Kim HY, Lee HA, Radu P, Dufour J-F. Association of modifiable metabolic risk factors and lifestyle with all-cause mortality in patients with hepatocellular carcinoma. *Sci Rep*. 2024; 14:15405.
37. Bell JA, Santos Ferreira DL, Fraser A, Soares ALG, Howe LD, Lawlor DA, Carslake D, Davey Smith G, O'Keefe LM. Sex differences in systemic metabolites at four life stages: cohort study with repeated metabolomics. *BMC Med*. 2021; 19:58.
38. Xu S-T, Sun M, Xiang Y. Global, regional, and national trends in type 2 diabetes mellitus burden among adolescents and young adults aged 10-24 years from 1990 to 2021: a trend analysis from the Global Burden of Disease Study 2021. *World J Pediatr*. 2025; 21:73-89.
39. Plaz Torres MC, Jaffe A, Perry R, Marabotto E, Strazzabosco M, Giannini EG. Diabetes medications and risk of HCC. *Hepatology*. 2022; 76:1880-1897.
40. Facciorusso A. The influence of diabetes in the pathogenesis and the clinical course of hepatocellular carcinoma: recent findings and new perspectives. *Curr Diabetes Rev*. 2013; 9:382-386.
41. Zhou P, Chang W-Y, Gong D-A, Xia J, Chen W, Huang L-Y, Liu R, Liu Y, Chen C, Wang K, Tang N, Huang A-L. High dietary fructose promotes hepatocellular carcinoma progression by enhancing O-GlcNAcylation *via* microbiota-derived acetate. *Cell Metab*. 2023; 35:1961-1975.e1966.
42. Grzymisławska M, Puch EA, Zawada A, Grzymisławski M. Do nutritional behaviors depend on biological sex and cultural gender? *Adv Clin Exp Med*. 2020; 29:165-172.
43. Zhang X, Coker OO, Chu ES, Fu K, Lau HCH, Wang Y-X, Chan AWH, Wei H, Yang X, Sung JJY, Yu J. Dietary cholesterol drives fatty liver-associated liver cancer by modulating gut microbiota and metabolites. *Gut*. 2021; 70:761-774.
44. Y M, W Y, T L, Y L, Tg S, J S, K W, El G, At C, X Z. Meat intake and risk of hepatocellular carcinoma in two large US prospective cohorts of women and men. *Int J Epidemiol*. 2019; 48.
45. Nuermaimaiti A, Chang L, Yan Y, Sun H, Xiao Y, Song S, Feng K, Lu Z, Ji H, Wang L. The role of sex hormones and receptors in HBV infection and development of HBV-related HCC. *J Med Virol*. 2023; 95:e29298.
46. Lee S-A, Kim H, Won Y-S, Seok S-H, Na Y, Shin H-B, Inn K-S, Kim B-J. Male-specific hepatitis B virus large surface protein variant W4P potentiates tumorigenicity and induces gender disparity. *Mol Cancer*. 2015; 14:23.
47. Li C-L, Li C-Y, Lin Y-Y, Ho M-C, Chen D-S, Chen P-J, Yeh S-H. Androgen Receptor Enhances Hepatic Telomerase Reverse Transcriptase Gene Transcription After Hepatitis B Virus Integration or Point Mutation in Promoter Region. *Hepatology*. 2019; 69:498-512.
48. Warnerdam DO, Kanaar R. Dealing with DNA damage: relationships between checkpoint and repair pathways. *Mutat Res*. 2010; 704:2-11.

49. Oshi M, Kim TH, Tokumaru Y, Yan L, Matsuyama R, Endo I, Cherkassky L, Takabe K. Enhanced DNA Repair Pathway is Associated with Cell Proliferation and Worse Survival in Hepatocellular Carcinoma (HCC). *Cancers* (Basel). 2021; 13:323.
50. Trzeciak AR, Barnes J, Ejiogu N, Foster K, Brant LJ, Zonderman AB, Evans MK. Age, sex, and race influence single-strand break repair capacity in a human population. *Free Radic Biol Med*. 2008; 45:1631-1641.
51. Grant EJ, Brenner A, Sugiyama H, Sakata R, Sadakane A, Utada M, Cahoon EK, Milder CM, Soda M, Cullings HM, Preston DL, Mabuchi K, Ozasa K. Solid Cancer Incidence among the Life Span Study of Atomic Bomb Survivors: 1958-2009. *Radiat Res*. 2017; 187:513-537.
52. Yang H, Sun L, Guan A, Yin H, Liu M, Mao X, Xu H, Zhao H, Lu X, Sang X, Zhong S, Chen Q, Mao Y. Unique TP53 neoantigen and the immune microenvironment in long-term survivors of Hepatocellular carcinoma. *Cancer Immunol Immunother*. 2021; 70:667-677.
53. Malorni W, Straface E, Matarrese P, Ascione B, Coinu R, Canu S, Galluzzo P, Marino M, Franconi F. Redox state and gender differences in vascular smooth muscle cells. *FEBS Lett*. 2008; 582:635-642.
54. Motawi TMK, Sadik NAH, Sabry D, Shahin NN, Fahim SA. rs2267531, a promoter SNP within glypican-3 gene in the X chromosome, is associated with hepatocellular carcinoma in Egyptians. *Sci Rep*. 2019; 9:6868.
55. Singh S, Kuftinec GN, Sarkar S. Non-alcoholic Fatty Liver Disease in South Asians: A Review of the Literature. *J Clin Transl Hepatol*. 2017; 5:76-81.
56. Liu H, Zheng J, Yang S, Zong Q, Wang Z, Liao X. Mir-454-3p induced WTX deficiency promotes hepatocellular carcinoma progressions through regulating TGF- $\beta$  signaling pathway. *J Cancer*. 2022; 13:1820-1829.
57. Yeh SH, Chen PJ, Shau WY, Chen YW, Lee PH, Chen JT, Chen DS. Chromosomal allelic imbalance evolving from liver cirrhosis to hepatocellular carcinoma. *Gastroenterology*. 2001; 121:699-709.
58. Liu F, Yuan J-H, Huang J-F, Yang F, Wang T-T, Ma J-Z, Zhang L, Zhou C-C, Wang F, Yu J, Zhou W-P, Sun S-H. Long noncoding RNA FTX inhibits hepatocellular carcinoma proliferation and metastasis by binding MCM2 and miR-374a. *Oncogene*. 2016; 35:5422-5434.
59. Chew V, Lai L, Pan L, *et al*. Delineation of an immunosuppressive gradient in hepatocellular carcinoma using high-dimensional proteomic and transcriptomic analyses. *Proc Natl Acad Sci U S A*. 2017; 114:E5900-E5909.
60. Behary J, Amorim N, Jiang X-T, *et al*. Gut microbiota impact on the peripheral immune response in non-alcoholic fatty liver disease related hepatocellular carcinoma. *Nat Commun*. 2021; 12:187.
61. Kwon H, Schafer JM, Song N-J, *et al*. Androgen conspires with the CD8<sup>+</sup> T cell exhaustion program and contributes to sex bias in cancer. *Sci Immunol*. 2022; 7:eabq2630.
62. Chakraborty B, Byemerwa J, Krebs T, Lim F, Chang C-Y, McDonnell DP. Estrogen Receptor Signaling in the Immune System. *Endocr Rev*. 2023; 44:117-141.
63. Wei Q, Guo P, Mu K, Zhang Y, Zhao W, Huai W, Qiu Y, Li T, Ma X, Liu Y, Chen X, Han L. Estrogen suppresses hepatocellular carcinoma cells through ER $\beta$ -mediated upregulation of the NLRP3 inflammasome. *Lab Invest*. 2015; 95:804-816.
64. Myojin Y, Kodama T, Sakamori R, *et al*. Interleukin-6 Is a Circulating Prognostic Biomarker for Hepatocellular Carcinoma Patients Treated with Combined Immunotherapy. *Cancers* (Basel). 2022; 14:883.
65. Naugler WE, Sakurai T, Kim S, Maeda S, Kim K, Elsharkawy AM, Karin M. Gender disparity in liver cancer due to sex differences in MyD88-dependent IL-6 production. *Science*. 2007; 317:121-124.
66. Yang C, Jin J, Yang Y, *et al*. Androgen receptor-mediated CD8<sup>+</sup> T cell stemness programs drive sex differences in antitumor immunity. *Immunity*. 2022; 55:1268-1283. e1269.
67. Lasser SA, Ozbay Kurt FG, Arkhypov I, Utikal J, Umansky V. Myeloid-derived suppressor cells in cancer and cancer therapy. *Nat Rev Clin Oncol*. 2024; 21:147-164.
68. Li F, Xing X, Jin Q, *et al*. Sex differences orchestrated by androgens at single-cell resolution. *Nature*. 2024; 629:193-200.
69. J M. TGF $\beta$  in Cancer. *Cell*. 2008; 134.
70. Shakiba E, Ramezani M, Sadeghi M. Evaluation of serum interleukin-6 levels in hepatocellular carcinoma patients: a systematic review and meta-analysis. *Clin Exp Hepatol*. 2018; 4:182-190.
71. Tian L-Y, Smit DJ, Jücker M. The Role of PI3K/AKT/mTOR Signaling in Hepatocellular Carcinoma Metabolism. *Int J Mol Sci*. 2023; 24:2652.
72. Gleeson TA, Kaiser C, Lawrence CB, Brough D, Allan SM, Green JP. The NLRP3 inflammasome is essential for IL-18 production in a murine model of macrophage activation syndrome. *Dis Model Mech*. 2024; 17:dmm050762.
73. Zou G, Tang Y, Yang J, Fu S, Li Y, Ren X, Zhou N, Zhao W, Gao J, Ruan Z, Jiang Z. Signal-induced NLRP3 phase separation initiates inflammasome activation. *Cell Res*. 2025.
74. Ahn S-M, Jang SJ, Shim JH, *et al*. Genomic portrait of resectable hepatocellular carcinomas: implications of RB1 and FGF19 aberrations for patient stratification. *Hepatology*. 2014; 60:1972-1982.
75. wheeler@bcm.edu CGARNEa, Network CGAR. Comprehensive and Integrative Genomic Characterization of Hepatocellular Carcinoma. *Cell*. 2017; 169:1327-1341. e1323.
76. Chang Y-S, Tu S-J, Chen H-D, Hsu M-H, Chen Y-C, Chao D-S, Chung C-C, Chou Y-P, Chang C-M, Lee Y-T, Yen J-C, Jeng L-B, Chang J-G. Integrated genomic analyses of hepatocellular carcinoma. *Hepatol Int*. 2023; 17:97-111.
77. Yang Q, Yan C, Gong Z. Activation of liver stromal cells is associated with male-biased liver tumor initiation in xmrk and Myc transgenic zebrafish. *Sci Rep*. 2017; 7:10315.
78. Xu C, Cheng S, Chen K, *et al*. Sex Differences in Genomic Features of Hepatitis B-Associated Hepatocellular Carcinoma With Distinct Antitumor Immunity. *Cell Mol Gastroenterol Hepatol*. 2023; 15:327-354.
79. Wu Y, Yao N, Feng Y, Tian Z, Yang Y, Zhao Y. Identification and characterization of sexual dimorphism-linked gene expression profile in hepatocellular carcinoma. *Oncol Rep*. 2019; 42:937-952.
80. Liang J, Chen W, Ye J, Ni C, Zhai W. Single-cell transcriptomics analysis reveals intratumoral heterogeneity and identifies a gene signature associated with prognosis of hepatocellular carcinoma. *Biosci Rep*. 2022; 42:BSR20212560.
81. Huang Y, Chen X, Wang L, Wang T, Tang X, Su

- X. Centromere Protein F (CENPF) Serves as a Potential Prognostic Biomarker and Target for Human Hepatocellular Carcinoma. *J Cancer*. 2021; 12:2933-2951.
82. Wang Y-F, Yuan S-X, Jiang H, Li Z-X, Yin H-Z, Tan J, Dai Z-H, Ge C-M, Sun S-H, Yang F. Spatial maps of hepatocellular carcinoma transcriptomes reveal spatial expression patterns in tumor immune microenvironment. *Theranostics*. 2022; 12:4163-4180.
83. Ji F, Zhang J, Liu N, Gu Y, Zhang Y, Huang P, Zhang N, Lin S, Pan R, Meng Z, Feng X-H, Roessler S, Zheng X, Ji J. Blocking hepatocarcinogenesis by a cytochrome P450 family member with female-preferential expression. *Gut*. 2022; 71:2313-2324.
84. Huang F-Y, Wong DK-H, Seto W-K, Lai C-L, Yuen M-F. Estradiol induces apoptosis *via* activation of miRNA-23a and p53: implication for gender difference in liver cancer development. *Oncotarget*. 2015; 6:34941-34952.
85. Gonçalves E, Poulos RC, Cai Z, *et al.* Pan-cancer proteomic map of 949 human cell lines. *Cancer Cell*. 2022; 40:835-849.e838.
86. Llovet JM, Montal R, Sia D, Finn RS. Molecular therapies and precision medicine for hepatocellular carcinoma. *Nat Rev Clin Oncol*. 2018; 15:599-616.
87. Jiang Y, Sun A, Zhao Y, *et al.* Proteomics identifies new therapeutic targets of early-stage hepatocellular carcinoma. *Nature*. 2019; 567:257-261.
88. Gu Z, Wang L, Dong Q, Xu K, Ye J, Shao X, Yang S, Lu C, Chang C, Hou Y, Zhai Y, Wang X, He F, Sun A. Aberrant LYZ expression in tumor cells serves as the potential biomarker and target for HCC and promotes tumor progression *via* csGRP78. *Proc Natl Acad Sci U S A*. 2023; 120:e2215744120.
89. Dai Z, Wang S, Guo X, Wang Y, Yin H, Tan J, Mu C, Sun S-H, Liu H, Yang F. Gender dimorphism in hepatocarcinogenesis-DNA methylation modification regulated X-chromosome inactivation escape molecule XIIST. *Clin Transl Med*. 2023; 13:e1518.
90. Li H, Rong Z, Wang H, Zhang N, Pu C, Zhao Y, Zheng X, Lei C, Liu Y, Luo X, Chen J, Wang F, Wang A, Wang J. Proteomic analysis revealed common, unique and systemic signatures in gender-dependent hepatocarcinogenesis. *Biol Sex Differ*. 2020; 11:46.
91. Rong Z, Fan T, Li H, Li J, Wang K, Wang X, Dong J, Chen J, Wang F, Wang J, Wang A. Differential Proteomic Analysis of Gender-dependent Hepatic Tumorigenesis in Hras12V Transgenic Mice. *Mol Cell Proteomics*. 2017; 16:1475-1490.
92. Schmidt DR, Patel R, Kirsch DG, Lewis CA, Vander Heiden MG, Locasale JW. Metabolomics in cancer research and emerging applications in clinical oncology. *CA Cancer J Clin*. 2021; 71:333-358.
93. Sun R, Zhang Z, Bao R, *et al.* Loss of SIRT5 promotes bile acid-induced immunosuppressive microenvironment and hepatocarcinogenesis. *J Hepatol*. 2022; 77:453-466.
94. Sun J, Ding J, Shen Q, *et al.* Decreased propionyl-CoA metabolism facilitates metabolic reprogramming and promotes hepatocellular carcinoma. *J Hepatol*. 2023; 78:627-642.
95. Cheng Y-W, Chen K-W, Kuo H-C, Kuo C-H, Lin W-H, Chen P-J, Yeh S-H. Specific diacylglycerols generated by hepatic lipogenesis stimulate the oncogenic androgen receptor activity in male hepatocytes. *Int J Obes (Lond)*. 2019; 43:2469-2479.
96. Manieri E, Herrera-Melle L, Mora A, Tomás-Loba A, Leiva-Vega L, Fernández DI, Rodríguez E, Morán L, Hernández-Cosido L, Torres JL, Seoane LM, Cubero FJ, Marcos M, Sabio G. Adiponectin accounts for gender differences in hepatocellular carcinoma incidence. *J Exp Med*. 2019; 216:1108-1119.
97. Salisbury DA, Casero D, Zhang Z, *et al.* Transcriptional regulation of N6-methyladenosine orchestrates sex-dimorphic metabolic traits. *Nat Metab*. 2021; 3:940-953.
98. Floreani A, Gabbia D, De Martin S. Are Gender Differences Important for Autoimmune Liver Diseases? *Life (Basel)*. 2024; 14:500.
99. Matsuki H, Hiroshima Y, Miyake K, Murakami T, Homma Y, Matsuyama R, Morioka D, Kurotaki D, Tamura T, Endo I. Reduction of gender-associated M2-like tumor-associated macrophages in the tumor microenvironment of patients with pancreatic cancer after neoadjuvant chemoradiotherapy. *J Hepatobiliary Pancreat Sci*. 2021; 28:174-182.

Received April 1, 2025; Revised April 16, 2025; Accepted April 19, 2025.

<sup>§</sup>These authors contributed equally to this work.

\*Address correspondence to:

Zhongjun Wu and Rui Liao, Department of Hepatobiliary Surgery, the First Affiliated Hospital of Chongqing Medical University, Chongqing, China.

E-mail: wzjtcy@126.com (ZW); E-mail: liaorui99@163.com (RL)

Released online in J-STAGE as advance publication April 22, 2025.



# Traditional Chinese medicine modulates hypothalamic neuropeptides for appetite regulation: A comprehensive review

Yuqi Wang<sup>1</sup>, Fanghua Qi<sup>1</sup>, Min Li<sup>2</sup>, Yuan Xu<sup>1</sup>, Li Dong<sup>3</sup>, Pingping Cai<sup>1,\*</sup>

<sup>1</sup> Department of Traditional Chinese Medicine, Shandong Provincial Hospital Affiliated with Shandong First Medical University, Ji'nan, China;

<sup>2</sup> Clinical Skills Training Center, Shandong Provincial Hospital Affiliated with Shandong First Medical University, Ji'nan, China;

<sup>3</sup> First School of Clinical Medicine, Shandong University of Traditional Chinese Medicine, Ji'nan, China.

**SUMMARY:** Obesity has emerged as a global health crisis, imposing substantial burdens on both individual well-being and socioeconomic development. The pathogenesis of obesity primarily stems from disrupted energy homeostasis, wherein the hypothalamus plays a pivotal role through its complex neuropeptide networks that regulate appetite and energy balance. Recent advances have highlighted the therapeutic potential of traditional Chinese medicine (TCM) in modulating hypothalamic appetite regulation. This comprehensive review systematically evaluates current evidence from PubMed and China National Knowledge Infrastructure databases, focusing on the mechanisms by which TCM interventions influence hypothalamic neuropeptide signaling pathways. Our analysis reveals that various TCM modalities, including bioactive compounds (e.g., berberine and, evodiamine), herbal formulations (e.g., Pingwei Powder, Fangji Huangqi Decoction), plant extracts (e.g., Cyclocarya paliurus aqueous extract), and Chinese patent medicines (e.g., Danzhi Jiangtang Capsules and Jingui Shenqi Pills), have significant effects on key appetite-regulating pathways. These effects are mediated through modulation of critical neuropeptide systems, particularly AgRP/NPY and POMC/CART neurons, as well as leptin signaling. These findings not only provide mechanistic insights into TCM's anti-obesity effects but also demonstrate the value of integrating traditional medicine with modern pharmacological approaches. The synergistic potential of TCM formulas, when combined with contemporary research methodologies, offers promising avenues for developing novel therapeutic strategies for obesity and related metabolic disorders.

**Keywords:** obesity, traditional Chinese medicine (TCM), hypothalamic neuropeptides, appetite regulation, energy homeostasis

## 1. Introduction

Obesity is a significant public health challenge worldwide. The World Obesity Alliance's 2023 World Obesity Map predicts that 1.9 billion people globally will be classified as obese by 2035, leading to an anticipated global economic impact of \$4.32 trillion (1). Obesity increases the risk of various health issues, including type 2 diabetes, cardiovascular disease, chronic kidney disease, gastrointestinal disorders, nonalcoholic fatty liver disease, cancer, respiratory ailments, dementia, and Alzheimer's disease (2). Moreover, for women of childbearing potential, a higher BMI is associated with a reduced likelihood of conception within 3 years following diagnosis (3). Consequently, reducing the incidence of obesity is an urgent global health concern.

Genetic and environmental factors promote the development and progression of obesity. Key contributors to the rising prevalence of obesity include changes in social and economic modes of production and

lifestyle changes, such as diet, nutrition, and exercise (4). A disequilibrium between energy intake and expenditure can lead to metabolic diseases like obesity and diabetes. Eating is the primary source of energy intake in the human body, and the hypothalamus plays a crucial role in regulating eating behaviors and energy balance (5). Therefore, controlling appetite and energy intake through hypothalamic mechanisms is essential to combating obesity.

To date, a number of pharmacological agents for weight management, including orlistat, liraglutide, lorcaserin, and diethylpropion, have received regulatory approval (6,7). However, the financial burden associated with these medications is substantial, and a growing array of adverse effects has been documented, encompassing cephalalgia, vertigo, asthenia, nausea, xerostomia, insomnia, anxiety, and constipation (8,9,10). These limitations necessitate the exploration of alternative therapeutic options, among which traditional Chinese medicine (TCM) holds significant promise.

TCM, with its holistic approach and utilization of natural compounds, offers a complementary perspective on appetite suppression and weight management. Many drugs have demonstrated the ability to regulate appetite and energy metabolism, which is closely related to the function of neuropeptides that modulate appetite in the hypothalamus, such as AgRP/NPY, POMC/CART and leptin (11). This paper reviews the effects of TCM monomers, formulas, extracts, single medicines, or Chinese patent medicines on appetite regulation mediated by hypothalamic neuropeptides in order to provide insights to develop traditional prescriptions and improve medicinal preparations. By capitalizing on the strengths of TCM, we can explore new avenues to address the global challenge of obesity and metabolic disorders.

## 2. Regulatory mechanism of the hypothalamus in feeding and energy consumption

Appetite is not only regulated by the energy steady-state system to meet the body's metabolic needs but is also regulated by the reward system to achieve steady-state regulation. The two systems form a complex neural circuit of mutual projection through various factors to comprehensively regulate appetite. Eating is reliable when most organisms are in a steady-state energy-deficient state but can be observed when energy is not required, and especially in the presence of highly palatable foods (12,13). The hypothalamus regulates energy metabolism through various nuclei, including the arcuate nucleus (ARC), ventromedial hypothalamus nucleus (VMH), dorsomedial hypothalamic nucleus (DMH), lateral hypothalamus (LH), parabrachial nucleus (PBN), and paraventricular nucleus (PVN). These nuclei interact through synaptic connections that affect each other while independently regulating energy homeostasis

(14). In the hypothalamus, there are mainly three types of neural circuits that affect appetite. These circuits have different characteristics that can affect appetite independently and interact with each other, thus forming three pillars of appetite control (15) (Figure 1).

### 2.1. Appetite-regulated neurons predominantly in the ARC region

The first pillar involves the expressing neurons in the hypothalamic ARC, they are primarily involved in food seeking but are less likely to normally drive food consumption. In the ARC, neuropeptide Y (NPY) and agouti-related protein (AgRP), which promote appetite, and pro-opiomelanocortin (POMC), which inhibits feeding, play essential roles in regulating appetite. When the ARC receives, integrates, and evaluates signals from the peripheral circulation, it secretes AgRP/NPY or POMC to the LH and PVN, generating corresponding feedback responses (16). During satiety, POMC cleaves to form the  $\alpha$ -melanocyte-stimulating hormone ( $\alpha$ -MSH), which binds to the melanocortin (MC) 3/4 receptor of POMC, and especially to MC-4R (17). This binding promotes the synthesis of PVN, which reduces appetite and enhances energy consumption. Additionally, it stimulates the release of thyrotropin-releasing hormone and corticotropin-releasing hormone to inhibit feeding and increase energy consumption. Conversely, in a hungry state, AgRP/NPY neurons secreted by ARC promote appetite and release NPY and AgRP. NPY directly stimulates food intake by activating the Y1 and Y5 receptors of NPY. The binding of AgRP to MC-3/4R and NPY to NPY-1/5R can antagonize the effects of  $\alpha$ -MSH and stimulate food intake (17) (Figure 2). Additionally, AgRP/NPY neurons can release the inhibitory

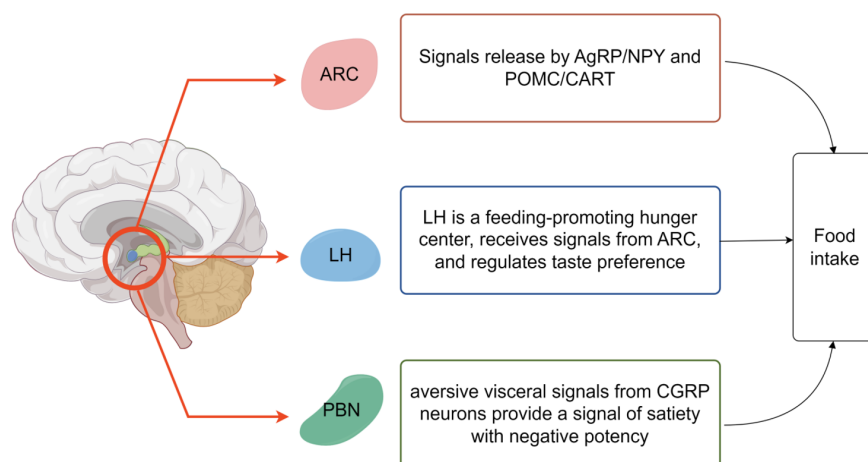


**Figure 1. In the hypothalamus, three main types of neural circuits affect appetite, including ARC, LHs, and PBN.** The interaction of these three pathways drives the initiation, maintenance, and termination of food consumption. AgRP and POMC neurons receive hunger or satiety signals and transmit them to LHs, which complete feeding behavior that can be counteracted by the loop of PBN<sup>CGRP</sup>.

neurotransmitter  $\gamma$ -aminobutyric acid, which acts on several neurons that inhibit appetite in the brain (18).

Leptin, a hormone secreted by white adipocytes, is regulated by fat content. This hormone is crucial in modulating the AgRP/NPY and POMC/cocaine amphetamine-regulated transcript (CART) neuronal pathways. The primary mechanism involves leptin inhibiting the AgRP/NPY neuronal pathway while stimulating the POMC/CART neuronal pathway (19). High levels of leptin act on the hypothalamus through blood circulation and bind to the leptin receptor (OB-R) in the ARC to regulate animal body weight and energy intake. Research has demonstrated that POMC/CART and AgRP/NPY neurons express the OB-Rb receptor, bind leptin to its receptor, and inhibit neuropeptide synthesis and release, thereby reducing appetite (20). *In vitro* studies indicate that glucagon-like peptide (GLP-1) directly stimulates POMC/CART neurons and indirectly inhibits the neurotransmission of AgRP/NPY neurons through  $\gamma$ -aminobutyric acid (GABA) -dependent signal transduction pathways, thereby inhibiting appetite and reducing energy intake (21).

Central and peripheral serotonin (5-hydroxytryptamine, 5-HT) modulate alimentary signals associated with energy homeostasis. There are at least fourteen 5-HT<sub>R</sub> subtypes expressed in the hypothalamus that regulate appetite and energy metabolism, such as 5-HT<sub>1BR</sub> and 5-HT<sub>2CR</sub> (22). 5-HT<sub>2CR</sub> is distributed in POMC neurons of ARC, while 5-HT<sub>1BR</sub> is expressed in AgRP/NPY neurons. The combination of 5-HT and 5-HT subtype receptors can regulate the expression of POMC/CART and AgRP/NPY neurons and result in inhibiting appetite and reducing

body weight (23).

## 2.2. LH-dominated appetite regulation circuit

The second pillar consists of circuits involving LH (Figure 3). LH is usually a feeding-promoting hunger center that receives both AgRP/NPY and POMC/CART neuronal projections from the arcuate nucleus and into the cerebral system and extracortical areas. It contains neurons that express melanin concentrating hormone (MCH), neurotensin (NT), and orexin. Melanin concentrate and neurotensin are factors that inhibit appetite. MCHs activate downstream G-protein-coupled receptors, including MCHR1 and MCHR2, and regulate food intake, energy balance, and other physiological functions by stimulating MCHR1 and MCHR2 receptors (24). Orexin is a factor that promotes appetite. Orexin can be divided into two neuropeptides, orexin A(OXA) and orexin B (OXB), whose common precursor is preorexin secreted by hypothalamic neurons (25). Orexin binds to two G-protein-coupled receptors, orexin 1 receptor (OX1R) and orexin 2 receptor (OX2R) (26). OX1R is mainly distributed in areas that control food intake, learning and memory, and reward (27).

Orexin-expressing neurons can be widely projected into the ARC (especially NPY neurons), VMH, DMH, PVN, and ventral capsular region (28). These neurons receive different inputs from the area of direct self-balance control and the area associated with hedonic or environmental feeding (29,30). Other studies have shown that photogenetic activation of LH inhibitory neurons marked by the vesicular GABA transporter leads

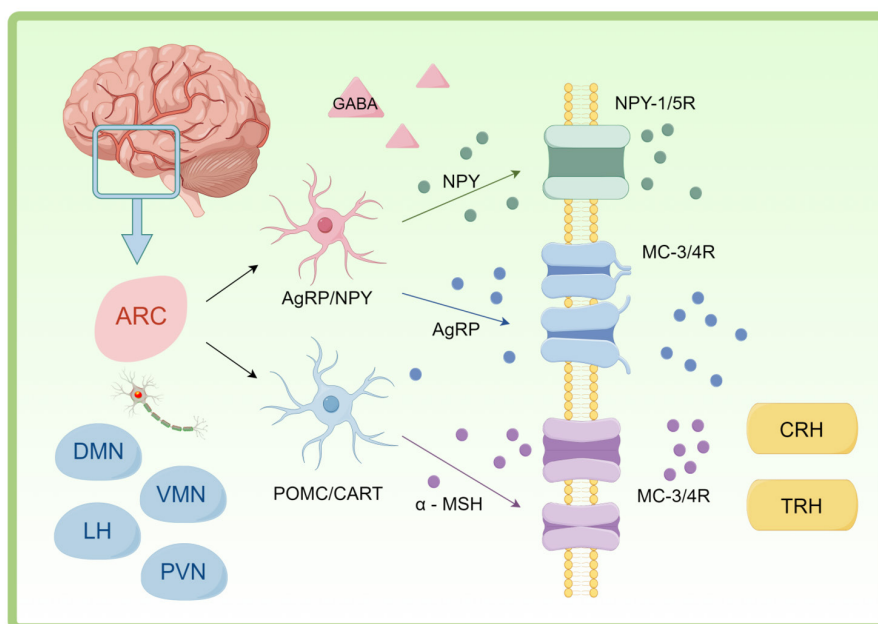


**Figure 2. Appetite-regulated neurons predominantly in the ARC region.** In the ARC, AgRP/NPY neurons and POMC/CART neurons modulate receptors NPY-1/5R, MC-3R, and MC-4R by releasing neuropeptides such as AgRP, NPY, and  $\alpha$ -MSH, thereby influencing appetite regulation and energy expenditure.

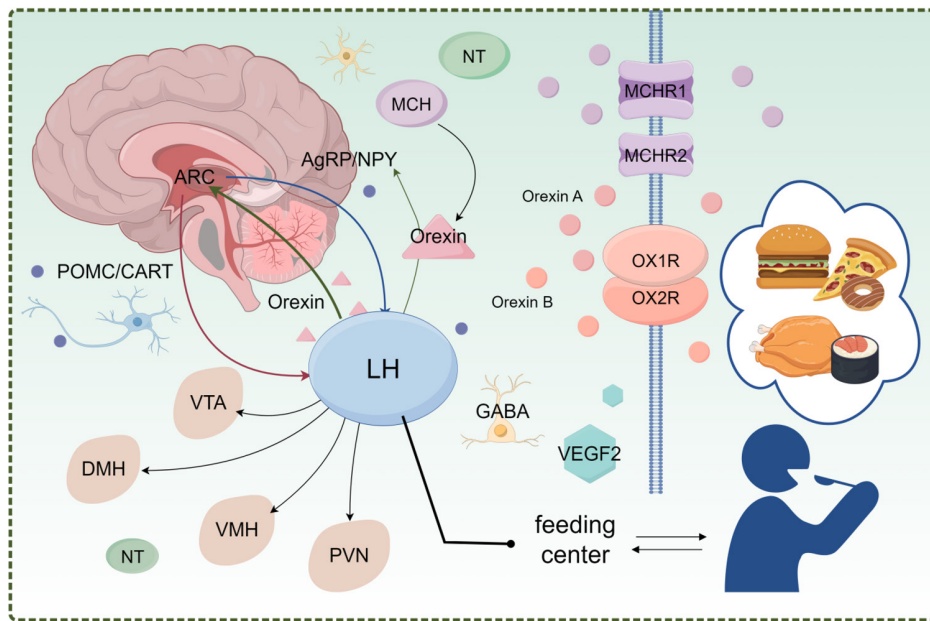


**Figure 3. LH-dominated appetite regulation circuit.** LH receives signals from AgRP/NPY and POMC/CART neuronal expression in ARCs and influences food intake by releasing MCHs, NTs, and orexin, while projecting signals into areas such as ARCs, DMHs, VMHs, and PVNs.

to feeding, and these manoeuvres are also beneficial (31). In contrast, activation of excitatory LH neurons expressing vesicular glutamate transporter type 2 inhibits feeding and leads to avoidance responses, while photoinhibition of these neurons is rewarding and leads to food consumption (32).

In most studies, evoked feeding was strongly associated with the reward characteristics of LH stimulation. LH neurons, for example, display different patterns of activity, including multiple stages of searching for and consuming food. LH activity regulates the hedonic quality of taste stimuli, suggesting the role of LH in the formation and maintenance of taste preference and aversion (33,34,35). In addition, taste sensory information enters the brain through the nucleus of the solitary tract (NTS) and reaches the LH through the PBN (36). This sensitivity to food palatability, coupled with exacerbated LH disturbance, suggests a role for the LH in promoting the consumption of palatable foods (37).

### 2.3. Mechanism of calcitonin gene-related peptide (CGRP) neurons in PBN

The third pillar consists mainly of CGRP neurons in the PBN. NTS is the main entry point for visceral, taste, hormone, and metabolic information into the brain, and PBN is the link between taste and visceral sensory information. These neurons effectively inhibit feeding when PBN is activated, but they do not increase food intake when inhibited. Studies have shown that activation of PBN neurons is associated with nausea (38), hormones causing satiety(39,40), and gastric dilatation-mediated visceral aversion (41,42).

CGRP neurons mediate the physiological effects of satiety, unlike PBN neurons that mediate the transmission of taste information (43), whose photogenetic activation strongly reduces food intake.  $PBN^{CGRP}$  neurons receive projections from excitatory Vglut 2-expressing neurons from NTS (44,45). When  $PBN^{CGRP}$  neurons are activated by signals associated with food intake, they provide a signal of satiety. Moreover, inhibition of  $PBN^{CGRP}$  neurons increases the duration of a meal without increasing total food consumption (46). As a result, the number of rounds of food consumption decreases over a fixed period of time, while the amount of food consumed increases within a round.

## 3. Effect of TCM on related factors in the hypothalamus

### 3.1. Effects of Chinese medicine monomers

The role of Chinese medicine monomers in the regulation of hypothalamic appetite is reported to be mainly in the neuropeptides AGRP/NPY and POMC/CART and leptin in ARCs. The following studies illustrate the effects of Chinese herbal monomers in this process (Figure 4 and Table 1).

Berberine in isoquinoline alkaloids is one of the main effective components of *Coptis chinensis* (Huanglian). According to TCM theory, *Coptis chinensis* Franch has effects of regulating the spleen and stomach, clearing heat and drying dampness, and eliminating fire and removing toxic substances, so it is one of the common TCMs used to treat obesity and diabetes. Modern studies have proven that berberine has a variety of



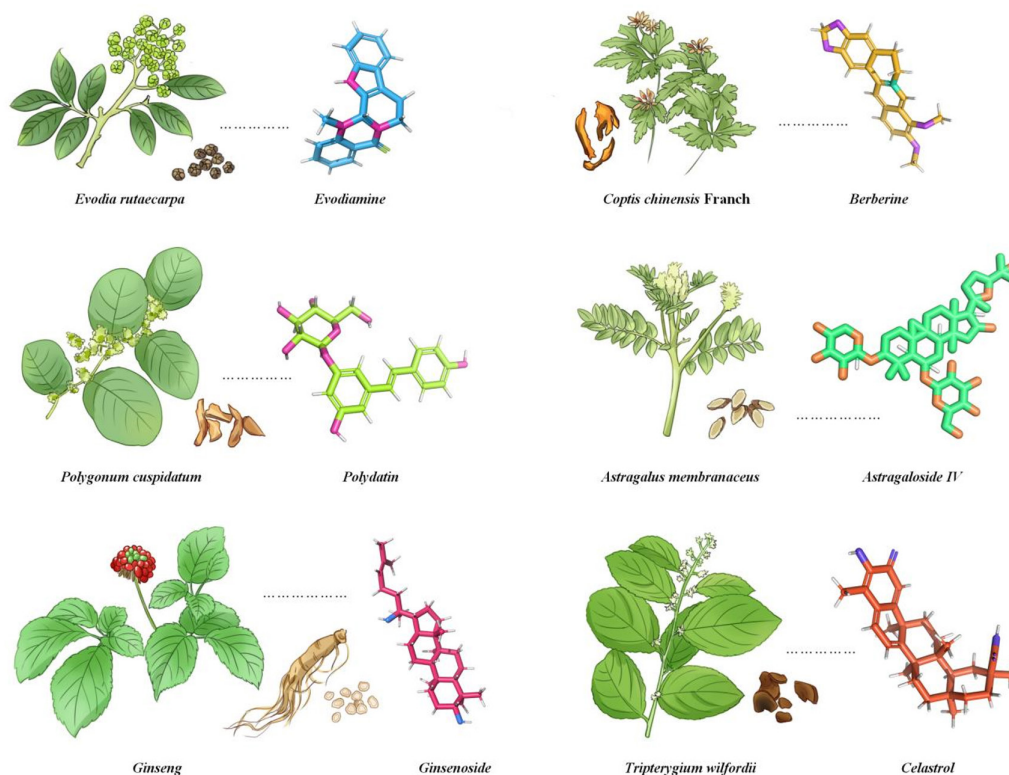


**Figure 4.** Several monomeric compounds derived from Chinese herbal medicines possess appetite-regulating effects. (A) *Evodia rutaecarpa* herbal plant and its processed slices; (B) 3D structural diagram of evodiamine; (C) *Coptis chinensis* Franch herbal plant and its processed slices; (D) 3D structural diagram of berberine; (E) *Polygonum cuspidatum* herbal plant and its processed slices; (F) 3D structural diagram of polydatin; (G) *Astragalus membranaceus* herbal plant and its processed slices; (H) 3D structural diagram of astragaloside IV; (I) *Ginseng* herbal plant and its processed slices; (J) 3D structural diagram of ginsenoside; (K) *Tripterygium wilfordii* herbal plant and its processed slices; (L) 3D structural diagram of celastrol. (Note: The Chinese herbal medicine illustrations and sliced herbs were modified and illustrated by the author based on reference images online. Image sources: <https://weibo.com>; <https://www.163.com>; <https://mp.weixin.qq.com>; <https://baike.baidu.com>; <http://www.dajiazhongyi.com/drug.php>; The 3D structural information on the compounds was obtained from the PubChem database, and the molecular models were rendered using the software PyMOL).

biological activities, including antioxidative action, anti-inflammatory action, anti-cancer action, immune regulation, and antibacterial activity (47). It can reduce blood glucose and blood lipids and inhibit lipid production (48). Park *et al.* demonstrated that berberine can reduce food intake, body weight, fat content, serum leptin, and glucose levels in mice fed a high-fat diet (49). The food intake of mice injected with NPY increased, compared to those injected with artificial cerebrospinal fluid, and the food intake of mice injected with berberine decreased significantly, while the serum glucose level in mice treated with NPY and berberine was significantly lower than that in mice injected with NPY.

Evodiamine is a tryptamine indole alkaloid and the principal bioactive compound in *Evodia rutaecarpa* (Wuzhuyu). Contemporary pharmacological studies have demonstrated that this compound has antineoplastic, cardioprotective, anti-ulcerative, antimicrobial, anti-inflammatory, and analgesic properties (50). A study has revealed that evodiamine exhibits a previously unidentified capacity to suppress adipogenesis through a mechanism involving the activation of ERK/MAPK signaling pathways, which subsequently down-regulated

the expression of adipogenic transcription factors and attenuated insulin-mediated Akt signaling (51). Shi *et al.* examined the impact of evodiamine on dietary consumption, body mass, and the levels of mRNA and peptide expression of appetite-regulating neuropeptides within the hypothalamus of male rats (52). Their findings demonstrated that intragastric administration of evodiamine at a dose of 40 mg/kg resulted in reduced food consumption and attenuated a body weight increase post-onset in rats. This was accompanied by elevated circulating leptin levels and a reduction in NPY and AgRP mRNA and peptide levels within the ARC. However, there were no significant alterations in the hypothalamic levels of POMC, CART, MCH, and MC4. Conversely, a lower dose of evodiamine (4 mg/kg) proved ineffective.

Astragaloside IV is one of the main components of *Astragalus membranaceus* (Huangqi) extract, which has many characteristics such as antioxidative action, anti-inflammatory action, and anti-apoptotic action. Thus far, numerous studies in cellular and animal models have shown that astragaloside IV is effective at protecting the cardiovascular system, lungs, kidneys, and the brain

Table 1. Several Chinese medicine monomers regulating appetite via the hypothalamus

| Monomers         | Source of Chinese herbal medicine           | Animals                          | Intervention                          | Functional mechanism   | Ref.    |
|------------------|---|----------------------------------|---------------------------------------|--|---------|
| Berberine        | <i>Coptis chinensis</i> (Huanglian)         | Mice fed a high-fat diet         | Intra-3rd ventricular microinjections | Decreases NPY levels   | (49)    |
| Evodiamine       | <i>Evodia rutaecarpa</i> (Wuzhuyu)          | Male rats                        | Intragastric administration           | Decreases AgRP/NPY mRNA levels and peptide expression  | (52)    |
| Astragaloside IV | <i>Astragalus membranaceus</i> (Huangqi)    | Fat-fed rats                     | Oral gavage                           | Increases p-STAT3, LepRb and POMC, decreases p-PI3K, SOCS3 and PTP1B                             | (55)    |
| Ginsenosides     | <i>Ginseng</i> (Renshen)                    | High fat diet induced obese mice | Intraperitoneal injection             | Lowers leptin levels   | (59)    |
| Celastrrol       | <i>Tripterygium wilfordii</i> (Leigongteng) | Diet-induced obese mice          | Intraperitoneal injection             | Enhances leptin sensitivity, suppresses PERK activity, increases phosphorylated STAT3 expression | (62,63) |
| Polydatin        | <i>Polygonum cuspidatum</i> (Huzhang)       | High-fat diet-induced obese mice | Oral gavage                           | Upregulates leptin levels  | (67)    |

(53,54). Jiang *et al.* found that astragaloside IV reduced leptin resistance in fat-fed rats by increasing p-signal transducer and activator of transcription 3 (STAT3), LepRb mRNA, and POMC mRNA and decreasing p-PI3K, suppressor of cytokine signaling (SOCS3), and protein tyrosine phosphatase-1B (PTP1B) mRNA in the hypothalamus (55). STAT3 modulates the suppression of AGRP/NPY neuronal activity and the facilitation of POMC/CART neuronal activation through its interaction with leptin and OB-R (56). Concurrently, the inhibition of SOCS3 and PTP1B expression augments STAT3 phosphorylation, thereby amplifying leptin signal transduction and ultimately having an anorexigenic effect (57). This pharmacological effect helps astragaloside IV prevent body weight gain and fat accumulation in rats with obesity induced by a high-fat diet, it alleviates metabolic disorders, and it reduces blood pressure and heart rate as well as noradrenaline levels in blood and kidney tissues.

Ginsenosides, which are extracted from ginseng (Renshen) with anti-obesity properties, have the ability to modulate metabolic processes and appetite regulation in murine models. A comprehensive review of previous *in vitro* and *in vivo* studies has indicated that ginseng and its ginsenosides enhance energy expenditure by activating the AMPK pathway and concurrently diminishing energy intake (58). Yao *et al.* demonstrated that ginsenosides inhibit ERS and regulate the phosphorylation of GT1-7 cells, a mouse hypothalamic gonadotropin-releasing hormone neuronal cell line, and STAT3 in the hypothalamus to reduce body weight and improve hepatic steatosis in mice with obesity induced by a high-fat diet (59). In that study, ginsenosides inhibited appetite, reduced body weight, visceral fat, body fat content, and blood glucose and leptin levels and improved glucose tolerance and blood lipids in obese mice.

Celastrrol is the most promising compound in *Tripterygium wilfordii* (Leigongteng) and has therapeutic effects on inflammatory diseases, cancer, neurodegenerative diseases, and other conditions such as diabetes, obesity, atherosclerosis, and hearing loss (60). A study has reported that celastrrol can reduce weight by regulating leptin sensitivity, energy metabolism, inflammation, lipid metabolism, and even intestinal microbiota (61). Liu *et al.* demonstrated that celastrrol mitigated ERS in the hypothalamus through the suppression of PERK activity, thereby increasing phosphorylated STAT3 expression and subsequently reducing food intake in mice (62). This indicates that celastrrol enhances leptin sensitivity, curtails energy expenditure, and induces weight loss in mice with obesity induced by a high-leptin diet. However, the compound showed no efficacy in ob/ob and db/db mouse models, implying that celastrrol functions as a leptin sensitizer. Similarly, Feng *et al.* demonstrated that celastrrol can enhance the sensitivity of leptin through interleukin-1 receptor 1 to inhibit appetite and weight loss (63). In

addition, the effect of celastrol has been found to be associated with the absence of PERK in arcuate nuclei POMC neurons, but specific mechanisms and PERK in other regions are still being examined (64).

Polydatin, one of the primary active components of *Polygonum cuspidatum* (Huzhang), has been shown in modern pharmacological studies to possess a broad spectrum of biological activities. These activities include the regulation of inflammation, oxidative stress, and apoptosis in key signaling pathways. Polydatin has demonstrated efficacy against cancer, against microbes, and providing protection for various systems, impacting the cardiovascular, nervous, endocrine, digestive, renal, and respiratory systems, as well as offering benefits for rheumatoid diseases, the skeletal system, and female health (65). *Polygonum cuspidatum* itself exhibits pharmacological properties such as dispelling dampness, alleviating jaundice, clearing heat, reducing toxins, activating blood, and removing stasis (66). Zheng *et al.* investigated the effects of polydatin on body weight control, glucose and lipid metabolism regulation, and combating inflammation in a mouse model of obesity induced by a high-fat diet (67). Polydatin reduced the weight of obese mice, regulated blood lipid levels, and significantly upregulated the expression of leptin mRNA and protein in the adipose tissue of obese mice.

### 3.2. Effects of TCM formulas

The absorption and metabolism of Chinese herbal decoctions and granules can also affect the hypothalamus (Table 2). They also play a role in regulating appetite by influencing AgRP/NPY, POMC/CART, leptin, and related factors.

Deng *et al.* conducted a clinical study on patients with simple obesity in which they were given Pingwei Powder, a combination of stir-fried *Rhizoma Atractylodis* (12 g), ginger-prepared *Cortex Magnoliae Officinalis* (9 g), *Pericarpium Citri Reticulatae* (6 g), and *Radix Glycyrrhizae Preparata* (3 g), and underwent ear acupoint treatment (68). This treatment resulted in a significant reduction in serum leptin and NPY levels.

Similarly, Li *et al.* treated simple obesity with Fangji Huangqi Decoction (*Fourstamen Stephania Root* 15 g, *Glycyrrhiza uralensis* 6 g, *Atractylodes macrocephala* Koidz 15 g, and *Astragalus membranaceus* 15 g) combined with abdominal massage (69). Although the drugs used differed from Pingwei Powder, the clinical trends were consistent. Fangji Huangqi Decoction can increase adiponectin levels, increase insulin hypersensitivity, enhance the inhibitory effect of insulin glycogen, and reduce blood lipid synthesis.

In a clinical trial, Jin *et al.* used Lianzhu Xiaoke Recipe containing *Coptis chinensis* Franch (30 g), parched *Rhizoma Atractylodis* (12 g), *Fructus Aurantii Immaturus* (10 g), *Cimicifugae* (10 g), *Pericarpium Citri Reticulatae* (12 g), parched *Rhizoma Pinelliae*

(10 g), *Crataegus pinnatifida* Bunge (30 g), *Massa Medicata Fermentata* (10 g), *Rhizoma Alismatis* (30 g), *Poria* (15 g), *Bombyx Batryticatus* (10 g), *Hirudo* (3 g), *Rhizoma Zingiberis* (10 g), *Jujubae Fructus* (10 g), and *Glycyrrhiza uralensis* (6 g) to treat patients with obesity and type II diabetes, with metformin hydrochloride as a comparison (70). The experimental data revealed a significant decrease in serum leptin and SOCS3 levels in the Chinese medicine group. In contrast, the difference in NPY levels before and after treatment was not statistically significant. The researchers concluded that the mechanisms of action of Lianzhu Xiaoke Decoction and metformin may be inconsistent and that further research is needed.

Bai *et al.* found that POMC expression in the hypothalamus of obese mice treated with Jiangtang No. 3 recipe (JTSHF) — a formulation consisting of *Ginseng*, *Bupleurum*, *Radix Paeoniae Rubra*, *Poria*, and 10 other traditional Chinese herbs in a 1:1:3:1 ratio of free decoction granules — was slightly higher than that in the model group. Additionally, AgRP levels decreased significantly, indicating that this recipe may help reduce food intake, lower body weight, and enhance glucose and lipid metabolism by influencing the expression of neuronal proteins associated with the hypothalamic feeding center (71). At the genus level, JTSHF increases the relative abundance of *Bacteroides*, *Prevotella*, and *Bacteroides* in the intestinal microflora and reduces the genera *Clostridium*, *Lactobacillus*, and *Oscillibacter*. JTSHF increased the content of short-chain fatty acids, increased the expression of GPR43/41, increased the expression of POMC, and decreased the expression of AgRP and NPY in the hypothalamus (72). Serum GLP-1 increased and ghrelin decreased after JTSHF intervention. Therefore, the authors believe that JTSHF plays an anti-diabetic role by affecting the composition, relative abundance and metabolites of intestinal flora, regulating a variety of intestinal brain peptides, affecting the feeding center of hypothalamus, and improving glycolipid metabolism.

Yang *et al.* reported that Wendan Decoction, consisting of *Citri Reticulatae Pericarpium* (10 g), *Pinelliae Rhizoma* (10 g), *Poria* (10 g), *Glycyrrhizae Radix Et Rhizoma* (3 g), *Caulis Bambusae in Taenia* (10 g), *Aurantii Fructus Immaturus* (10 g), *Zingiberis Rhizoma Recens* (5 slices), and *Jujubae Fructus*, effectively reduced body weight in obese rats on a high-fat diet, significantly improved the expression of leptin receptors and POMC mRNA in the hypothalamus, and reduced the level of leptin and OB-R in peripheral blood while reducing body weight (73).

Some medicines can also increase appetite-promoting factors. For example, Wang *et al.* observed changes in feeding behavior, body mass, Ob-R, AgRP, and NPY in rats with chronic restraint stress, revealing a possible mechanism of decreased food consumption and slow growth of body mass in rats with chronic stress.

**Table 2. Several Chinese medicine formulas regulating appetite via the hypothalamus**

| Compound                 | Constituents   | Efficacy   | Sample type                                   | Functional mechanisms   | Ref.    |
|--------------------------|--|--|---|---|---------|
| Pingwei Powder           | <i>Rhizoma Atractylodis</i> , ginger-prepared <i>Cortex Magnoliae Officinalis</i> , <i>Pericarpium Citri Reticulatae</i> , and <i>Radix Glycyrrhizae Preparata</i>   | Decreases body weight, BMI, and body fat percentage  | Simple obese patients                         | Reduces serum leptin and NPY levels   | (68)    |
| Fangji Huangqi Decoction | <i>Fourstamen Stephania Root</i> , <i>Glycyrrhiza uralensis</i> , <i>Atractylodes macrocephala</i> Koidz, and <i>Astragalus membranaceus</i>   | Decreases body weight while enhancing blood glucose, lipid, and blood pressure levels  | Simple obese patients                         | Reduces serum leptin and NPY levels, increases adiponectin levels                         | (69)    |
| Lianzhu Xiaoke recipe    | <i>Coptis chinensis</i> Franch, parched <i>Rhizoma Atractylodis</i> , <i>Fructus Aurantii Immaturus</i> , <i>Cimicifugae</i> , <i>Pericarpium Citri Reticulatae</i> , parched <i>Rhizoma Pinelliae</i> , <i>Crataegus pinnatifida</i> Bunge, <i>Massa Medicata Fermentata</i> , <i>Rhizoma Alismatis</i> , <i>Poria</i> , <i>Bombyx Batryticatus</i> , <i>Hirudo</i> , <i>Rhizoma Zingiberis</i> , <i>Jujubae Fructus</i> , and <i>Glycyrrhiza uralensis</i> | Lowers blood glucose, blood lipids, and fasting insulin levels, increases serum GLP-1 levels, and improves carotid atherosclerotic plaques | Obese patients with type 2 diabetes           | Reduces serum leptin and SOCS-3 levels  | (70)    |
| Jiangtang No. 3 recipe   | <i>Panax ginseng</i> C.A.Mey, <i>Radix bupleuri</i> , <i>Rehmannia glutinosa</i> (Gaertn.) DC., <i>Salvia miltiorrhiza</i> Bunge, <i>Coptis chinensis</i> Franch   | Lowers fasting and postprandial blood glucose levels and improves lipid levels   | Mice with type 2 diabetes fed a high-fat diet | Reduces AgRP levels, increases POMC levels  | (71,72) |
| Wendan Decoction         | <i>Citri Reticulatae Pericarpium</i> , <i>Pinelliae Rhizoma</i> , <i>Poria</i> , <i>Glycyrrhizae Radix Et Rhizoma</i> , <i>Caulis Bambusae in Taenia</i> , <i>Aurantii Fructus Immaturus</i> , <i>Zingiberis Rhizoma Recens</i> , and <i>Jujubae Fructus</i>   | Inhibits obesity   | High fat diet induced obese rats              | Improves the expression of POMC, reduces the level of leptin and OB-R in peripheral blood | (73)    |
| Xiaoyao Powder           | <i>Bupleurum</i> , <i>Angelica sinensis</i> , <i>Radix Paeoniae Alba</i> , <i>Rhizoma Atractylodis Macrocephalae</i> , <i>Radix Glycyrrhizae</i> , <i>Rhizoma Zingiberis Recens</i> , <i>Herba Menthae</i>   | Improves stress resistance and appetite  | Rats after chronic immobilization stress      | Reduces Ob-R levels in ARCs, and increases AgRP and NPY levels                            | (74)    |
| Liujiunzi Decoction      | <i>Radix Ginseng</i> , <i>Rhizoma Atractylodis Macrocephalae</i> , <i>Poria</i> , <i>Radix Glycyrrhizae</i> , <i>Pericarpium Citri Reticulatae</i> , and <i>Rhizoma Pinelliae</i>  | Ameliorates cisplatin-induced injuries in the gastric antrum, liver, and ileum, and alleviates chemotherapy-induced anorexia               | Rats with anorexia                            | Decreases serum leptin levels, down-regulates CART and POMC, up-regulates NPY and AgRP    | (75)    |



Concurrently, Xiaoyao Powder (*Bupleurum*, *Angelica sinensis*, *Radix Paeoniae Alba*, *Rhizoma Atractylodis Macrocephalae*, *Radix Glycyrrhizae*, *Rhizoma Zingiberis Recens*, *Herba Menthae*) was selected as the intervention drug (74). The results indicated that Xiaoyao Powder effectively alleviated the symptoms of decreased appetite and reduced body weight under chronic restraint stress. This may be related to the inhibition of Ob-R protein and gene expression in ARCs and the upregulation of AgRP and NPY protein and gene expression.

In the treatment of different diseases, formulas affect the appetite-regulating neuropeptides of the hypothalamus differently. Liujunzi Decoction originates from the Medical Biography in the Ming dynasty and consists of six types of herbal medicines such as *Radix Ginseng*, *Rhizoma Atractylodis Macrocephalae*, *Poria*, *Radix Glycyrrhizae*, *Pericarpium Citri Reticulatae*, and *Rhizoma Pinelliae*. It benefits qi and invigorates the spleen and dries dampness to eliminate phlegm. Dai *et al.* created a rat model of anorexia by intraperitoneal injection of cisplatin to evaluate the efficacy of Liujunzi Decoction (75). Results showed that Liujunzi Decoction alleviated injury to the gastric antrum, liver, and ileum induced by cisplatin, decreased the serum leptin level, and also decreased the levels of ghrelin, IL-6 and growth differentiation factor 15. In the antrum and hypothalamus, Liujunzi Decoction inhibited cisplatin-induced activation of the JAK-STAT signaling pathway, resulting in down-regulation of transcription levels of the downstream anorexia-related neuropeptides CART, POMC, and TRH and up-regulation of expression of the hypothalamic appetite-related peptides NPY and AGRP.

### 3.3. Effects of a single medicine or extract

There are two types of Chinese medicine extracts and a type of lyophilized powder that can regulate appetite-related neuropeptides. These are *Cyclocarya paliurus* (Qingqianliu) aqueous extract, *Ginkgo biloba* (Yinxing) extract, and *Ziziphi Spinosae Semen* freeze-dried powder (Table 3).

*Cyclocarya paliurus* (Batalin) Iljinskaja, an indigenous and rare monocotyledonous species from Southern China, is renowned for its extensive traditional medicinal properties. These include clearing heat, detoxification, increasing saliva production, quenching thirst, anti-inflammatory action, insecticidal action, dispelling wind, and relieving itchiness. Additionally, it demonstrates efficacy in the prevention and management of diabetes, hypertension, hyperlipidemia, dizziness, and edema as well as in reducing cholesterol and modulating immune system functions (76). To reduce obesity, *Cyclocarya paliurus* ethanol leaf extracts primarily alleviate glucose metabolism disorders by reducing glucose absorption, modulating lipid profiles, regulating the insulin signaling pathway, decreasing  $\beta$ -cell apoptosis, enhancing insulin synthesis and secretion, altering

**Table 3. Several Chinese medicines or extracts regulating appetite via the hypothalamus**

| Medicine or extract                               | Efficacy   | Animals                             | Functional mechanism  | Ref.    |
|---|--|-------------------------------------|---|---------|
| <i>Cyclocarya paliurus</i> aqueous extract        | Clears heat, detoxifies, increases saliva production, anti-inflammatory action, etc.         | Obese rats with metabolic syndrome  | Upregulates POMC, downregulates NPY   | (79)    |
| <i>Ginkgo biloba</i> extract                      | Promotes blood circulation and dispels blood stasis, removes turbidity and reduces blood fat | Diet induced obese rats             | Decreases the activity of 5-HT transporter, upregulates 5-HT2C serotonin receptor, POMC, and CART | (81-83) |
| <i>Ziziphi Spinosae Semen</i> freeze-dried powder | Nourishes the heart and tonifies the liver, calms the heart and tranquilizes the mind        | Rats under 24 h continuous darkness | Increases leptin and POMC levels, decreases NPY levels  | (85)    |

the composition of the gut microbiota, and inhibiting  $\alpha$ -glucosidase activity (77). In rats with diabetes induced by a high-fat diet and streptozotocin, both the ethanol and aqueous extracts of *Cyclocarya paliurus* demonstrated comparable antihyperglycemic, antihyperlipidemic, and antioxidant properties, with no significant differences observed between the two extracts (78). Xu *et al.* used Cg-Leprecp/NDmcr SHR/cp rats as an obesity and metabolic syndrome model to investigate the effects of *Cyclocarya paliurus* aqueous extract (CPAE) (79). Their findings indicated that CPAE administration significantly decreased food consumption, body weight, organ weight, adiposity, and BMI in SHR/cp rats. Additionally, CPAE treatment resulted in a reduction in fasting blood glucose, fasting serum insulin, HOMA-IR, serum free fatty acids, serum malondialdehyde, serum superoxide dismutase, and serum total glutathione levels. Moreover, CPAE markedly increased the phosphorylation levels of InsR, IRS1, PI3Kp85, Akt, and FoXO1, and upregulated the protein expression of POMC in the hypothalamus while significantly downregulating NPY expression.

*Ginkgo biloba* has demonstrated effects both centrally and peripherally, influencing the electrochemical, physiological, neurological, and vascular systems in animal models (80). *Ginkgo biloba* extract (GBE), derived from the desiccated foliage of the plant, is regarded as one of the most effective extracts for therapeutic applications. In a pilot study, Banin *et al.* established that GBE markedly diminished food consumption and body fat accumulation while averting diet-induced hyperglycemia and dyslipidemia in obese rats. On this basis, the ovaries of female rats were removed to simulate menopause, and GBE was given by gavage for 14 days (81). Banin *et al.* showed that GBE decreased the activity of 5-HT transporter, increase the local concentration of 5-HT, and improved appetite and alleviated obesity caused by an estrogen deficiency in climacteric rats (82). A separate study indicated that a single oral administration of GBE significantly upregulated the hypothalamic gene expression of anorexigenic mediators in male rats, such as the 5-HT<sub>2C</sub> serotonin receptor and the neuropeptides POMC and CART, while there were no observable changes in the expression of orexigenic mediators (83).

*Ziziphi Spinosae Semen* has the effects of alleviating anxiety, tranquillizing and hypnosis, preventing depression, and preventing convulsions (84). Chinese medicine theory holds that *Ziziphi Spinosae Semen* has the effects of tonifying the liver and calming the heart, and arresting sweating and promoting the production of bodily fluids. It can be used to treat insomnia due to deficiency and restlessness, palpitations, body deficiencies and sweating, and thirst due to disturbed bodily fluids. Xu *et al.* reported that the lyophilized powder of *Ziziphi Spinosae Semen* increased the levels of leptin and POMC in the hypothalamus of rats and decreased the levels of NPY so as to correct the

disturbance of awakening from sleep and an abnormal rate of energy metabolism caused by 24 h of darkness (85).

### 3.4. Effects of Chinese patent medicines

Three other Chinese patent medicines have also been shown to regulate appetite *via* the hypothalamus, and their mechanisms of action are reported in the following studies (Table 4). These studies suggest that these medicines influence the hypothalamic pathways by modulating neuropeptide expression and other signaling pathway activity.

Danzhi Jiangtang capsules, consisting of *Radix Pseudostellariae*, *Radix Rehmanniae*, *Semen Cuscutae*, *Cortex Moutan*, and *Hirudo*, are traditionally used to enhance qi, nourish yin, and promote blood circulation. Bi *et al.* found that Danzhi Jiangtang Capsules can promote the secretion of  $\alpha$ -MSH and inhibit AgRP secretion in the hypothalamus (86). These capsules can improve the feeding behavior of mice, reduce their body weight, alleviate obesity, and lower the risk of diabetes. Their clinical study also showed that Danzhi Jiangtang Capsules can improve the polyfeeding behavior of diabetes patients and that they have the effects of reducing body weight, regulating blood lipids, and reducing BMI.

Jingui Shenqi pills (JSPs) were initially documented in the classical medical text Essentials from the Golden Cabinet (*Jin Guì Yào Lǜè*). The formulation includes *Radix Rehmanniae*, *Rhizoma Dioscoreae*, *Fructus Corni*, *Poria*, *Cortex Moutan*, *Rhizoma Alismatis*, *Ramulus Cinnamomi*, and *Radix Aconiti Lateralis Preparata*. Zhang *et al.* evaluated the function of JSPs in mice with type 2 diabetes (87). Results indicated that JSPs effectively inhibited appetite and led to a steady decline in body weight, fasting blood glucose, and oral glucose tolerance in diabetic mice. In addition, JSPs result in increased dendritic length and branching, which protects hypothalamic neurons and synaptic structures. The expression and activation of POMC increased significantly, while the expression and activation of AgRP decreased when primary hypothalamic neurons were treated with 10% JSPs-rich serum, and these effects may be related to the regulation of PI3K.

There are also drugs in Chinese patent medicines that promote appetite. Child compound Endothelium corneum, consisting of *Endothelium Corneum Gigeriae Galli* and *Massa Medicata Fermentata*, has the effects of invigorating the spleen, stimulating appetite, promoting digestion, and removing food stagnancy. In functional dyspepsia, child compound Endothelium corneum has been shown to inhibit the hyperactive POMC/Stat3/Akt pathway in the rat hypothalamus and enhance gastrointestinal motility by rebalancing the homeostasis of the brain-intestine-microbiota axis in rats (88).

Table 4. Several Chinese patent medicines regulating appetite via the hypothalamus

| Chinese patent medicine            | Constituents  | Efficacy  | Animals                        | Functional mechanisms  | Ref. |
|------------------------------------|---|---|--------------------------------|--|------|
| Danzhi Jiangtang Capsules          | <i>Radix Pseudostellariae</i> , <i>Radix Rehmanniae</i> , <i>Semen Cuscutae</i> , <i>Cortex Moutan</i> , and <i>Hirudo</i>  | Nourishes Yin and moistens dryness, promotes blood circulation and dispels blood stasis       | Male db/db mice                | Promotes the secretion of $\alpha$ -MSH and inhibit AgRP secretion | (86) |
| Jingui Shengqi pills               | <i>Radix Rehmanniae</i> , <i>Rhizoma Dioscoreae</i> , <i>Fructus Corni</i> , <i>Poria</i> , <i>Cortex Moutan</i> , <i>Rhizoma Alismatis</i> , <i>Ramulus Cinnamomi</i> , and <i>Radix Aconiti Lateralis Preparata</i> | Warms and tonifies kidney-yang, dissipates Qi and promotes water circulation                  | Mice with type 2 diabetes      | Increases POMC, decreases AgRP                                     | (87) |
| Child compound Endothelium corneum | <i>Endothelium Corneum Gigeriae Galli</i> and <i>Massa Medicata Fermentata</i>  | Invigorates the spleen and stimulates appetite, promotes digestion and removes food stagnancy | Rats with functional dyspepsia | Increases NPY  | (88) |

4. Discussion and prospects

In modern medicine, factors like genetics, lifestyle, diet, and pathology affect drug outcomes, underscoring the need for individualized treatments. Chinese medicine formulas, with their complex components and multi-target mechanisms, offer unique therapeutic effects under various individual- and disease-related conditions, in contrast to modern drugs with a single target. This highlights TCM's advantage in maintaining internal balance and its flexibility in appetite regulation. Most appetite-suppressing medicines in TCM function by invigorating the spleen, removing dampness, promoting blood circulation, and regulating qi, aligning with the "spleen-main movement" theory. These medicines act through various mechanisms, affecting appetite and demonstrating TCM's multi-level approach to hypothalamus regulation. For instance, Xiaoyao Powder targets the liver and spleen simultaneously, achieving a balance through overall regulation rather than focusing on a single organ or pathway. TCM's adaptability shows its potential in comprehensive appetite regulation.

Several monomeric components from TCM have been shown to regulate appetite. While studies on these monomers help explain TCM mechanisms, their clinical effects often differ from those of single or combined herbal formulations. TCM formulas contain diverse chemical components targeting multiple pathways, helping to balance various organs. TCM can also affect the expression of neuropeptides related to the regulation of the appetite of the hypothalamus through a variety of signaling pathways, such as the PI3K/Akt signalin pathway, the autophagy pathway regulated by AMPK, and the PERK-mediated endoplasmic reticulum stress in the hypothalamus. Different TCM formulations can exhibit similar mechanisms, and the same drug's efficacy may vary with different formulas and diseases. Exploring the synergistic effects of these formulas could reveal their overall benefits. In order to identify more cost-effective pharmaceutical ingredients, the focus of future research can be gradually extended to the interaction of neuropeptides with downstream pathways. Exploring the synergistic effects of these pathways might reveal novel therapeutic strategies for metabolic disorders. Integrating TCM with modern pharmacology could potentially optimize treatment efficacy and minimize adverse effects, offering holistic approaches to appetite regulation.

Drug toxicity to the liver and kidneys must be considered. For instance, further studies on evodiamine have revealed its potential liver, heart, and kidney toxicity, which is dose- and time-dependent (50). This indicates that future research should carefully consider the dosage and timing of new drugs. TCM formulas can reduce toxicity and enhance efficacy, making them potentially more suitable for long-term use. However, TCM formulas are complex, with numerous interactions

among different herbs. Thus, studying the mechanisms of TCM's toxic adverse effects and understanding these interactions at a molecular level is crucial. By integrating traditional practices with modern pharmacology, toxic components and their pathways can be identified, improving the safety of long-term TCM use and reducing adverse reactions, thus maximizing the benefits of Chinese medicine.

In addition, improving oral bioavailability is a significant challenge in the development of new drugs from TCM monomers. Berberine, despite its wide array of pharmacological activities, has low bioavailability due to poor solubility, low permeability, P-glycoprotein efflux, and hepatic and intestinal metabolism. Long-term oral administration of berberine may also alter gut flora and affect other physiological functions, limiting its clinical use (48). Previous studies orally administered TCM formulas, extracts, and patent medicines, but monomers were given both orally and *via* injection. To provide convenient long-term treatment, enhancing oral bioavailability is crucial for TCM research and application. Modern drug development emphasizes drug efficacy and safety; improving bioavailability can impact treatment outcomes and enable more scientific evaluations of TCM's efficacy and toxicity, facilitating new drug development and promoting TCM in the global market.

According to current research, appetite-regulating mechanisms of the hypothalamus have not been fully elucidated, and especially their role in LH and PBN. A few studies have clearly shown that the mechanism of appetite control is related to the regulation of orexin and its receptors, MCHs, and CGRP neurons, but the potential role of TCMs in affecting that mechanism cannot be denied. Further investigation into how TCMs influence these neural circuits could unveil novel pathways for appetite regulation. Of course, we cannot ignore other biological processes involved in weight reduction, such as crocin, which inhibits obesity by inhibiting adipocyte differentiation and promoting lipolysis (89). This discussion with the nervous system will help us better understand the role of TCM in it.

Therefore, extensive research is essential to exploring the mechanisms of action of TCM, given its multi-target and multi-pathway nature. The primary objective is translating basic research into clinical use to identify compounds with improved efficacy, safety, and fewer adverse reactions. Moreover, research and development should focus on creating a wide range of adaptable, highly cost-effective, and user-friendly formulations to provide new avenues for preventing and treating obesity.

## 5. Conclusions

TCMs may affect appetite mechanisms in the hypothalamus, helping to control appetite, reduce body weight, and improve metabolic outcomes. Using

ancient remedies in conjunction with modern scientific understanding, TCM can help to develop new, more effective treatments for obesity. Integrating traditional and modern medicine provides a fresh perspective on treating metabolic disorders, where long-term therapeutic options remain limited. This synergy between ancient wisdom and contemporary science can foster innovative therapeutic strategies, potentially unlocking novel pathways for metabolic regulation. Exploring these integrative approaches might also reveal previously untapped mechanisms, enhancing our ability to combat obesity and related metabolic diseases more effectively.

## Acknowledgements

We thank all of the collaborators and participants in the review.

**Funding:** This work was supported by the National Research and Training Program for Outstanding Clinical Talents in Traditional Chinese Medicine (grant number: National Letter of TCM Practitioners No. 1 (2022) and the 2023 Qilu Biancang Traditional Chinese Medicine talent training project (Lu health Letter No. [2024] 78).

**Conflict of Interest:** The authors have no conflicts of interest to disclose.

## References

- Loos RJF, Yeo GSH. The genetics of obesity: From discovery to biology. *Nat Rev Genet.* 2022; 23:120-133.
- Miller E, Edelman S, Campos C, Anderson JE, Parkin CG, Polonsky WH. Inadequate insurance coverage for overweight/obesity management. *Am J Manag Care.* 2024; 30:365-371.
- Haase CL, Varbo A, Laursen PN, Schnecke V, Balen AH. Association between body mass index, weight loss and the chance of pregnancy in women with polycystic ovary syndrome and overweight or obesity: A retrospective cohort study in the UK. *Hum Reprod.* 2023; 38:471-481.
- Chinese Medical Association Endocrinology Branch, Chinese Association of Traditional Chinese Medicine Diabetes Branch, Chinese Association of Physicians Surgeons Branch Board of Obesity and Diabetes Surgeons, Chinese Association of Physicians Surgeons Branch Board of Obesity and Diabetes Surgeons, Chinese Association of Research Hospitals Diabetes and Obesity Surgical Committee. Multidisciplinary clinical consensus on diagnosis and treatment of obesity (2021 edition). *Chin J Endocrin Metab.* 2021; 37:959-972. (in Chinese)
- Hill JO, Wyatt HR, Peters JC. Energy balance and obesity. *Circulation.* 2012; 126:126-132.
- Solas M, Milagro FI, Martínez-Urbistondo D, Ramirez MJ, Martínez JA. Precision obesity treatments including pharmacogenetic and nutrigenetic approaches. *Trends Pharmacol Sci.* 2016; 37:575-593.
- Gadde KM, Apolzan JW, Berthoud HR. Pharmacotherapy for patients with obesity. *Clin Chem.* 2018; 64:118-129.
- Smith SR, Weissman NJ, Anderson CM, Sanchez M, Chuang E, Stubbe S, Bays H, Shanahan WR; Behavioral



- Modification and Lorcaserin for Overweight and Obesity Management (BLOOM) Study Group. Multicenter, placebo-controlled trial of lorcaserin for weight management. *N Engl J Med.* 2010; 363:245-256.
9. Aronne LJ, Wadden TA, Peterson C, Winslow D, Odeh S, Gadde KM. Evaluation of phentermine and topiramate versus phentermine/topiramate extended-release in obese adults. *Obesity (Silver Spring).* 2013; 21:2163-2171.
10. Pi-Sunyer X, Astrup A, Fujioka K, Greenway F, Halpern A, Krempf M, Lau DC, le Roux CW, Violante Ortiz R, Jensen CB, Wilding JP; SCALE Obesity and Prediabetes NN8022-1839 Study Group. A randomized, controlled trial of 3.0 mg of liraglutide in weight management. *N Engl J Med.* 2015; 373:11-22.
11. Zhu Y, Tao F. Research progress on appetite suppression by traditional Chinese herbal medicines based on appetite regulation mechanism. *Shanghai J Trad Chin Med.* 2022; 56:79-86. (in Chinese)
12. Morton GJ, Meek TH, Schwartz MW. Neurobiology of food intake in health and disease. *Nat Rev Neurosci.* 2014; 15:367-378.
13. Saper CB, Chou TC, Elmquist JK. The need to feed: Homeostatic and hedonic control of eating. *Neuron.* 2002; 36:199-211.
14. Yu Mengxian, Fang Penghua, Zhang Zhenwen. The role of hypothalamic neuropeptides in the central nervous system regulation of energy metabolism. *China J Modern Med.* 2022; 32:45-50. (in Chinese)
15. Sternson SM, Eisel AK. Three pillars for the neural control of appetite. *Annu Rev Physiol.* 2017; 79:401-423.
16. Waterson MJ, Horvath TL. Neuronal regulation of energy homeostasis: Beyond the hypothalamus and feeding. *Cell Metab.* 2015; 22:962-970.
17. Chen J, Cheng M, Wang L, Zhang L, Xu D, Cao P, Wang F, Herzog H, Song S, Zhan C. A vagal-NTS neural pathway that stimulates feeding. *Curr Biol.* 2020; 30:3986-3998.
18. Vohra MS, Benchoula K, Serpell CJ, Hwa WE. AgRP/ NPY and POMC neurons in the arcuate nucleus and their potential role in treatment of obesity. *Eur J Pharmacol.* 2022; 915:174611.
19. Tung YC, Piper SJ, Yeung D, O'Rahilly S, Coll AP. A comparative study of the central effects of specific proopiomelanocortin (POMC)-derived melanocortin peptides on food intake and body weight in POMC null mice. *Endocrinology.* 2006; 147:5940-5947.
20. Wang X, Wang S, Fang C, Wang J, Kuang X, Zhao D, Wang Y. Changes of appetite regulation factors in hypothalamic arcuate nucleus of rats after chronic immobilization stress. *Chin J Pathophys.* 2019; 35:473-478. (in Chinese)
21. Secher A, Jelsing J, Baquero AF, *et al.* The arcuate nucleus mediates GLP-1 receptor agonist liraglutide-dependent weight loss. *J Clin Invest.* 2014; 124:4473-4488.
22. Nonogaki K. Serotonin conflict in sleep-feeding. *Vitam Horm.* 2012; 89:223-239.
23. Nonogaki K. The regulatory role of the central and peripheral serotonin network on feeding signals in metabolic diseases. *Int J Mol Sci.* 2022; 23:1600.
24. He Q, Yuan Q, Shan H, Wu C, Gu Y, Wu K, Hu W, Zhang Y, He X, Xu HE, Zhao LH.. Mechanisms of ligand recognition and activation of melanin-concentrating hormone receptors. *Cell Discov.* 2024; 10:48.
25. Grady FS, Boes AD, Geerling JC. A century searching for the neurons necessary for wakefulness. *Front Neurosci.* 2022; 16:930514.
26. Yin J, Babaoglu K, Brautigam CA, Clark L, Shao Z, Scheuermann TH, Harrell CM, Gotter AL, Roecker AJ, Winrow CJ, Renger JJ, Coleman PJ, Rosenbaum DM. Structure and ligand-binding mechanism of the human OX1 and OX2 orexin receptors. *Nat Struct Mol Biol.* 2016; 23:293-299.
27. Mirbolouk B, Khakpour-Taleghani B, Rostampour M, Jafari A, Rohampour K. Enhanced low-gamma band power in the hippocampus and prefrontal cortex in a rat model of depression is reversed by orexin-1 receptor antagonism. *IBRO Neurosci Rep.* 2023; 15:386-394.
28. de La Serre CB, Kim YJ, Moran TH, Bi S. Dorsomedial hypothalamic NPY affects cholecystokinin-induced satiety *via* modulation of brain stem catecholamine neuronal signaling. *Am J Physiol Regul Integr Comp Physiol.* 2016; 311:R930-R939.
29. Stratford TR, Wirtshafter D. Lateral hypothalamic involvement in feeding elicited from the ventral pallidum. *Eur J Neurosci.* 2013; 37:648-653.
30. Petrovich GD, Setlow B, Holland PC, Gallagher M. Amygdalo-hypothalamic circuit allows learned cues to override satiety and promote eating. *J Neurosci.* 2002; 22:8748-8753.
31. Jennings JH, Ung RL, Resendez SL, Stamatakis AM, Taylor JG, Huang J, Veleta K, Kantak PA, Aita M, Shilling-Scriver K, Ramakrishnan C, Deisseroth K, Otte S, Stuber GD. Visualizing hypothalamic network dynamics for appetitive and consummatory behaviors. *Cell.* 2015; 160:516-527.
32. Jennings JH, Rizzi G, Stamatakis AM, Ung RL, Stuber GD. The inhibitory circuit architecture of the lateral hypothalamus orchestrates feeding. *Science.* 2013; 341:1517-1521.
33. Touzani K, Sclafani A. Conditioned flavor preference and aversion: role of the lateral hypothalamus. *Behav Neurosci.* 2001; 115:84-93.
34. Touzani K, Sclafani A. Lateral hypothalamic lesions impair flavour-nutrient and flavour-toxin trace learning in rats. *Eur J Neurosci.* 2002; 16:2425-2433.
35. Li JX, Yoshida T, Monk KJ, Katz DB. Lateral hypothalamus contains two types of palatability-related taste responses with distinct dynamics. *J Neurosci.* 2013; 33:9462-9473.
36. Tokita K, Armstrong WE, St John SJ, Boughter JD Jr. Activation of lateral hypothalamus-projecting parabrachial neurons by intraorally delivered gustatory stimuli. *Front Neural Circuits.* 2014; 8:86.
37. Wiepkema PR. Positive feedbacks at work during feeding. *Behaviour.* 1971; 39:266-273.
38. Reilly S. The parabrachial nucleus and conditioned taste aversion. *Brain Res Bull.* 1999; 48:239-254.
39. Alhadeff AL, Hayes MR, Grill HJ. Leptin receptor signaling in the lateral parabrachial nucleus contributes to the control of food intake. *Am J Physiol Regul Integr Comp Physiol.* 2014; 307:R1338-1344.
40. Alhadeff AL, Baird JP, Swick JC, Hayes MR, Grill HJ. Glucagon-like Peptide-1 receptor signaling in the lateral parabrachial nucleus contributes to the control of food intake and motivation to feed. *Neuropsychopharmacol.* 2014; 39:2233-2243.
41. Baird JP, Travers JB, Travers SP. Parametric analysis of gastric distension responses in the parabrachial nucleus. *Am J Physiol Regul Integr Comp Physiol.* 2001; 281:R1568-1580.
42. Sabbatini M, Molinari C, Grossini E, Mary DASG, Vacca

- G, Cannas M. Retraction Note: The pattern of c-Fos immunoreactivity in the hindbrain of the rat following stomach distension. *Exp Brain Res*. 2024; 242:987.
43. Carter ME, Soden ME, Zweifel LS, Palmiter RD. Genetic identification of a neural circuit that suppresses appetite. *Nature*. 2013; 503:111-114.
44. Wu Q, Clark MS, Palmiter RD. Deciphering a neuronal circuit that mediates appetite. *Nature*. 2012; 48:594-597.
45. Travagli RA, Hermann GE, Browning KN, Rogers RC. Brainstem circuits regulating gastric function. *Annu Rev Physiol*. 2006; 68:279-305.
46. Campos CA, Bowen AJ, Schwartz MW, Palmiter RD. Parabrachial CGRP neurons control meal termination. *Cell Metab*. 2016; 23:811-820.
47. Cui Y, Zhou Q, Jin M, Jiang S, Shang P, Dong X, Li L. Research progress on pharmacological effects and bioavailability of berberine. *Naunyn Schmiedeberg Arch Pharmacol*. 2024; 397:8485-8514.
48. Sun R, Kong B, Yang N, *et al*. The hypoglycemic effect of berberine and berberrubine involves modulation of intestinal farnesoid X receptor signaling pathway and inhibition of hepatic gluconeogenesis. *Drug Metab Dispos*. 2021; 49:276-286.
49. Park HJ, Jung E, Shim I. Berberine for appetite suppressant and prevention of obesity. *Biomed Res Int*. 2020; 2020:3891806.
50. Lin L, Liu Y, Tang R, Ding S, Lin H, Li H. Evodiamine: A extremely potential drug development candidate of alkaloids from *Evodia rutaecarpa*. *Int J Nanomedicine*. 2024; 19:9843-9870.
51. Wang T, Wang Y, Kontani Y, Kobayashi Y, Sato Y, Mori N, Yamashita H. Evodiamine improves diet-induced obesity in a uncoupling protein-1-independent manner: Involvement of antiadipogenic mechanism and extracellularly regulated kinase/mitogen-activated protein kinase signaling. *Endocrinol*. 2008; 149:358-366.
52. Shi J, Yan J, Lei Q, Zhao J, Chen K, Yang D, Zhao X, Zhang Y. Intragastric administration of evodiamine suppresses NPY and AgRP gene expression in the hypothalamus and decreases food intake in rats. *Brain Res*. 2009; 1247:71-78.
53. Fu J, Wang Z, Huang L, Zheng S, Wang D, Chen S, Zhang H, Yang S. Review of the botanical characteristics, phytochemistry, and pharmacology of *Astragalus membranaceus* (Huangqi). *Phytother Res*. 2014; 28:1275-1283.
54. Zhang J, Wu C, Gao L, Du G, Qin X. Astragaloside IV derived from *Astragalus membranaceus*: A research review on the pharmacological effects. *Adv Pharmacol*. 2020; 87:89-112.
55. Jiang P, Ma D, Wang X, Wang Y, Bi Y, Yang J, Wang X, Li X. Astragaloside IV prevents obesity-associated hypertension by improving pro-inflammatory reaction and leptin resistance. *Mol Cells*. 2018; 41:244-255.
56. Kwon O, Kim KW, Kim MS. Leptin signalling pathways in hypothalamic neurons. *Cell Mol Life Sci*. 2016; 73:1457-1477.
57. Pan WW, Myers MG Jr. Leptin and the maintenance of elevated body weight. *Nat Rev Neurosci*. 2018; 19:95-105.
58. Li Z, Ji GE. Ginseng and obesity. *J Ginseng Res*. 2018; 42:1-8.
59. Yao Y. Ginsenosides reduce body weight and ameliorate hepatic steatosis in high fat diet-induced obese mice *via* endoplasmic reticulum stress and p-STAT3/STAT3 signaling. *Mol Med Rep*. 2020; 21:1059-1070.
60. Cascão R, Fonseca JE, Moita LF. Celastrol: A spectrum of treatment opportunities in chronic diseases. *Front Med (Lausanne)*. 2017; 4:69.
61. Xu S, Feng Y, He W, Xu W, Xu W, Yang H, Li X. Celastrol in metabolic diseases: Progress and application prospects. *Pharmacol Res*. 2021; 167:105572.
62. Liu J, Lee J, Salazar Hernandez MA, Mazitschek R, Ozcan U. Treatment of obesity with celastrol. *Cell*. 2015; 161:999-1011.
63. Feng X, Guan D, Auen T, Choi JW, Salazar Hernández MA, Lee J, Chun H, Faruk F, Kaplun E, Herbert Z, Copps KD, Ozcan U. IL1R1 is required for celastrol's leptin-sensitization and antiobesity effects. *Nat Med*. 2019; 25:575-582.
64. He Z, Lieu L, Dong Y, *et al*. PERK in POMC neurons connects celastrol with metabolism. *JCI Insight*. 2021; 6:e145306.
65. Karami A, Fakhri S, Kooshki L, Khan H. Polydatin: Pharmacological mechanisms, therapeutic targets, biological activities, and health benefits. *Molecules*. 2022; 27:6474.
66. Liu LT, Guo G, Wu M, Zhang WG. The progress of the research on cardio-vascular effects and acting mechanism of polydatin. *Chin J Integr Med*. 2012; 18:714-719.
67. Zheng L, Wu J, Mo J, Guo L, Wu X, Bao Y. Polydatin inhibits adipose tissue inflammation and ameliorates lipid metabolism in high-fat-fed mice. *Biomed Res Int*. 2019; 2019:7196535.
68. Deng C, Zhang Y, Cen M, Cai J, Lai Y. Effects of Pingwei Powder combined with auricular point therapy on serum levels of NPY and leptin in simple obesity patients. *Guangzhou Medical Journal*. 2018; 49:19-22. (in Chinese)
69. Li Y, Shen X, Yuan J. Treatment of simple obesity with spleen deficiency and dampness obstruction by combination of Fangji Huangqi Decoction and Xunjingpu Method. *Modern J Integrated Trad Chin Western Med*. 2020; 29:2924-2927. (in Chinese)
70. Jin K, Li P, Zhang F, Wei G, Ji L, Xu L, Lu Z, Wang Y, Li H, Zhu S, Yan Y. Effect of Lianzhu Xiaoke recipe on glucose and lipid metabolism and inflammatory factors of type 2 diabetes patients. *Acta Chinese Med*. 2023; 38:1095-1101. (in Chinese)
71. Bai Y, Bao X, Zhao D, Zhu R, Li R, Tian Y, Mo F, Gao S. Mechanism study of Jiang Tang San Hao Formula improving glucolipid metabolism in diet-induced obese mice. *China J Trad Chin Med Pharmacy*. 2020; 35:2253-2258. (in Chinese)
72. Bai Y, Zhao Y, Jin J, Ye Z, Fan H, Zhao D, Gao S. Jiang Tang San Hao Formula exerts its anti-diabetic effect by affecting the gut-microbiota-brain axis. *Phytomedicine*. 2024; 135:156100.
73. Yang H, Yu S, Wang P, Shu Q, Cheng S. The mechanism of regulating leptin resistance in obesity and the influence of adjusting methylation of OB-R, POMC gene promoter of Wendan Decoction[J]. *World J Integrated Trad Western Med*. 2020; 6:23-30. (in Chinese)
74. Wang X, Wang S, Fang C, Wang J, Kuang X, Zhao D, Wang Y. Expression of Ob-R, AgRP and NPY in rat hypothalamic arcuate nucleus after chronic immobilization stress and the regulation of Xiaoyao Powder. *China J Trad Chin Med Pharmacy*. 2018; 33:2798-2802. (in Chinese)
75. Dai Y, Chen S, Li Y, Zhang G, Bi P, Nie K. Liujunzi Decoction ameliorated cisplatin-induced anorexia

- by inhibiting the JAK-STAT signaling pathway and coordinating anorexigenic and orexigenic neuropeptides in rats. *J Ethnopharmacol.* 2022; 285:114840.
76. Chen Z, Jian Y, Wu Q, Wu J, Sheng W, Jiang S, Shehla N, Aman S, Wang W. *Cyclocarya paliurus* (Batalin) Iljinskaja: Botany, ethnopharmacology, phytochemistry and pharmacology. *J Ethnopharmacol.* 2022; 285:114912.
77. Wang X, Tang L, Ping W, Su Q, Ouyang S, Su J. Progress in research on the alleviation of glucose metabolism disorders in type 2 diabetes using *Cyclocarya paliurus*. *Nutrients.* 2022; 14:3169.
78. Wang Q, Jiang C, Fang S, Wang J, Ji Y, Shang X, Ni Y, Yin Z, Zhang J. Antihyperglycemic, antihyperlipidemic and antioxidant effects of ethanol and aqueous extracts of *Cyclocarya paliurus* leaves in type 2 diabetic rats. *J Ethnopharmacol.* 2013; 150:1119-1127.
79. Xu G, Yoshitomi H, Sun W, Guo X, Wu L, Guo X, Qin L, Fan Y, Xu T, Liu T, Gao M. *Cyclocarya paliurus* (Batal.) Iljinskaja Aqueous Extract (CPAE) ameliorates obesity by improving insulin signaling in the hypothalamus of a metabolic syndrome rat model. *Evid Based Complement Alternat Med.* 2017; 2017:4602153.
80. Diamond BJ, Shiflett SC, Feiwei N, Matheis RJ, Noskin O, Richards JA, Schoenberger NE. Ginkgo biloba extract: Mechanisms and clinical indications. *Arch Phys Med Rehabil.* 2000; 81:668-678.
81. Banin RM, Hirata BK, Andrade IS, Zemdeg JC, Clemente AP, Dornellas AP, Boldarine VT, Estadella D, Albuquerque KT, Oyama LM, Ribeiro EB, Telles MM. Beneficial effects of Ginkgo biloba extract on insulin signaling cascade, dyslipidemia, and body adiposity of diet-induced obese rats. *Braz J Med Biol Res.* 2014; 47:780-788.
82. Banin RM, de Andrade IS, Cerutti SM, Oyama LM, Telles MM, Ribeiro EB. Ginkgo biloba extract (GbE) stimulates the hypothalamic serotonergic system and attenuates obesity in ovariectomized rats. *Front Pharmacol.* 2017; 8:605.
83. Machado MMF, Pereira JP, Hirata BKS, Júlio VS, Banin RM, Andrade HM, Ribeiro EB, Cerutti SM, Telles MM. A single dose of Ginkgo biloba extract induces gene expression of hypothalamic anorexigenic effectors in male rats. *Brain Sci.* 2021; 11:1602.
84. Li J H, Tang Q L, Guo J Q, Wang Q, Zhu S, Wang Y, Yang C, Gao S, Liu J, Gao R, Wang J, Ye X, Pan X, Zang L. Effective components of Semen Ziziphi Spinosae for sedative-hypnotic based on receptor ligand binding assay. *Chinese Pharmacolog Bull.* 2016; 32:508-513. (in Chinese)
85. Xu W, Ruan Y, Bian H, Wang Y, Yu S, Li T, Huang L. Study on the effect of Zizyphus jujube kernel freeze-dried powder on sleep awakening state and energy metabolism rate in rats. *Chinese Pharmacological Bulletin.* 2022; 38:305-310. (in Chinese)
86. Bi Z, Lu Y, Zhang Y, Li J, Zhou H, Lv X, Fang C. Research on the regulation effects of Danzhi Jiangtang capsule on feeding behavior and brain feeding center alpha-melanocyte stimulating hormone and agouti-related protein in db/db mice. *J Changchun Univ Chin Med.* 2024; 40:44-49. (in Chinese)
87. Zhang S, Zhang Y, Wen Z, Yang Y, Bu T, Wei R, Chen Y, Ni Q. Jinkui Shenqi pills ameliorate diabetes by regulating hypothalamic insulin resistance and POMC/AgRP expression and activity. *Phytomedicine.* 2024; 126:155297.
88. He Y, Yang C, Wang P, Yang L, Wu H, Liu H, Qi M, Guo Z, Li J, Shi H, Wu X, Hu Z. Child compound Endothelium corneum attenuates gastrointestinal dysmotility through regulating the homeostasis of brain-gut-microbiota axis in functional dyspepsia rats. *J Ethnopharmacol.* 2019; 240:111953.
89. Gu M, Luo L, Fang K. Crocin inhibits obesity *via* AMPK-dependent inhibition of adipocyte differentiation and promotion of lipolysis. *Biosci Trends.* 2018; 12:587-594.

Received March 26, 2025; Revised June 5, 2025; Accepted June 13, 2025.

*\*Address correspondence to:*

Pingping Cai, Department of Traditional Chinese Medicine, Shandong Provincial Hospital Affiliated with Shandong First Medical University, Ji'nan 250021, China.

E-mail: pingpingcai@126.com

Released online in J-STAGE as advance publication June 15, 2025.

# Advancing precision medicine in immune checkpoint blockade for HIV/AIDS: Current strategies and future directions

Xiangyi Tang<sup>1,2</sup>, Cheng Wang<sup>1</sup>, Xiling Zhang<sup>1,2</sup>, Qibin Liao<sup>2</sup>, Hongzhou Lu<sup>1,2,\*</sup>

<sup>1</sup> School of Public Health Bengbu Medical University, Bengbu, China;

<sup>2</sup> The Third People's Hospital of Shenzhen, National Clinical Research Center for Infectious Diseases and The Second Affiliated Hospital of Southern University of Science and Technology, Shenzhen, China.

**SUMMARY:** Acquired immunodeficiency syndrome (AIDS)/human immunodeficiency virus (HIV) patients experience significant increase in their survival and decline in the mortality with the advent of antiretroviral therapy (ART). Nonetheless, ART alone still cannot completely cure AIDS/HIV patients. Furthermore, the virus remains latent in resting CD4<sup>+</sup>T cells for extended periods, posing a continuous threat to AIDS/HIV patients. Immune checkpoint blockades (ICBs), as a promising immunotherapy, inaugurate new pathways for AIDS/HIV cure or remission given their capability to break down the latency limit of HIV, and promote the regeneration and activation of HIV-specific T cells. However, not all AIDS/HIV patients respond to immune checkpoint inhibitors (ICIs), similar to that encountered in cancer patients, accompanied by the risk of severe immune-related adverse events (irAEs) in some cases. Accordingly, the present study was conducted to explore the possibility of personalized medicine tailored to the host discrepancy, with purposes of achieving better treatment outcomes, higher objective response rates, and fewer irAEs. Strategies for ICIs based on individual differences are documented to be conducive to improving therapeutic outcomes for patients. Therefore, this study intended to improving the therapeutic efficacy of ICIs in AIDS/HIV patients within the context of precision immunotherapy, including monotherapy and combination strategies, as well as the application of predictive biomarkers.

**Keywords:** AIDS/HIV, immune checkpoint blockade, T cell exhaustion, precision immunotherapy, predictive biomarkers

## 1. Introduction

Acquired immunodeficiency syndrome (AIDS) remains a significant infectious disease. Antiretroviral therapy (ART) is the standard treatment for AIDS/human immunodeficiency virus (HIV) patients, aiding in the restoration of their immune system that has been compromised by the virus (1). However, rather than completely eliminating the virus, ART merely suppresses the replication of the virus to levels that are undetectable in the blood. In this way, it can significantly decrease the risk of disease progression and transmission, ultimately, a functional cure of AIDS patients (2).

Nevertheless, complete immune reconstitution is not achieved in 10-40 percent of infected individuals (3), which may be related to factors such as sustained immune activation, thymic hypoplasia, intestinal flora disruption, and heterogeneity of viral reservoirs (4). In recent years, with the rapid development in the field of immunotherapy, immunomodulatory therapies such as immune checkpoint blockades (ICBs) have received

widespread attention. These drugs have not only demonstrated significant efficacy in oncology treatment, but have also made important progress in exploring the treatment of chronic infectious diseases such as HIV, hepatitis B, and tuberculosis (5). To date, the Food and Drug Administration has approved a total of 25 drugs in 8 classes of ICIs, some of which have entered clinical trials in HIV-infected patients. It is worth noting that the application of ICIs in HIV treatment is becoming increasingly promising as research progresses: a variety of novel monotherapy regimens and combination strategies are currently undergoing phase I and II clinical trials in HIV-infected patients, and the clinical use of such drugs is expected to expand significantly in the future (6,7).

Clinical trials of ICIs in patients with HIV have highlighted several critical issues that require the utmost attention of clinicians, investigators, and regulatory agencies (1). The main areas of concern are differences in adverse effects after individualized immunotherapy (3) effects on CD4<sup>+</sup> T-cell dynamics (4) characteristics



of viral load fluctuations, and (5) heterogeneity in final clinical outcomes. These differences highlight the particular importance of individualized treatment strategies in HIV-infected patients (8-10). Current research focuses on exploring biomarkers that can predict the benefit of ICI therapy, overcoming the variability of treatment response by developing precise treatment regimens, and ultimately achieving the goal of converting non-responders into responders. This review systematically summarizes innovative strategies to enhance the effectiveness of ICI therapy within the framework of precision medicine, including but not limited to biomarker screening based on tumor microenvironmental characteristics, treatment timing optimization, and combination therapy regimen design. These research advances not only provide new ideas to improve the clinical management of HIV-infected patients but also represent an important opportunity to achieve breakthroughs in the field of ICI immunotherapy.

## 2. Immune checkpoint inhibitors and T cell exhaustion in HIV

Immune checkpoints were first discovered and applied for the treatment of cancers (11), enabling a dramatic shift in the traditional therapeutic paradigm. Back to the end of the last century, a special immunoglobulin on the surface of CD4<sup>+</sup> T cells and CD8<sup>+</sup> T cells, was accidentally found by scientists, naming cytotoxic T-lymphocyte antigen 4 (CTLA-4). Another immune

checkpoint was fortunately discovered shortly afterwards. When studying the mechanism of programmed cell death in mice, a professor of immunology from Kyoto University in Japan accidentally discovered a key gene involved in programmed cell death, *i.e.*, programmed cell death protein 1 (PD-1). Since then, many new immune checkpoints were observed and involved in studies on underlying mechanisms. Currently, PD-1 monoclonal antibodies (mAbs) are common therapeutic agents clinically. Multiple ICIs, such as Ipilimumab, Nivolumab, and Atezolizumab, when combined with other drugs, have become potent tools in the treatment of various diseases. Subsequently, the clinical application of ICI has been extended to the management of HIV and related coinfections. A large number of clinical drug trials have been carried out for verification, with the achievement of remarkable results in some studies. Validation of the effectiveness and safety of drugs has laid a foundation for the development of immunotherapy-oriented precision treatment strategies (Figure 1).

Intense immune activation may lead to T-cell depletion, CD4<sup>+</sup> T-cell expression and CD8<sup>+</sup> T-cell expression. Consequently, the viral replication cannot be controlled during HIV infection. CD4<sup>+</sup> T cells are T lymphocytes that express T cell receptors that can promote the antibody and CTL response. In the HIV-infected state, CD4<sup>+</sup> T cells are depleted, resulting in the loss of their antiviral CTL response and their ability to control viral load. PD-1 expression on HIV-specific T cells is a major marker of T cell exhaustion that may

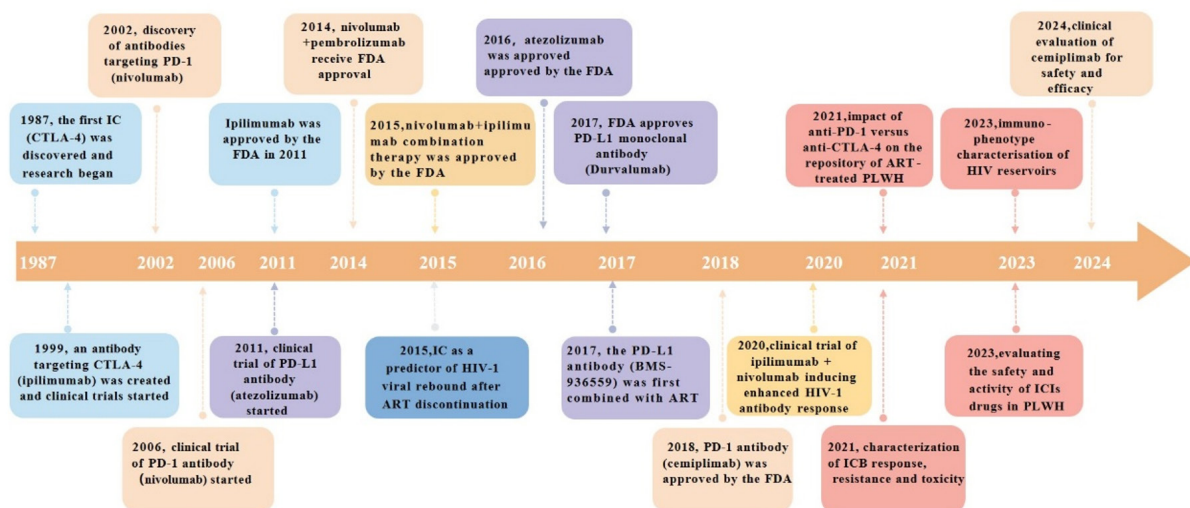


**Figure 1. Immune checkpoint discovery and clinical studies of ICB in HIV treatment.** Major immune checkpoints and checkpoint inhibitors in HIV therapy. In 1987 CTLA-4 became the first immune checkpoint in history to be discovered, and in 1999 ipilimumab was created and began clinical trials and was approved for marketing by the FDA in 2011 (blue section). In the same year, an antibody targeting PD-L1 (atezolizumab) also began a clinical trial component. 2002, the discovery of the first antibody targeting PD-1 (nivolumab) and subsequent clinical trials, while different antibodies including pembrolizumab and cemiplimab were also developed for clinical therapy (orange part). Since then, PD-L1 antibodies including durvalumab and BMS-936559 were introduced and applied to clinical treatment (purple section). The yellow part of the figure shows the combination strategy of immune checkpoint inhibitors and the application in HIV treatment. The grey part is one of the indicators that IC may be regarded as a predictor of viral rebound after ART treatment interruption. The red part indicates the clinical safety and efficacy assessment of combination therapy with ICIs. IC, immune checkpoint; FDA, US Food and Drug Administration; ICB, immune checkpoint blockade; ICIs, immune checkpoint inhibitors; ART, antiretroviral therapy; PLWH, people living with HIV.

indicate disease progression. PD-1 expression has been confirmed to correlate with reduced CD8<sup>+</sup> T cell function, viral load and CD4 T cell counts (12).

It is possible for receptor surface drivers to sufficiently activate ligands, and tyrosine phosphorylation at the cytoplasmic ends of cells to activate inhibitory signals mediated by transduction factors, thus preventing the generation of T cell receptor-mediated activation signals (13). For example, in immune cells, PD-1 signaling depends mainly on the core factor tyrosine phosphatase SHP-2, which may be recruited to PD-1 after binding to its ligand PD-L1. Further phosphorylation of ITSM can induce the conversion of SHP-2 to an active conformation, reduce the phosphorylation of CD3 and CD28, and thus exert a negative regulation on the signal strength of TCR. However, unlike PD-1, CTLA-4 lacks the ITSM motif bound to SHP-2, suggesting a possible indirect recruitment. In the large immune signaling network, it is critical to uncover the mechanisms of the checkpoint signaling pathways, which may provide potential reference for subsequent development of ICIs. In general, the invasion of pathogens (e.e., bacteria or viruses) may trigger a range of immune responses in the host. During the development of HIV infection, there may be gradual change in the mechanism underlying the involvement of HIV-specific CD4<sup>+</sup> and CD8<sup>+</sup> T cells in the durable antiviral work, eventually leading to a dysfunction of inhibiting viral expansion. PD-1, CTLA-4 and other inhibitory receptors are expressed on HIV-specific cells. Binding of these immune checkpoints to corresponding ligands may inactivate T cells, promoting virus to evade surveillance by the host immune system. In other words, dysfunctional CD4<sup>+</sup> and CD8<sup>+</sup> T cells both stem from the upregulation of inhibitory immune checkpoints. Among them, PD-1 is a well-studied immune checkpoint causing the dysfunction of HIV-specific CD4<sup>+</sup> and CD8<sup>+</sup> T cells, which may stimulate disease progression and loss of antiviral function (14). Although great attention has been attached to CD8<sup>+</sup> T cell function, HIV-specific CD4<sup>+</sup> T cells were also enhanced in ICBs. An *in vitro* study revealed that PD-1 blockade enhanced the proliferation of HIV-specific CD4<sup>+</sup> T cells and production of IFN $\gamma$ , IL-2, IL-13 and IL-21, providing superior evidence for ICBs (14,15). In view of the above, the use of ICBs may partly restore the function of HIV-specific T cells, and enhance the host immune response to control the progression of HIV infection eventually. In this regard, immune intervention may be benefited from a comprehensive understanding of the role of immune checkpoints in HIV-specific T cells. Currently, most HIV patients, except for a few "elite controllers", still require traditional antiviral therapies. The application of anti-HIV treatment aims to control the virus and clean virus reservoir on the surface of infected T cells. Given the suppressed immune checkpoint expression, namely, on the premise of ART virus cannot be eradicated, the existence of latent virus is one of the

factors for a lifelong treatment in the targeted patients. Immune checkpoint proteins were found to impair HIV-specific cytotoxic functions by promoting latent infected cells, leading to HIV persistence. Therefore, intervention using ICBs can be adopted, as an adjuvant strategy, prior to antiviral therapy, which may to some extent reverse latent infection to reduce the number of HIV reservoirs (16) (Figure 2).

### 3. The activity and safety of ICBs in PLWH

ICBs are a frequent therapeutic option for cancer patients, but not including people living with HIV (PLWH) usually. It may be attributed to the immunological deficiencies in HIV-infected patients, raising concerns among clinical researchers about their safety and impact. However, the clinical value of ICBs in HIV patients has been proposed and demonstrated in several recent studies. Here, we will continue to expound the clinical use of ICBs in PLWH to clarify these controversies. In our study, available clinical data on immune checkpoints in HIV patients are gathered to answer questions related to the efficacy and safety of ICBs and to decipher potential influential factors (Table 1-2).

#### 3.1. Effect of ICIs on viral load and CD4<sup>+</sup> T cells in PLWH

HIV viral load and CD4<sup>+</sup> T lymphocyte counts are important indicators in the clinical management of HIV patients. In a phase 1 clinical trial of PD-1, CD4<sup>+</sup> T cell counts increased in patients treated by PD-1 inhibitors (5), revealing potential correlation between CD4<sup>+</sup> T cell counts and PD-1 inhibitors. In another study of 8 AIDS patients treated with cemiplimab (PD-1), Gay CL *et al.* (17) found that a single infusion of anti-PD-L1 antibody (BMS-936559) increased HIV-1 Gag-specific CD8<sup>+</sup> T cell responses in 2 of 6 participants, with no significant change in median CD4<sup>+</sup> T cell counts, CD4<sup>+</sup> percentage, or CD4/CD8 ratio, and a decrease in CA-RNA in CD4<sup>+</sup> T cells from 201 to 194. There was no significant difference in CA-DNA from 435 to 513. The standard HIV RNA levels remained at <40 copies/mL in all participants, and the ratio of HIV DNA to RNA/DNA in 8 participants unchanged from baseline after 28 days of observation.

Furthermore, in a prior research investigating the efficacy of different doses of CTLA-4 therapy in 24 HIV patients, Colston E *et al.* (10) found that 2 participants (8.3%) exhibited a significant reduction in HIV-1 RNA levels, but 8 (33.3%) showed no significant change in HIV RNA levels, all from the low-dose treatment group. Conversely, 14 participants (58.3%) demonstrated significantly increased HIV RNA levels. All individuals with obviously elevated HIV RNA (except for 1 patient) were from the high-dose group. Therefore, CTLA-4 treatment regimens showed no significant difference in

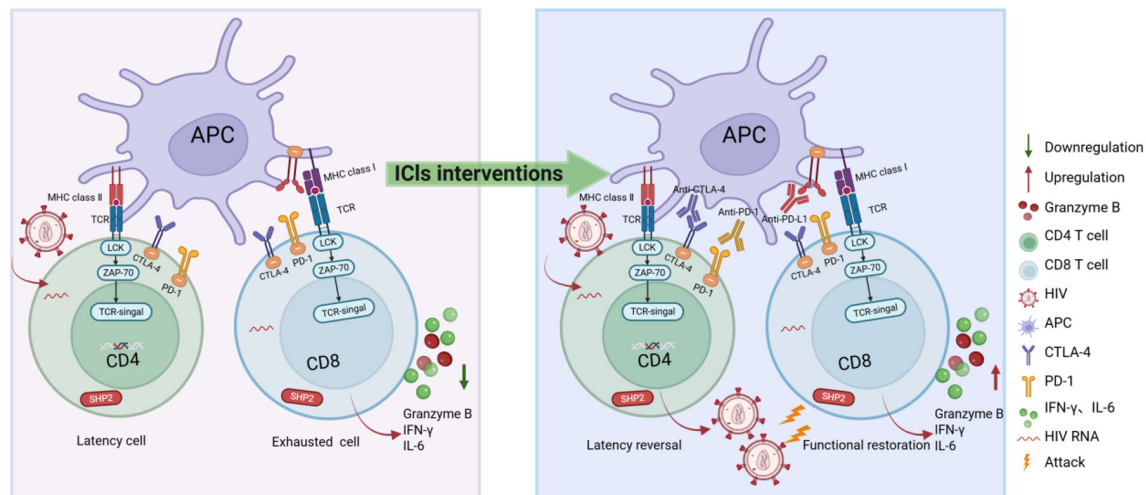


**Figure 2. Immune checkpoint therapy drugs suppress HIV.** After HIV infection of the host, the virus enters the receptors of CD4 T cells and hijacks the host machinery for replication. During chronic infection, sustained viral antigen exposure leads to overactivation of the CD8 T-cell TCR signaling pathway, triggering high expression of immune checkpoint molecules, leading to T-cell depletion, loss of cytotoxicity, and reduced proliferative capacity. At the same time, HIV infection leads to massive depletion of CD4 T cells, and some infected cells enter a latent state, forming a viral reservoir. Immune checkpoint inhibitors (e.g., anti-PD-1 antibodies) can block inhibitory signals and partially restore the antiviral function of CD8 T cells. However, ICI may also activate latently infected CD4 T cells and induce HIV proviral transcription. Created with BioRender.com. **Abbreviations:** MHC class I: Major Histocompatibility Complex class I; MHC class II: Major Histocompatibility Complex class II; TCR: T-Cell Receptor; LCK: Lymphocyte-specific protein tyrosine kinase; CTLA-4: Cytotoxic T-Lymphocyte-Associated Protein 4; PD-1: Programmed Death-1; PD-L1: Programmed Death-Ligand 1; TCR signal: T-Cell Receptor signal; SHP2: Src Homology 2 Domain-containing Phosphatase 2; Granzyme B: Granzyme B; IFN- $\gamma$ : Interferon-gamma; IL-6: Interleukin-6; HIV: Human Immunodeficiency Virus; ICIs: Immune Checkpoint Inhibitors; Anti-CTLA-4: Anti-CTLA-4 Antibody; Anti-PD-1: Anti-PD-1 Antibody; Anti-PD-L1: Anti-PD-L1 Antibody; HIV RNA: HIV Ribonucleic Acid.

its overall control of viral load, and viral replication may be potentially activated in some cases when using high-dose regimen. This study may provide important insights into the effect of different dose regimens on changes in HIV RNA levels, offering a valuable basis for further investigation. Anyway, it should be acknowledged that there are still limitations in these studies, such as small number and range of subjects, despite the confirmation of potential benefit of ICB on CD4<sup>+</sup> T cells and HIV RNA viral load in HIV patients.

### 3.2. Clinical response of ICIs in PLWH

With the success of ICBs in the field of oncology, this therapy has been applied in the treatment of patients with HIV-associated tumors, with some clinical benefit achieved. However, HIV patients with different tumor types may respond differently to treatment. Kaposi's sarcoma (KS) and non-small cell lung cancer (NSCLC) are two of the most representative tumor types in clinical trials of ICB for patients with HIV-associated tumors. Our literature retrieval obtained eight studies on the use of ICBs for HIV-associated tumor treatment (ClinicalTrials.gov), including five studies involving both KS and NSCLC (Table 1). In a phase 2 clinical trial of patients with HIV-KS, 12% of these participants had a complete response to PD-1 therapy, 59% had a partial response, while the overall response rate was 71% (95% CI 44-90) (17). Nevertheless, in another study involving

6 cases of HIV-KS, only 2 patients reached stable disease (lasting  $\geq 24$  weeks), and notably, one participant died of severe diffuse KSHV-associated polyclonal B-cell lymphocyte proliferation (5). In another on HIV-NSCLC, from real-world studies, the objective response rate (ORR) for these patients was 31% after the use of ICBs, with ORRs of 38% and 25% for first- and second-line patients, respectively ( $P = 0.06$ ), with no significant inter-group difference (8). Significantly, patients with melanoma had an ORR of 69%, compared to only 11% for those with head and neck squamous cell carcinoma (HNSCC) (NCT03094286). Altogether, ICBs may produce varied therapeutic response for HIV combined with different tumor types, with a maximum ORR of 69% and a minimum of only 11%. Given objective factors such as limited samples, multi-center studies with expanded sample size should be performed on ICBs for patients with HIV-associated tumors (19). Overall, the ORR of ICBs was superbly around 70% in both KS and melanoma, but only 11% in HNSCC. In the future, multi-cohort studies should be conducted with expanded sample size and type for further verification.

As described in the above studies, all patients received ART, with no significant difference in baseline CD4 + T cell count ( $> 200$ ). Baseline CD4 + T lymphocyte count emerges as a pivotal prognostic biomarker, with its clinical predictive value rooted in its central role in orchestrating adaptive immune responses (8,19). The tumor microenvironment (TME) exhibits

Table 1. Clinical trials of checkpoint blockades in HIV infection

| Trials      | Region               | Phase | Drug                 | Treatment  | Participants | Characteristic             | Efficiency   | irAES  | Ref. |
|-------------|----------------------|-------|----------------------|--|--------------|----------------------------|--|--|------|
| NCT03469804 | France               | 2     | Pembrolizumab (PD-1) | 200 mg, every 3 weeks for 6 months   | 30           | HIV-related Kaposi sarcoma | /  | 12% (2/17) Grade $\geq 3$  | 18   |
| NCT02595866 | United States        | 1     | Pembrolizumab (PD-1) | 200 mg, every 3 weeks  | 30           | HIV and advanced cancer    | 23% (7/30) had detectable HIV viremia; no significant viral load breakthrough                  | 73% (22/30) irAEs (Grade 1-2); 20% (6/30) Grade $\geq 3$         | 5    |
| NCT03239899 | United States        | 1     | Pembrolizumab (PD-1) | Single dose of 2 mg/kg at Week 0   | 20           | HIV infection              | /  | /  | 39   |
| NCT04091932 | China                | 2     | Pembrolizumab (PD-1) | 2 mg/kg, every for 3 months  | 10           | AIDS-related PML           | Data under analysis  | /  | 40   |
| NCT03367754 | United States        | 1     | Pembrolizumab (PD-1) | 200 mg   | 60           | HIV infection              | /  | /  | 41   |
| NCT04514484 | United States        | 1     | Nivolumab (PD-1)     | Day 1 every 28 days for up to 1 year   | 18           | HIV and advanced cancer    | /  | /  | 42   |
| NCT03304093 | France               | 2     | Nivolumab (PD-1)     | 3 mg/kg, every 2 weeks   | 16           | HIV infection              | /  | /  | 39   |
| NCT05187429 | Australia, Singapore | 1, 2  | Nivolumab (PD-1)     | Cohort A: 0.1/0.3/1.0 mg/kg single dose on Day 7; Cohort B: Single dose on Day 0 | 42           | HIV infection              | /  | /  | 43   |
| NCT03316274 | United States        | 1     | Nivolumab (PD-1)     | Cohort A: 10 mg every 2 weeks for 4 doses; Cohort B: Response-based dosing       | 12           | HIV-related Kaposi sarcoma | /  | /  | 44   |
| NCT04929028 | United States        | 2     | Nivolumab (PD-1)     | Cohort A: 1 mg/kg for 12 weeks; Cohort B: 2.5 mg/kg for 12 weeks                 | 53           | HIV-associated anal cancer | /  | /  | 45   |
| NCT03787095 | United States        | 1, 2  | Cemiplimab (PD-1)    | 0.3/1/3/10 mg/kg at weeks 0 and 6  | 5            | HIV infection              | 25% (1/4) increased HIV-1-specific T-cell responses and transiently increased HIV-1 expression | 100% (4/4) experienced Grade 1-2                                 | 9    |
| NCT03407105 | United States        | 1     | Ipilimumab (CTLA-4)  | 0.1, 1, 3, or 5 mg/kg 2 or 4 doses of every 28                                   | 24           | HIV infection              | 41.7% (10/24) CD4+ counts increased; 16.7% (4/24) decreased                                    | 37.5% (9/24) Grade 1; 41.7% (10/24) Grade 2; 4.2% (1/24) Grade 3 | 10   |
| NCT02028403 | United States        | 1     | BMS-936559 (PD-L1)   | 0.3 mg/kg single dose  | 8            | HIV infection              | 33.3% (2/6) increased HIV-1 CD8+ responses   | 16.7% (1/6) asymptomatic hypophysitis                            | 17   |



Table 1. Clinical trials of checkpoint blockades in HIV infection (continued)

| Trials      | Region        | Phase | Drug               | Treatment   | Participants | Characteristic  | Efficiency   | irAES | Ref. |
|-------------|---------------|-------|--------------------|---|--------------|---|--|-------|------|
| NCT03330143 | China         | 2     | ASC22 (PD-L1)      | Cohort A: 1 mg/kg for 12 weeks;<br>Cohort B: 2.5 mg/kg for 12 weeks | 30           | HIV infection   | Latent reservoir activation analysis ongoing   | /     | 46   |
| NCT04499053 | United States | 2     | Durvalumab (PD-L1) | 1500 mg, every 3 weeks for 4 cycles                                 | 18           | HIV-infected with NSCLC   | /  | /     | 47   |
| NCT03094286 | Spain         | 2     | Durvalumab (PD-L1) | 1500 mg, every 4 weeks  | 20           | HIV-1-infected CD4+ and CD8+ T-cell counts and patients with plasma HIV-1 viremia remained stable advanced cancer | 75% (15/20) Grade 1; 50% (10/20) Grade 2; 5% (1/20) Grade 3; 5% (1/20) Grade 4; 10% (2/20) Grade 5 |       | 19   |

Table 2. Clinical trials of immune checkpoint combination therapy in HIV

| Trials      | Region        | Phase | Combination Drug  | Treatment   | Participant | Characteristic                         | Effency  | irAES                                       | Ref. |
|-------------|---------------|-------|---|---|-------------|--|--|---|------|
| NCT05129189 | China         | 2     | ASC22 (PD-L1) + Chidamide (HDACi)                                 | ASC22: 2 mg/kg every 2 weeks  | 15          | HIV infection                          | CA-HIV RNA increased from baseline to week 4; CA-RNA/DNA ratio returned to baseline by week 24. Plasma HIV VL showed no significant change from baseline at weeks 4 and 8. | 46.7% (7/15) Grade 1-2; 6.7% (1/15) Grade 3 | 28   |
| NCT05646082 | UK            | 1     | Dostarlimab (PD-1) + cART   | Dostarlimab: 500 mg every 3 weeks (first 4 doses), then 1000 mg every 6 weeks until week 48   | 20          | HIV-associated Kaposi sarcoma          | /  | /   | 48   |
| NCT03354936 | France        | /     | Pembrolizumab (PD-1) or Durvalumab (PD-L1) or Ipilimumab (CTLA-4) | /   | 50          | HIV-infected and cancer                | /  | /   | 49   |
| NCT05597800 | Italy         | 2     | Nivolumab (PD-1) + Ipilimumab (CTLA-4)                            | Nivolumab 3 mg/kg + Ipilimumab 1 mg/kg every 3 weeks for 4 cycles   | 30          | HIV infection with NSCLC               | /  | /   | 50   |
| NCT02408861 | United States | 1     | Nivolumab (PD-1) + Ipilimumab (CTLA-4)                            | Cohort A: nivolumab 30 minutes on day 1;<br>Cohort B: ipilimumab 90 minutes on day 1 of every third cycle of nivolumab; Cohort C: Ipilimumab 90 minutes on day 1 of every sixth cycle of nivolumab. Treatment repeats every 14 days for up to 46 cycles | 96          | HIV-related classical Hodgkin lymphoma | /  | /   | 51   |

remarkable variability across varied cancer types (20), resulting in profound impact on the therapeutic outcomes. This variability was strikingly evident in a cohort of 461 NSCLC patients. The study demonstrated that in tumors with high PD-1 expression, the level of programmed death-ligand 1 (PD-L1) emerged as a pivotal predictor of therapeutic response (21). Moreover, the abundance of host-derived cells within the TME plays a decisive role in shaping treatment outcomes. The therapeutic sensitivity and resistance may be dictated collectively by the intricate interplay between host cells and tumor cells, which is mediated through cytokine secretion, immune response modulation, and bidirectional signaling. Consequently, variations in host cell density across tumors may result in divergent responses to immunotherapy.

### 3.3. Immune-related adverse events (irAEs) associated with ICI in PLWH

In real-world studies, approximately 20% of HIV patients experienced any grade of irAEs, with a rate of grade  $\geq 3$  irAEs reaching 7.7% in this group of patients. Specifically, 19% and 39% of HIV patients treated with ICBs combined chemotherapy or targeted agents experienced any grade of irAEs, with 5.9% and 13% experiencing grade  $\geq 3$  irAEs. and 13%, respectively. Moreover, irAEs of any grade occurred in 16% of PWH with baseline CD4<sup>+</sup> T-cell counts  $< 200$  cells/ $\mu$ L, and 7.8% of which were grade  $\geq 3$ . Of these, the most common irAEs were pneumonia and endocrine, both at 4.7%; moreover, 4% of PWH with baseline CD4<sup>+</sup> T-cell counts  $\geq 200$  cells/ $\mu$ L experienced any grade of irAEs, 9.9% of which were grade  $\geq 3$  (8). Collectively, the frequency of irAEs varies considerably among HIV-infected individuals, depending on the treatment strategies and host CD4<sup>+</sup> T cells.

The occurrence of irAEs may be related to multiple different risk factors, which were reported to be associated with the type of tumors found (22,23), over-expression of PD-1/PD-L1 and smoking history. However, studies on the use of ICBs in HIV patients are currently limited to efficacy, necessitating further in-depth investigation on irAEs. Special attention should be given to the study of irAEs in HIV patients, a special group of immunodeficient population.

### 3.4. Cooperation benefits: Combined immune checkpoint therapy strategies

The combination of anti-PD-1 and anti-CTLA-4 therapies has previously been shown in SIV studies to reverse latency compared to ICB monotherapy (24). Recently, in a clinical trial on the combination of PD-1 and CTLA-4, Harper J et.al. found a 1.44-fold (interquartile range, 1.16-1.89) increase in median CA-US HIV RNA in patients receiving nabulizumab+ibritumomab compared

with nabulizumab monotherapy ( $P = 0.031$ ) (25), offering a useful perspective for combination therapy.

As for clinical trials on ICBs in HIV patients, the majority of patients also adhere to ART during treatment. In patients with viremic HIV patients, a study of CTLA-4 (ipilimumab) found a smaller increase in baseline HIV-1 RNA in patients who were not on ART compared to those who were on ART (0.93 vs. 0.8), yet without significant difference between groups (10). Moreover, in clinical trials on the use of ICBs alone versus jointly, combination therapy with PD-1 and CTLA-4 in patients with HIV resulted in improved latency reversal efficiency, as evidenced by a rise in HIV ART, and monitoring of the change in HIV virus load in 43% of PWH who received nivolumab+ipilimumab in this context, these HIV virus load data point before or after the initiation of ICBs (8). Thus, HIV RNA was increase, yet without statistical significance, during treatment for HIV patients treated with ART or not with ICBs.

In another phase II clinical trial of ASC22 (PD-1) combined with histone deacetylase (HDAC) inhibitors in HIV patients, conducted by a research team from Shanghai, China, compared to the baseline level, CA HIV RNA levels increased progressively at week 4 and significantly increased by week 8 (4.27-fold,  $P = 0.004$ ), but gradually declined after week 8 and returned to the baseline by week 24 (26). Therefore, PD-1 combination therapy may have potential in activating the latent reservoir.

With respect to the above, ICBs therapy still has some problems in its safety and efficacy, despite successive clinical trials in HIV patients. Firstly, similar to cancer patients, irAEs are inevitable in HIV patients treated with ICBs and cover all grades, necessitating more effective risk mitigation strategies. Furthermore, the majority of ICBs currently used in HIV patients are inhibitors targeting PD-1/PD-L1 and CTLA-4. There is inadequate investigation on other antibody drugs including TIGIT, LAG-3, and TIM-3, which may restrict our understanding of the safety and efficacy of ICBs. For example, HVEM and BLAT could negatively regulate T cells, and TIGIT was significantly up-regulated in clonally competent pairs of latent cells, according to the study of HIV on immune cell phenotype library. Secondly, the host is also a pivotal factor affecting the efficacy of ICBs. There are early studies showing that gender, age and heredity can affect the effect of ICBs (27,28). The clinical trials of ICBs on AIDS patients are mostly concentrated on males, blacks or whites, etc., and distributed in developed countries and regions such as Europe and the United States. A study of combination therapy with ICBs for HIV patients in Shanghai, China, provides an important clinical basis for promoting the treatment program (26), while AIDS occurs frequently in some developing countries and regions such as Africa. As described previously, ICBs are commonly adopted for patients with HIV-associated tumors, mainly

for NSCLC and KS patients, exhibiting cancer type-dependent varied response rates. Besides, T-cell failure is an important hallmark of chronic infectious diseases, and HIV patients are predominately prone to acquiring various opportunistic infections caused by autoimmune deficiencies, including hepatitis B and tuberculosis, *etc.* At this study, there is a need to conduct additional clinical trials of ICBs for patients with HIV-associated tumors. In terms of therapeutic strategies, preliminary findings support the importance of combining ICBs, which, by integrating the complementary advantages of different mechanistic therapies, have demonstrated significant breakthroughs in viral clearance, immune reconstitution, and long-term control, and that the ICI combination strategy is currently the most promising strategic pathway to achieving a functional cure for HIV (Figure 3).

#### 4. Immune checkpoint: Research progress as biomarkers for disease prediction

ICBs have emerged as a promising strategy to restore antiviral immunity in PLWH. However, the heterogeneous responses of CD4<sup>+</sup> and CD8<sup>+</sup> T cell subsets to ICBs highlight the necessity for precision-guided therapeutic approaches. To improve efficacy, sophisticated immunotherapeutic strategies may be found by integrating the findings of recent clinical and preclinical studies.

Nevertheless, there is currently a lack of sufficient biomarker research for AIDS patients, but it is also important to validate the already identified biomarkers clinically. More comprehensive strategies are required to provide precise selection criteria for patients undergoing ICI-based monotherapy or combination therapy.

##### 4.1. Monitoring of ICIs Efficacy

An intimate correlation of PD-1 expression has previously been established with the depletion of CD8<sup>+</sup> T cell function, yet without the discovery of direct effect of PD-1 on CD8<sup>+</sup> T cell counts. Therefore, PD-1 may act primarily by inhibiting the antiviral activity of cytotoxic T cells, rather than directly regulating its counts. Furthermore, PD-1 expression was significantly associated with reduced CD4<sup>+</sup> T cell counts, which could be recovered after using a PD-1 inhibitor (5). Another study documented a significant elevation of the HIV RNA in 58.3% of participants in the high-dose group of CTLA-4 inhibitors, possibly related to excessive immune activation, which might result in expanded viral repertoire or increased inflammatory response (12). Specifically, the PD-1 pathway mainly affects the count and function of CD4<sup>+</sup> T cells, while the regulation of CTLA-4 is more complex and dose-dependent (10). A precise regulation is required to balance the immune reconstitution and viral control when applying ICIs for

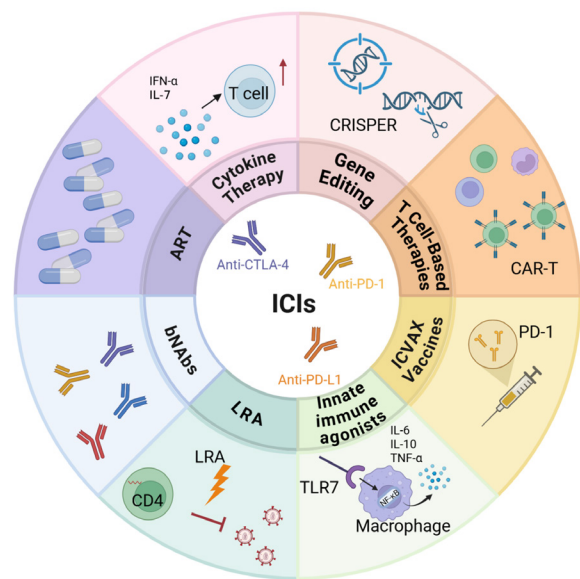


**Figure 3. Schematic Overview of ICI Based Combination Strategies.** The following strategies can be used to intervene in HIV treatment based on ICI therapy combined with other treatments. Treatments such as gene editing CRISPR-Cas9 target viral DNA or host genes to remove the viral reservoir. Latency reversal agents (LRA) such as histone deacetylase inhibitors (HDACi), which expose the latent virus to the immune system by activating it, or drug therapy. In cytokine therapy, cytokines such as IFN- $\alpha$ , and IL-7 enhance HIV-specific T cell survival and killing and modulate follicular helper T cell function to combat HIV. Various immunotherapies have been developed based on the body's immune system, and T cell immunotherapy targets and removes HIV-infected host cells by modifying T cells. Innate immune agonists enhance the antiviral immune response by activating pattern recognition receptors (PRRs). HIV-neutralising antibodies block the onset of infection by interfering with the entry of HIV-1 into target cells, primarily by binding to viral infectious process exposures. Therapeutic vaccines (*e.g.*, ICBVAX) are designed to activate specific B/T cell immune responses by delivering HIV antigens to establish long-lasting immune memory. When it comes to immune checkpoint inhibitor therapy, combination therapy such as ICI in combination with ART synergistically reduces the viral reservoir by controlling viral replication while restoring T-cell function as compared to single inhibitor therapy. Created with BioRender.com. Abbreviations: ICI: immune checkpoint inhibitor; ART: antiretroviral therapy; LRA: latency reversing agent; CAR-T: chimeric antigen receptor T cell; TLR: toll-like receptor; bNAbs: broadly neutralising antibodies ; IFN- $\alpha$ : interferon-alpha.

HIV treatment. PD-1 inhibitors can improve the number and function of CD4<sup>+</sup> T cells, providing a new strategy for immune recovery in HIV patients, with additional attention on its safety and resistance during long-term medication. At present, in order to balance the antiviral effect with the risk of immunopathology, there is a need to determine the optimal dose of CTLA-4 inhibitors by more clinical trials.

##### 4.2. Immune activation and inflammatory markers

The modulatory effects of ICIs on CD38 expression during HIV infection reveal a novel dimension of virus-host interactions. As a multifunctional immunoregulatory molecule (29), CD38 critically influences T cell

functionality and disease progression, with genetic deficiency of CD38 directly impairing regulatory T cell development and accelerating autoimmune disorders (30). Notably, while PD-1/PD-L1 checkpoint blockade demonstrates remarkable efficacy in solid tumors, HIV exploits CD4+ T cell surface co-receptors (CCR5/CXCR4) to upregulate immune markers such as CD38, thereby establishing a proviral immune microenvironment. In this pathological context, therapeutic application of ICIs may further upregulate CD38 expression through IFN- $\gamma$ -mediated immune activation, potentially contributing to ICI resistance (31). So far, there is limited investigations into HIV-associated immune marker dynamics under checkpoint inhibition, necessitating further studies of mechanisms to delineate these regulatory networks.

#### 4.3. Combined therapy strategies

In terms of combined therapies available at present, dual blockade of PD-1/CTLA-4 has demonstrated significant therapeutic potential in HIV management recently. Preclinical SIV models and subsequent clinical trial data consistently indicate that such combination therapy can activate latent viral reservoirs more effectively compared to monotherapy. For example, Rahman *et al.* classified SIV treatment into treatment with PD-1 + vaccine and vaccine only under ART inhibition, and DNA vaccination induced high-frequency proliferation of CD8+ T cells with cytolytic potential. In their research, after analytical treatment interruption, SIV-specific IFN $\lambda$ + CD4+ and CD8+ T cells expanded further for 2 to 4 weeks

in the vaccine + PD-1 group, preserving the function and breadth of antiviral T cells after ART interruption (26). Noticeably, two SIVs (50%) in the other PD-1 blockade + vaccine group died of AIDS symptoms during the experiment, whereas all eight (100%) SIVs survived in the other two vaccine-only and control groups throughout the study. The median fold change in SIV plasma viral load relative to set point was 1.82-fold in the PD-1 blockade + vaccine group, accounting for double the fold change in the vaccine-only group; moreover, PD-1 blockade accelerated potential reservoir reactivation and AIDS progression in chronically SIV-infected rhesus macaques after ART interruption. However, at this study, there is insufficient SIV trials that provide a valid basis for ICBs + vaccine therapy in the treatment HIV. Importantly, existing data all suggested that effective activation of potential reservoirs provides robust evidence, which should be validated in the clinical setting (27).

Furthermore, other combination therapies are also available for application. ICIs have made remarkable progress in tumor treatment, among which TIM 3 + PD-1 therapy show excellent immunomodulatory ability, offering another novel solution for tumor immunotherapy. It is worth noting that the successful experience of these ICIs in tumor treatment also provides additional insights for HIV treatment. As we known, it is crucial to restore and maintain the immune function of patients during HIV treatment. In view of this, it highlights the clinical significance and research value of ICIs for the treatment of HIV (32). Meanwhile, IB1321 is regarded as the first dual-targeting IC (TIGIT/PD-1) bispecific antibody

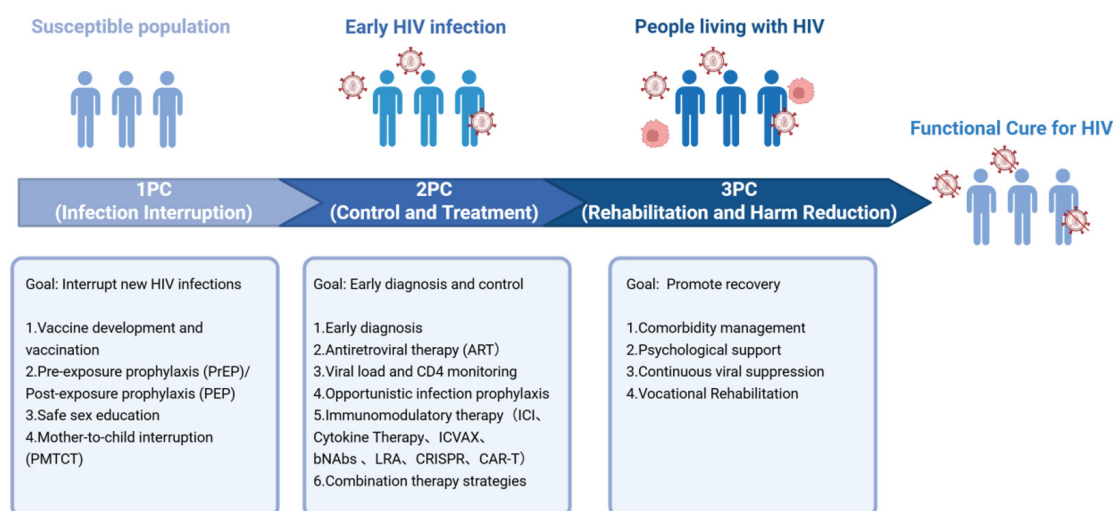


**Figure 4. Tertiary prevention and control strategies to achieve a functional cure for HIV.** In pursuit of a functional cure for HIV, a three-dimensional prevention and control system of prevention, interruption, and cure is being built. The vaccine-driven source prevention and control system includes prevention in high-risk groups and research and development of innovative vaccines. Secondary prevention is based on post-infection treatment-based interventions, and the immunomodulatory combination strategy of immunotherapy highlights the unique advantages and development potential of many HIV treatments, making a major step forward in achieving a functional cure for HIV. Tertiary prevention focuses on recovery promotion and harm reduction, supported by multidimensional strategies that encourage sustained technological innovation and policy synergy networks. *Abbreviations:* PC: prevention and control. Created with BioRender.com.



available clinically, which has been highly concerned considering its performance in tumor treatment. A study was designed to evaluate the safety, tolerability, and antitumor activity (NCT04911894) of IBI321 in 16 patients with advanced malignant solid tumors who did not respond to standard therapy. Corresponding data are not yet available, although the trial is currently completed. In the future, we will continue to focus on the therapeutic outcome of IBI321, aiming at providing possible foundation for the effectiveness and safety of HIV treatment, and advancing HIV treatment (33).

Besides, TLR7 is an innate immune receptor that recognizes single- and short double-stranded RNA. It is a active participant in antiviral immunity that functions to stimulate dendritic cell maturation, promote cytokine secretion and antigen presentation, thereby enhancing the adaptive immune response. Vesatolimod (GS-9620) is a potent and selective TLR7 agonist that can moderately induce PBMC infection to produce HIV, activate T cells, and enhance antibody-mediated HIV + CD4 T cell killing *in vitro*. For example, by establishing a rhesus macaque model with chronic SIV infection and long-term ART inhibition, a previous study investigated the therapeutic potential of PD-1 blocking antibodies alone or in combination with the TLR7 agonist vesatolimod (34). However, this combination therapy generated no significant effectiveness. More in-depth statistical analyses of the collected data should be conducted to search for possible subgroup effects or treatment effects under specific conditions, and actively explore the possibility of combination regimens with other immunomodulators or antiviral drugs to form a more effective treatment combination.

#### 4.4 Other influential factors related to precision therapy

Safety must be taken into consideration for patients before treatment, and CD4 cell count is a protective factor to reduce the risk of irAEs. Biomarker detection should also be performed throughout the whole process (8). Meanwhile, individual differences have been reported in the response to ICIs, even with the occurrence of severe irAEs in some patients (35), thus necessitating biomarker detection for predicting disease progression. These biomarkers may serve dual predictive roles. To be specific and firstly, biomarkers can determine whether baseline levels of immune checkpoint molecules can forecast the therapeutic efficacy of ICBs (36). Secondly, it can benefit the assessment of the correlation of dynamic changes in these markers during treatment with subsequent development of drug resistance and irAEs (37).

For instance, in the treatment of melanoma, the biweekly 10 mg/kg pembrolizumab regimen demonstrated marginally reduced ORR compared to the triweekly 10 mg/kg schedule (33.7% vs. 32.9%), whereas the 3 mg/kg ipilimumab cohort exhibited

significantly lower ORR than the pembrolizumab group (11.9% vs. 33.7%) (38). In HIV immunotherapy trials, 90% of high-dose regimen recipients showed significant elevation in the absolute counts of CD4<sup>+</sup> T cells, yet with the absence of linear correlation between CD4<sup>+</sup> percentage changes and absolute count increments underscores, requiring expanded sample sizes to validate dose-response relationships (10). Furthermore, spatial multi-omics profiling can be integrated to decode the potential associations between patient-specific biomarker signatures and therapeutic responses, which may facilitate the elucidation of spatial regulatory mechanisms of immunotherapy sensitivity within the TME (21). In addition, pharmacokinetic monitoring models linking biomarker trajectories to ICI plasma concentrations may also contribute to enhanced efficacy prediction accuracy and guide personalized therapeutic optimization.

## 5. Conclusion

In conclusion, patients with HIV may not be able to benefit equally from ICBs given the existing clinical data. It is necessary to consider precision medicine, and to improve the selection of appropriate ICBs therapies for an individual with a view to maximising the therapeutic benefit. Biomarkers can assist in disease diagnosis and prognosis, and guide personalized treatment, which is an important tool for the implementation of precision medicine. Biomarkers may benefit the determination of appropriate treatment regimens during ICB therapy. However, due to the complexity of HIV itself and the challenge of uncovering its associated biomarkers, mining biomarkers is still one of the most important means to advance the functional cure of AID patients.

Massive existing studies have reported the expression of TIGIT, TIM-3, LAG-3, *etc.* on T cells of HIV patients, and relevant *in vitro* studies have documented the potential of ICBs.

Currently, available choices of ICBs are limited as relevant clinical trials are still in the preliminary stage. In combination therapy, dual-target ICB therapy can activate the viral latent reservoir. ICBs in combination with vaccines have shown potential in reducing latent reservoirs. In the comparison of pre- and post-treatment DNA reservoirs, the viral reservoirs after treatment using vaccine in combination with PD-1 therapy were reduced even more significantly as (3.5 vs. 2.1) levels compared to DNA vaccine only. However, there are few trials on the use of ICBs + vaccine in SIV, necessitating further investigation concerning the on-going gap in clinical validation.

However, there are several questions that need to be answered about its strategy in combination with ICB therapy, despite the indispensability of conventional ART as described above. The first problem is it necessary to use ART through the course of ICB therapy. Consequently, multi-cohort studies are required to

investigate the viral suppression with ART and the viral suppression utility of ICBs.

The second problem is how should ICI be applied as a predictive marker after ART treatment interruption. ICB has been revealed to be a new and effective modality for patients when ART treatment is interrupted after the emergence of drug resistance and viraemia, *etc.*. Extensive studies have documented the value of PD-1 in indicating depletion or even activation. For instance, the effects of PD-1, TIM-3, and LAG-3 in the CD4+ and CD8+ T cells in predicting a significant effect on viral rebound, suggesting a role in strongly predicting viraemic relapse events after treatment interruption. The final question is whether resistance or increased drug toxicity occurs during treatment using ICB as an immunosuppressant for ART. Currently, the core treatment option for HIV remains ART, with limitations such as the inability to clear latent viral reservoirs, the need for lifelong medication, and the potential risk of drug resistance, which warrants a thorough investigation of the use of combination treatment strategies as opposed to monotherapy.

The immune system is a key breakthrough in achieving a functional cure for HIV. For example, strategies such as activating the self-regenerative capacity of immune cells, precisely targeting latent viral reservoirs, and developing therapeutic vaccines and broad-spectrum neutralizing antibodies hold the promise of achieving a functional cure for HIV without the need for lifelong drug therapy.

To achieve this long-term goal, it is necessary to integrate diversified therapeutic means: combining cutting edge technological breakthroughs with traditional interventions, and constructing a prevention and control system of prevention and control at the source - early blockade - immune reconstruction, to promote a paradigm shift from passive control to active elimination of HIV treatment.

The first level of the prevention and control system is vaccine-driven, focusing on the protection of susceptible populations and the research and development of innovative vaccines. For example, the development of the latest therapeutic vaccine, IVCAX, is based on the regulation of immune checkpoints on effector T-cells to achieve functional inhibition by suppressing viral replication, marking an important advance in vaccine development.

The second tier of the prevention and control system focuses on early intervention after infection, forming a network of 'early screening and early treatment - virus reservoir monitoring - joint immune regulation'. Currently, the synergistic strategy of immune checkpoint inhibitors (ICIs) and antiretroviral therapy (ART) has highlighted its unique advantages: while ART controls viral replication, ICIs can restore T-cell function and target the removal of latent infected cells, significantly reducing the size of the viral reservoir.

The third level of prevention and control focuses on immune reconstitution and long-term recovery, such as remodeling the immune function through the establishment of an autologous memory T-cell bank or targeting the glucose metabolism pathway to enhance the persistence of CD8+ T-cells, which provides long-term immune protection for patients.

In summary, a functional cure for HIV requires a multi-dimensional strategy: continuous promotion of technological innovations (*e.g.*, gene editing, innate immune agonists, chimeric antigen receptor T cells, *etc.*), improvement of the policy synergy network, and construction of a global HIV governance framework. Through the technological empowerment of the three-tier prevention and control system, it is expected to achieve effective control of new infections and a significant increase in the functional cure rate in the future, providing a replicable and innovative model for the prevention and control of chronic infectious diseases.

**Funding:** This study was supported by grants from the National Key Research and Development Program of China (2024YFC2311101, 2023YFC2306700, 2023YFC2306703, 2023YFC2306400, 2023YFC2306401, 2022YFC2304401), the Special Funds for Strategic Emerging Industry of Shenzhen (F-2022-Z99-502266), the Shenzhen High-level Hospital Construction Fund (G2022091, XKJS-CRGRK-008).

**Conflict of Interest:** The authors declare that the research was conducted in the absence of any commercial or financial relationships that could be construed as a potential conflict of interest.

## References

1. Liu XJ, McGoogan JM, Wu ZY. Human immunodeficiency virus/acquired immunodeficiency syndrome prevalence, incidence, and mortality in China, 1990 to 2017: a secondary analysis of the Global Burden of Disease Study 2017 data. *Chin Med J (Engl)*. 2021; 134:1175-1180.
2. Abana CZ, Lampitey H, Bonney EY, Kyei GB. HIV cure strategies: which ones are appropriate for Africa? *Cell Mol Life Sci*. 2022; 79:400.
3. Wu X, Wu G, Ma P, *et al*. Immediate and long-term outcomes after treat-all among people living with HIV in China: an interrupted time series analysis. *Infect Dis Poverty*. 2023; 12:73.
4. Deeks SG, Archin N, Cannon P, Collins S, Jones RB, de Jong MWP, Lambotte O, Lamplough R, Ndung'u T, Sugarman J, Tiemessen CT, Vandekerckhove L, Lewin SR; International AIDS Society (IAS) Global Scientific Strategy working group. Research priorities for an HIV cure: International AIDS Society Global Scientific Strategy 2021. *Nat Med*. 2021; 27:2085-2098.
5. Uldrick TS, Gonçalves PH, Abdul-Hay M, *et al*. Assessment of the Safety of Pembrolizumab in Patients

- With HIV and Advanced Cancer – A Phase 1 Study. *JAMA Oncol.* 2019; 5:1332-1339.
6. Yi M, Zheng X, Niu M, Zhu S, Ge H, Wu K. Combination strategies with PD-1/PD-L1 blockade: current advances and future directions. *Mol Cancer.* 2022; 21:28.
7. Boyer Z, Palmer S. Targeting Immune Checkpoint Molecules to Eliminate Latent HIV. *Front Immunol.* 2018; 9:2339.
8. El Zarif T, Nassar AH, Adib E, *et al.* Safety and Activity of Immune Checkpoint Inhibitors in People Living With HIV and Cancer: A Real-World Report From the CATCH-IT Consortium. *J Clin Oncol.* 2023; 41:3712-3723.
9. Gay CL, Bosch RJ, McKhann A, *et al.* Safety and Immune Responses Following Anti-PD-1 Monoclonal Antibody Infusions in Healthy Persons With Human Immunodeficiency Virus on Antiretroviral Therapy. *Open Forum Infect Dis.* 2024; 11:ofad694.
10. Colston E, Grasela D, Gardiner D, Bucy RP, Vakkalagadda B, Korman AJ, Lowy I. An open-label, multiple ascending dose study of the anti-CTLA-4 antibody ipilimumab in viremic HIV patients. *PLoS One.* 2018; 13:e0198158.
11. Gougis P, Jochum F, Abbar B, Dumas E, Bihan K, Lebrun-Vignes B, Moslehi J, Spano JP, Laas E, Hotton J, Reyat F, Hamy AS, Salem JE. Clinical spectrum and evolution of immune-checkpoint inhibitors toxicities over a decade – a worldwide perspective. *EClinicalMedicine.* 2024; 70:102536.
12. Fenwick C, Joo V, Jacquier P, Noto A, Banga R, Perreau M, Pantaleo G. T-cell exhaustion in HIV infection. *Immunol Rev.* 2019; 292:149-163.
13. Baldanzi G. Immune Checkpoint Receptors Signaling in T Cells. *Int J Mol Sci.* 2022; 23:3529.
14. Brunet-Ratnasingham E, Morou A, Dubé M, Niessl J, Baxter AE, Tastet O, Brassard N, Ortega-Delgado G, Charlebois R, Freeman GJ, Tremblay C, Routy JP, Kaufmann DE. Immune checkpoint expression on HIV-specific CD4<sup>+</sup> T cells and response to their blockade are dependent on lineage and function. *EBioMedicine.* 2022; 84:104254.
15. Porichis F, Kwon DS, Zupkosky J, Tighe DP, McMullen A, Brockman MA, Pavlik DF, Rodriguez-Garcia M, Pereyra F, Freeman GJ, Kavanagh DG, Kaufmann DE. Responsiveness of HIV-specific CD4 T cells to PD-1 blockade. *Blood.* 2011; 118:965-974.
16. Gubser C, Chiu C, Lewin SR, Rasmussen TA. Immune checkpoint blockade in HIV. *EBioMedicine.* 2022; 76:103840.
17. Gay CL, Bosch RJ, Ritz J, *et al.* Clinical Trial of the Anti-PD-L1 Antibody BMS-936559 in HIV-1 Infected Participants on Suppressive Antiretroviral Therapy. *J Infect Dis.* 2017; 215:1725-1733.
18. Delyon J, Biard L, Renaud M, *et al.* PD-1 blockade with pembrolizumab in classic or endemic Kaposi's sarcoma: a multicentre, single-arm, phase 2 study. *Lancet Oncol.* 2022; 23:491-500.
19. Gonzalez-Cao M, Morán T, Dalmau J, *et al.* Assessment of the Feasibility and Safety of Durvalumab for Treatment of Solid Tumors in Patients With HIV-1 Infection: The Phase 2 DURVAST Study. *JAMA Oncol.* 2020; 6:1063-1067.
20. Sinha N, Sinha S, Valero C, Schäffer AA, Aldape K, Litchfield K, Chan TA, Morris LGT, Ruppin E. Immune Determinants of the Association between Tumor Mutational Burden and Immunotherapy Response across Cancer Types. *Cancer Res.* 2022; 82:2076-2083.
21. Deng H, Zhao Y, Cai X, Chen H, Cheng B, Zhong R, Li F, Xiong S, Li J, Liu J, He J, Liang W. PD-L1 expression and Tumor mutation burden as Pathological response biomarkers of Neoadjuvant immunotherapy for Early-stage Non-small cell lung cancer: A systematic review and meta-analysis. *Crit Rev Oncol Hematol.* 2022; 170:103582.
22. Morad G, Helmink BA, Sharma P, Wargo JA. Hallmarks of response, resistance, and toxicity to immune checkpoint blockade. *Cell.* 2021; 184:5309-5537.
23. Lopez-Olivo MA, Kachira JJ, Abdel-Wahab N, Pundole X, Aldrich JD, Carey P, Khan M, Geng Y, Pratt G, Suarez-Almazor ME. A systematic review and meta-analysis of observational studies and uncontrolled trials reporting on the use of checkpoint blockers in patients with cancer and pre-existing autoimmune disease. *Eur J Cancer.* 2024; 207:114148.
24. Harper J, Gordon S, Chan CN, *et al.* CTLA-4 and PD-1 dual blockade induces SIV reactivation without control of rebound after antiretroviral therapy interruption. *Nat Med.* 2020; 26:519-528.
25. Rasmussen TA, Rajdev L, Rhodes A, *et al.* Impact of Anti-PD-1 and Anti-CTLA-4 on the Human Immunodeficiency Virus (HIV) Reservoir in People Living With HIV With Cancer on Antiretroviral Therapy: The AIDS Malignancy Consortium 095 Study. *Clin Infect Dis.* 2021; 73:e1973-e1981.
26. Rahman SA, Yagnik B, Bally AP, Morrow KN, Wang S, Vanderford TH, Freeman GJ, Ahmed R, Amara RR. PD-1 blockade and vaccination provide therapeutic benefit against SIV by inducing broad and functional CD8<sup>+</sup> T cells in lymphoid tissue. *Sci Immunol.* 2021; 6:eabh3034.
27. Wu C, He Y, Zhao J, Luo K, Wen Z, Zhang Y, Li M, Cui Y, Liu Z, Wang C, Han Z, Li G, Feng F, Li P, Chen L, Sun C. Exacerbated AIDS Progression by PD-1 Blockade during Therapeutic Vaccination in Chronically Simian Immunodeficiency Virus-Infected Rhesus Macaques after Interruption of Antiretroviral Therapy. *J Virol.* 2022; 96:e0178521.
28. Wu L, Zheng Z, Xun J, *et al.* Anti-PD-L1 antibody ASC22 in combination with a histone deacetylase inhibitor chidamide as a "shock and kill" strategy for ART-free virological control: a phase II single-arm study. *Signal Transduct Target Ther.* 2024; 9:231.
29. Lu L, Wang J, Yang Q, Xie X, Huang Y. The role of CD38 in HIV infection. *AIDS Res Ther.* 2021; 18:11.
30. Li W, Liang L, Liao Q, Li Y, Zhou Y. CD38: An important regulator of T cell function. *Biomed Pharmacother.* 2022; 153:113395.
31. Angelicola S, Ruzzi F, Landuzzi L, Scalambra L, Gelsomino F, Ardizzoni A, Nanni P, Lollini PL, Palladini A. IFN- $\gamma$  and CD38 in Hyperprogressive Cancer Development. *Cancers (Basel).* 2021; 13:309.
32. Spreafico A, Janku F, Rodon JA, *et al.* A phase I study of Sym021, an anti-PD-1 antibody, alone and in combination with Sym022 (anti-LAG-3) or Sym023 (anti-TIM-3). *Ann Oncol.* 2019; 30(Suppl 5):v488-v489.
33. U.S. National Library of Medicine. A Study of Dose Escalation of IBI321 in Patients With Advanced Solid Tumors. NCT04911894. <https://clinicaltrials.gov/study/NCT04911894> (accessed August 6, 2024).
34. Bekerman E, Hesselgesser J, Carr B, Nagel M, Hung M, Wang A, Stapleton L, von Gegerfelt A, Elyard HA, Lifson JD, Geleziunas R. PD-1 Blockade and TLR7 Activation Lack Therapeutic Benefit in Chronic

- Simian Immunodeficiency Virus-Infected Macaques on Antiretroviral Therapy. *Antimicrob Agents Chemother.* 2019; 63:e01163-19.
35. Lau JSY, McMahon JH, Gubser C, Solomon A, Chiu CYH, Dantanarayana A, Chea S, Tennakoon S, Zerbato JM, Garlick J, Morcilla V, Palmer S, Lewin SR, Rasmussen TA. The impact of immune checkpoint therapy on the latent reservoir in HIV-infected individuals with cancer on antiretroviral therapy. *AIDS.* 2021; 35:1631-1636.
36. Dhodapkar KM, Duffy A, Dhodapkar MV. Role of B cells in immune-related adverse events following checkpoint blockade. *Immunol Rev.* 2023; 318:89-95.
37. Cariou PL, Pobel C, Michot JM, Danlos FX, Besse B, Carbonnel F, Mariette X, Marabelle A, Messayke S, Robert C, Routier E, Noël N, Lambotte O. Impact of immunosuppressive agents on the management of immune-related adverse events of immune checkpoint blockers. *Eur J Cancer.* 2024; 204:114065.
38. Qiu J, Cheng Z, Jiang Z, Gan L, Zhang Z, Xie Z. Immunomodulatory Precision: A Narrative Review Exploring the Critical Role of Immune Checkpoint Inhibitors in Cancer Treatment. *Int J Mol Sci.* 2024; 25:5490.
39. Benito JM, Restrepo C, García-Foncillas J, Rallón N. Immune checkpoint inhibitors as potential therapy for reverting T-cell exhaustion and reverting HIV latency in people living with HIV. *Front Immunol.* 2023; 14:1270881.
40. U.S. National Library of Medicine. Treatment of PD-1 Inhibitor in AIDS-associated PML (TPAP). NCT04091932. <https://clinicaltrials.gov/study/NCT04091932> (accessed August 6, 2024).
41. U.S. National Library of Medicine. A Single Dose of Pembrolizumab in HIV-Infected People. NCT03367754. <https://clinicaltrials.gov/study/NCT03367754> (accessed August 6, 2024).
42. U.S. National Library of Medicine. Testing the Combination of the Anti-cancer Drugs XL184 (Cabozantinib) and Nivolumab in Patients With Advanced Cancer and HIV. NCT04514484. <https://clinicaltrials.gov/study/NCT04514484> (accessed August 6, 2024).
43. U.S. National Library of Medicine. Low Dose Nivolumab in Adults Living With HIV on Antiretroviral Therapy (NIVO-LD). NCT05187429. <https://clinicaltrials.gov/study/NCT05187429> (accessed June 16, 2024).
44. U.S. National Library of Medicine. Intra-lesional Nivolumab Therapy for Limited Cutaneous Kaposi Sarcoma. NCT03316274. <https://clinicaltrials.gov/study/NCT03316274> (accessed June 16, 2024).
45. U.S. National Library of Medicine. Therapy Adapted for High Risk and Low Risk HIV-Associated Anal Cancer. NCT04929028. <https://clinicaltrials.gov/study/NCT04929028> (accessed August 6, 2024).
46. U.S. National Library of Medicine. Study to Evaluate Safety, Tolerance and Efficacy of ASC22 Combined With ART in Subjects With HIV. NCT05330143. <https://clinicaltrials.gov/study/NCT05330143> (accessed August 6, 2024).
47. U.S. National Library of Medicine. Durvalumab and Tremelimumab in Combination With Chemotherapy in Virus-infected Patients With Non-small Cell Lung Cancer. NCT04499053. <https://clinicaltrials.gov/study/NCT04499053> (accessed June 16, 2024).
48. U.S. National Library of Medicine. Preliminary Assessment of Safety and Tolerability of Dostarlimab in Combination Antiretroviral Therapy (cART) Refractory HIV Associated Kaposi Sarcoma (STARKAP). NCT05646082. <https://clinicaltrials.gov/study/NCT05646082> (accessed June 16, 2024).
49. U.S. National Library of Medicine. ANRS CO24 OncoVIHAC (Onco VIH Anti Checkpoint). NCT03354936. <https://clinicaltrials.gov/study/NCT03354936> (accessed June 16, 2024).
50. U.S. National Library of Medicine. Nivolumab/Ipilimumab and Chemotherapy Combination in Advanced NSCLC Patients With HIV, HBV, HCV and Long Covid Syndrome (LUNGVI). NCT05597800. <https://clinicaltrials.gov/study/NCT05597800> (accessed June 16, 2024).
51. U.S. National Library of Medicine. Nivolumab and Ipilimumab in Treating Patients With HIV Associated Relapsed or Refractory Classical Hodgkin Lymphoma or Solid Tumors That Are Metastatic or Cannot Be Removed by Surgery. NCT02408861. <https://clinicaltrials.gov/study/NCT02408861> (accessed June 16, 2024).

Received March 12, 2025; Revised April 18, 2025; Accepted April 26, 2025.

\*Address correspondence to:

Hongzhou Lu, The Third People's Hospital of Shenzhen, National Clinical Research Center for Infectious Diseases and The Second Affiliated Hospital of Southern University of Science and Technology, Shenzhen, Guangdong, China.  
E-mail: luhongzhou@szsy.sustech.edu.cn

Released online in J-STAGE as advance publication April 29, 2025.



# Multimodal treatment of colorectal liver metastases: Where are we? Current strategies and future perspectives

Caterina Accardo<sup>1</sup>, Ivan Vella<sup>1</sup>, Fabrizio di Francesco<sup>1</sup>, Sergio Rizzo<sup>2</sup>, Sergio Calamia<sup>1</sup>, Alessandro Tropea<sup>1</sup>, Pasquale Bonsignore<sup>1</sup>, Sergio Li Petri<sup>1</sup>, Salvatore Gruttadauria<sup>1,3,\*</sup>

<sup>1</sup> Department for the Treatment and Study of Abdominal Diseases and Abdominal Transplantation, Istituto di Ricovero e Cura a Carattere Scientifico- Istituto Mediterraneo per i Trapianti e Terapie ad alta specializzazione (IRCCS-ISMETT), University of Pittsburgh Medical Center (UPMC), Palermo, Italy;

<sup>2</sup> Medical Oncology Service, Istituto di Ricovero e Cura a Carattere Scientifico- Istituto Mediterraneo per i Trapianti e Terapie ad alta specializzazione (IRCCS-ISMETT), University of Pittsburgh Medical Center (UPMC), Palermo, Italy;

<sup>3</sup> Department of Surgery and Medical and Surgical Specialties, University of Catania, Catania, Italy.

**SUMMARY:** Despite the continued high prevalence of colorectal cancer in the Western world, recent years have witnessed a decline in its mortality rate, largely attributable to the sustained advancement of multimodal treatment modalities for metastatic patients. One persisting issue is lack of consensus between different centres and multidisciplinary teams regarding definition of resectability, the duration of chemotherapy treatment, and surgical strategy. This narrative review outlines current multimodal treatment of patients with colon cancer metastatic to the liver and/or lung in different clinical scenarios. Currently, there are multiple multimodal strategies that can be employed to enhance resectability in these patients. These include novel and sophisticated target therapies (such as novel immunotherapeutic modalities and micro RNAs), complex resections utilising parenchyma-sparing techniques, liver transplantation, and cytoreductive strategies in patients for whom a curative option is not feasible. It is the responsibility of the scientific community to establish standardised protocols across different centres, based on the most recent evidence, while maintaining a high degree of personalisation of treatment for each individual patient. It seems likely that artificial intelligence (AI) will play a significant role in achieving this goal.

**Keywords:** liver metastases, colorectal cancer, multidisciplinary approach, surgical strategy

## 1. Introduction

Colorectal cancer represents the third most prevalent cancer diagnosis globally and is the second leading cause of cancer-related mortality (1), although there has been a gradual improvement in survival for these patients over the last few decades (2). In fact, there have been remarkable advances in the management of metastatic colorectal cancer (mCRC). These developments can be attributed to several factors, including the evolution of liver surgery techniques with a reduction in mortality and morbidity, the introduction of new procedures that enhance the future liver remnant (such as portal vein embolization, two-stage hepatectomy [TSH], and associated liver partition and portal vein ligation for staged hepatectomy [ALPPS]), and the enhanced efficacy of chemotherapy (3-5). In addition, the selection criteria for resection of colorectal liver metastasis (CRLM) have changed significantly, becoming less stringent regarding the number and size of metastases, the presence of extrahepatic disease (EHD), patient age limits and

resection margins (6).

Despite being the only potentially curative strategy for CRLM, surgery remains underused (7). This is probably in part because there are still misconceptions about the distinction between resectable and unresectable disease, and it can be difficult to identify ideal windows for surgery that fit with the multimodal management of these patients (8). The majority of patients with metastatic disease are seen exclusively by medical oncologists for systemic therapy to manage metastatic disease, which often means that the oncologist is the only specialist to review the resectability of the disease (9,10). Furthermore, there is frequently a lack of agreement on strategy and decision-making even among experienced hepatobiliary surgeons themselves (11).

So much remains to be done to optimize multimodal treatment of these patients, with protocols that are as standardised as possible, but at the same time tailored to each individual patient. It is not easy, and it is precisely by reviewing evolution of thinking in CRLM treatment that we can understand future prospects.

## 2. Metachronous CRLM

According to a recent European multi-societal consensus (12), "early metachronous metastases" are those absent at presentation but detected within 12 months of the primary tumor, while "late metachronous metastases" are those detected after 12 months.

Currently, there is no absolute evidence on whether or not neoadjuvant treatment is indicated in all cases of metachronous CRLM. In a 2010 study by Adam *et al.* on a multicenter cohort of 1,471 patients with metachronous CRLM who underwent liver resection (LR) with or without neoadjuvant chemotherapy, univariate analysis showed that preoperative chemotherapy did not affect overall survival (OS) (60% at 5 years in both groups); however, postoperative chemotherapy was associated with better OS (65% vs. 55% at 5 years,  $p < 0.01$ ) (13). In the ESMO Clinical Practice Guidelines, the metachronous onset of CRLM could be an oncological contraindication to upfront surgery (14), and in fact, historically, metachronous onset has been considered a biological predictor of poor prognosis (15). However, some studies in the literature suggest that upfront resection should be considered in cases of a single small nodule that does not require major hepatectomy or indicate high morbidity (16).

## 3. Synchronous CRLM

### 3.1. Defining resectability

Each clinical case of a patient with CRLM should be presented to a multidisciplinary team at the time of initial diagnosis (17) to assess resectability and determine a precise multimodal treatment pathway (18). The criteria for R0 resectability of CRLM (the only way, apart from liver transplantation, to cure the disease after effective chemotherapy) depend on technical and oncological (prognostic) criteria and experience of the multidisciplinary team (MDT). Considerations when assessing resectability must include an assessment of disease burden (*i.e.*, size, number and distribution of CRLM) (19), impression of the disease biology (*i.e.*, rate of disease progression, suspicion of EHD, timing of presentation in relation to primary colorectal tumor, sidedness of primary colorectal tumor, RAS/BRAF mutation status, microsatellite instability [MSI] status) (20), and technical aspects. Over the years, different definitions of resectability have been given in the case of CRLM (21-25) and Table 1 summarizes them according to their temporal evolution. Evolution of the definition reflects the progressive technological and technical-surgical development (three-dimensional study of the liver, increasingly effective hepatic hypertrophy techniques, more accurate imaging, *etc.*) and the appearance of effective chemotherapies, which have pushed the limits of surgical indication. Surgical

thinking has progressively evolved: from the indication only in cases with a number of CRLM  $< 4$ , absence of extrahepatic metastases and obtaining an R0 margin of at least 1 cm (26) up to increasingly less stringent criteria in terms of number of metastases (27), surgical margin (28) and presence of resectable extrahepatic disease or vascular infiltration. Currently, it is considered resectable if complete resection with tumor-free margins is possible, with preservation of at least 20-30% of total liver volume, adequate vascular inflow and outflow, and effective biliary drainage (29). Technically, therefore, resectability is not limited by number, size or bilobar metastatic involvement if tumors can be resected leaving sufficient residual liver (14).

Patients defined as initially unresectable could undergo a reassessment of resectability, preferably within 2-3 months of starting therapy, as proposed by an expert consensus (30).

### 3.2. Patients with unresectable CRLM

In the case of initially unresectable liver metastasis, chemotherapy is the only viable treatment option. While traditional chemotherapy has historically demonstrated efficacy in suppressing tumor growth, the advent of novel chemotherapy agents and molecularly targeted drugs has led to a paradigm shift in the treatment landscape. These new agents have been shown to induce tumor shrinkage and, in selected cases, complete remission. Consequently, liver metastasis that was initially deemed unresectable may become resectable through the use of chemotherapy, a process known as conversion therapy.

Bismuth *et al.* first reported the possibility that chemotherapy may convert unresectable disease to resectable disease (31). It is estimated that approximately 15% of patients undergoing systemic chemotherapy and 30-50% of those undergoing regional chemotherapy are converted to resectable status (32-35). A study by Sugiyama and colleagues identified patients with specific clinical profiles, including a left-sided primary tumor, absence of extrahepatic metastases, H1 or H2 grade, and treatment with molecularly targeted agents, who were potential candidates for conversion hepatectomy with the goal of cytoreduction, and they demonstrated favorable outcomes (36).

The question of how long a patient should remain on downstaging chemotherapy prior to resection is still open to debate within the medical community. Some proponents of this approach advocate for surgical intervention as soon as the patient is deemed resectable (37), while others advocate achieving highest tumor response (with a median duration of approximately four months) (38). A recent review on optimal duration of chemotherapy in colorectal cancer according to indications posits that when the objective is a conversion strategy, a relatively limited number of cycles (four to six cycles) should be administered, with re-staging and

**Table 1. The anatomical definition of "resectability" in the case of CRLMs, according to different studies in different time periods**

| Author, Year (Ref.)                        | N patients | Country                                      | Anatomical definition of resectability  |
|--|------------|--|---|
| Ekberg <i>et al.</i> , 1986 (26)           | 72         | Sweden                                       | Resectable if < 4 lesions, absence of extrahepatic metastases, possibility of obtaining a surgical margin of at least 1 cm  |
| Charnsangavej C, <i>et al.</i> , 2006 (26) | -          | USA  | Resectable if is possible to preserve two contiguous hepatic segments, preservation of adequate vascular inflow and outflow as well as biliary drainage, and the ability to preserve adequate FLR > 20% in a healthy liver).<br>(The presence of extrahepatic disease should no longer be considered an absolute contraindication to hepatic resection.)  |
| Rees M, <i>et al.</i> , 2008 (19)          | 929        | United Kingdom                               | Complete resection of all CRLM, regardless of size, number, distribution, or width of resection margin, while preserving a sufficient volume of FLR 25-30% in case of normal liver  |
| Adam R, <i>et al.</i> , 2012 (29)          | -          | International Consensus                      | Potential for complete resection with tumor-free margins (R0 resection), with preservation of at least two disease-free liver segments with viable vascular inflow, outflow, and biliary drainage and an FLR volume of 30%.   |
| Worni M, <i>et al.</i> , 2014 (21)         | -          | USA  | Appropriate medical candidate for surgery; possibility to plan R0 resection irrespective of size and multiplicity; sufficient FLR<br><i>Note:</i> The presence of limited extrahepatic disease that is amenable to resection is a relative contraindication.  |
| Viganò L, <i>et al.</i> , 2015 (27)        | 849        | Italy, Switzerland                           | Surgical indication even if > 8 metastases in the absence of risk factors (good response to chemotherapy, absence of extrahepatic disease, non-rectal location)   |
| Phelip JM, <i>et al.</i> , 2016 (22)       | 26         | France                                       | Borderline resectable: number of metastases ≤ 8 and/or ≤ 6 segments of liver involved whatever the size of the metastases, without infiltration of any hepatic veins and without infiltration of both hepatic arteries or both portal vein branches; absence of more than 2 potentially resectable extrahepatic (e.g., pulmonary) metastases, and at least one metastasis measurable by CT scan or MRI. |
| Allard MA, <i>et al.</i> , 2017 (28)       | 12,406     | Multicentre                                  | Even in cases with CRLM > 10, with R0/R1 resection we obtain better survival rates than with chemotherapy alone.  |
| Pietrantonio F, <i>et al.</i> , 2017 (25)  | 31         | Italy  | Borderline resectable: tumor involvement of > 1 hepatic vein, or > 4 hepatic segments, need for 2-stage hepatectomy or radiofrequency ablation, and/or biologically (high risk): ≥ 4 metastatic nodules, or synchronous metastases.   |
| Huiskens J, <i>et al.</i> , 2019 (27)      | 181        | Netherlands                                  | The ability to obtain a complete resection of all lesions in one single surgical procedure ( <i>i.e.</i> , excluding 2-stage resections and/or use of portal vein embolization) by resection only ( <i>i.e.</i> excluding the use of additional ablative treatments or other local methods), leaving an estimated FLR of 25-30% in uncompromised livers, or 35-40% in compromised livers.               |
| Ichida H, <i>et al.</i> , 2019 (23)        | 245        | Japan  | Resectable: ≤ 3 lesions, tumor size <5 cm; absence of extra-hepatic metastases; FLR > 30%.<br>Borderline resectable: > 4 lesions; tumor size > 5 cm; presence of resectable extra-hepatic metastases. FLR < 30%   |
| Nieuwenhuizen S, <i>et al.</i> , 2020 (24) | -          | Netherlands                                  | Easily resectable: ≤ 3 adjacent segments removed; FLR > 40%; < 1 hepatic vein involved; contralateral portal pedicle and inferior caval vein free from tumor.<br>Difficultly resectable: >3 adjacent segments removed; FLR < 40%; perihilar resections or biliary and/or vascular resection required; involvement of contralateral portal pedicle and inferior caval.                                   |
| Dijkstra M, <i>et al.</i> , 2021 (20)      | 520        | Netherlands                                  | CRLM are resectable at the discretion of the performing oncological or hepatobiliary surgeon.   |
| Cervantes A, <i>et al.</i> , 2022 (28)     | -          | European Society for Medical Oncology (ESMO) | Resectability is not limited by number, size or bilobar metastatic involvement, if tumours may be resected leaving sufficient FLR > 30%.  |

Table 1 The anatomical definition of 'resectability' in the case of CRLMs, according to different studies in different time periods. CRLM: colorectal liver metastasis; FLR: future liver remnant.

re-evaluation for surgery as soon as possible in most cases (39). Shortly before, a retrospective work on a multicentre cohort of 2,793 patients with unresectable CRLM undergoing conversion chemotherapy that aimed to assess systemic treatment characteristics impacting outcome after hepatectomy, revealed that short (< 7 or < 13 cycles in 1st or 2nd line) preoperative chemotherapy duration was independently associated with longer OS (HR: 0.85,  $p = 0.046$ ), DFS (HR: 0.81,  $p = 0.016$ ) and hepatic-specific relapse-free survival (HR: 0.80,  $p = 0.05$ ) (40).

Thus, what is currently emerging in the literature is that an excessive duration of chemotherapy can be disadvantageous and does not increase patients' OS, may instead lead to liver toxicity (41,42). Prospective studies may define optimal duration in terms of the balance between conversion to resectability, short duration (to reduce cytotoxic effects and prevent missing metastasis) and maximum biological effect.

According to latest ASCO guidelines (43), it is recommended that doublet backbone chemotherapy (FOLFOX or FOLFIRI) be offered as a first-line therapy for patients with initially unresectable MSS or pMMR CRLMs. In selected cases, triplet backbone chemotherapy (FOLFOXIRI) may also be offered as a first-line therapy. For patients with a right-sided mCRC, in the first-line treatment bevacizumab is recommended, an anti-vascular endothelial growth factor (anti-VEGF) antibody. This is typically used in conjunction with FOLFOX or FOLFOXIRI, which has been shown to produce high rates of pathologic responses and necrosis of CRLM (44,45). First-line therapy with pembrolizumab should be offered to patients with MSI-H or dMMR CRLM (46), while first-line therapy with anti-EGFR therapy plus doublet chemotherapy should be offered to patients with MSS or pMMR left-sided RAS wild-type mCRC (47,48). Finally, new target therapies are emerging for mCRC with RAS mutation, sometimes associated with anti-EGFR, such as Adagrasib or Divaragrasib, which are starting to show promising results (49).

### 3.3. Patients with resectable CRLM

Adjuvant chemotherapy during the perioperative period can confer survival benefits to patients with resectable CRLM (50). A 2015 consensus from the EGOSLIM group strongly recommended the use of neoadjuvant chemotherapy in these cases, reiterating the fact that synchronous CRLM has less favorable cancer biology and lower expected survival rates than metachronous CRLM (51). The value of neoadjuvant treatment is also evident in more recent series, particularly in patients with high-risk metastases. It is, therefore, necessary to identify a subgroup of patients who may benefit more from neoadjuvant treatment than others with resectable disease. A retrospective study of 322 patients conducted

in 2022 demonstrated that neoadjuvant treatment can enhance OS in patients with resectable CRLM and high clinical risk scores, as proposed by Fong *et al.* (52). In a more recent study by Ninomiya *et al.* on a multi-institutional cohort, CRLM were classified into three grades (A, B and C) based on the combination of the H-stage (H1:  $\leq 4$  lesions and  $\leq 5$  cm, H2:  $\geq 5$  lesions or  $> 5$  cm, H3:  $\geq 5$  lesions and  $> 5$  cm), the lymph node status of the primary tumor (pN0/1:  $\leq 3$  metastases, pN2:  $\geq 4$  metastases), and the presence of resectable extrahepatic metastases. The findings of this study indicate that patients with synchronous grade B/C CRLM may be suitable candidates for neoadjuvant chemotherapy (53). On the contrary, a recent meta-analysis from 2024, which included 24 studies on 8,700 patients, indicated favorable OS in the upfront surgery group (OR 1.21, 95% CI: 1.06-1.38) and favorable disease-free survival in the upfront surgery group (OR 1.71, 95% CI: 1.38-2.12). These findings suggest that neoadjuvant chemotherapy offers no additional benefit for resectable colorectal cancer with liver metastases. Consequently, upfront surgery should be considered the preferred treatment option (54). Another recent review (55) on the use of neoadjuvant chemotherapy (NAC) in CRLM points out that the available literature does not really show a clear superiority of NAC over upfront surgery when considering endpoints such as OS and disease free survival (DFS) in resectable CRLM. However, NAC certainly offers advantages in controlling micrometastases (56), increasing the rate of R0/R1 resections (57) or in selecting patients who progress during systemic treatment (cases in which surgery may be futile). Thus, in the near future, we will probably tend to stratify more resectable CRLM patients according to risk (58,59), for example by analysing circulating tumour DNA (60,61) as well as by evaluating validated clinical risk scores (52,62). The aim is to identify patients at diagnosis with resectable forms of CRLM who may benefit from preoperative short NAC in terms of OS, DFS, increased chance of curative resection R0/R1 or other patient benefits. Further prospective studies on this topic are needed.

### 3.4. Synchronous lung metastases

It is becoming increasingly common for patients with colorectal cancer to present with advanced disease, including synchronous liver and lung metastases. Studies available in the literature show a five-year survival rate ranging from 40 to 70% in cases of liver and lung metastases (both synchronous and metachronous) undergoing surgery with radical intent (63,64); so the general concept that emerges is that with complete resection we gain an oncological advantage for these patients (65).

In cases of peripheral and resectable lung localizations, a simultaneous approach is recommended,



if feasible, utilizing a single abdominal incision to initially resect the liver metastases, followed by a transdiaphragmatic approach for resection of the lung metastases (66). This approach has been described in the literature as superior to staged resection in terms of blood loss and costs with a similar impact on survival (67). According to the authors, the transdiaphragmatic approach is associated with a number of advantages, including avoidance of two separate anaesthesia episodes and two separate hospital admissions. Furthermore, it eliminates the need for a thoracic incision to resect the lung metastasis. An additional benefit of the transdiaphragmatic approach is that surgeons are able to palpate tiny lung metastases and localise them more accurately than with the video-assisted transthoracic approach, which lacks this capability. In 2021, Jalil *et al.* also proposed a single-port approach with transdiaphragmatic videoassisted thoracoscopy, with less invasiveness and functional impact on the diaphragm but identical ability to achieve R0 resection (68). The transdiaphragmatic approach to pulmonary metastases is recommended in the literature also in cases of laparoscopic liver resections, still ensuring an aggressive approach with less invasiveness (69).

Although it is the most widely supported oncological strategy, the combined resection rate remains low in the few studies available in the literature. In a recent Swedish study based on a national register, 1923 patients with liver and lung metastases from colorectal cancer registered between 2008 and 2016 were considered. Of these, complete resection of all tumour sites (colon, liver and lung) was performed in only 44 patients. These patients who underwent simultaneous resection were the youngest in the cohort and presented more frequently with right-sided colon cancer than those who were resected only in the liver. In addition, those who were operated on exclusively on the primary more frequently had a higher American Society of Anaesthesiologists (ASA) score. According to the authors of this study, the low rate of combined resection is again to be attributed to a different understanding of resectability between oncologist and surgeon and to heterogeneity in assessment of the MDT (70). An aggressive surgical strategy is therefore proposed in strictly selected patients, which is why in the context of oncology recommendations an attempt was made to identify additional predictors of prognosis in these multimetastatic patients. In a 2017 Korean study, a single-centre experience of combined surgical resection of liver and lung metastases in 66 patients who had already undergone resection of the primary tumour, it emerged that the timing of presentation (synchronous or metachronous, within or after 3 months from colonic resection, *ed.*) is not a negative prognostic factor as it has no impact on OS unlike the number and location of hepatic localizations (71). And further studies have been conducted over the years on this subject by identifying prognostic factors as CEA, rectal primary cancer,

bilateral lung metastasis and multiple metastases (72,73).

Another frequently observed scenario involves patients presenting with resectable liver metastases and innumerable, thus unresectable, lung metastases. In such patients, the natural history of mCRC is determined by the progression of liver metastases rather than lung metastases. Such patients rarely present with symptoms of respiratory distress or other pulmonary complications. Moreover, lung metastases can be effectively managed with alternative chemotherapy regimens.

A recent study examined the efficacy of surgical intervention in patients with synchronous liver and lung metastases and compared three treatment modalities: resection of liver metastases only, resection of liver and lung metastases, and palliative chemotherapy. The patients who underwent resection of liver metastases only exhibited an intermediate survival rate between those who underwent resection of both liver and lung metastases and those who underwent palliative chemotherapy (74). This suggests that in the clinical scenario of inoperable lung metastases, resection of liver lesions alone may offer a survival benefit over chemotherapy alone.

A randomized controlled trial (LUNA, liver resection with unresectable pulmonary nodules for colorectal adenocarcinoma; NCT02738606) is ongoing to objectively determine the benefit of LR alone in these patients (75).

### 3.5. Liver-first?

According to an international consensus (51), if both the primary tumor and metastases are resectable, synchronous resection can be performed in selected patients undergoing limited hepatectomy. An even more recent consensus (12) recommends that when upfront synchronous LR is to be performed together with colectomy, the LR component should be a minor hepatectomy.

For rectal tumors, preoperative radiotherapy is the standard of care, but not for high rectal tumors or T2 tumors, and single-stage surgery should not be performed (51).

In a retrospective analysis of 7,360 patients (4,415 primary-first, 552 liver-first, and 2,393 simultaneous resections) from the LiverMetSurvey registry (76), the liver-first approach is associated with longer survival than the alternative approaches (3-year survival 65.9% *vs.* primary-first 60.4%: hazard ratio [HR] 1.321,  $p = 0.031$ ; *vs.* simultaneous resections 54.4%: HR 1.624,  $p < 0.001$ ).

The liver-first approach is recommended when there are specific liver-related criteria, such as borderline resectability, that favor hepatectomy first after systemic chemotherapy. A retrospective study of 217 patients by the Strasbourg group identifies synchronous CRLM, right colon tumors, persistently high preoperative CEA

levels and lack of adjuvant treatment as prognostic factors associated with limited survival when comparing patients undergoing primary-first and simultaneous resection approaches (77). In a more recent paper on 658 patients, comparing simultaneous, liver-first, and colorectal-first strategies for the surgical treatment of synchronous colorectal liver metastases, a simultaneous approach was not associated with worse OS or morbidity compared with a liver-first approach (78).

Determining the optimal surgical strategy for each patient with CRLM is a complex process. A multitude of critical factors must be considered, including the location and extent of the primary tumor and liver metastases, the patient's performance status, the presence of symptoms, and the presence of underlying comorbidities. It is important to note that not all patients are suitable for all treatment options (51).

### 3.6. Adjuvant treatment

Adjuvant chemotherapy following curative liver resection of CRLM is not a standard protocol in all medical centres (79) and the data provided by the literature considered are incomplete, as the patients analysed are often not stratified according to risk categories. Some randomised controlled trials on adjuvant chemotherapy after CRLM resection have recently demonstrated an extension in the duration of DFS, although no such extension has been observed in OS (80,81). On the other hand, there are some studies showing that both OS and DFS are improved in patients with synchronous CRLM in the adjuvant chemotherapy group (79,82). In any case, there is a benefit for the patient, as long as the duration is not excessive (with an associated increase in toxicity). In a clinical trial on however a small number of patients (no. 28), a 3-month treatment with CAPOX appears to be safe and effective (83). Indeed, the actual duration of the treatment still remains unclear. So even if there is no real difference in OS, a better DFS still has a beneficial impact on the patient, so adjuvant chemotherapy continues to be recommended by the guidelines. It is the opinion of experts that, in the absence of prior chemotherapy for metastatic disease, the recommendation is for chemotherapy (low level of evidence – expert opinion), with options being FOLFOX or CAPOX, unless patients have been recently (< 6-12 months) exposed to oxaliplatin-based adjuvant chemotherapy for stage II or III colorectal cancer (84,85).

In the context of metachronous liver metastases, a retrospective study of 75 patients who underwent curative resection of metachronous CRLM revealed that survival at 10 and OS were enhanced when adjuvant chemotherapy was administered post-surgery (86), but there are actually no consistent results in the literature. Certainly, the identification of risk scores as proposed by Chinese colleagues could help us in this regard (87): the prognostic score was based on five clinical factors

such as lymph node spread of the primary tumour, size of the largest metachronous focus > 5 cm, presence of multiple liver metastases, preoperative CEA level > 200 ng/mL and recurrence-free interval from the time of resection of the primary tumour to the appearance of the metachronous metastasis of less than 12 months. The findings revealed that there was no significant difference in 3-year recurrence-free survival (RFS) and OS between the adjuvant chemotherapy and observation groups. However, when patients were stratified according to risk, 3-year RFS and OS were comparable between the groups in patients with the lowest risk. A similar result was demonstrated by Nakai *et al.* (88).

Probably in the future, circulating tumor DNA (ctDNA)-based molecular residual disease will help us to stratify patients as candidates for systemic treatment after curative resection (89).

### 4. Systemic Therapy

*Novel therapies*; The recent open-label, multicenter, randomized, phase III study (CAIRO5) from the Dutch Colorectal Cancer Study Group corroborates the findings of previous studies that FOLFOXIRI-bevacizumab is the preferred treatment for patients with initially unresectable CRLM, provided that the primary tumor is right-sided or mutated at the RAS or BRAFV600E level. In patients with a left-sided tumor and wild-type RAS and BRAFV600E, the addition of panitumumab to FOLFOX or FOLFIRI demonstrated no clinical benefit over bevacizumab but was associated with increased toxicity. These treatments have the potential to reduce tumor size and render the tumor amenable to curative treatment (45).

The emergence of *novel immunotherapeutic modalities*, including cancer vaccines and adoptive cell transfer therapies, has begun to transform the landscape of CRLM treatment (90). In a phase II clinical trial of a dendritic cell (DC) vaccine in colon cancer liver metastasis patients with disease-free resection margins, Rodriguez *et al.* observed a clear tendency for the DC group to exhibit a reduction in tumor recurrence and an extension in disease-free survival compared with the control group. The median disease-free survival for the DC group was 9.53 months, compared with 25.26 months for the control group (91).

*Chimeric antigen receptor T-cell (CAR-T)* therapy may represent a promising approach for the treatment of CRLM. A phase I trial of CAR-T therapy targeting CEA in patients with mCRC has yielded encouraging results (92).

Furthermore, the potential therapeutic role of *microRNAs* (miRNAs) in CRLM is becoming increasingly evident. Prior research has demonstrated the potential of miRNAs as prognostic biomarkers for CRLM patients (93,94).

Although the evidence is still preliminary, there are also data indicating that the addition of a *fecal microbiota*

*transplantation* (FMT) to a treatment regimen may be beneficial for patients with mCRC (95). A phase II trial is currently underway to assess the efficacy of FMT in combination with either pembrolizumab or nivolumab (programmed death-1 pathway (PD-1) inhibitors) in mCRC patients who have not responded to anti-PD-1 therapy (NCT04729322).

Recently, research has also shown that *nanosystems* can effectively deliver anticancer drugs to target mCRC. A study conducted in 2021 demonstrated successful synthesis and characterization of a nanocarrier capable of recognizing mCRC cells in secondary organs (96).

## 5. Surgical Strategies

In the 1980s, indications for resective liver surgery were very limited, and less than 10% of patients were candidates for surgery.

The expansion of technical indications for LR is based on three key factors: the improvement of the efficacy of systemic chemotherapy, the improvement of liver surgery techniques and the expansion of knowledge about liver regeneration (97). Patients with extensive disease, including those with synchronous disease, bilobar disease, and extensive numbers of nodules, are now eligible for aggressive surgical intervention (98). It is now widely accepted that the number and lobar location of metastases are less important in determining resectability than the presence of adequate inflow, outflow and a functional liver remnant (99). Any discussion of optimal timing and candidates for surgical intervention should involve a multidisciplinary team comprising medical oncologists, surgical oncologists, radiologists, pathologists, interventional radiologists, radiation oncologists, and geneticists. This approach goes beyond simply considering the technical feasibility of a given procedure.

Furthermore, there is considerable variation in the hospital and surgeon practice patterns regarding the definition of resectability (100).

### 5.1. ALPPS, TSH and LVD

As progress continues, expanded indications are giving way to new operative strategies, including TSH and ALPPS. Recently, an interventional radiology technique has also emerged with the aim of hypertrophying the future liver remnant (FLR): liver venous deprivation (LVD).

The TSH, with a portal vein ligation or portal vein embolisation (PVE) in the first stage, has been developed to facilitate resection in patients with an inadequate FLR (4,101). Typically, the desired degree of hypertrophy is not reached for a period of 4-8 weeks; thus, 1/3 of patients unfortunately experience disease progression during this waiting time and the survival of patients who drop out is lower than that of patients treated only with

chemotherapy (102). This is the historical reason for development of the ALPPS: by associating portal vein ligation with in situ transection of the parenchyma during the first stage, a more rapid hypertrophy is induced with a lower risk of tumour progression (103). ALPPS was, however, in early studies on the subject, correlated with high morbidity and mortality rates (5).

Despite historical evidence indicating that ALPPS is associated with elevated postoperative mortality and complication rates, several modifications have been introduced over time (T-ALPPS (104), RALPPS (105), p-ALPPS (106), *etc.*), resulting in a reduction in perioperative mortality to 3.8% (107). More recently, the LIGRO trial found that compared with traditional TSH, ALPPS can improve resection rate (92% vs. 57%) without changing the surgical margins, complication rates, or short-term mortality (108). In 2019, the ALPPS registry group published benchmark values for ALPPS (109) as well as a preoperative ALPPS risk score to evaluate possible candidates (110). Nevertheless, a prospective study on the subject indicates that the strategy remains relatively uncommon in Europe (nine countries included in the study (111)) on the other hand, TSH with PVE is described as safe and effective in the treatment of extensive bilobar metastases with both laparoscopic and open techniques (112), also remembering that an ALPPS technique can be a rescue in case of TSH/PVE with insufficient hypertrophy, with adequate oncological results (113). Finally, according to a systematic review and meta-analysis in 2022 (114), the superiority of one technique over the other cannot be determined.

In 2016 (115), the Montpellier group described a new interventional radiology technique with the aim of rapid hypertrophy of the FLR: the LVD technique, which consisted of adding suprahepatic venous deprivation to the classic portal vein embolisation in a single interventional radiology procedure. Although in recent retrospective cohorts the technique can induce hypertrophy rates similar to ALPPS with reduced hospital stay (116), randomised multicentre studies are needed to define what will be the gold standard for hypertrophy in the near future.

### 5.2. Parenchymal-sparing vs. major hepatectomy and the concept of repeated hepatectomy

The treatment of multiple and small CRLM has recently evolved from predominantly anatomic resections, such as major hepatectomy or extended hemihepatectomy, to parenchymal-sparing approaches for both unilateral and bilateral lesions.

A meta-analysis regarding anatomical versus non-anatomical resections showed that surgical margins, OS, and DFS did not differ significantly between the two groups (117).

Torzilli *et al.* validated use of intraoperative

ultrasonography (IOUS) and subsequently demonstrated that this technique (IOUS-guided parenchymal-sparing hepatectomy [PSH]) could also be employed for lesions near the hepatocaval confluence, a location that would otherwise necessitate a significant hepatectomy with the potential for vascular reconstruction (118). PSH for solitary lesions with a diameter of less than 3 cm does not result in an increased recurrence rate and has been linked to improved survival outcomes. This is due to the fact that it enhances the possibility of successful salvage in cases of liver recurrence (119). In fact, this technique could reduce the number of major hepatectomies by up to 80%, and subsequent recurrences can be re-resected with excellent 5-year OS (120). This concept of repeated hepatectomy, repeated LR of CRLM, can achieve comparable perioperative mortality and long-term survival rates with primary LR (121). It is true that PSH may result in a certain risk of intrahepatic recurrence, however it has comparable results to anatomical resection in terms of hepatic recurrence free survival at 3 and 5 years, as analysed in a recent meta-analysis. The most recent data therefore strengthen its application in this category of patients (122).

### 5.3. Role of minimally invasive surgery

Laparoscopic liver resection (LLR) has been the accepted standard of care for peripheral lesions in the so-called "laparoscopic segments" II, III, V, and VI for over a decade (123). However, the utilization of minimally invasive surgery (MIS) for hepatic lobectomy remains more constrained and has been considerably slower in achieving widespread acceptance. A recent consensus statement recommends the use of minimally invasive techniques as appropriate options for both primary tumor and liver metastases (12). Indeed, two randomized clinical trials, OSLO-COMET (124) and LapOpHuva (125), compared laparoscopic and laparotomic resections in two heterogeneous cohorts of patients. The results demonstrated the efficacy of laparoscopy for CRLM with equivalent oncologic outcomes, a faster return to work, and reduced perioperative morbidity, length of stay (LOS) and perioperative pain.

The advent of robotic liver surgery has led to an increase in the utilization of MIS for all LR. The robotic surgical system has been shown to be particularly beneficial in facilitating the completion of complex procedures such as major lobectomies, which have a higher conversion rate to open surgery when attempted laparoscopically (126). A recent multicenter retrospective analysis comparing robotic liver resection (RLR) with LLR revealed that RLR was associated with lower rates of R1 resection (16.9 vs. 28.8%,  $p = 0.025$ ). Furthermore, the benefit of RLR over LLR was observed to be greater for more challenging operations or for lesions located in posterosuperior segments (127).

It is important to note that, in contrast to the

comparison between open liver resection (OLR) and LLR, there are currently no randomized trials that specifically examine RLR. Nonetheless, the first international recommendations are beginning to emerge (128).

Furthermore, it is important to note that MIS facilitates a more expeditious resumption of postoperative chemotherapy, which has a beneficial impact on natural history of the disease (129).

Notwithstanding the aforementioned data, it is imperative to acknowledge that although MIS has been regarded as a viable option for a long time, recently published quality benchmarks, based on over 11,000 patients worldwide, have been established with the objective of offering patients the most efficacious oncological outcomes and the fewest possible postoperative complications (130).

## 6. Locoregional therapy

Local treatments for CRLM include hepatic arterial infusion chemotherapy (HAIC), radiofrequency ablation (RFA) or microwave ablation (MWA), stereotactic body radiotherapy (SBRT) and selective internal radiotherapy (SIRT).

The combination of HAIC and systemic chemotherapy has been demonstrated to enhance the response rate of patients undergoing first-line chemotherapy to a level exceeding 90% and to elevate the response rate of previously treated patients with unresectable CRLM to 85% (131,132). As demonstrated in the phase II/III PACHA trial, adjuvant HAIC with oxaliplatin has been shown to increase OS in patients at high risk of recurrence (133). Additionally, data from four prospective trials on HAIC combined with systemic chemotherapy after LR have demonstrated excellent long-term survival, with modern-era patients demonstrating 5-year survival rates of up to 78% and 10-year survival rates of 61% (134).

In patients with unresectable CRLM, the long-term results of the recent EORTC-CLOCC trial demonstrated that the combination of RFA ( $\pm$  surgical resection) and chemotherapy yielded an 8-year survival rate of 35.9%, in comparison with 8.9% observed in patients treated with chemotherapy alone (135).

In a recent publication reporting 465 ablations, microwave cancer destruction was shown to be an effective and durable therapeutic modality. In cases where the tumor was 1 cm or less, complete death of the cancer cells was achieved in 99% of cases (136). Karagkounis *et al.* demonstrated that factors associated with local recurrence on multivariate analysis included increasing size as a continuous variable (HR: 1.04, 95% CI: 1.01-1.08;  $p = 0.006$ ) and subcapsular location (HR: 2, 95% CI: 1.09-3.65;  $p = 0.02$ ). In addition, they observed that the cumulative rate of local recurrence at two years was 6.8% for tumors  $\leq 10$  mm, 12.4% for tumors of 11-



20 mm, and 30.2% for tumors > 20 mm (137). It thus emerges that as the size of the lesions (CRLM < 1 cm in diameter) decreases, the effectiveness of the method increases. A recent multi-centre prospective trial has therefore confirmed that local destruction is effective in small CRLM (138), especially in patients who are more fragile and exposed to the possible complications of surgical treatment.

Given the minimal periprocedural complications associated with local ablative therapies and their demonstrated efficacy in treating small tumors, there has been growing interest in comparing ablative therapy with hepatectomy for resectable CRLM. Consequently, a randomized phase III clinical trial, the COLLISION trial, is currently in progress with the target of demonstrating the non-inferiority of ablative therapy (RFA or MWA) to hepatectomy for resectable disease (139). The results are awaited, and although the gold standard is currently considered to be liver resection in cases where the disease is resectable, local destruction must be considered in several cases: patients with poor functional reserve with small metastases who cannot undergo surgery (140) or associated with resection to avoid major hepatectomy (with better surgical outcomes) (141).

SBRT has been shown to be an effective and safe local therapy in patients with unresectable CRLM, with the potential to achieve a high local control rate (142). The SIFLOX trial was designed to compare the efficacy of SIRT in combination with systemic chemotherapy versus systemic chemotherapy alone in treatment of unresectable CRLM. The findings demonstrated that SIRT can extend progression-free survival and enhance response rates in the liver (143).

Subgroup analyses in relevant studies have demonstrated that SBRT provides superior local control compared to RFA for tumours measuring over 2 cm. However, for tumours measuring 2 cm or smaller, RFA has been shown to be superior (144).

## 7. Combined liver resection and tumor ablation

In the context of parenchymal preservation, a significant number of surgeons will utilize ablation in cases of deeper parenchymal lesions, where attempted resection would result in an unacceptably small FLR, or when the aim is to achieve limited resections. The prevailing view is that this approach, when combined with appropriately timed systemic therapy, can result in a cure or, at the very least, a significant disease-free interval. To illustrate, the recent CLOCC trial was a randomized phase II trial that was terminated prematurely following evidence that combined surgery with RFA of otherwise unresectable tumors in conjunction with systemic therapy was associated with a significant improvement in OS (145). In the context of a parenchymal-sparing strategy, the combination of RFA and LR is safe with regard to oncological outcomes when the appropriate

criteria are adhered to (small-size lesions, oligometastatic disease *etc.*) (146). A recent nationwide population-based propensity score-matched study from the Netherlands (147) has revealed that combined resection and ablation should be available and considered as an alternative to resection alone in any patient with multiple metastases.

## 8. Disappearing liver metastasis

In the context of modern chemotherapeutics, treatment effects may result in the disappearance of CRLM on standard preoperative imaging. The prevailing view in the past has been that all areas of known disease, whether quiescent or otherwise, should be resected. This implies that if the disease was initially identified on a scan, it should be included in the resection field. In patients with unidentified and untreated disappearing liver metastases (DLMs), local recurrence at the site of the original tumor has been observed in up to 59% of cases (148). The idea of the past has been gradually confirmed by more recent studies. A systematic review on the subject published in 2025 (149) confirms the increased risk of local recurrence in the case of unresected DLMs, suggesting that all primary sites should be removed.

In a study comprising 40 patients with 126 DLMs, van Vledder *et al.* identified that the occurrence of > 3 metastases prior to chemotherapy (OR 13.1;  $p < 0.001$ ) and the number of preoperative chemotherapy cycles (OR 1.18;  $p = 0.03$ ) were independently associated with the development of DLMs. These findings contribute to the growing body of evidence from studies of this nature, which facilitate the identification of preoperative risk factors for the development of DLMs (148).

Furthermore, a recent series of studies has demonstrated that utilization of Eovist-based magnetic resonance imaging or contrast-enhanced ultrasound techniques can effectively identify up to 55% of disappearing lesions, with 69% of these cases exhibiting residual disease (150). Thus, in the case of DLMs, it would be appropriate to perform preoperative staging with CT and MRI and perform an aggressive surgical strategy (151). In addition, intraoperative ultrasound with contrast enhancement (CEIOUS) should be routinely adopted for the intraoperative detection of DLMs (152). In light of increased pre- and intra-operative diagnostic accuracy of DLMs, it could follow that, should these investigations prove negative, a decision could be made to postpone resection and opt for close surveillance. Some works in the literature support this possibility, which did not describe a statistically significant difference in overall survival between patients with resected DLMs and patients with DLMs left in place (153). Moreover, in the absence of recommendations on the management of DLMs, the attitude of surgeons varies greatly depending on the clinical case, with obvious reticence to perform surgery when *e.g.* they are only localisations that are no longer visible on preoperative

imaging (154), instead of suggesting close surveillance (155).

So, despite the enhanced understanding of this clinical situation, surgeons' dispositions remain markedly disparate, as evidenced by another recent review examining the attitudes of 67 surgeons from 25 disparate countries (154).

There is a clear need for quality prospective studies and consensus building to define the best management on a case-by-case basis.

## 9. Liver transplantation

Liver transplantation (LT) for unresectable CRLM was initially investigated in the SECA trials, which demonstrated a 5-year OS rate of up to 83% (156). The results of TransMet, a prospective randomized trial on the subject, have recently been published (157): a total of 94 patients were randomly assigned and included in the intention-to-treat population, with 47 patients receiving LT plus chemotherapy and 47 receiving chemotherapy alone. The 5-year OS rate for the intention-to-treat population was 56.6% (95% CI: 43.2-74.1) for LT plus chemotherapy and 12.6% (5.2-30.1) for chemotherapy alone. The HR was 0.37 (95% CI: 0.21-0.65), with a *p*-value of 0.0003. The 5-year OS rates were 73.3% (95% CI: 59.6-90.0) and 9.3% (3.2-26.8) for the LT plus chemotherapy and chemotherapy alone groups, respectively.

It can be postulated that there may be a threshold tumor load for which LR yields an acceptable survival rate. Consequently, it might be hypothesized that LT could provide a survival benefit over LR in a subset of patients with a high tumor load. However, the situation in Norway with regard to the availability of grafts for liver transplantation is much rosier than in the rest of the world, which is constantly faced with the problem of organ shortage. This is the reason why this therapeutic option can only be offered to a highly selected group of patients: patients under 70 years of age with excellent performance status, no extrahepatic disease or lymph node metastases and a primary left colon operated at least one year previously (with a T stage < 4), after an excellent response to chemotherapy (158,159). In all other cases, only palliative strategies can be proposed (such as cytoreductive surgery for patients with good performance status). The strict selection criteria are justified not only by the shortage of organs but also by the realisation that adherence to these criteria is essential to achieve post-transplant survival rates in line with conventional indications (160). When considering liver transplantation for CRLM as a treatment option, it is more important to discuss biological resectability than technical resectability, in the interest of providing the best treatment to those with the best prognostic predictive factors. In fact, as a recent review points out, an Oslo score of 1 or less, metabolic tumour volume on PET/

CT less than 70 cm<sup>3</sup>, metachronous disease or tumour burden score (TBS) less than 9 are predictive of better post-transplant outcomes (160).

The experience accrued over the course of these years provides clear evidence that the prognosis following LT for colorectal liver metastases is dependent on the morphological and biological characteristics of the tumor, including tumor burden, metabolic tumor volume, genetic phenotype and response to chemotherapy (161,162).

On the one hand, the use of small segmental grafts from deceased or living donors could be a way to expand the donor pool with less impact on the waiting list for deceased donor transplantation and minimal risk to the donor in the case of living donor liver transplantation (163). On the other hand, in addition to increasing the pool of available organs, we need to know more about the biological aspects of the tumour in order to define increasingly targeted indications (164).

## 10. Cytoreductive surgery

As we move forward in the era of highly efficacious chemotherapy, it becomes pertinent to consider the role of resection in patients with multifocal bilateral disease, where the initial tumor load could not be fully excised through R0 or R1 resection. In such patients, LT is becoming an appealing treatment with promising results, as discussed. However, it seems that the feasibility of this approach may be limited by the organ shortage and the rigorous selection criteria. This is particularly the case for young patients with "liver-only" disease, in the absence of obvious comorbidities, who represent a small fraction of patients. For patients who are unable to be transplanted (*e.g.*, due to age ≥ 70 years, limited EHD, or LT not available) but who are responding very well to chemotherapy and has an excellent performance status to tolerate an aggressive surgical strategy, it may be worthwhile exploring the possibility of cytoreductive surgery (165-167). There is currently little literature available on debulking surgery in this patient category, and prospective studies on the subject are awaited.

The currently available data do not allow us to propose clear recommendations regarding patient selection and appropriate threshold for tumor cytoreduction or on optimal duration of chemotherapy before debulking surgery. Nevertheless, a number of findings appear to indicate that a cytoreductive approach may be a valuable option for patients with unresectable multinodular CRLM who are responding to systemic treatment, similar to the benefits typically observed in patients who achieve a partial or complete response to chemotherapy. It may be beneficial to consider this approach on a case-by-case basis, with input from a multidisciplinary team with expertise in liver surgery, to identify suitable candidates and ensure use of an effective systemic perioperative chemotherapy (168).

## 11. Artificial intelligence

It seems that the use of AI may offer a potential advantage in the early diagnosis and management of CRLM (169,170). As previously mentioned, there are a number of factors to consider when providing clinical and surgical care for a patient with liver metastases from the colon-rectum. It is often the case that the decision-making process is complex and varies from one center to another, depending on the clinical judgment of the local multidisciplinary team (11). Given the numerous variables involved, it is becoming increasingly clear that AI-related technologies can offer valuable assistance. As outlined in a recent review by Rompianesi *et al.* (169), which provides a comprehensive overview of potential applications of AI in this field, the Radiomics Intelligent Analysis Toolkit-based analysis platform developed by Li *et al.* (171) is a promising approach. Construction of individualized nomograms was made possible by the use of maximum-level enhanced computed tomography images in the portal venous phase and patients' clinical information (age, sex, CEA and carbohydrate antigen 19-9) to predict development of CRLM in patients with colorectal cancer. A recent systematic meta-analysis (172) describes that in 11 of the 14 included studies, radiomics is able to predict prognosis and better select patients for treatment strategy candidating itself as a useful future diagnostic-predictive tool. It might be of interest to consider, for instance, the development of other AI-based predictive models, such as those designed to predict response to chemotherapy treatment (173) or local ablative treatment (174), or AI-based techniques to determine the correct surgical margin depending on the clinical case (175). The utilisation of machine learning algorithms for development of prognostic indicators, such as those capable of predicting early recurrence, has already been extensively explored in experimental settings (176). Translation of these algorithms into clinical practice holds significant potential for enhancing patient care. It is evident that the progressive implementation of AI in clinical practice appears to be an inevitable phenomenon. Recent studies have demonstrated a promising experimental basis for this development. However, it is important to acknowledge limitations that currently exist, which are not insignificant. The training of AI systems necessitates substantial datasets, which, in clinical contexts, would demand the establishment of extensive, multi-centre data databases, accompanied by all the concomitant privacy concerns that this would entail. Moreover, it is imperative to consider the ethical implications, as the machine can merely suggest but cannot supplant the clinical sensibilities of medical professionals. Finally, It is evident that the technical capabilities of disparate medical institutions, contingent on their respective economic capacities, could act as a hindrance to the extensive implementation of AI in clinical practice.

## 12. Prognostic scores

Predicting prognosis can help identify patients who may benefit from different treatments. For many years, a clinical outcome established by Fong *et al.* is widely used to predict the prognosis of patients with CRLM. They identified seven significant independent predictors of poor long-term outcomes, which they believe may be useful to consider in future studies: positive margins, EHD, positive primary nodal disease, disease-free interval between primary disease and metastases less than 12 months, more than one liver tumor, the largest liver tumor > 5 cm, and CEA levels > 200 ng/mL. The last five of these criteria were used to create a preoperative scoring system that has been shown to accurately predict prognosis (15). Today, it has become increasingly common to make prognostic predictions based on other technologies, such as radiomics, genomics, and proteomics (177-179).

It would seem that RAS mutation status may also have an impact on outcomes independent of the chosen local therapy (180,181). For patients with RAS-mutant tumors, there is an earlier onset of local tumor progression regardless of the size of the tumor (182); they also tend to have positive and narrower margins after LR (183). Indeed, the rate of margin positivity was higher in patients with a RAS mutation than in patients with wild-type RAS (11.4% vs. 5.4%,  $p = 0.007$ ) in the aforementioned study. In patients who later presented with liver-first recurrence, the width of the resection margin was significantly smaller in patients with a RAS mutation than in patients with wild-type RAS (4 mm vs. 7 mm,  $p = 0.031$ ).

A recent study indicated that a "triple mutation" in TP53, RAS, and SMAD4 was associated with inferior overall and recurrence-free survival in CRLM patients compared with double mutations in any two of the three genes (184).

A recent retrospective analysis of the randomized phase III study, NEW EPOC, has classified metastases into three molecular subtypes from a biological perspective. The analysis demonstrates that the biologically derived molecular subtypes of CRLM and integrated clinical-molecular risk groups are highly prognostic. This novel molecular classification requires further investigation as a potential predictive biomarker for the development of personalized systemic treatments for colorectal liver metastases (185). The field of molecular mechanisms of CRLM remains relatively unexplored, and it is likely to yield new insights into the development of personalized treatments for these patients.

## 13. Conclusions

Over the past decade, there have been notable advancements in the diagnosis and treatment of

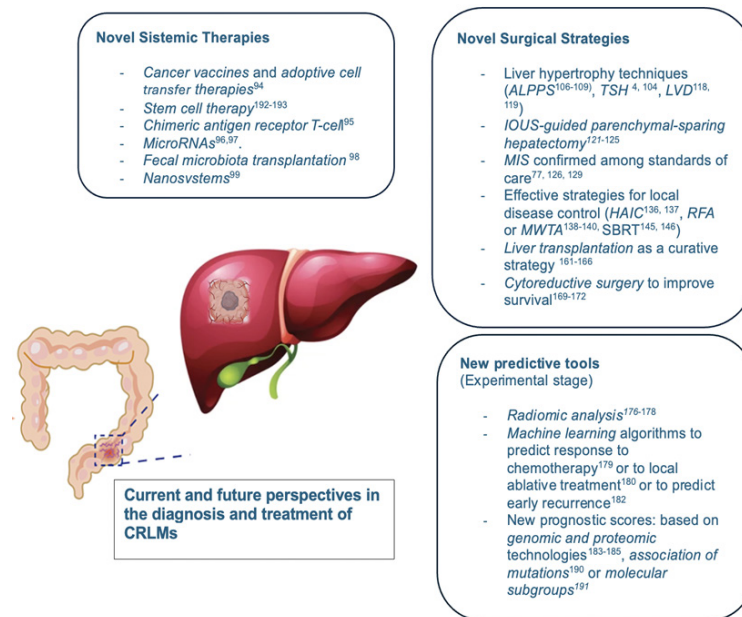


**Figure 1. Current and future perspectives in the diagnosis and treatment of CRLMs.** ALPPS: Associating Liver Partition and Portal vein ligation for Staged hepatectomy; TSH: Two-Stage Hepatectomy; LVD: Liver Venous Deprivation; IOUS: Intra-Operative UltraSound; MIS: Minimally Invasive Surgery; HAIC: Hepatic Arterial Infusion chemotherapy; RFA: RadioFrequency Ablation; MWTA: Micro-Wave ThermoAblation; SBRT: Stereotactic Body Radiation Therapy.

CRLM, as outlined in this review and summarized in Figure 1. The multiplicity of proposed treatments and the divergence of opinion regarding the definition of resectability and the treatment of these patients in different centers necessitates further efforts to standardize treatment protocols, which must, nevertheless, be tailored to each case. Individualized treatment remains a key research topic in the future. The goal is to perform surgical resection or LT in selected cases; however, the introduction of new treatments and new technologies permits the advancement of the boundaries of knowledge and an increase in survival rates in these patients, as it is being attempted with a better understanding of tumour biology and personalized medicine (186,187). Probably, AI will suggest the appropriate treatment pathway in terms of oncological outcome and patient safety based on individual patient variables, with a targeted but standard pathway in different centers.

**Funding:** None.

**Conflict of Interest:** The authors have no conflicts of interest to disclose.

## References

1. International Agency for Research on Cancer WHO, Others. Estimated number of deaths in 2020, worldwide, both sexes, all ages. Available at: <https://gco.iarc.fr/today/online-analysis-pie.2020>. (accessed March 9, 2020).
2. Kow AWC. Hepatic metastasis from colorectal cancer. J Gastrointest Oncol. 2019; 10:1274-1298.
3. Makuuchi M, Thai BL, Takayasu K, Takayama T, Kosuge T, Gunvén P, Yamazaki S, Hasegawa H, Ozaki H. Preoperative portal embolization to increase safety of major hepatectomy for hilar bile duct carcinoma: a preliminary report. Surgery. 1990; 107:521-527.
4. Adam R, Laurent A, Azoulay D, Castaing D, Bismuth H. Two-stage hepatectomy: A planned strategy to treat irresectable liver tumors. Ann Surg. 2000; 232:777-785.
5. Schnitzbauer AA, Lang SA, Goessmann H *et al*. Right portal vein ligation combined with in situ splitting induces rapid left lateral liver lobe hypertrophy enabling 2-staged extended right hepatic resection in small-for-size settings. Ann Surg. 2012; 255:405-414.
6. Adam R, Kitano Y. Multidisciplinary approach of liver metastases from colorectal cancer. Ann Gastroenterol Surg. 2019; 3:50-56.
7. Ivey GD, Johnston FM, Azad NS, Christenson ES, Lafaro KJ, Shubert CR. Current surgical management strategies for colorectal cancer liver metastases. Cancers (Basel). 2022; 14:1063.
8. Chandra P, Sacks GD. Contemporary Surgical Management of Colorectal Liver Metastases. Cancers (Basel). 2024; 16:941.
9. Krell RW, Reames BN, Hendren S, Frankel TL, Pawlik TM, Chung M, Kwon D, Wong SL. Surgical referral for colorectal liver metastases: A population-based survey. Ann Surg Oncol. 2015; 22:2179-2194.
10. Wei AC, Jarnagin WR. Questioning why more patients with colorectal liver metastases are not referred for metastasectomy. JAMA Surg. 2020; 155:909-910.
11. Ignatavicius P, Oberkofler CE, Chapman WC *et al*. Choices of therapeutic strategies for colorectal liver metastases among expert liver surgeons: A throw of the Dice? Ann Surg. 2020; 272:715-722.
12. Siriwardena AK, Serrablo A, Fretland ÅA *et al*. Multisocietal European consensus on the terminology,



- diagnosis, and management of patients with synchronous colorectal cancer and liver metastases: an E-AHPBA consensus in partnership with ESSO, ESCP, ESGAR, and CIRSE. *Br J Surg.* 2023; 110:1161-1170.
13. Adam R, Bhangu P, Poston G, Mirza D, Nuzzo G, Barroso E, Ijzermans J, Hubert C, Ruers T, Capussotti L, Ouellet JF, Laurent C, Cugat E, Colombo PE, Milicevic M. Is perioperative chemotherapy useful for solitary, metachronous, colorectal liver metastases? *Ann Surg.* 2010; 252:774-787.
14. Cervantes A, Adam R, Roselló S, Arnold D, Normanno N, Taïeb J, Seligmann J, De Baere T, Osterlund P, Yoshino T, Martinelli E. Metastatic colorectal cancer: ESMO clinical practice guideline for diagnosis, treatment and follow-up. *Ann Oncol.* 2023; 34:10-32.
15. Fong Y, Fortner J, Sun RL, Brennan MF, Blumgart LH. Clinical score for predicting recurrence after hepatic resection for metastatic colorectal cancer: analysis of 1001 consecutive cases. *Ann Surg.* 1999; 230:309-321.
16. Cohen R, Platell CF. Metachronous colorectal cancer metastasis: Who, what, when and what to do about it. *J Surg Oncol.* 2024; 129:71-77.
17. Beets G, Sebag-Montefiore D, Andritsch E *et al.* ECCO essential requirements for quality cancer care: Colorectal cancer. A critical review. *Crit Rev Oncol Hematol.* 2017; 110:81-93.
18. Osterlund P, Salminen T, Soveri L-M *et al.* Repeated centralized multidisciplinary team assessment of resectability, clinical behavior, and outcomes in 1086 Finnish metastatic colorectal cancer patients (RAXO): A nationwide prospective intervention study. *Lancet Reg Health Eur.* 2021; 3:100049.
19. Rees M, Tekkis PP, Welsh FK, O'Rourke T, John TG. Evaluation of long-term survival after hepatic resection for metastatic colorectal cancer: a multifactorial model of 929 patients. *Ann Surg.* 2008; 247:125-35.
20. Dijkstra M, Nieuwenhuizen S, Puijk RS, Timmer FEF, Geboers B, Schouten EAC, Opperman J, Scheffer HJ, de Vries JJJ, Versteeg KS, Lissenberg-Witte BI, van den Tol MP, Meijerink MR. Primary tumor sidedness, RAS and BRAF mutations and MSI status as prognostic factors in patients with colorectal liver metastases treated with surgery and thermal ablation: results from the Amsterdam Colorectal Liver Met Registry (AmCORE). *Biomedicines.* 2021; 9:962.
21. Worni M, Shah KN, Clary BM. Colorectal cancer with potentially resectable hepatic metastases: optimizing treatment. *Curr Oncol Rep.* 2014; 16:407.
22. Phelip JM, Mineur L, De la Fouchardière C, Chatelut E, Quesada JL, Roblin X, Pezet D, Mendoza C, Buc E, Rivoire M. High resectability rate of initially unresectable colorectal liver metastases after UGT1A1-Adapted High-Dose irinotecan combined with LV5FU2 and cetuximab: A multicenter phase II study (ERBIFORT). *Ann Surg Oncol.* 2016; 23:2161-2166.
23. Ichida H, Mise Y, Ito H, Ishizawa T, Inoue Y, Takahashi Y, Shinozaki E, Yamaguchi K, Saiura A. Optimal indication criteria for neoadjuvant chemotherapy in patients with resectable colorectal liver metastases. *World J Surg Oncol.* 2019; 17:100.
24. Nieuwenhuizen S, Puijk RS, van den Bemd B *et al.* Resectability and ablatability criteria for the Treatment of Liver Only Colorectal Metastases: Multidisciplinary consensus document from the COLLISION Trial Group. *Cancers (Basel).* 2020; 12:1779.
25. Pietrantonio F, Di Bartolomeo M, Cotsoglou C *et al.* Perioperative triplet chemotherapy and cetuximab in patients with RAS wild type high recurrence risk or borderline resectable colorectal cancer liver metastases. *Clin Colorectal Cancer.* 2017; 16:e191-e198.
26. Ekberg H, Tranberg KG, Andersson R, Lundstedt C, Hägerstrand I, Ranstam J, Bengmark S. Determinants of survival in liver resection for colorectal secondaries. *Br J Surg.* 1986; 73:727-731.
27. Viganò L, Capussotti L, Majno P, Toso C, Ferrero A, De Rosa G, Rubbia-Brandt L, Mentha G. Liver resection in patients with eight or more colorectal liver metastases. *Br J Surg.* 2015; 102:92-101.
28. Allard MA, Adam R, Giuliani F *et al.* Long-term outcomes of patients with 10 or more colorectal liver metastases. *Br J Cancer.* 2017; 117:604-611.
29. Huiskens J, Bolhuis K, Engelbrecht MR, De Jong KP, Kazemier G, Liem MS, Verhoef C, de Wilt JH, Punt CJ, van Gulik TM; Dutch colorectal cancer group. Outcomes of resectability assessment of the Dutch Colorectal Cancer Group Liver Metastases Expert Panel. *J Am Coll Surg.* 2019; 229:523-532.e2.
30. Adam R, De Gramont A, Figueras J, Guthrie A, Kokudo N, Kunstlinger F, Loyer E, Poston G, Rougier P, Rubbia-Brandt L, Sobrero A, Tabernero J, Teh C, Van Cutsem E; Jean-Nicolas Vauthey of the EGOSLIM (Expert Group on OncoSurgery management of Liver Metastases) group. The oncosurgery approach to managing liver metastases from colorectal cancer: a multidisciplinary international consensus. *Oncologist.* 2012; 17:1225-1239.
31. Bismuth H, Adam R, Lévi F, Farabos C, Waechter F, Castaing D, Majno P, Engerran L. Resection of nonresectable liver metastases from colorectal cancer after neoadjuvant chemotherapy. *Ann Surg.* 1996; 224:509-522.
32. Alberts SR, Horvath WL, Sternfeld WC, Goldberg RM, Mahoney MR, Dakhil SR, Levitt R, Rowland K, Nair S, Sargent DJ, Donohue JH. Oxaliplatin, fluorouracil, and leucovorin for patients with unresectable liver-only metastases from colorectal cancer: a North Central Cancer Treatment Group phase II study. *J Clin Oncol.* 2005; 23:9243-9249.
33. Adam R, Wicherts DA, de Haas RJ, Ciacio O, Lévi F, Paule B, Ducreux M, Azoulay D, Bismuth H, Castaing D. Patients with initially unresectable colorectal liver metastases: is there a possibility of cure? *J Clin Oncol.* 2009; 27:1829-1835.
34. Folprecht G, Gruenberger T, Bechstein W *et al.* Survival of patients with initially unresectable colorectal liver metastases treated with FOLFOX/cetuximab or FOLFIRI/cetuximab in a multidisciplinary concept (CELIM study). *Ann Oncol.* 2014; 25:1018-25.
35. Huiskens J, van Gulik TM, van Lienden KP *et al.* Treatment strategies in colorectal cancer patients with initially unresectable liver-only metastases, a study protocol of the randomised phase 3 CAIRO5 study of the Dutch Colorectal Cancer Group (DCCG). *BMC Cancer.* 2015; 15:365.
36. Sugiyama M, Uehara H, Shin Y, Shiokawa K, Fujimoto Y, Mano Y, Komoda M, Nakashima Y, Sugimachi K, Yamamoto M, Morita M, Toh Y. Indications for conversion hepatectomy for initially unresectable colorectal cancer with liver metastasis. *Surg Today.* 2022; 52:633-642.
37. Adam R, Avisar E, Ariche A, Giachetti S, Azoulay D, Castaing D, Kunstlinger F, Levi F, Bismuth F. Five-year survival following hepatic resection after neoadjuvant

- therapy for nonresectable colorectal. *Ann Surg Oncol.* 2001; 8:347-53.
38. Kemeny NE, Melendez FD, Capanu M, Paty PB, Fong Y, Schwartz LH, Jarnagin WR, Patel D, D'Angelica M. Conversion to resectability using hepatic artery infusion plus systemic chemotherapy for the treatment of unresectable liver metastases from colorectal carcinoma. *J Clin Oncol.* 2009; 27:3465-3471.
39. Damato A, Ghidini M, Dottorini L, Tomasello G, Iaculli A, Ghidini A, Luciani A, Petrelli F. Chemotherapy duration for various indications in colorectal cancer: a review. *Curr Oncol Rep.* 2023; 25:341-352.
40. Innominato PF, Cailliez V, Allard M-A *et al.* Impact of preoperative chemotherapy features on patient outcomes after hepatectomy for initially unresectable colorectal cancer liver metastases: A LiverMetSurvey Analysis. *Cancers (Basel).* 2022; 14:4340.
41. Calistri L, Rastrelli V, Nardi C, Maraghelli D, Vidali S, Pietragalla M, Colagrande S. Imaging of the chemotherapy-induced hepatic damage: Yellow liver, blue liver, and pseudocirrhosis. *World J Gastroenterol.* 2021; 27:7866-7893.
42. Donati F, Cioni D, Guarino S, Mazzeo ML, Neri E, Boraschi P. Chemotherapy-Induced liver injury in patients with colorectal liver metastases: Findings from MR Imaging. *Diagnostics (Basel).* 2022; 12:867.
43. Morris VK, Kennedy EB, Baxter NN *et al.* Treatment of Metastatic Colorectal Cancer: ASCO Guideline. *J Clin Oncol.* 2023; 41:678-700.
44. Masi G, Loupakis F, Salvatore L, Fornaro L, Cremolini C, Cupini S, Ciarlo A, Del Monte F, Cortesi E, Amoroso D, Granetto C, Fontanini G, Sensi E, Lupi C, Andreuccetti M, Falcone A. Bevacizumab with FOLFOXIRI (irinotecan, oxaliplatin, fluorouracil, and folinate) as first-line treatment for metastatic colorectal cancer: a phase 2 trial. *Lancet Oncol.* 2010; 11:845-852.
45. First-line systemic treatment strategies in patients with initially unresectable colorectal cancer liver metastases (CAIRO5): an open-label, multicentre, randomised, controlled, phase 3 study from the Dutch Colorectal Cancer Group. *Lancet Oncol.* 2023; 24:757-771.
46. André T, Shiu K-K, Kim TW *et al.* Pembrolizumab in Microsatellite-Instability-High Advanced Colorectal Cancer. *N Engl J Med.* 2020; 383:2207-2218.
47. Heinemann V, von Weikersthal LF, Decker T *et al.* FOLFIRI plus cetuximab or bevacizumab for advanced colorectal cancer: final survival and per-protocol analysis of FIRE-3, a randomised clinical trial. *Br J Cancer.* 2021; 124:587-594.
48. Brulé SY, Jonker DJ, Karapetis CS, O'Callaghan CJ, Moore MJ, Wong R, Tebbutt NC, Underhill C, Yip D, Zalberg JR, Tu D, Goodwin RA. Location of colon cancer (right-sided versus left-sided) as a prognostic factor and a predictor of benefit from cetuximab in NCIC CO.17. *Eur J Cancer.* 2015; 51:1405-1414.
49. Yaeger R, Uboha NV, Pelster MS *et al.* Efficacy and Safety of Adagrasib plus Cetuximab in Patients with KRASG12C-Mutated Metastatic Colorectal Cancer. *Cancer Discov.* 2024; 14:982-993.
50. Sorbye H, Mauer M, Gruenberger T *et al.* Predictive factors for the benefit of perioperative FOLFOX for resectable liver metastasis in colorectal cancer patients (EORTC Intergroup Trial 40983). *Ann Surg.* 2012; 255:534-539.
51. Adam R, de Gramont A, Figueras J *et al.* Managing synchronous liver metastases from colorectal cancer: a multidisciplinary international consensus. *Cancer Treat Rev.* 2015; 41:729-741.
52. Chen FL, Wang YY, Liu W, Xing BC. Neoadjuvant chemotherapy improves overall survival in resectable colorectal liver metastases patients with high clinical risk scores-- A retrospective, propensity score matching analysis. *Front Oncol.* 2022; 12:973418.
53. Ninomiya M, Emi Y, Motomura T, Tomino T, Iguchi T, Kayashima H, Harada N, Uchiyama H, Nishizaki T, Higashi H, Kuwano H. Efficacy of neoadjuvant chemotherapy in patients with high-risk resectable colorectal liver metastases. *Int J Clin Oncol.* 2021; 26:2255-2264.
54. Burasakarn P, Hongjinda S, Fuengfoo P, Thienhiran A. Neoadjuvant chemotherapy versus upfront surgery for resectable colorectal liver metastases: A systemic review and meta-analysis. *Surg Pract.* 2024; 28:16-26.
55. Bernardi L, Roesel R, Aghayan DL, Majno-Hurst PE, De Dosso S, Cristaudi A. Preoperative chemotherapy in upfront resectable colorectal liver metastases: New elements for an old dilemma? *Cancer Treat Rev.* 2024; 124:102696.
56. Nishioka Y, Shindoh J, Yoshioka R, Gono W, Abe H, Okura N, Yoshida S, Sakamoto Y, Hasegawa K, Fukayama M, Kokudo N. Clinical Impact of Preoperative Chemotherapy on Microscopic Cancer Spread Surrounding Colorectal Liver Metastases. *Ann Surg Oncol.* 2017; 24:2326-2333.
57. Laurent C, Adam JP, Denost Q, Smith D, Saric J, Chiche L. Significance of R1 Resection for Advanced Colorectal Liver Metastases in the Era of Modern Effective Chemotherapy. *World J Surg.* 2016; 40:1191-1199.
58. Jiang YJ, Zhou SC, Chen JH, Liang JW. Oncological outcomes of neoadjuvant chemotherapy in patients with resectable synchronous colorectal liver metastasis: A result from a propensity score matching study. *Front Oncol.* 2022; 12:951540.
59. Noda T, Takahashi H, Tei M *et al.* Clinical outcomes of neoadjuvant chemotherapy for resectable colorectal liver metastasis with intermediate risk of postoperative recurrence: A multi-institutional retrospective study. *Ann Gastroenterol Surg.* 2022; 7:479-490.
60. Liu W, Jin KM, Zhang MH, Bao Q, Liu M, Xu D, Wang K, Xing BC. Recurrence prediction by circulating tumor DNA in the patient with colorectal liver metastases after hepatectomy: A prospective biomarker study. *Ann Surg Oncol.* 2023; 30:4916-4926.
61. Jones RP, Pugh SA, Graham J, Primrose JN, Barriuso J. Circulating tumour DNA as a biomarker in resectable and irresectable stage IV colorectal cancer; a systematic review and meta-analysis. *Eur J Cancer.* 2021; 144:368-381.
62. Ayez N, van der Stok EP, Grünhagen DJ, Rothbarth J, van Meerten E, Eggermont AM, Verhoef C. The use of neo-adjuvant chemotherapy in patients with resectable colorectal liver metastases: Clinical risk score as possible discriminator. *Eur J Surg Oncol.* 2015; 41:859-867.
63. Engstrand J, Sterner J, Hasselgren K, Stromberg C, Stureson C. Treatment intention and outcome in patients with simultaneously diagnosed liver and lung metastases from colorectal cancer. *Eur J Surg Oncol.* 2022; 48:1799-1806.
64. Matsumura M, Yamashita S, Ishizawa T, Akamatsu N, Kaneko J, Arita J, Nakajima J, Kokudo N, Hasegawa

- K. Oncological benefit of complete metastasectomy for simultaneous colorectal liver and lung metastases. *Am J Surg*. 2020; 219:80-87.
65. Handy JR, Bremner RM, Crocenzi TS, Detterbeck FC, Fernando HC, Fidiias PM, Firestone S, Johnstone CA, Lanuti M, Little VR, Kesler KA, Mitchell JD, Pass HI, Ross HJ, Varghese TK. Expert consensus document on pulmonary metastasectomy. *Ann Thorac Surg*. 2019; 107:631-649.
66. Mise Y, Mehran RJ, Aloia TA, Vauthey JN. Simultaneous lung resection *via* a transdiaphragmatic approach in patients undergoing liver resection for synchronous liver and lung metastases. *Surgery*. 2014; 156:1197-1203.
67. De Bellis M, Kawaguchi Y, Duwe G, Tran Cao HS, Mehran RJ, Vauthey JN. Short- and long-term outcomes of a transdiaphragmatic approach for simultaneous resection of colorectal liver and lung metastases. *J Gastrointest Surg*. 2021; 25:641-649.
68. Abdel Jalil R, Abou Chaar MK, Shihadeh OM, Al-Qudah O, Gharaibeh A, Aldimashki L, Dabous A, Ghanem R, Al-Edwan A. Transdiaphragmatic single-port video-assisted thoracoscopic surgery; a novel approach for pulmonary metastasectomy through laparotomy incision - case series. *J Cardiothorac Surg*. 2021; 16:18.
69. Lerut P, Nuytens F, D'Hondt M. Combined Minimal Invasive Transdiaphragmatic Resections of Peripheral Colorectal Lung Metastases in Patients Undergoing Laparoscopic Liver Resections. *Ann Surg Oncol*. 2016; 23:885.
70. Engstrand J, Taflin H, Rystedt JL, Hemmingsson O, Urdzik J, Sandström P, Björnsson B, Hasselgren K. The resection rate of synchronously detected liver and lung metastasis from colorectal cancer is low-a national registry-based study. *Cancers (Basel)*. 2023; 15:1434.
71. Jeong S, Heo JS, Park JY, Choi DW, Choi SH. Surgical resection of synchronous and metachronous lung and liver metastases of colorectal cancers. *Ann Surg Treat Res*. 2017; 92:82-89.
72. Miller G, Biernacki P, Kemeny NE, Gonen M, Downey R, Jarnagin WR, D'Angelica M, Fong Y, Blumgart LH, DeMatteo RP. Outcomes after resection of synchronous or metachronous hepatic and pulmonary colorectal metastases. *J Am Coll Surg*. 2007; 205:231-238.
73. Lee SH, Kim SH, Lim JH, Kim SH, Lee JG, Kim DJ, Choi GH, Choi JS, Kim KS. Aggressive surgical resection for concomitant liver and lung metastasis in colorectal cancer. *Korean J Hepatobiliary Pancreat Surg*. 2016; 20:110-115.
74. Mise Y, Kopetz S, Mehran RJ, Aloia TA, Conrad C, Brudvik KW, Taggart MW, Vauthey JN. Is complete liver resection without resection of synchronous lung metastases justified? *Ann Surg Oncol*. 2015; 22:1585-1592.
75. Chun YS, Mehran RJ, Tzeng C-WD, Kee BK, Dasari A, Sepesi B, Conrad C, Aloia TA, Kopetz S, Vauthey JN. LUNA: A randomized phase II trial of liver resection plus chemotherapy or chemotherapy alone in patients with unresectable lung and resectable liver metastases from colorectal adenocarcinoma. *J Clin Orthod*. 35: TPS3625. [https://doi.org/10.1200/JCO.2017.35.15\\_suppl.TPS362](https://doi.org/10.1200/JCO.2017.35.15_suppl.TPS362)
76. Giuliani F, Viganò L, De Rose AM *et al*. Liver-First Approach for Synchronous Colorectal Metastases: Analysis of 7360 Patients from the LiverMetSurvey Registry. *Ann Surg Oncol*. 2021; 28:8198-8208.
77. Addeo P, Foguene M, Guerra M, Cusumano C, Paul C, Faitot F, Fiore L, De Mathelin P, Bachellier P. Predicting Limited Survival After Resection of Synchronous Colorectal Liver Metastases: a Propensity Score Matched Comparison Between The Primary First And The Simultaneous Strategy. *J Gastrointest Surg*. 2023; 27:1141-1151.
78. Frühling P, Strömberg C, Isaksson B, Urdzik J. A comparison of the simultaneous, liver-first, and colorectal-first strategies for surgical treatment of synchronous colorectal liver metastases at two major liver-surgery institutions in Sweden. *HPB (Oxford)*. 2023; 25:26-36.
79. Takeda K, Kikuchi Y, Sawada YU, Kumamoto T, Watanabe J, Kuniski C, Misumi T, Endo I. Efficacy of Adjuvant Chemotherapy Following Curative Resection of Colorectal Cancer Liver Metastases. *Anticancer Res*. 2022; 42:5497-5505.
80. Hasegawa K, Saiura A, Takayama T *et al*. Adjuvant Oral Uracil-Tegafur with Leucovorin for Colorectal Cancer Liver Metastases: A Randomized Controlled Trial. *PLoS One*. 2016; 11:e0162400.
81. Kanemitsu Y, Shimizu Y, Mizusawa J *et al*. Hepatectomy Followed by mFOLFOX6 Versus Hepatectomy Alone for Liver-Only Metastatic Colorectal Cancer (JCOG0603): A Phase II or III Randomized Controlled Trial. *J Clin Oncol*. 2021; 39:3789-3799.
82. Kobayashi S, Beppu T, Honda G *et al*. Survival Benefit of and Indications for Adjuvant Chemotherapy for Resected Colorectal Liver Metastases-a Japanese Nationwide Survey. *J Gastrointest Surg*. 2020; 24:1244-1260.
83. Satake H, Hashida H, Tanioka H *et al*. Hepatectomy Followed by Adjuvant Chemotherapy with 3-Month Capecitabine Plus Oxaliplatin for Colorectal Cancer Liver Metastases. *Oncologist*. 2021; 26:e1125-e1132.
84. Van Cutsem E, Cervantes A, Adam R *et al*. ESMO consensus guidelines for the management of patients with metastatic colorectal cancer. *Ann Oncol*. 2016; 27:1386-1422.
85. Yoshino T, Arnold D, Taniguchi H *et al*. Pan-Asian adapted ESMO consensus guidelines for the management of patients with metastatic colorectal cancer: a JSMO-ESMO initiative endorsed by CSCO, KACO, MOS, SSO and TOS. *Ann Oncol*. 2018; 29:44-70.
86. Kelm M, Schollbach J, Anger F, Wiegner A, Klein I, Germer CT, Schlegel N, Kunzmann V, Löb S. Prognostic impact of additive chemotherapy after curative resection of metachronous colorectal liver metastasis: a single-centre retrospective study. *BMC Cancer*. 2021; 21:490.
87. Pan Z, Peng J, Lin J, Chen G, Wu X, Lu Z, Deng Y, Zhao Y, Sui Q, Wan D. Is there a survival benefit from adjuvant chemotherapy for patients with liver oligometastases from colorectal cancer after curative resection? *Cancer Commun (Lond)*. 2018; 38:29.
88. Nakai T, Ishikawa H, Tokoro T, Okuno K. The clinical risk score predicts the effectiveness of adjuvant chemotherapy for colorectal liver metastasis. *World J Surg*. 2015; 39:1527-1536.
89. Kataoka K, Mori K, Nakamura Y *et al*. Survival benefit of adjuvant chemotherapy based on molecular residual disease detection in resected colorectal liver metastases: subgroup analysis from CIRCULATE-Japan GALAXY. *Ann Oncol*. 2024; 35:1015-1025.
90. Kamal Y, Schmit SL, Frost HR, Amos CI. The tumor microenvironment of colorectal cancer metastases: opportunities in cancer immunotherapy. *Immunotherapy*. 2020; 12:1083-1100.



91. Rodriguez J, Castañón E, Perez-Gracia JL *et al.* A randomized phase II clinical trial of dendritic cell vaccination following complete resection of colon cancer liver metastasis. *J Immunother Cancer*. 2018; 6:96.
92. Zhang C, Wang Z, Yang Z *et al.* Phase I Escalating-Dose Trial of CAR-T Therapy Targeting CEA<sup>+</sup> Metastatic Colorectal Cancers. *Mol Ther*. 2017; 25:1248-1258.
93. Sahu SS, Dey S, Nabinger SC, Jiang G, Bates A, Tanaka H, Liu Y, Kota J. The Role and Therapeutic Potential of miRNAs in Colorectal Liver Metastasis. *Sci Rep*. 2019; 9:15803.
94. Balacescu O, Sur D, Cainap C, Visan S, Cruceriu D, Manzat-Saplan R, Muresan MS, Balacescu L, Lisencu C, Irimie A. The Impact of miRNA in Colorectal Cancer Progression and Its Liver Metastases. *Int J Mol Sci*. 2018; 19:3711.
95. Zhang J, Wu K, Shi C, Li G. Cancer Immunotherapy: Fecal Microbiota Transplantation Brings Light. *Curr Treat Options Oncol*. 2022; 23:1777-1792.
96. Bouzo BL, Lores S, Jatal R, Alijas S, Alonso MJ, Conejos-Sánchez I, de la Fuente M. Sphingomyelin nanosystems loaded with uroguanylin and etoposide for treating metastatic colorectal cancer. *Sci Rep*. 2021; 11:17213.
97. Heinrich S. The current role of liver surgery in the treatment of colorectal liver metastases. *Hepatobiliary Surg Nutr*. 2019; 8:552-554.
98. Weber SM, Jarnagin WR, DeMatteo RP, Blumgart LH, Fong Y. Survival after resection of multiple hepatic colorectal metastases. *Ann Surg Oncol*. 2000; 7:643-650.
99. Adams RB, Aloia TA, Loyer E, Pawlik TM, Taouli B, Vauthey JN; Americas Hepato-Pancreato-Biliary Association; Society of Surgical Oncology; Society for Surgery of the Alimentary Tract. Selection for hepatic resection of colorectal liver metastases: expert consensus statement. *HPB (Oxford)*. 2013; 15:91-103.
100. Mohammad WM, Martel G, Mimeault R, Fairfull-Smith RJ, Auer RC, Balaa FK. Evaluating agreement regarding the resectability of colorectal liver metastases: a national case-based survey of hepatic surgeons. *HPB (Oxford)*. 2012; 14:291-297.
101. Brouquet A, Abdalla EK, Kopetz S, Garrett CR, Overman MJ, Eng C, Andreou A, Loyer EM, Madoff DC, Curley SA, Vauthey JN. High survival rate after two-stage resection of advanced colorectal liver metastases: response-based selection and complete resection define outcome. *J Clin Oncol*. 2011; 29:1083-1090.
102. Giuliani F, Ardito F, Ferrero A, Aldrighetti L, Ercolani G, Grande G, Ratti F, Giovannini I, Federico B, Pinna AD, Capussotti L, Nuzzo G. Tumor progression during preoperative chemotherapy predicts failure to complete 2-stage hepatectomy for colorectal liver metastases: results of an Italian multicenter analysis of 130 patients. *J Am Coll Surg*. 2014; 219:285-294.
103. Lau WY, Lai EC, Lau SH. Associating liver partition and portal vein ligation for staged hepatectomy: the current role and development. *Hepatobiliary Pancreat Dis Int*. 2017; 16:17-26.
104. Robles R, Parrilla P, López-Conesa A, Brusadin R, de la Peña J, Fuster M, García-López JA, Hernández E. Tourniquet modification of the associating liver partition and portal ligation for staged hepatectomy procedure. *Br J Surg*. 2014; 101:1129-1134.
105. Gall TM, Sodergren MH, Frampton AE, Fan R, Spalding DR, Habib NA, Pai M, Jackson JE, Tait P, Jiao LR. Radio-frequency-assisted Liver Partition with Portal vein ligation (RALPP) for liver regeneration. *Ann Surg*. 2015; 261:e45-e46.
106. Petrowsky H, Györi G, de Oliveira M, Lesurtel M, Clavien PA. Is partial-ALPPS safer than ALPPS? A single-center experience. *Ann Surg*. 2015; 261:e90- e92.
107. Linecker M, Björnsson B, Stavrou GA *et al.* Risk Adjustment in ALPPS Is Associated With a Dramatic Decrease in Early Mortality and Morbidity. *Ann Surg*. 2017; 266:779-786.
108. Sandström P, Røsek BI, Sparrelid E, Larsen PN, Larsson AL, Lindell G, Schultz NA, Bjørneth BA, Isaksson B, Rizell M, Björnsson B. ALPPS improves resectability compared with conventional two-stage hepatectomy in patients with advanced colorectal liver metastasis: Results from a scandinavian multicenter randomized controlled trial (LIGRO Trial). *Ann Surg*. 2018; 267:833-840.
109. Raptis DA, Linecker M, Kambakamba P *et al.* Defining Benchmark Outcomes for ALPPS. *Ann Surg*. 2019; 270:835-841.
110. Linecker M, Stavrou GA, Oldhafer KJ *et al.* The ALPPS Risk Score: Avoiding Futile Use of ALPPS. *Ann Surg*. 2016; 264:763-771.
111. Collienne M, Neven A, Caballero C *et al.* EORTC 1409 GITCG/ESSO 01 - A prospective colorectal liver metastasis database for borderline or initially unresectable diseases (CLIMB): Lessons learnt from real life. From paradigm to unmet need. *Eur J Surg Oncol*. 2023; 49:107081.
112. Knitter S, Sauer L, Hillebrandt KH, Moosburner S, Fehrenbach U, Auer TA, Raschok N, Lurje G, Krenzien F, Pratschke J, Schöning W. Extended right hepatectomy following clearance of the left liver lobe and portal vein embolization for curatively intended treatment of extensive bilobar colorectal liver metastases: A single-center case series. *Curr Oncol*. 2024; 31:1145-1161.
113. Bednarsch J, Czigan Z, Sharmeen S, van der Kroft G, Strnad P, Ulmer TF, Isfort P, Bruners P, Lurje G, Neumann UP. ALPPS versus two-stage hepatectomy for colorectal liver metastases--a comparative retrospective cohort study. *World J Surg Oncol*. 2020; 18:140.
114. Diaz Vico T, Granero Castro P, Alcover Navarro L, Suárez Sánchez A, Mihic Góngora L, Montalvá Orón EM, Maupoey Ibáñez J, Truán Alonso N, González-Pinto Arrillaga I, Granero Trancón JE. Two stage hepatectomy (TSH) versus ALPPS for initially unresectable colorectal liver metastases: A systematic review and meta-analysis. *Eur J Surg Oncol*. 2023; 49:550-559.
115. Guiu B, Chevallier P, Denys A, Delhom E, Pierredon-Foulongne MA, Rouanet P, Fabre JM, Quenet F, Herrero A, Panaro F, Baudin G, Ramos J. Simultaneous trans-hepatic portal and hepatic vein embolization before major hepatectomy: the liver venous deprivation technique. *Eur Radiol*. 2016; 26:4259-4267.
116. Cassese G, Troisi RI, Khayat S, Quenet F, Tomassini F, Panaro F, Guiu B. Liver venous deprivation versus associating liver partition and portal vein ligation for staged hepatectomy for colo-rectal liver metastases: a comparison of early and late kinetic growth rates, and perioperative and oncological outcomes. *Surg Oncol*. 2022; 43:101812.
117. Sui CJ, Cao L, Li B, Yang JM, Wang SJ, Su X, Zhou YM. Anatomical versus nonanatomical resection of colorectal liver metastases: a meta-analysis. *Int J Colorectal Dis*. 2012; 27:939-946.
118. Torzilli G, Montorsi M, Del Fabbro D, Palmisano A,



- Donadon M, Makuuchi M. Ultrasonographically guided surgical approach to liver tumours involving the hepatic veins close to the caval confluence. *Br J Surg.* 2006; 93:1238-1246.
119. Mise Y, Aloia TA, Brudvik KW, Schwarz L, Vauthey JN, Conrad C. Parenchymal-sparing Hepatectomy in Colorectal Liver Metastasis Improves Salvageability and Survival. *Ann Surg.* 2016; 263:146-152.
120. Kokudo N, Tada K, Seki M, Ohta H, Azekura K, Ueno M, Matsubara T, Takahashi T, Nakajima T, Muto T. Anatomical major resection versus nonanatomical limited resection for liver metastases from colorectal carcinoma. *Am J Surg.* 2001; 181:153-159.
121. Petrowsky H, Gonen M, Jarnagin W, Lorenz M, DeMatteo R, Heinrich S, Encke A, Blumgart L, Fong Y. Second liver resections are safe and effective treatment for recurrent hepatic metastases from colorectal cancer: a bi-institutional analysis. *Ann Surg.* 2002; 235:863-871.
122. Wang K, Liu Y, Hao M, Li H, Liang X, Yuan D, Ding L. Clinical outcomes of parenchymal-sparing versus anatomic resection for colorectal liver metastases: A systematic review and meta-analysis. *World J Surg Oncol.* 2023; 21:241.
123. Buell JF, Cherqui D, Geller DA *et al.* The international position on laparoscopic liver surgery: The Louisville Statement, 2008. *Ann Surg.* 2009; 250:825-830.
124. Aghayan D, Fretland Å, Kazaryan A, Dagenborg V, Fagerland M, Flatmark K, Edwin B. 411P Laparoscopic versus open liver resection for colorectal cancer liver metastases: Five-year actual survival of the previously reported randomized controlled trial – The OSLO-COMET Trial. *Ann Oncol.* 2022; 33(Suppl): S724. <http://dx.doi.org/10.1016/j.annonc.2022.07.549>
125. Robles-Campos R, Lopez-Lopez V, Brusadin R, Lopez-Conesa A, Gil-Vazquez PJ, Navarro-Barrios Á, Parrilla P. Open versus minimally invasive liver surgery for colorectal liver metastases (LapOpHuva): a prospective randomized controlled trial. *Surg Endosc.* 2019; 33:3926-3936.
126. Tsung A, Geller DA, Sukato DC, Sabbaghian S, Tohme S, Steel J, Marsh W, Reddy SK, Bartlett DL. Robotic versus laparoscopic hepatectomy: a matched comparison. *Ann Surg.* 2014; 259:549-555.
127. Masetti M, Fallani G, Ratti F, Ferrero A, Giuliani F, Cillo U, Guglielmi A, Ettore GM, Torzilli G, Vincenti L, Ercolani G, Cipressi C, Lombardi R, Aldrighetti L, Jovine E. Minimally invasive treatment of colorectal liver metastases: does robotic surgery provide any technical advantages over laparoscopy? A multicenter analysis from the IGoMILS (Italian Group of Minimally Invasive Liver Surgery) registry. *Updates Surg.* 2022; 74:535-545.
128. Vreeland TJ, Collings AT, Ozair A *et al.* SAGES/AHPBA guidelines for the use of minimally invasive surgery for the surgical treatment of colorectal liver metastases (CRLM). *Surg Endosc.* 2023; 37:2508-2516.
129. Tohme S, Goswami J, Han K, Chidi AP, Geller DA, Reddy S, Gleisner A, Tsung A. Minimally invasive resection of colorectal cancer liver metastases leads to an earlier initiation of chemotherapy compared to open surgery. *J Gastrointest Surg.* 2015; 19:2199-2206.
130. Goh BKP, Han H-S, Chen K-H *et al.* Defining Global Benchmarks for Laparoscopic Liver Resections: An International Multicenter Study. *Ann Surg.* 2023; 277:e839-e848.
131. Tan HL, Lee M, Vellayappan BA, Neo WT, Yong WP. The Role of Liver-Directed Therapy in Metastatic Colorectal Cancer. *Curr Colorectal Cancer Rep.* 2018; 14:129-137.
132. Pak LM, Kemeny NE, Capanu M, Chou JF, Boucher T, Cercek A, Balachandran VP, Kingham TP, Allen PJ, DeMatteo RP, Jarnagin WR, D'Angelica MI. Prospective phase II trial of combination hepatic artery infusion and systemic chemotherapy for unresectable colorectal liver metastases: Long term results and curative potential. *J Surg Oncol.* 2018; 117:634-643.
133. Goéré D, Pignon JP, Gelli M, Elias D, Benhaim L, Deschamps F, Caramella C, Boige V, Ducreux M, de Baere T, Malka D. Postoperative hepatic arterial chemotherapy in high-risk patients as adjuvant treatment after resection of colorectal liver metastases - a randomized phase II/III trial - PACHA-01 (NCT02494973). *BMC Cancer.* 2018; 18:787.
134. Kemeny NE, Chou JF, Boucher TM, Capanu M, DeMatteo RP, Jarnagin WR, Allen PJ, Fong YC, Cercek A, D'Angelica MI. Updated long-term survival for patients with metastatic colorectal cancer treated with liver resection followed by hepatic arterial infusion and systemic chemotherapy. *J Surg Oncol.* 2016; 113:477-484.
135. Macbeth F, Farewell V, Treasure T. RE: Local Treatment of Unresectable Colorectal Liver Metastases: Results of a Randomized Phase II Trial. *J Natl Cancer Inst.* 2017; 109.
136. Leung U, Kuk D, D'Angelica MI, Kingham TP, Allen PJ, DeMatteo RP, Jarnagin WR, Fong Y. Long-term outcomes following microwave ablation for liver malignancies. *Br J Surg.* 2015; 102:85-91.
137. Karagkounis G, McIntyre SM, Wang T, Chou JF, Nasar N, Gonen M, Balachandran VP, Wei AC, Soares KC, Drebin JA, D'Angelica MI, Jarnagin WR, Kingham TP. Rates and patterns of recurrence after microwave ablation of colorectal liver metastases: A per lesion analysis of 416 tumors in the era of 2.45 GHz generators. *Ann Surg Oncol.* 2023; 30:6571-6578.
138. Tinguely P, Ruiter SJS, Engstrand J, de Haas RJ, Nilsson H, Candinas D, de Jong KP, Freedman J. A prospective multicentre trial on survival after Microwave Ablation Versus Resection for Resectable Colorectal liver metastases (MAVERRIC). *Eur J Cancer.* 2023; 187:65-76.
139. Meijerink MR, van der Lei S, Dijkstra M *et al.* Thermal ablation versus surgical resection of small-size colorectal liver metastases (COLLISION): an international, randomised, controlled, phase 3 non-inferiority trial. *Lancet Oncol.* 2025; 26:187-199.
140. Tinguely P, Laurell G, Enander A, Engstrand J, Freedman J. Ablation versus resection for resectable colorectal liver metastases - Health care related cost and survival analyses from a quasi-randomised study. *Eur J Surg Oncol.* 2023; 49:416-425.
141. Liu M, Wang Y, Wang K, Bao Q, Wang H, Jin K, Liu W, Yan X, Xing B. Combined ablation and resection (CARE) for resectable colorectal cancer liver Metastases-A propensity score matching study. *Eur J Surg Oncol.* 2023; 49:106931.
142. Scorsetti M, Comito T, Tozzi A, Navarria P, Fogliata A, Clerici E, Mancosu P, Reggiori G, Rimassa L, Torzilli G, Tomatis S, Santoro A, Cozzi L. Final results of a phase II trial for stereotactic body radiation therapy for patients with inoperable liver metastases from colorectal cancer. *J Cancer Res Clin Oncol.* 2015; 141:543-553.
143. van Hazel GA, Heinemann V, Sharma NK *et al.* SIRFLOX: Randomized Phase III Trial Comparing First-Line mFOLFOX6 (Plus or Minus Bevacizumab) Versus

- mFOLFOX6 (Plus or Minus Bevacizumab) Plus Selective Internal Radiation Therapy in Patients With Metastatic Colorectal Cancer. *J Clin Oncol.* 2016; 34:1723-1731.
144. Jackson WC, Tao Y, Mendiratta-Lala M, Bazzi L, Wahl DR, Schipper MJ, Feng M, Cuneo KC, Lawrence TS, Owen D. Comparison of Stereotactic Body Radiation Therapy and Radiofrequency Ablation in the Treatment of Intrahepatic Metastases. *Int J Radiat Oncol Biol Phys.* 2018; 100:950-958.
145. Ruers T, Punt CJA, van Coevorden F, Pierie JP, Rinkes IB, Ledermann JA, Poston GJ, Bechstein WO, Lentz MA, Mauer ME, Cutsem EV, Lutz MP, Nordlinger B. Radiofrequency ablation (RFA) combined with chemotherapy for unresectable colorectal liver metastases (CRC LM): Long-term survival results of a randomized phase II study of the EORTC-NCRI CCSG-ALM Intergroup 40004 (CLOCC). *J Clin Oncol.* 2015; 33:3501. [https://doi.org/10.1200/jco.2015.33.15\\_suppl.3501](https://doi.org/10.1200/jco.2015.33.15_suppl.3501)
146. Giannone F, Grollemund A, Felli E, Mayer T, Cherkaoui Z, Schuster C, Pessaux P. Combining radiofrequency ablation with hepatic resection for liver-only colorectal metastases: A propensity-score based analysis of long-term outcomes. *Ann Surg Oncol.* 2023; 30:4856-4866.
147. de Graaff MR, Klaase JM, den Dulk M *et al.* Trends and overall survival after combined liver resection and thermal ablation of colorectal liver metastases: a nationwide population-based propensity score-matched study. *HPB (Oxford).* 2024; 26:34-43.
148. van Vledder MG, de Jong MC, Pawlik TM, Schulick RD, Diaz LA, Choti MA. Disappearing colorectal liver metastases after chemotherapy: should we be concerned? *J Gastrointest Surg.* 2010; 14:1691-1700.
149. Papakonstantinou M, Fantakis A, Torzilli G, Donadon M, Chatzikomnitsa P, Giakoustidis D, Papadopoulos VN, Giakoustidis A. A systematic review of disappearing colorectal liver metastases: Resection or no resection? *J Clin Med.* 2025; 14:1147.
150. Tani K, Shindoh J, Akamatsu N, Arita J, Kaneko J, Sakamoto Y, Hasegawa K, Kokudo N. Management of disappearing lesions after chemotherapy for colorectal liver metastases: Relation between detectability and residual tumors. *J Surg Oncol.* 2018; 117:191-197.
151. Kuhlmann K, van Hilst J, Fisher S, Poston G. Management of disappearing colorectal liver metastases. *Eur J Surg Oncol.* 2016; 42:1798-1805.
152. Anselmo A, Cascone C, Siragusa L, Sensi B, Materazzo M, Riccetti C, Bacchiocchi G, Ielpo B, Rosso E, Tisone G. Disappearing colorectal liver metastases: Do we really need a ghostbuster? *Healthcare (Basel).* 2022; 10:1898.
153. Barimani D, Kauppila JH, Stureson C, Sparrelid E. Imaging in disappearing colorectal liver metastases and their accuracy: a systematic review. *World J Surg Oncol.* 2020; 18:264.
154. Ghazanfar MA, Abdelhamid A, Aldrighetti L *et al.* The dilemma of the disappearing colorectal liver metastases: defining international trends in management. *HPB (Oxford).* 2023; 25:446-453.
155. Owen JW, Fowler KJ, Doyle MB, Saad NE, Linehan DC, Chapman WC. Colorectal liver metastases: disappearing lesions in the era of Eovist hepatobiliary magnetic resonance imaging. *HPB (Oxford).* 2016; 18:296-303.
156. Dueland S, Syversveen T, Solheim JM, Solberg S, Grut H, Bjørneth BA, Hagness M, Line PD. Survival following liver transplantation for patients with nonresectable liver-only colorectal metastases. *Ann Surg.* 2020; 271:212-218.
157. Adam R, Piedvache C, Chiche L *et al.* Liver transplantation plus chemotherapy versus chemotherapy alone in patients with permanently unresectable colorectal liver metastases (TransMet): results from a multicentre, open-label, prospective, randomised controlled trial. *Lancet.* 2024; 404:1107-1118.
158. Maspero M, Sposito C, Virdis M, Citterio D, Pietrantonio F, Bhoori S, Belli F, Mazzaferro V. Liver transplantation for hepatic metastases from colorectal cancer: Current knowledge and open issues. *Cancers (Basel).* 2023; 15:345.
159. Chávez-Villa M, Ruffolo LI, Line PD, Dueland S, Tomiyama K, Hernandez-Alejandro R. Emerging Role of Liver Transplantation for Unresectable Colorectal Liver Metastases. *J Clin Oncol.* 2024; 42:1098-1101.
160. Line PD, Dueland S. Transplantation for colorectal liver metastasis. *Curr Opin Organ Transplant.* 2024; 29:23-29.
161. Line PD, Dueland S. Liver transplantation for secondary liver tumours: The difficult balance between survival and recurrence. *J Hepatol.* 2020; 73:1557-1562.
162. Lanari J, Hagness M, Sartori A, Rosso E, Gringeri E, Dueland S, Cillo U, Line PD. Liver transplantation versus liver resection for colorectal liver metastasis: a survival benefit analysis in patients stratified according to tumor burden score. *Transpl Int.* 2021; 34:1722-1732.
163. Nadalin S, Settmacher U, Rauchfuß F, Balci D, Königsrainer A, Line PD. RAPID procedure for colorectal cancer liver metastasis. *Int J Surg.* 2020; 82S:93-96.
164. Søreide K. Liver transplantation for non-resectable colorectal liver metastases: The thin red line. *Br J Cancer.* 2023; 128:1794-1796.
165. Adam R, Accardo C, Allard MA. Cytoreductive surgery for colorectal liver metastases: is it worthwhile? *Minerva Surg.* 2022; 77:433-440.
166. Adam R, Kitano Y, Abdelrafee A, Allard MA, Baba H. Debulking surgery for colorectal liver metastases: Foolish or chance? *Surg Oncol.* 2020; 33:266-269.
167. Kalil JA, Krzywon L, Zlotnik O, Perrier H, Petrillo SK, Chaudhury P, Schadde E, Metrakos P. Debulking hepatectomy for colorectal liver metastasis conveys survival benefit. *Cancers (Basel).* 2024; 16:1730.
168. Stewart CL, Warner S, Ito K, Raoof M, Wu GX, Kessler J, Kim JY, Fong Y. Cytoreduction for colorectal metastases: liver, lung, peritoneum, lymph nodes, bone, brain. When does it palliate, prolong survival, and potentially cure? *Curr Probl Surg.* 2018; 55:330-379.
169. Rompianesi G, Pegoraro F, Ceresa CD, Montalti R, Troisi RI. Artificial intelligence in the diagnosis and management of colorectal cancer liver metastases. *World J Gastroenterol.* 2022; 28:108-122.
170. Han T, Zhu J, Chen X, Chen R, Jiang Y, Wang S, Xu D, Shen G, Zheng J, Xu C. Application of artificial intelligence in a real-world research for predicting the risk of liver metastasis in T1 colorectal cancer. *Cancer Cell Int.* 2022; 22:28.
171. Li M, Li X, Guo Y, Miao Z, Liu X, Guo S, Zhang H. Development and assessment of an individualized nomogram to predict colorectal cancer liver metastases. *Quant Imaging Med Surg.* 2020; 10:397-414.
172. Wesdorp NJ, van Goor VJ, Kemna R, Jansma EP, van Waesberghe JHTM, Swijnenburg RJ, Punt CJA, Huiskens J, Kazemier G. Advanced image analytics predicting clinical outcomes in patients with colorectal liver metastases: A systematic review of the literature. *Surg*

- Oncol. 2021; 38:101578.
173. Wei J, Cheng J, Gu D, Chai F, Hong N, Wang Y, Tian J. Deep learning-based radiomics predicts response to chemotherapy in colorectal liver metastases. *Med Phys.* 2021; 48:513-522.
174. Taghavi M, Staal F, Gomez Munoz F, Imani F, Meek DB, Simões R, Klompenhouwer LG, van der Heide UA, Beets-Tan RGH, Maas M. CT-Based Radiomics Analysis Before Thermal Ablation to Predict Local Tumor Progression for Colorectal Liver Metastases. *Cardiovasc Intervent Radiol.* 2021; 44:913-920.
175. Bertsimas D, Margonis GA, Sujichantararat S *et al.* Using Artificial Intelligence to Find the Optimal Margin Width in Hepatectomy for Colorectal Cancer Liver Metastases. *JAMA Surg.* 2022; 157:e221819.
176. Kawashima J, Endo Y, Woldesenbet S *et al.* Preoperative identification of early extrahepatic recurrence after hepatectomy for colorectal liver metastases: A machine learning approach. *World J Surg.* 2024; 48:2760-2771.
177. Dohan A, Gallix B, Guiu B *et al.* Early evaluation using a radiomic signature of unresectable hepatic metastases to predict outcome in patients with colorectal cancer treated with FOLFIRI and bevacizumab. *Gut.* 2020; 69:531-539.
178. Grünhagen D. Predicting prognosis in colorectal liver metastases. *Hepatobiliary Surg Nutr.* 2019; 8:643-645.
179. Ma YS, Huang T, Zhong XM, Zhang HW, Cong XL, Xu H, Lu GX, Yu F, Xue SB, Lv ZW, Fu D. Proteogenomic characterization and comprehensive integrative genomic analysis of human colorectal cancer liver metastasis. *Mol Cancer.* 2018; 17:139.
180. Kawaguchi Y, Lillemoe HA, Vauthey JN. Gene mutation and surgical technique: Suggestion or more? *Surg Oncol.* 2020; 33:210-215.
181. Jiang BB, Yan K, Zhang ZY, Yang W, Wu W, Yin SS, Chen MH. The value of KRAS gene status in predicting local tumor progression of colorectal liver metastases following radiofrequency ablation. *Int J Hyperthermia.* 2019; 36:211-219.
182. Odisio BC, Yamashita S, Huang SY, Harmoush S, Kopetz SE, Ahrar K, Shin Chun Y, Conrad C, Aloia TA, Gupta S, Hicks ME, Vauthey JN. Local tumour progression after percutaneous ablation of colorectal liver metastases according to RAS mutation status. *Br J Surg.* 2017; 104:760-768.
183. Brudvik KW, Mise Y, Chung MH, Chun YS, Kopetz SE, Passot G, Conrad C, Maru DM, Aloia TA, Vauthey JN. RAS Mutation Predicts Positive Resection Margins and Narrower Resection Margins in Patients Undergoing Resection of Colorectal Liver Metastases. *Ann Surg Oncol.* 2016; 23:2635-43.
184. Kawaguchi Y, Kopetz S, Newhook TE, De Bellis M, Chun YS, Tzeng CD, Aloia TA, Vauthey JN. Mutation Status of RAS, TP53, and SMAD4 is Superior to Mutation Status of RAS Alone for Predicting Prognosis after Resection of Colorectal Liver Metastases. *Clin Cancer Res.* 2019; 25:5843-5851.
185. Katipally RR, Martinez CA, Pugh SA, Bridgewater JA, Primrose JN, Domingo E, Maughan TS, Talamonti MS, Posner MC, Weichselbaum RR, Pitroda SP; with the S:CORT Consortium. Integrated Clinical-Molecular Classification of Colorectal Liver Metastases: A Biomarker Analysis of the Phase 3 New EPOC Randomized Clinical Trial. *JAMA Oncol.* 2023; 9:1245-1254.
186. Patsalias A, Kozovska Z. Personalized medicine: Stem cells in colorectal cancer treatment. *Biomed Pharmacother.* 2021; 141:111821.
187. Garza Treviño EN, Quiroz Reyes AG, Rojas Murillo JA, de la Garza Kalife DA, Delgado Gonzalez P, Islas JF, Estrada Rodriguez AE, Gonzalez Villarreal CA. Cell therapy as target therapy against colon cancer stem cells. *Int J Mol Sci.* 2023; 24:8163.

Received January 11, 2025; Revised March 4, 2025; Accepted March 16, 2025.

*\*Address correspondence to:*

Salvatore Gruttadauria, IRCCS-ISMETT, University of Pittsburgh Medical Center (UPMC), 90127 Palermo, Italy.  
E-mail: sgruttadauria@ismett.edu

Released online in J-STAGE as advance publication March 18, 2025.

# Advancing hepatobiliary diagnosis and treatment using shortwave-infrared fluorescence imaging with ICG-C9

Kosuke Hatta<sup>1</sup>, Ryota Tanaka<sup>1,\*</sup>, Kenjiro Kimura<sup>1</sup>, Naoki Yamashita<sup>2</sup>, Jie Li<sup>2</sup>, Terufusa Kunisada<sup>2</sup>, Takeaki Ishizawa<sup>1</sup>

<sup>1</sup>Department of Hepato-Biliary-Pancreatic Surgery, Osaka Metropolitan University Graduate School of Medicine, Osaka, Japan;

<sup>2</sup>R&D Technology Center, Tamron Co., Ltd., Saitama, Japan.

**SUMMARY:** Indocyanine green (ICG)-C9, a novel cyanine dye developed by the Center for Biosystems Dynamics Research at RIKEN, provides significant advantages over conventional ICG due to its detectability *via* shortwave-infrared (SWIR) fluorescence imaging. Unlike standard ICG, ICG-C9 facilitates SWIR imaging and displays therapeutic potential when conjugated with antibodies *in vivo*, suggesting broader applicability across various cancer types. This study evaluated the efficacy of SWIR fluorescence imaging with ICG-C9 in comparison with existing near-infrared (NIR) imaging techniques. We assessed excretion kinetics and the relationship between excitation and fluorescence wavelengths for ICG-C9 and ICG following intravenous administration in BALB/c-nu mice. Tumor uptake was evaluated using a cell-line-derived subcutaneous tumor model from HuH-7 cells, representing hepatocellular carcinoma. Variables including dose, administration route, and exposure time were optimized for comparison. Maximum fluorescence intensity for ICG-C9 was observed with an excitation wavelength of 915 nm and fluorescence emission wavelengths >950 nm within the SWIR spectrum. Both ICG-C9 and ICG followed similar excretion pathways, involving hepatic uptake and biliary excretion. Tumor uptake of ICG-C9 was confirmed under similar conditions to ICG. ICG-C9 demonstrates promising potential as an alternative to NIR fluorescence imaging with ICG, offering unique properties that may enhance imaging capabilities. However, further research is required to establish its clinical applicability and broader therapeutic utility.

**Keywords:** shortwave-infrared, near-infrared, fluorescence imaging, indocyanine green, hepatocellular carcinoma

## 1. Introduction

The Center for Biosystems Dynamics Research at RIKEN has developed indocyanine green (ICG)-based  $\pi$ -conjugation-extended cyanine dyes, specifically ICG-C9 and ICG-C11. These dyes emit fluorescence in the shortwave-infrared (SWIR) spectrum at wavelengths of 922 nm and 1,010 nm, respectively, when dissolved in water. Using antibody conjugates with ICG-C9 and ICG-C11, researchers have demonstrated multiplexed SWIR fluorescence molecular imaging of breast tumors, visualizing both surface receptors and tumor vasculature in live mice (1,2).

Currently, near-infrared (NIR) fluorescence imaging with ICG is widely employed across various medical fields for diagnostic and therapeutic purposes (3-7). In hepatobiliary surgery, NIR fluorescence imaging has been utilized since its introduction (8), facilitating applications such as intraoperative fluorescence guidance and photodynamic therapy (9-13). Specifically, during

laparoscopic cholecystectomy and hepatectomy for liver cancer, intraoperative NIR fluorescence imaging with ICG has been associated with a reduced risk of bile duct injuries (14,15) and improved patient prognosis (16). However, NIR imaging has limitations, including autofluorescence interference and inadequate visualization of deep tissues (17,18). In contrast, SWIR fluorescence imaging, operating within the 1,000 to 1,400 nm wavelength range, offers significant advantages, including reduced tissue absorption and light scattering. These properties allow for superior imaging of deeper tissues (19,20), enhancing its potential for diagnostic and therapeutic applications in oncology (21-24).

Despite growing interest in SWIR fluorescence imaging for hepatobiliary surgery, its clinical adoption remains limited, primarily due to the lack of suitable imaging devices and fluorescent probes (25). To address this gap, this study evaluates the potential of SWIR fluorescence imaging with ICG-C9 as an effective alternative to NIR imaging for hepatobiliary diseases.



We analyzed the fluorescence characteristics and pharmacokinetics of ICG-C9 and assessed its uptake in hepatocellular carcinoma models.

## 2. Materials and Methods

### 2.1. Equipment for fluorescence imaging system

The fluorescence imaging system used in this study comprised the following components: an industrial lens (SMA11F25, Tamron Co., Ltd., Saitama, Japan) capable of covering a broad spectral range from visible light to the SWIR band; three fluorescence filters supplied by Semrock Inc. (Rochester, NY, USA) — an  $857 \pm 15$  nm band-pass filter (FF01-857), a 950 nm long-pass filter (FF01-937), and a 1000 nm long-pass filter (BLP01-980); a cooled monochrome SWIR camera (BH-71IGA, BITRAN Co., Ltd., Saitama, Japan) equipped with a SWIR image sensor (IMX990AABJ-C, Sony Semiconductor Solutions Co., Kanagawa, Japan); and two fiber-coupled lasers (HANGZHOU NAKU TECHNOLOGY Co., Ltd., Hangzhou, Zhejiang, China) with excitation wavelengths of 808 nm and 915 nm, along with beam expanders (ThorLabs Inc., Newton, NJ, USA). The fluorescence filters were used to detect emission wavelengths of  $857 \pm 15$  nm,  $> 950$  nm, and  $> 1,000$  nm. The camera captured monochrome images corresponding to the red, green, and blue channels of the light emitted by the RGB light source (Leimac Co., Ltd, Tokyo, Japan), enabling the generation of RGB images. The lens was positioned 60 cm above the targets, and the light power density was maintained at 20 mW/cm<sup>2</sup> (Supplementary Figures S1 and S2, <https://www.biosciencetrends.com/action/getSupplementalData.php?ID=256>). Fluorescence intensity data were processed using ImageJ software (National Institutes of Health, NIH).

### 2.2. Fluorescence intensity of ICG and ICG-C9 *in vitro*

ICG and ICG-C9, kindly provided by Dr. Takashi Jin (Center for Biosystems Dynamics Research, RIKEN, Osaka, Japan), were dissolved in 1% bovine serum albumin (BSA) to a final concentration of 0.1 mg/mL. Fluorescence intensities of both dyes were measured for all combinations of excitation wavelengths (808 nm and 915 nm) and emission wavelengths (840–873 nm,  $> 950$  nm, and  $> 1,000$  nm). The exposure time for all measurements was standardized at 30 ms.

### 2.3. Animals

BALB/c nude mice aged 5–6 weeks ( $n = 18$ ) were procured from Oriental Yeast Co., Ltd. (Tokyo, Japan). The mice were housed under specific pathogen-free conditions, maintained at a 12-hour light/dark cycle, and provided with autoclaved food and tap water throughout

the study. Anesthesia was induced with 3% isoflurane and maintained at 1–2% isoflurane during implantation procedures and intravenous injections. The animal experimental protocol was reviewed and approved by the Institutional Animal Care and Use Committee (Approval no. 23061), adhering to Japanese regulations and ethical guidelines for animal experimentation. Humane euthanasia was performed under isoflurane anesthesia prior to autopsy.

### 2.4. Pharmacokinetics of ICG and ICG-C9

ICG and ICG-C9 were prepared as solutions in 1% BSA in water and administered intravenously to 12 mice. Six mice received ICG and six received ICG-C9. A bolus injection of 0.5 mg/kg in 100  $\mu$ L of water was delivered *via* the tail vein. Post-administration, mice were euthanized at predetermined intervals — 15 min, 30 min, 3 h, 6 h, and 24 h — to evaluate the distribution of the fluorescent dyes in excretory organs. Imaging was conducted as follows: Mice injected with ICG were imaged using an excitation wavelength of 808 nm and emission wavelengths ranging from 840 to 873 nm. Mice injected with ICG-C9 were imaged using an excitation wavelength of 915 nm and emission wavelengths  $> 950$  nm. The exposure time for all imaging procedures was set to 30 ms.

### 2.5. Tumor cell line and xenograft model

HuH-7 cells, a well-differentiated human hepatoma cell line (26), were obtained from the Japanese Collection of Research Bioresources (JCRB) Cell Bank (Osaka, Japan). The cells were cultured in Dulbecco's Modified Eagle's Medium (DMEM, #044-29765, Fujifilm Wako, Tokyo, Japan) supplemented with 10% fetal bovine serum (FBS, #175012, Nichirei Bioscience, Tokyo, Japan) and 1% penicillin–streptomycin (P/S, #168-23191, Fujifilm Wako, Tokyo, Japan) and incubated at 37°C in a humidified atmosphere containing 5% CO<sub>2</sub> and 95% air. For harvesting, cells were briefly treated with 0.25% (w/v) trypsin–1 mmol/L EDTA solution (#209-16941, Fujifilm Wako, Tokyo, Japan).

After continuous culture, HuH-7 cells were collected into tubes, washed with phosphate-buffered saline (PBS, #045-29795, Fujifilm Wako, Tokyo, Japan), and resuspended in serum-free medium. Each mouse received a subcutaneous injection of  $5 \times 10^6$  HuH-7 cells in 0.1 mL of serum-free medium containing 33% Matrigel (#356234, Corning, Tokyo, Japan) into the left flank.

### 2.6. Fluorescence imaging of subcutaneous xenograft models

ICG and ICG-C9 were administered intravenously *via* the tail vein to six mice (three mice per dye) once tumor sizes reached approximately 200 mm<sup>3</sup>, around three

weeks after HuH-7 cell transplantation. Fluorescence imaging was performed 24 h post-administration. The dyes were delivered as bolus injections at doses of 0.5, 2.5, or 7.5 mg/kg in volumes of 100, 100, and 300  $\mu$ L of water, respectively. To avoid hemodynamic instability (27), the 7.5 mg/kg dose in a 300  $\mu$ L volume was divided into three 100  $\mu$ L aliquots and administered over a period of three days (100  $\mu$ L/day). Tumors were excised from the mice after euthanasia and imaged using fluorescence techniques. Tumors from mice treated with ICG were imaged with an excitation wavelength of 808 nm and an emission range of 840–873 nm, whereas those from mice treated with ICG-C9 were imaged with an excitation wavelength of 915 nm and an emission range of > 950 nm. For each condition, images were acquired with exposure times of 30, 80, and 300 ms.

## 2.7. Fluorescence microscopy

The cellular uptake of ICG and ICG-C9 in tumors derived from the HuH-7 human hepatoma cell line was evaluated using fluorescence microscopy. Tumors were harvested from mice administered 7.5 mg/kg of either ICG or ICG-C9. Pathological specimens were fixed

in formalin, sectioned into 7  $\mu$ m slices, and stained with hematoxylin and eosin (H&E). Fluorescence microscopy images were acquired using a BZ-X810 microscope (Keyence, Osaka, Japan). The exposure time for image acquisition was set to 3 s. Composite images were generated by stitching multiple images captured with a 20 $\times$  objective lens, utilizing the integrated imaging system of the microscope. To directly visualize fluorescence signals in the specimens without using fluorescent antibodies, an ICG filter (OP-87767; Keyence) was employed. This filter provided a 710–760 nm excitation window and an 810–875 nm emission window, enabling NIR imaging.

## 3. Results

### 3.1. Fluorescence intensity of ICG and ICG-C9 *in vitro*

For ICG, maximum fluorescence intensity was observed at an excitation wavelength of 808 nm, with emission wavelengths ranging from 840 to 873 nm. Fluorescence intensity was significantly reduced at an excitation wavelength of 915 nm. In contrast, ICG-C9 exhibited maximum fluorescence intensity at an excitation

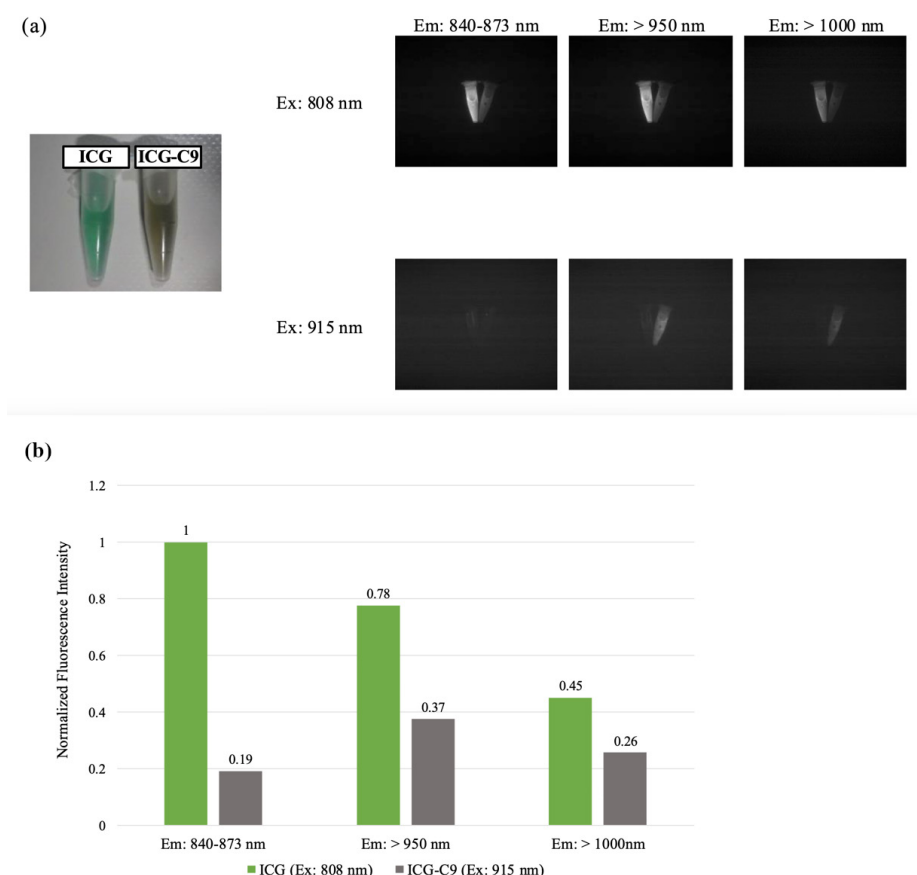


**Figure 1. Fluorescence intensities of ICG and ICG-C9** (a) Fluorescence intensities were measured under various combinations of excitation wavelengths (808 nm and 915 nm) and emission wavelengths (840–873 nm, > 950 nm, and >1,000 nm), with an exposure time of 30 ms. (b) ICG showed maximum fluorescence intensity at an excitation wavelength of 808 nm and emission wavelengths of 840–873 nm. In contrast, ICG-C9 exhibited maximum fluorescence intensity at an excitation wavelength of 915 nm and emission wavelengths of > 950 nm. ICG-C9 exhibited weaker fluorescence intensity than ICG.

wavelength of 915 nm, with emission wavelengths exceeding 950 nm (Figure 1a). Despite maintaining consistent exposure times and light power intensities, ICG-C9 displayed weaker fluorescence intensity than ICG under these conditions (Figure 1b).

### 3.2. Pharmacokinetics of ICG and ICG-C9

Similar to ICG, ICG-C9 was selectively taken up from the bloodstream into the liver and rapidly excreted into the bile (Figure 2a). Fifteen min post-intravenous administration of ICG, hepatic fluorescence reached near-maximum levels, followed by excretion into the bile and distribution in the intestinal tract. After 3 h, intestinal fluorescence increased, while at 24 h, minimal fluorescence remained in the liver or intestinal tract. In contrast, 6 h post-administration of ICG-C9, fluorescence persisted in the liver, whereas ICG fluorescence was minimal (Figure 2b). These findings suggest that ICG-C9 displays a slower excretion rate than ICG.

### 3.3. Fluorescence imaging of subcutaneous xenograft models

Fluorescence from ICG or ICG-C9 was not detectable at low doses (0.5 mg/kg). ICG fluorescence was detectable at doses of 2.5 mg/kg or higher, while ICG-C9 required a dose of 7.5 mg/kg for detection (Figure 3a). The fluorescence intensity of ICG-C9 was lower than that of ICG; however, with an extended exposure time of 300 ms, ICG-C9 uptake became detectable. Both dyes were taken up into the HuH-7 human hepatoma cell line tumors, demonstrating similar tumor-targeting properties (Figure 3b).

### 3.4. Fluorescence microscopy

Fluorescence signals from both ICG and ICG-C9 were observed in HuH-7 tumors, confirming similar uptake characteristics at the microscopic level. Fluorescence localized to both tumor periphery and interior regions (Figure 4a). At the cellular level, fluorescence was

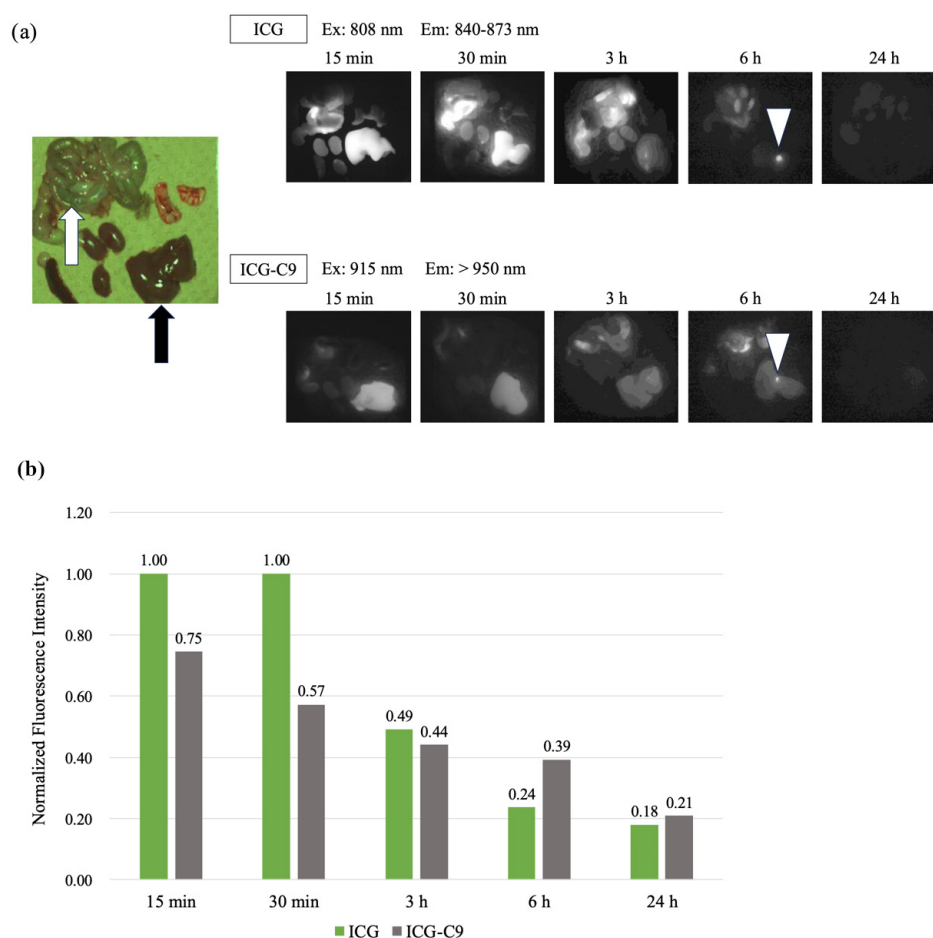


**Figure 2. ICG and ICG-C9 distribution in excretory organs (a)** Anatomical indicators: black arrow, liver; white arrow, intestine; white triangle, gallbladder. ICG and ICG-C9 were administered intravenously, and their distribution in excretory organs was analyzed at various time points post-administration. Both dyes were selectively taken up by the liver from the bloodstream and rapidly excreted into bile. No fluorescence signals were detectable in excretory organs 24 h after administration. **(b)** Fluorescence intensity in the liver following ICG and ICG-C9 administration. Six hours after ICG-C9 administration, detectable fluorescence persisted in the liver, whereas fluorescence from ICG was minimal. This suggests that ICG-C9 exhibits a slower excretion rate than ICG.

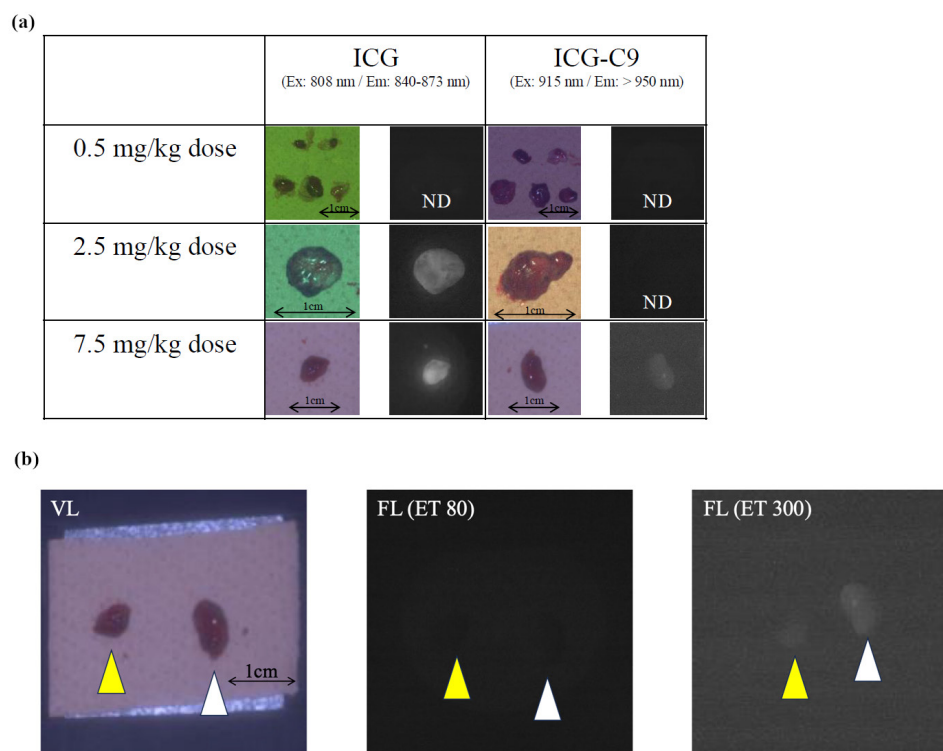


**Figure 3. ICG and ICG-C9 uptake in tumors (a)** Non-detectable (ND). A cell-line-derived subcutaneous tumor model from HuH-7 cells, representing hepatocellular carcinoma, was used to evaluate tumor uptake of ICG-C9 and compare it with ICG uptake. Fluorescence imaging was conducted 24 h post-administration. Tumors from mice treated with ICG were imaged using an excitation wavelength of 808 nm and emission wavelengths ranging from 840 to 873 nm, whereas tumors treated with ICG-C9 were imaged using an excitation wavelength of 915 nm and emission wavelengths of > 950 nm. ICG was detectable at a dose of 2.5 mg/kg with a 30 ms exposure time, whereas ICG-C9 required a dose of 7.5 mg/kg and a 300 ms exposure time for detection. **(b)** Panels: Left — tumors under visible light; center — fluorescence imaging with an 80 ms exposure time; right — fluorescence imaging with a 300 ms exposure time. A yellow triangle identifies a tumor from a mouse treated with ICG, while a white triangle marks a tumor from a mouse treated with ICG-C9. Fluorescence intensity for ICG-C9 was lower compared with ICG. Additionally, ICG-C9 was only detectable under the longer exposure time (300 ms), demonstrating that, like ICG, ICG-C9 is taken up by HuH-7-derived tumors.

predominantly found in the cytoplasm of HuH-7 cells, with no fluorescence observed in the nucleus (Figure 4b). The fluorescence intensity of ICG-C9 was lower than that of ICG, likely due to the shorter excitation and emission wavelength range of the filter used.

#### 4. Discussion

This study highlights several advantages of ICG-C9, making it a promising alternative to conventional ICG for fluorescence imaging. One of the primary advantages of ICG-C9 is its fluorescence properties, with peak intensity achieved at an excitation wavelength of 915 nm and emission wavelengths > 950 nm in the SWIR spectrum. Moreover, ICG-C9 is one of the few biocompatible and water-soluble SWIR fluorescent probes, making it suitable for biomedical research and holding great potential to accelerate the clinical translation of SWIR fluorescence imaging. However, ICG-C9 exhibits lower fluorescence intensity than ICG under identical excitation density and exposure conditions due to its reduced quantum yield in aqueous solutions (2). Consequently, achieving optimal fluorescence with ICG-C9 may require higher doses, extended exposure times, or increased

excitation light intensity. In this study, detectable fluorescence from the HuH-7 cell line tumor model was achieved with a dose of 7.5 mg/kg and an exposure time of 300 ms, while shorter exposure times (*e.g.*, 80 ms or less) resulted in insufficient fluorescence. While the required dose (7.5 mg/kg) and exposure time (300 ms) used in this study may not be directly applicable to real-time surgical imaging, our findings suggest potential for improving signal detection by adjusting excitation power and exposure conditions.

ICG-C9 shares similar excretion properties with ICG, with both being taken up by the liver from the bloodstream and excreted into bile. This characteristic enables intraoperative fluorescence cholangiography following intravenous administration of ICG-C9, as the excreted dye emits a fluorescence signal. Currently, intraoperative NIR fluorescence imaging using ICG during laparoscopic cholecystectomy is used to visualize biliary structures (8,28), reducing the risk of bile duct injuries (14,15). However, its effectiveness can be limited in patients with obesity or cholecystitis due to increased tissue thickness around the biliary structures (29,30). SWIR fluorescence, in contrast, displays reduced tissue absorption and scattering and



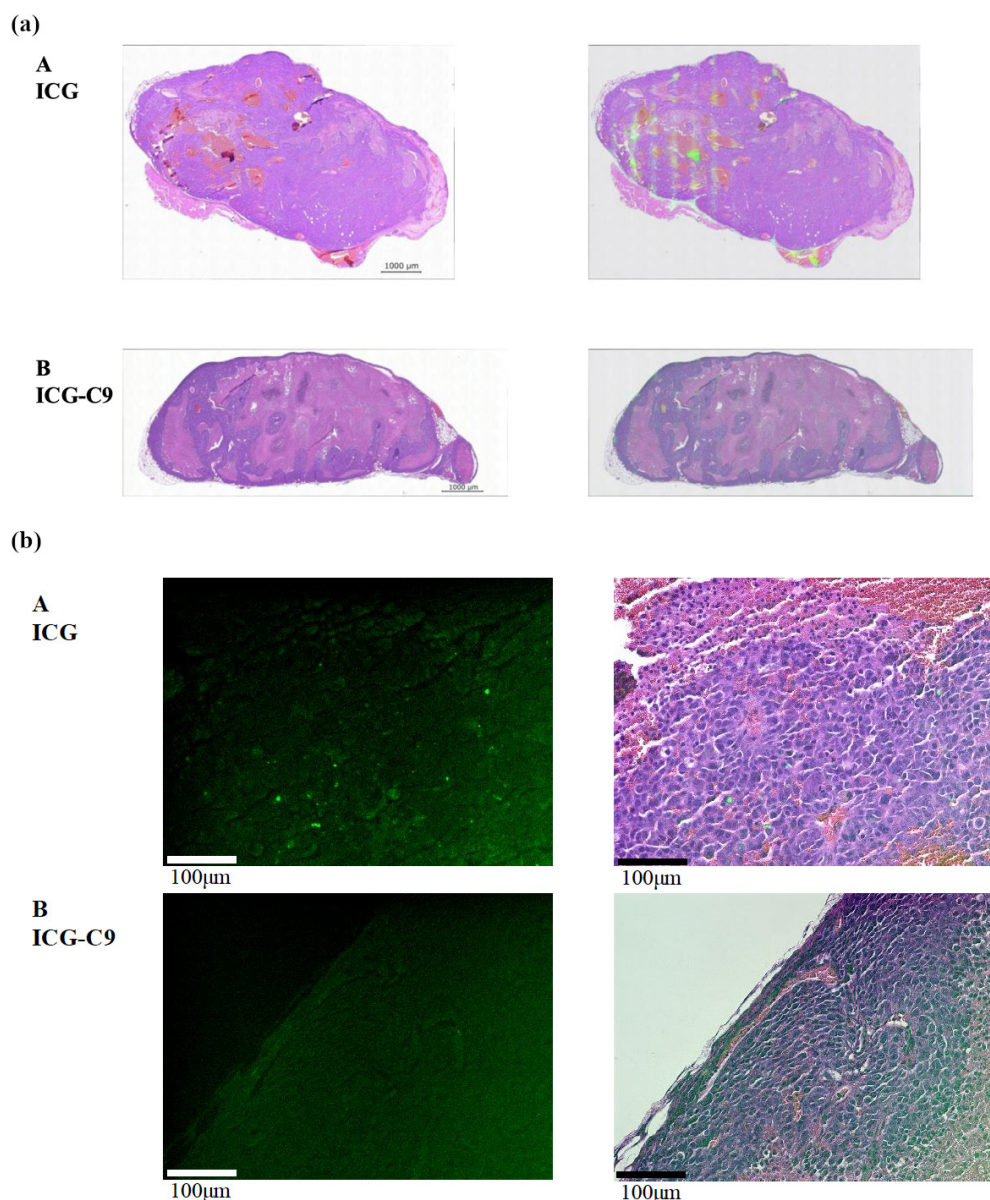


**Figure 4. Microscopical analysis of tumors from mice administered 7.5 mg/kg doses of ICG or ICG-C9** (a) Left panel: cancer tissues stained with hematoxylin and eosin (H&E). Right panel: merged images showing fluorescence from ICG (A) or ICG-C9 (B) within cancer tissues. Both ICG and ICG-C9 demonstrated fluorescence within HuH-7 tumors, confirming similar uptake properties at the microscopic level. Fluorescence was localized to both the tumor periphery and interior regions. (b) Left panel: fluorescence images under a 20× objective lens. Right panel: merged images showing fluorescence. For both ICG and ICG-C9, fluorescence was confined to the cytoplasm of HuH-7 cells, with no signal detected in the nucleus.

is less affected by autofluorescence (19,20). This makes ICG-C9 particularly suited for deep tissue visualization. Nevertheless, the bile excretion properties of ICG-C9 may pose challenges, such as excessive liver background fluorescence, which could obscure bile duct visualization (31,32). The extended  $\pi$ -conjugated system of ICG-C9 increases its hydrophobicity, enhancing stronger protein and membrane binding (2). Although this leads to greater tissue accumulation, it also results in slower excretion, which may contribute to prolonged background fluorescence. Moreover, our findings suggest that ICG-C9 exhibits slower excretion compared to conventional ICG. However, like ICG, hepatic washout

following administration was observed. This indicates that employing a delayed imaging protocol—allowing sufficient time after administration—may enhance tumor-to-background contrast and reduce interference with bile duct visualization. In clinical practice, ICG-C9 may need to be administered earlier than the typical timing used for ICG. Nevertheless, further investigation is required to determine the optimal timing of administration for effective imaging.

A significant advantage of ICG-C9 is its ability to accumulate in HuH-7 human hepatoma cell line tumors, similar to ICG. The mechanism by which ICG highlights hepatocellular carcinoma (HCC)

involves the retention of ICG within the tumor after it is washed out from the surrounding liver tissue. This occurs because well-differentiated HCC maintains the expression of ICG uptake transporters, such as Na<sup>+</sup>/taurocholate cotransporting polypeptide and organic anion-transporting polypeptide 8, although at lower levels than normal liver tissue. However, morphological and functional impairments in the biliary excretion system within HCC prevent the efficient elimination of ICG, leading to its accumulation in the tumor (33). This mechanism has also been demonstrated in subcutaneous tumor mouse models using HuH-7 cells (13). The transporters involved in the uptake of ICG-C9 remain unknown; however, this study suggests that ICG-C9 shares bile excretory properties similar to those of ICG. Utilizing bile stasis around the tumor, ICG-C9 may enhance the sensitivity of intraoperative fluorescence imaging techniques for poorly differentiated HCC and liver metastases, allowing fluorescent visualization of tumor rims (10,34). SWIR imaging has been shown to provide higher sensitivity and improved target-to-background contrast when compared with NIR imaging, thereby making it a powerful tool for guiding liver cancer resections (25). Given that ICG-C9 exhibits its most intense fluorescence in the SWIR spectrum, it holds great potential for enhancing tumor imaging during surgery. Specifically, the combination of conventional NIR imaging using ICG and SWIR imaging using ICG-C9 may enable double-color imaging—such as distinguishing cancerous tissue from hepatic segments (10,35) and visualizing bile ducts and blood vessels (8,28). Similar to how ICG fluorescence imaging enables real-time, high-sensitivity detection of small, grossly unidentifiable liver tumors (10), it may facilitate the identification of deeper or previously undetectable lesions. Additionally, studies have demonstrated the utility of ICG-labeled antibodies for target cell imaging with NIR fluorescence and for ICG-based phototherapy in hepatocellular carcinoma (13,36). These approaches could also be adapted to SWIR imaging with ICG-C9, enabling multi-color imaging by labeling different antibodies with ICG and ICG-C9 and switching excitation wavelengths (2). This capability could broaden therapeutic applications, including more precise and targeted cancer treatments.

Despite its potential, this study has several limitations. Although ICG-C9 is bile-excreted, its fluorescence intensity in macroscopic observations was weaker than expected, likely due to its inherently lower fluorescence intensity compared with ICG. Another potential factor could be the camera-to-object distance used in this experiment, which was substantially greater than the typical distance in conventional endoscopic or handheld fluorescence observation devices. In clinical practice, shorter distances between the imaging device and the target tissue are expected to enhance excitation light delivery and fluorescence signal capture,

potentially improving the visibility of ICG-C9-labeled tumors. Therefore, the performance of ICG-C9 observed in our experimental setup may underestimate its true potential under surgical conditions. The large camera-to-object distance, relative to the size of the object, may have resulted in insufficient excitation or signal detection. Furthermore, the excitation light intensity used in this study (20 mW/cm<sup>2</sup>) may have been relatively low, which could have further limited the efficiency of fluorescence excitation and detection. In this study, a cell line-derived subcutaneous xenograft model was used to evaluate the *in vivo* performance of ICG-C9. However, this model lacks the heterogeneity and biological complexity of actual patient tumor. Moreover, because the tumors were implanted subcutaneously, we were unable to assess fluorescence differences between tumor and paraneoplastic tissues. As a result, it remains unclear whether ICG-C9 was specifically taken up by tumor cells in this model. Additionally, the small sample size, and limited range of cell lines tested constrain the generalizability of the findings. Further research is warranted to investigate whether other human hepatoma cell lines exhibit similar preferential uptake of ICG-C9 and to confirm its utility in SWIR fluorescence imaging. To better replicate clinical conditions and evaluate tumor-specific uptake, future studies should incorporate patient-derived xenograft models that more accurately reflect the biological diversity of human tumors. Furthermore, liver transplant xenograft models would enable direct comparison between tumor and normal hepatocytes, providing more precise insights into the specificity of ICG-C9 accumulation. While ICG is considered a safe fluorescence dye (37), the cytotoxicity profile of ICG-C9 — though ICG-C9 exhibits a concentration-dependent cytotoxicity profile similar to conventional ICG based on the 3-(4,5-dimethylthiazol-2-yl)-2,5-diphenyltetrazolium bromide assays in HeLa cells (2) — requires further validation. Future studies should focus on characterizing the pharmacokinetics, tumor accumulation, and tissue penetration capabilities of SWIR light when using ICG-C9. Moreover, optimizing imaging parameters such as dose, exposure time, and excitation light intensity will be crucial for maximizing the clinical utility of SWIR imaging with ICG-C9.

In conclusion, our study demonstrated that ICG-C9, like ICG, is excreted *via* bile and exhibits fluorescence in the SWIR range. Additionally, ICG-C9 was effectively taken up by tumors derived from a human hepatoma cell line. These findings suggest that ICG-C9 holds potential for applications in hepatobiliary surgery and as a therapeutic agent when conjugated with antibodies. However, further studies are necessary to evaluate its safety, efficacy, and clinical utility. Addressing key issues such as fluorescence intensity, pharmacokinetics, and generalizability is essential to enhance the translational relevance of our study.

## Acknowledgements

Authors acknowledge Dr. Takashi Jin (Center for Biosystems Dynamics Research, RIKEN, Osaka, Japan) for donating ICG and ICG-C9, and Keyence (Osaka, Japan) for microscopic imaging.

**Funding:** This study was supported by R&D Technology Center, Tamron Co. The study sponsor had no role in study design; in the collection, analysis, and interpretation of data; in the writing of the report; or in the decision to submit the paper for publication.

**Conflict of Interest:** R&D Technology Center, Tamron Co. provided the fluorescence imaging system for this study.

**Data Availability Statement:** The datasets generated and analyzed during the current study are available from the corresponding author upon reasonable request.

## References

- Swamy MMM, Murai Y, Monde K, Tsuboi S, Jin T. Shortwave-infrared fluorescent molecular imaging probes based on  $\pi$ -conjugation extended indocyanine green. *Bioconjug Chem*. 2021; 32:1541-1547.
- Swamy MMM, Murai Y, Monde K, Tsuboi S, Swamy AK, Jin T. Biocompatible and water-soluble shortwave-infrared (SWIR)-emitting cyanine-based fluorescent probes for *in vivo* multiplexed molecular imaging. *ACS Appl Mater Interfaces*. 2024; 16:17253-17266.
- Kitai T, Inomoto T, Miwa M, Shikayama T. Fluorescence navigation with indocyanine green for detecting sentinel lymph nodes in breast cancer. *Breast Cancer*. 2005; 12:211-215.
- Kusano M, Tajima Y, Yamazaki K, Kato M, Watanabe M, Miwa M. Sentinel node mapping guided by indocyanine green fluorescence imaging: A new method for sentinel node navigation surgery in gastrointestinal cancer. *Dig Surg*. 2008; 25:103-108.
- Ogata F, Azuma R, Kikuchi M, Koshima I, Morimoto Y. Novel lymphography using indocyanine green dye for near-infrared fluorescence labeling. *Ann Plast Surg*. 2007; 58:652-655.
- Raabe A, Nakaji P, Beck J, Kim LJ, Hsu FP, Kamerman JD, Seifert V, Spetzler RF. Prospective evaluation of surgical microscope-integrated intraoperative near-infrared indocyanine green videoangiography during aneurysm surgery. *J Neurosurg*. 2005; 103:982-989.
- Rubens FD, Ruel M, Fremes SE. A new and simplified method for coronary and graft imaging during CABG. *Heart Surg Forum*. 2002; 5:141-144.
- Ishizawa T, Bandai Y, Kokudo N. Fluorescent cholangiography using indocyanine green for laparoscopic cholecystectomy: an initial experience. *Arch Surg*. 2009; 144:381-382.
- Inoue Y, Arita J, Sakamoto T, Ono Y, Takahashi M, Takahashi Y, Kokudo N, Saiura A. Anatomical liver resections guided by 3-dimensional parenchymal staining using fusion indocyanine green fluorescence imaging. *Ann Surg*. 2015; 262:105-111.
- Ishizawa T, Fukushima N, Shibahara J, Masuda K, Tamura S, Aoki T, Hasegawa K, Beck Y, Fukayama M, Kokudo N. Real-time identification of liver cancers by using indocyanine green fluorescent imaging. *Cancer*. 2009; 115:2491-2504.
- Ishizawa T, Saiura A, Kokudo N. Clinical application of indocyanine green-fluorescence imaging during hepatectomy. *Hepatobiliary Surg Nutr*. 2016; 5:322-328.
- Ishizawa T, Tamura S, Masuda K, Aoki T, Hasegawa K, Imamura H, Beck Y, Kokudo N. Intraoperative fluorescent cholangiography using indocyanine green: A biliary road map for safe surgery. *J Am Coll Surg*. 2009; 208:e1-e4.
- Kaneko J, Inagaki Y, Ishizawa T, Gao J, Tang W, Aoki T, Sakamoto Y, Hasegawa K, Sugawara Y, Kokudo N. Photodynamic therapy for human hepatoma-cell-line tumors utilizing biliary excretion properties of indocyanine green. *J Gastroenterol*. 2014; 49:110-116.
- Dip F, LoMenzo E, Sarotto L, *et al*. Randomized trial of near-infrared incisionless fluorescent cholangiography. *Ann Surg*. 2019; 270:992-999.
- Pesce A, Piccolo G, La Greca G, Puleo S. Utility of fluorescent cholangiography during laparoscopic cholecystectomy: a systematic review. *World J Gastroenterol*. 2015; 21:7877-7883.
- He K, Hong X, Chi C, Cai C, An Y, Li P, Liu X, Shan H, Tian J, Li J. Efficacy of near-infrared fluorescence-guided hepatectomy for the detection of colorectal liver metastases: a randomized controlled trial. *J Am Coll Surg*. 2022; 234:130-137.
- Sordillo LA, Pu Y, Pratavieira S, Budansky Y, Alfano RR. Deep optical imaging of tissue using the second and third near-infrared spectral windows. *J Biomed Opt*. 2014; 19:056004.
- Carr JA, Franke D, Caram JR, Perkinson CF, Saif M, Askoxylakis V, Datta M, Fukumura D, Jain RK, Bawendi MG, Bruns OT. Shortwave infrared fluorescence imaging with the clinically approved near-infrared dye indocyanine green. *Proc Natl Acad Sci U S A*. 2018; 115:4465-4470.
- Ding F, Zhan Y, Lu X, Sun Y. Recent advances in near-infrared II fluorophores for multifunctional biomedical imaging. *Chem Sci*. 2018; 9:4370-4380.
- Smith AM, Mancini MC, Nie S. Bioimaging: second window for *in vivo* imaging. *Nat Nanotechnol*. 2009; 4:710-711.
- Suo Y, Wu F, Xu P, Shi H, Wang T, Liu H, Cheng Z. NIR-II fluorescence endoscopy for targeted imaging of colorectal cancer. *Adv Healthc Mater*. 2019; 8:e1900974.
- Dai H, Shen Q, Shao J, Wang W, Gao F, Dong X. Small molecular NIR-II fluorophores for cancer phototheranostics. *Innovation (Camb)*. 2021; 2:100082.
- Iida T, Kiya S, Kubota K, Jin T, Seiyama A, Nomura Y. Monte Carlo modeling of shortwave-infrared fluorescence photon migration in voxelized media for the detection of breast cancer. *Diagnostics (Basel)*. 2020; 10:961.
- Fan X, Yang J, Ni H, Xia Q, Liu X, Wu T, Li L, Prasad PN, Liu C, Lin H, Qian J. Initial experience of NIR-II fluorescence imaging-guided surgery in foot and ankle surgery. *Engineering*. 2024; 40:19-27.
- Hu Z, Fang C, Li B, *et al*. First-in-human liver-tumour surgery guided by multispectral fluorescence imaging in the visible and near-infrared-I/II windows. *Nat Biomed Eng*. 2020; 4:259-271.
- Nakabayashi H, Taketa K, Miyano K, Yamane T, Sato J. Growth of human hepatoma cells lines with differentiated functions in chemically defined medium. *Cancer Res*.



- 1982; 42:3858-3863.
27. Diehl KH, Hull R, Morton D, Pfister R, Rabemampianina Y, Smith D, Vidal JM, van de Vorstenbosch C, European Federation of Pharmaceutical Industries Association and European Centre for the Validation of Alternative Methods. A good practice guide to the administration of substances and removal of blood, including routes and volumes. *J Appl Toxicol.* 2001; 21:15-23.
28. Dip F, Roy M, Menzo EL, Simpfendorfer C, Szomstein S, Rosenthal RJ. Routine use of fluorescent incisionless cholangiography as a new imaging modality during laparoscopic cholecystectomy. *Surg Endosc.* 2015; 29:1621-1626.
29. Daskalaki D, Fernandes E, Wang X, Bianco FM, Elli EF, Ayloo S, Masrur M, Milone L, Giulianotti PC. Indocyanine green (ICG) fluorescent cholangiography during robotic cholecystectomy: results of 184 consecutive cases in a single institution. *Surg Innov.* 2014; 21:615-621.
30. Igami T, Nojiri M, Shinohara K, Ebata T, Yokoyama Y, Sugawara G, Mizuno T, Yamaguchi J, Nagino M. Clinical value and pitfalls of fluorescent cholangiography during single-incision laparoscopic cholecystectomy. *Surg Today.* 2016; 46:1443-1450.
31. Esposito C, Alberti D, Settini A, Pecorelli S, Boroni G, Montanaro B, Escolino M. Indocyanine green (ICG) fluorescent cholangiography during laparoscopic cholecystectomy using RUBINA™ technology: preliminary experience in two pediatric surgery centers. *Surg Endosc.* 2021; 35:6366-6373.
32. Kono Y, Ishizawa T, Tani K, Harada N, Kaneko J, Saiura A, Bandai Y, Kokudo N. Techniques of fluorescence cholangiography during laparoscopic cholecystectomy for better delineation of the bile duct anatomy. *Medicine (Baltimore).* 2015; 94:e1005.
33. Ishizawa T, Masuda K, Urano Y, Kawaguchi Y, Satou S, Kaneko J, Hasegawa K, Shibahara J, Fukayama M, Tsuji S, Midorikawa Y, Aburatani H, Kokudo N. Mechanistic background and clinical applications of indocyanine green fluorescence imaging of hepatocellular carcinoma. *Ann Surg Oncol.* 2014; 21:440-448.
34. van der Vorst JR, Hutteman M, Mieog JS, de Rooij KE, Kaijzel EL, Löwik CW, Putter H, Kuppen PJ, Frangioni JV, van de Velde CJ, Vahrmeijer AL. Near-infrared fluorescence imaging of liver metastases in rats using indocyanine green. *J Surg Res.* 2012; 174:266-271.
35. Ishizawa T, Zuker NB, Kokudo N, Gayet B. Positive and negative staining of hepatic segments by use of fluorescent imaging techniques during laparoscopic hepatectomy. *Arch Surg.* 2012; 147:393-394.
36. Jin T, Tsuboi S, Komatsuzaki A, Imamura Y, Muranaka Y, Sakata T, Yasuda H. Enhancement of aqueous stability and fluorescence brightness of indocyanine green using small calix[4]arene micelles for near-infrared fluorescence imaging. *MedChemComm.* 2016; 7:623-631.
37. Obana A, Miki T, Hayashi K, *et al.* Survey of complications of indocyanine green angiography in Japan. *Am J Ophthalmol.* 1994; 118:749-753.

Received April 14, 2025; Revised June 4, 2025; Accepted June 9, 2025.

*\*Address correspondence to:*

Ryota Tanaka, Department of Hepato-Biliary-Pancreatic Surgery, Osaka Metropolitan University Graduate School of Medicine, Osaka 545-8585, Japan.  
E-mail: taanaakaa3364@gmail.com

Released online in J-STAGE as advance publication June 14, 2025.



# SNRPA promotes hepatocellular carcinoma proliferation and lenvatinib resistance *via* B7-H6-STAT3/AKT axis by facilitating B7-H6 pre-mRNA maturation

Jiejun Hu<sup>1,§</sup>, Junhua Gong<sup>1,§</sup>, Xia Shu<sup>2</sup>, Xin Dai<sup>1</sup>, Dong Cai<sup>1</sup>, Zhibo Zhao<sup>1</sup>, Jinhao Li<sup>1</sup>, Guochao Zhong<sup>1,\*</sup>, Jianping Gong<sup>1,\*</sup>

<sup>1</sup>Department of Hepatobiliary Surgery, The Second Affiliated Hospital of Chongqing Medical University, Chongqing, China;

<sup>2</sup>Department of Gastroenterology, The First People's Hospital of Longquanyi District, Chengdu, China.

**SUMMARY:** The pre-mRNAs splicing is important mechanisms of hepatocellular carcinoma (HCC) progression. Hence, this study aimed to explore the function and corresponding mechanisms of small nuclear ribonucleoprotein polypeptide A (SNRPA), a vital RNAs splicing molecule, in HCC. Here, the University of Alabama at Birmingham CANcer data analysis portal (UALCAN), western blotting, and immunohistochemistry indicated that SNRPA levels were elevated in HCC tissues. Moreover, high expression of SNRPA was correlated with unfavorable clinicopathologic features and poor survival in HCC patients. A series of *in vitro* and *in vivo* gain/loss-of-function experiments reported that SNRPA promoted the proliferation of HCC cells. Integrated nanopore full-length cDNA sequencing and RNA-binding protein immunoprecipitation sequencing revealed that B7 homologue 6 (B7-H6) was a potential target of SNRPA. Subsequently, western blotting and flow cytometry showed that SNRPA activated B7-H6-STAT3/AKT signaling axis in HCC cells with promotion of G1-S transition in the cell cycle and inhibition of cell apoptosis. Mechanistically, RNA-binding protein immunoprecipitation and polymerase chain reaction with using exon-exon and exon-intron junction primers revealed that SNRPA facilitated B7-H6 pre-mRNA maturation by binding to it directly and contributing to its intron 2 splicing. Moreover, drug sensitivity test found that SNRPA induced HCC cell resistance to lenvatinib. Finally, restoration experiments demonstrated that the effects of SNRPA on HCC cells relied on B7-H6 expression. Taken together, SNRPA promotes HCC growth and lenvatinib resistance *via* B7-H6-STAT3/AKT axis through facilitating B7-H6 pre-mRNA maturation by maintaining its intron 2 splicing. Thus, SNRPA may be a promising target for HCC therapy and lenvatinib resistance reversion.

**Keywords:** hepatocellular carcinoma, SNRPA, B7-H6, pre-mRNA maturation, lenvatinib resistance

## 1. Introduction

Hepatocellular carcinoma (HCC) is the sixth most frequent type of cancer, and the third leading cause of cancer-related death worldwide (1). For the past several decades, surgery (including liver resection and transplantation) remains a primary treatment modality for patients with early-stage HCC (2,3). Although numerous molecular target drugs, such as tyrosine kinase inhibitors (TKIs) and immune checkpoint inhibitors (ICIs), have been utilized for the treatment of patients with advanced-stage HCC, their effects were limited (4,5). This is mainly due to the heterogeneity in the etiology of HCC and various factors resulting in drug resistance (6,7). Therefore, there is an urgent need to discover novel molecular targets for HCC therapy and reversion of drug resistance.

The splicing and removal of the introns of pre-mRNAs is an important process in pre-mRNA maturation. In this process, normal and abnormal splicing are regulated to produce various transcripts with different functions (alternative splicing), thereby enriching the genetic diversity (8-10). In recent years, accumulating evidence indicates that both normal and abnormal pre-mRNA splicing play an essential role in tumor progression, therapeutic resistance, and adaptation to harsh microenvironments (11-14). The small nuclear ribonucleoprotein polypeptide A (SNRPA) gene coding the U1A protein is a major component of the spliceosome U1 small nuclear ribonucleoprotein, which is intimately associated with RNA splicing, modification, and decay (15-17). Several studies have reported that SNRPA enhanced tumor progression in gastric cancer and colorectal cancer (18-20). Using bioinformatic analysis,

Zhang *et al.* found that elevated SNRPA expression was associated with poor survival in HCC patients (21). In addition, it was recently reported that SNRPA promoted HCC metastasis with microvascular invasion (22). However, above studies have not demonstrated that SNRPA aggravates HCC and other cancers *via* pre-mRNA splicing, which is the most essential and direct function of SNRPA. Thus, in this study, we sought to identify the mechanism of pre-mRNA splicing driven by SNRPA in HCC progression.

Coded by the NCR3LG1 gene, B7 homologue 6 (B7-H6) protein is a new member of the B7 family discovered by Brandt *et al.* in 2009 using bioinformatics and mass spectrometry (23). Human B7-H6 is rarely detected in normal human tissues; nevertheless, it was frequently present in various human tumors (23,24), including HCC, breast cancer, and gastric cancer (25-27). As a transmembrane protein, B7-H6 plays an important role in tumorigenesis *via* an immunological mechanism (28-30). In recent years, an increasing number of studies find that B7-H6 promotes tumor progression by regulating cell cycle and apoptosis *via* a non-immunological action. This process primarily includes the activation of signal transducer and activator of transcription 3 (STAT3), protein kinase B (AKT), and extracellular signal-regulated kinase (ERK) signaling pathways (27,31-33). Considering the absence of B7-H6 in normal tissues and its relative abundance among tumor tissues, its expression may be a response to tumorigenesis. Naturally, the study of the mechanism underlying the expression of B7-H6 in tumors may provide a novel treatment modality for patients with HCC.

In this study, we identified that SNRPA-B7-H6-STAT3/AKT axis plays a critical role in HCC cell proliferation and lenvatinib resistance through a mechanism of B7-H6 pre-mRNA maturation facilitated by SNRPA. Collectively, SNRPA may be a promising target molecule for HCC therapy and reversal of resistance to lenvatinib in HCC patients.

## 2. Materials and Methods

### 2.1. Human tissue samples

Initially, 12 pairs of fresh HCC tissues and matched para-tumor tissues from the Second Affiliated Hospital of Chongqing Medical University (Chongqing, China) were collected to detect the SNRPA expression through western blotting. A total of 85 and 97 pairs of HCC tissues and corresponding adjacent tumor tissues, respectively, were obtained from the Second Affiliated Hospital of Chongqing Medical University and OUTDO BIOTECH (cat.no. HLivH180Su31; OUTDO BIOTECH, Shanghai, China). The tissues were utilized in immunohistochemistry staining to detect the SNRPA protein levels and analyze the correlation of SNRPA expression and the survival of patients with

HCC. The selection criteria were as follows. Inclusion criteria: 1) patients were diagnosed as HCC by biopsy after surgery, 2) patients had no immunodeficiency disease; exclusion criteria: 1) patients suffered from other cancers, 2) patients had received chemotherapy, radiofrequency ablation, or molecular targeted therapy before liver resection. This research was approved by the Ethics Committee of the Second Affiliated Hospital of Chongqing Medical University (approval number RER2022-637A). All patients provided informed consent.

### 2.2. Xenograft models

Indicated HCC cells ( $2.5 \times 10^6$ /mice) were suspended in cool phosphate buffer saline and subsequently injected into the right hindlimb of nude mice (male, 4-week-old) subcutaneously. Additionally, we sought to investigate the impact of SNRPA on the sensitivity of HCC cells to lenvatinib *in vivo*. For this purpose, 10 days after the transplantation of indicated cells, the nude mice received treatment with lenvatinib once daily (10 mg/kg) *via* oral gavage. Tumor size was measured with a caliper every 3 days; the formula for the size calculation was as follows: volume = (length  $\times$  width<sup>2</sup>)/2 cm<sup>3</sup>. Three weeks after implantation, the nude mice were killed by cervical dislocation and the tumors were removed. These experiments were approved by the Animal Ethics Committee of Chongqing Medical University (approval number RER2021-136X).

### 2.3. Other Methods

Detailed materials and methods including western blotting, immunohistochemistry, cell culture, lentivirus infection, cell counting Kit-8 test, EdU assay, colony formation assay, scratch wound healing assay, nanopore full-length cDNA sequencing, RNA-binding protein immunoprecipitation, flow cytometry for cell cycle analysis, flow cytometry for cell apoptosis detection, small-interfering RNA transfection, reverse transcription-polymerase chain reaction, quantitative real-time polymerase chain reaction, bioinformatic analysis, and statistical analysis are described in Supplemental Data. Additionally, antibodies, primers, and targeted sequences used in this project can be found in Supplemental Tables S1-S5 (<https://www.biosciencetrends.com/supplementaldata/253>).

## 3. Results

3.1. SNRPA is frequently elevated in HCC tissues, and its elevation predicts poor survival in HCC patients.

Analysis using the UALCAN revealed that both the mRNA (Figure 1A) and protein (Figure 1B) levels of SNRPA were increased in HCC tissues compared

with normal liver tissues. In addition, the expression of SNRPA was higher in patients with stages 2–3 HCC than in those with stage 1 HCC (Figure 1C). Subsequently, genes positively associated with SNRPA were subjected to KEGG analysis by DAVID; among the enriched KEGG pathways, "cell cycle" was highly related to HCC progression (Figure 1D). Furthermore, western blotting demonstrated that SNRPA protein expression was significantly upregulated in HCC tissues compared with paired para-tumor tissues (Figure 1E). Moreover, immunohistochemistry assay indicated that SNRPA were frequently elevated both in the Chongqing cohort of 85 HCC patients and OUTDO BIOTECH cohort of 97 HCC patients (Figure 1F). The relationship between SNRPA levels and clinicopathological features was analyzed with the chi-squared test, and the results showed that SNRPA levels were positively correlated with tumor size in HCC patients from the above-mentioned cohorts (Supplemental Tables S6, S7, <https://www.biosciencetrends.com/supplementaldata/253>). Notably, SNRPA expression was positively related to tumor TNM stage only in HCC patients from the Chongqing cohort (Supplemental Tables S6, S7, <https://www.biosciencetrends.com/supplementaldata/253>). Subsequently, Kaplan–Meier analysis, as well as univariate and multivariate Cox proportional hazards regression models demonstrated that overall survival was poorer in HCC patients with high levels of SNRPA than in those with low levels of SNRPA in both the Chongqing and OUTDO BIOTECH cohorts. In addition, high expression of SNRPA was an independent predictor of the poor overall survival in HCC patients from the OUTDO BIOTECH cohort (Figure 1G, H and Supplemental Figure S1A, B, <https://www.biosciencetrends.com/supplementaldata/253>). Meanwhile, in the Chongqing cohort, HCC patients with high levels of SNRPA suffered from a shorter disease-free survival versus those with low levels of SNRPA. Notably, high SNRPA expression was an independent risk factor for tumor recurrence in HCC (Figure 1I and Supplemental Figure S1C, <https://www.biosciencetrends.com/supplementaldata/253>). Moreover, we used the Gene Expression Profiling Interactive Analysis (GEPIA) to analyze TCGA-LIHC samples, the results further showed that high expression of SNRPA was closely associated with a poor prognosis in HCC patients (Supplemental Figure S2A, B, <https://www.biosciencetrends.com/supplementaldata/253>). Collectively, these data indicate that SNRPA is elevated in HCC, and its elevation is related to unfavorable clinicopathologic features and poor survival in HCC patients. It is therefore likely that SNRPA plays a vital role in HCC progression.

### 3.2. SNRPA promotes HCC cell proliferation both *in vitro* and *in vivo*.

Western blotting revealed that SNRPA was highly

expressed in Huh-7 and SK-Hep-1 cells, whereas it was lowly expressed in Hep 3B cells (Supplemental Figure S3A, <https://www.biosciencetrends.com/supplementaldata/253>). Based on these results, we silenced SNRPA expression in Huh-7 and SK-Hep-1 cells, and overexpressed SNRPA in Hep 3B cells through lentivirus infection. The efficiency of SNRPA knockdown (Supplemental Figure S3B, <https://www.biosciencetrends.com/supplementaldata/253>) and overexpression (Supplemental Figure S3C, <https://www.biosciencetrends.com/supplementaldata/253>) was identified by western blotting. Knockdown of SNRPA significantly suppressed the proliferation of Huh-7 and SK-Hep-1 cells, whereas SNRPA overexpression significantly promoted the proliferation of Hep 3B cells, as demonstrated by CCK-8, EdU, and colony formation assays (Figure 2A–F). However, wound healing assay demonstrated that SNRPA knockdown or overexpression did not affect the migration of HCC cells (Supplemental Figure S4A, B, <https://www.biosciencetrends.com/supplementaldata/253>). We also established nude mouse subcutaneous xenograft models and found that SNRPA silencing could significantly inhibit the growth of Huh-7 and SK-Hep-1 cells *in vivo* (Figure 2G, H and Supplemental Figure S5A, B, <https://www.biosciencetrends.com/supplementaldata/253>). Furthermore, immunohistochemistry staining of xenograft tumor tissues illustrated that Ki-67 expression was decreased in tumor tissues from the SNRPA knockdown groups compared with the negative control groups (Supplemental Figure S5C, D, <https://www.biosciencetrends.com/supplementaldata/253>). Overall, the above data suggest that SNRPA promotes HCC cell proliferation both *in vitro* and *in vivo*.

### 3.3. SNRPA activates the B7-H6-STAT3/AKT signaling axis in HCC cells with promotion of G1-S transition in the cell cycle and inhibition of cell apoptosis.

Firstly, we detected significantly changed transcripts after SNRPA silencing using nanopore full-length cDNA sequencing in Huh-7 cells. The sequencing identified 348 transcripts with significant difference ( $|\text{fold change}| \geq 2$ ;  $P < 0.05$ ) between the SNRPA knockdown and negative control groups (Supplemental Figure S6A, B, <https://www.biosciencetrends.com/supplementaldata/253>). Moreover, RIP-sequencing with using anti-SNRPA antibody identified numerous putative SNRPA binding peaks in Huh-7 cells (Supplemental Figure S6C, D, <https://www.biosciencetrends.com/supplementaldata/253>). RIP-sequencing assay showed that on both single-transcript and whole-transcriptome levels, SNRPA always dominantly combined with the CDS zones (Supplemental Figure S6E, F, <https://www.biosciencetrends.com/supplementaldata/253>). This observation suggested that SNRPA plays an essential

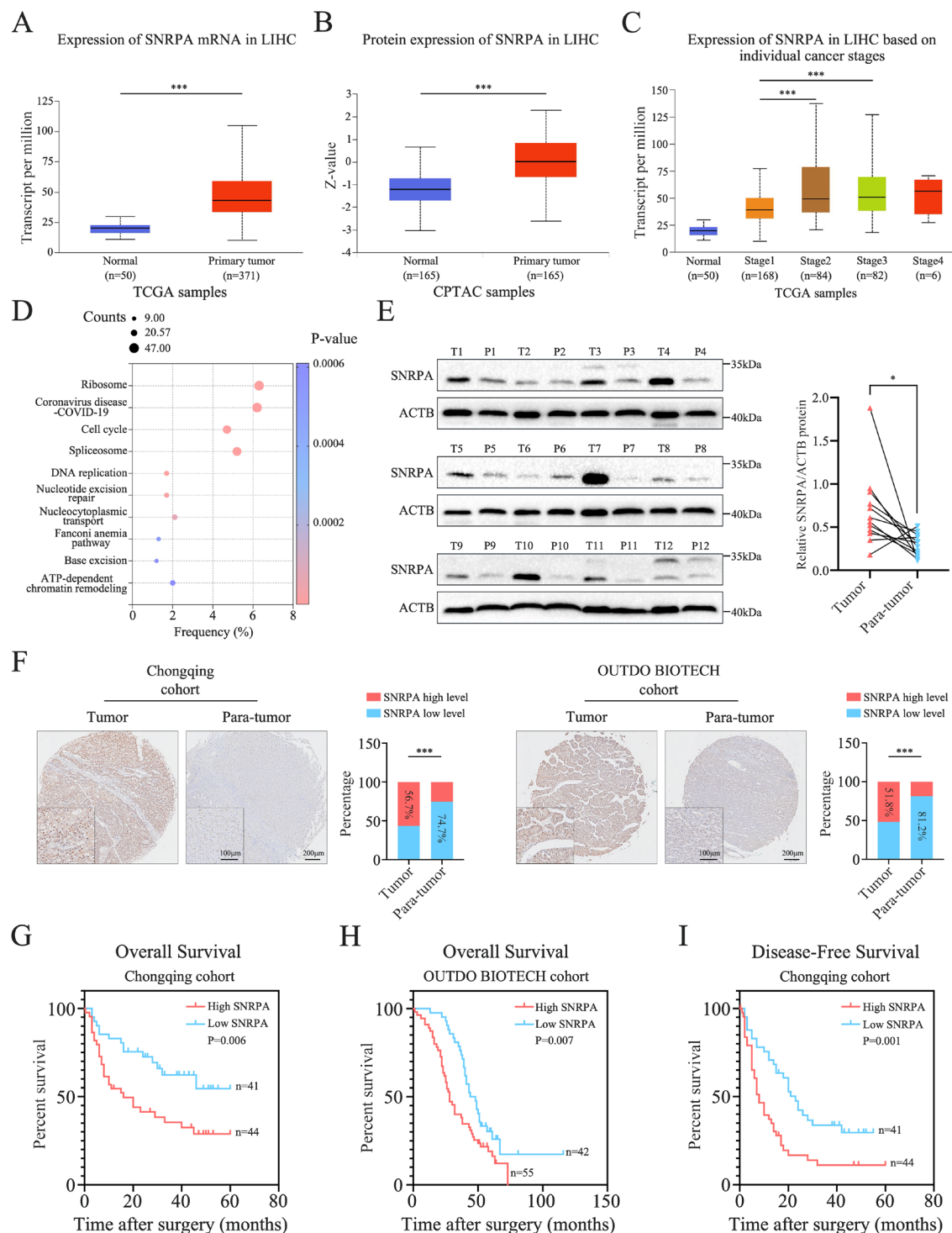


**Figure 1. SNRPA is frequently elevated in HCC tissues, which predicts a poor survival in HCC patients.** (A) UALCAN analysis of SNRPA mRNA levels in HCC tissues and normal liver tissues from TCGA samples. (B) SNRPA protein expression in HCC tissues and normal liver tissues from CPTAC samples acquired by UALCAN analysis. (C) UALCAN analysis showing SNRPA mRNA expression at different cancer stages. (D) Enriched KEGG pathways of SNRPA positively correlated genes acquired from DAVID analysis. (E) Western blot showing SNRPA levels in HCC tissues and matched para-tumor tissues. (F) IHC staining analysis of SNRPA expression in HCC tissues and paired para-tumor tissues from Chongqing (left panel) and OUTDO BIOTECH (right panel) cohorts. (G and H) Kaplan-Meier analysis showing the association between SNRPA levels and overall survival of HCC patients from Chongqing (G) and OUTDO BIOTECH (H) cohorts. (I) Kaplan-Meier analysis showing the correlation between SNRPA expression and disease-free survival of patients with HCC from Chongqing cohort. Continuous data were shown as the mean  $\pm$  standard deviation (SD). \* $P < 0.05$ , \*\*\* $P < 0.001$ .



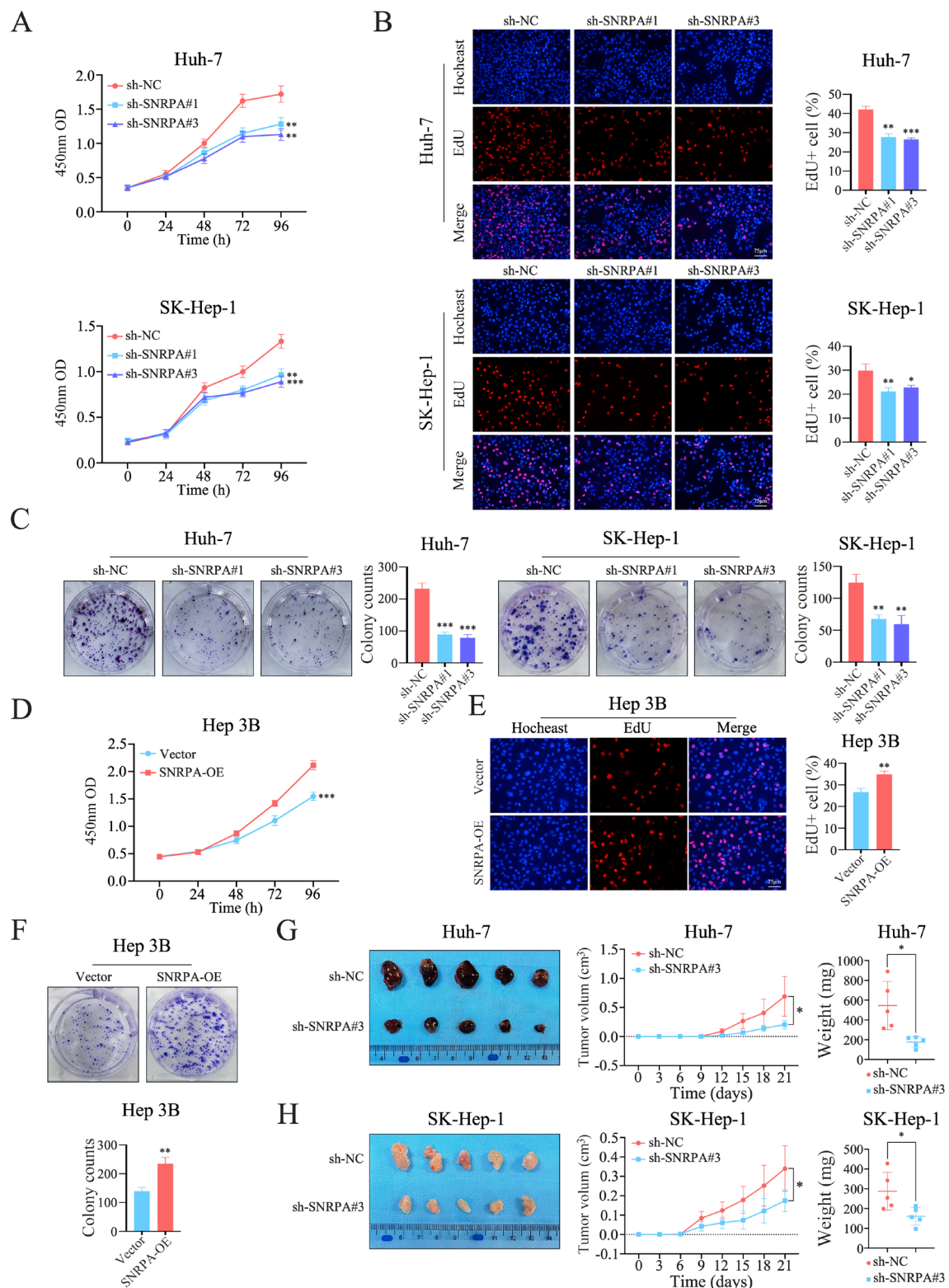


**Figure 2. SNRPA promotes HCC cell proliferation both *in vitro* and *in vivo*.** (A) CCK-8 test, (B) EdU staining, and (C) Colony formation assay to detect the proliferative ability of Huh-7 and SK-Hep-1 cells after SNRPA silencing. (D) CCK-8 assay, (E) EdU test, and (F) Colony formation assay to analyze Hep 3B cell proliferative activity after SNRPA overexpression. (G and H) Subcutaneous xenograft models of Huh-7 (G) and SK-Hep-1 (H) cells to assess the influence of SNRPA knockdown on tumor growth. Continuous data were presented as the mean  $\pm$  SD. \* $P$  < 0.05, \*\* $P$  < 0.01, \*\*\* $P$  < 0.001.

role in pre-mRNA splicing. Finally, we intersected the transcripts whose levels showed significant changes ( $|\text{fold change}| \geq 2$ ;  $P\text{-value} < 0.05$ ) after SNRPA knockdown according to nanopore full-length cDNA sequencing with the transcripts that were annotated by significantly enriched SNRPA binding peaks ( $\text{fold enrichment} \geq 5$ ;  $P < 0.05$ ) identified through RIP sequencing. Surprisingly, the ENST00000338965 transcript of the NCR3LG1 gene encoding B7-H6 protein was downregulated after SNRPA knockdown, and it combined directly with SNRPA (Figure 3A). It has been reported that B7-H6 promotes tumor growth, inhibits cell apoptosis, and accelerates G1-S transition in the cell cycle in several types of cancer, also including HCC among them; these effects are driven by ERK, AKT, and STAT3 signaling pathways (27, 31, 33). Subsequently, western blotting was performed to detect the B7-H6 related pathway activity after SNRPA silencing or overexpression in HCC cells. The results revealed that SNRPA knockdown decreased the B7-H6 expression, as well as the relative levels of phosphorylated-STAT3 (p-STAT3) and p-AKT in Huh-7 and SK-Hep-1 cells. In contrast, SNRPA overexpression significantly upregulated the B7-H6 expression and the phosphorylation levels of STAT3 and AKT in Hep 3B cells (Figure 3B). However, there were no apparent changes in relative p-ERK levels after SNRPA knockdown or overexpression (Figure 3B). Immunohistochemistry staining also showed that the levels of B7-H6, p-STAT3, and p-AKT were markedly decreased in xenograft tumor tissues from the SNRPA silencing groups compared with xenograft tumor tissues from the negative control groups (Supplemental Figure S7A, B, <https://www.biosciencetrends.com/supplementaldata/253>). Moreover, as demonstrated by flow cytometry assays, SNRPA knockdown blocked G1-S transition in the cell cycle and induced apoptosis in Huh-7 and SK-Hep1 cells (Figure 3C and Supplemental Figure S8, <https://www.biosciencetrends.com/supplementaldata/253>). In contrast, SNRPA overexpression promoted G1-S transition (Figure 3D) and inhibited the apoptosis in Hep 3B cells (Figure 3E). Western blotting showed that the levels of cyclin dependent kinase 4 (CDK4) and CDK6 were evidently declined after SNRPA silencing in Huh-7 and SK-Hep-1 cells. Meanwhile, the levels of cleaved-caspase3 in Huh-7 and SK-Hep-1 cells were markedly elevated after SNRPA silencing, whereas SNRPA overexpression in Hep 3B cells exerted an opposite effect (Figure 3F), which was consistent with the results from flow cytometry. However, downregulation or upregulation of SNRPA expression did not significantly alter the levels of cyclin D1 (CCND1) (Figure 3F). Taken together, it is possible that SNRPA promotes HCC cell proliferation *via* B7-H6-STAT3/AKT axis-mediated inhibition of apoptosis and promotion of G1-S transition in the cell cycle.

### 3.4. SNRPA facilitates B7-H6 pre-mRNA maturation *via* its intron 2 splicing.

We analyzed the underlying SNRPA-binding sequences within the B7-H6 pre-mRNA based on the RIP-sequencing data. The results showed that there were three significantly enriched SNRPA binding peaks on B7-H6 pre-mRNA, namely Peak 1, Peak 2, and Peak 3 (Figure 4A). In detail, Peak 1 spanned the whole intron 2 of B7-H6 pre-mRNA, whereas Peak 2 and Peak 3 were located on exon 5 (Figure 4A). Interestingly, between the Peak 2 and Peak 3 zones, B7-H6 pre-mRNA was alternatively spliced into two transcripts, namely variant 1, which encodes B7-H6 protein, and variant 2, which is eliminated *via* the nonsense-mediated decay pathway (Figure 4B). According to the location of SNRPA binding peaks on B7-H6 pre-mRNA, we formulated two hypotheses regarding the mechanism of SNRPA involved in elevating B7-H6 protein expression. Firstly, SNRPA promotes the B7-H6 pre-mRNA maturation by facilitating its intron 2 splicing to increase the B7-H6 protein levels; Secondly, SNRPA enhances the transformation of variant 2 to variant 1 of B7-H6 to upregulate its protein levels. To determine these hypotheses, we firstly precipitated the endogenous SNRPA protein in wild-type Huh-7 cells and exogenous SNRPA protein in SNRPA overexpression Hep 3B cells with using anti-SNRPA and anti-FLAG antibodies, respectively (Figure 4C). Subsequently, analysis of the immunoprecipitated RNA through RT-PCR with agarose gel electrophoresis and qRT-PCR showed that both endogenous and exogenous SNRPA protein could combine with Peak 1, Peak 2, and Peak 3 of B7-H6 pre-mRNA (Figure 4D, E). Finally, we designed four pairs of specific exon-exon and exon-intron junction primers to study the effect of SNRPA on B7-H6 pre-mRNA fate (Figure 4F). The qRT-PCR results showed that SNRPA silencing significantly decreased the levels of B7-H6 mature mRNA in both Huh-7 and SK-Hep-1 cells, while an opposite result was obtained in Hep 3B cells after SNRPA overexpression. Nevertheless, the B7-H6 pre-mRNA levels increased moderately in Huh-7 cells after SNRPA silencing; whereas, they remained stable in SK-Hep-1 cells after SNRPA knockdown and Hep 3B cells after SNRPA overexpression (Figure 4G and Supplemental Figure S9A, <https://www.biosciencetrends.com/supplementaldata/253>). Overall, the above data indicated that SNRPA promoted the transformation of B7-H6 pre-mRNA to mature mRNA; however, this effect only altered the levels of B7-H6 mature mRNA and did not change the pre-mRNA levels in SK-Hep-1 and Hep 3B cells. This was probably caused by the coupling of splicing and transcription (34) or pre-mRNA decay after a splicing defect (35). On the other hand, SNRPA knockdown in Huh-7 and SK-Hep-1 cells inhibited both the B7-H6 variant 1 and variant 2 mRNA expression, while SNRPA

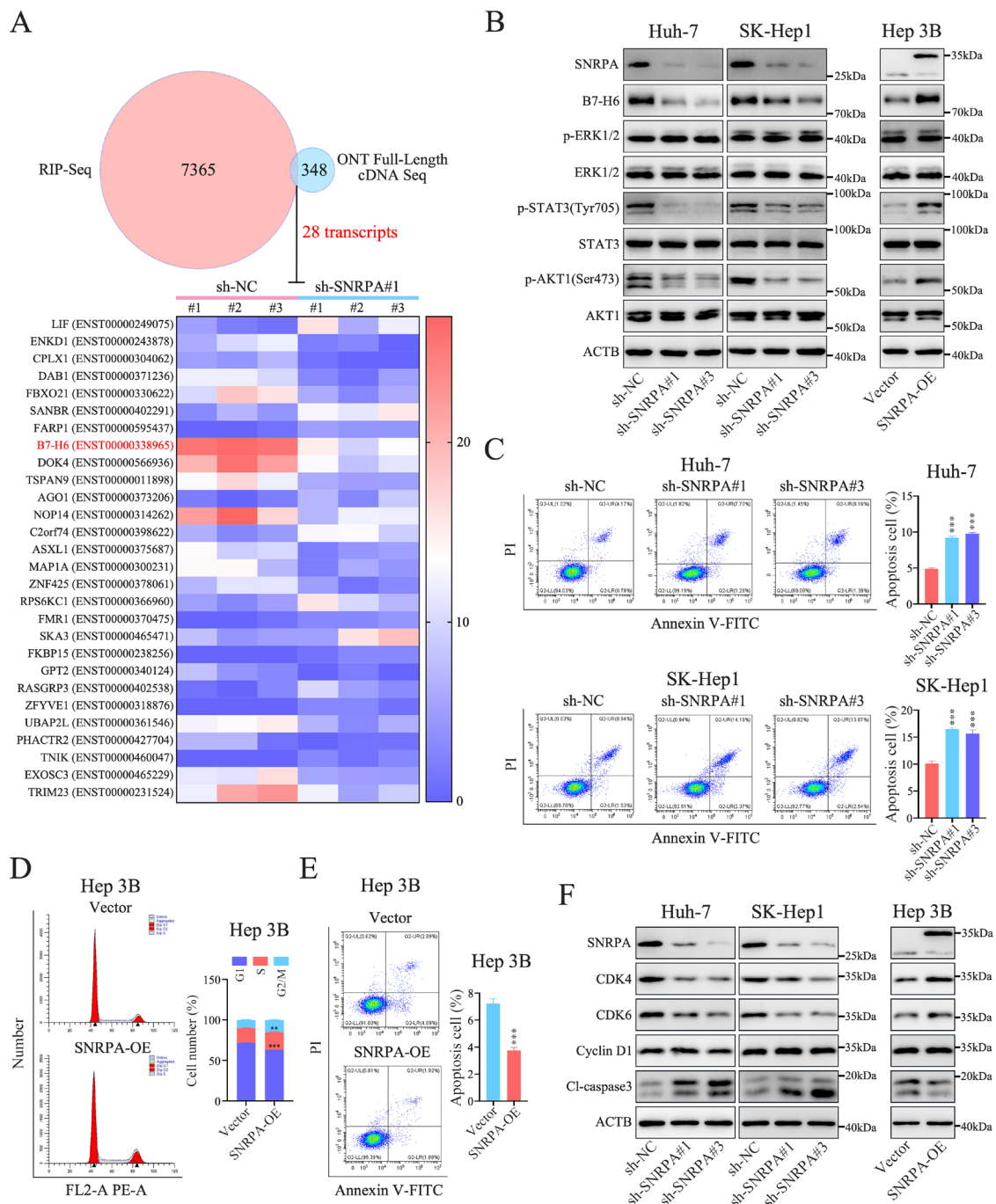


**Figure 3. SNRPA activates B7-H6-STAT3/AKT signaling pathways in HCC cells.** (A) Venn diagram and heatmap showing the intersection of transcripts whose levels changed significantly ( $|\text{fold change}| \geq 2$ ;  $P\text{-value} < 0.05$ ) after SNRPA knockdown according to nanopore full-length cDNA sequencing with transcripts annotated by significantly enriched SNRPA binding peaks (fold enrichment  $\geq 5$ ;  $P < 0.05$ ) identified through RIP sequencing. (B) Western blot to detect the effect of SNRPA on B7-H6-ERK/STAT3/AKT signaling pathways in HCC cells. (C) Flow cytometry analysis for cell apoptosis in Huh-7 and SK-Hep-1 cells after SNRPA silencing. (D and E) Flow cytometry analysis for the cell cycle (D) and apoptosis (E) in Hep 3B cells after SNRPA overexpression. (F) Western blot showing the affection of SNRPA on the cell cycle and apoptosis related gene expression in HCC cells. Continuous data were reported as the mean  $\pm$  SD. \*\* $P < 0.01$ , \*\*\* $P < 0.001$ .

overexpression had an opposite effect in Hep 3B cells (Figure 4H and Supplemental Figure S9B, <https://www.biosciencetrends.com/supplementaldata/253>). Collectively, the results above indicate that SNRPA increases B7-H6 protein levels in HCC cells at least in part by facilitating its pre-mRNA maturation *via* intron 2 splicing.

### 3.5. SNRPA enhances HCC cell resistance to lenvatinib.

The acquirement of resistance to TKIs in HCC treatment is partly due to the complementary activation of the STAT3 and AKT signaling pathways (36-38). Thus, we further investigated the impact of SNRPA on the sensitivity of HCC cells to lenvatinib. Using dose-



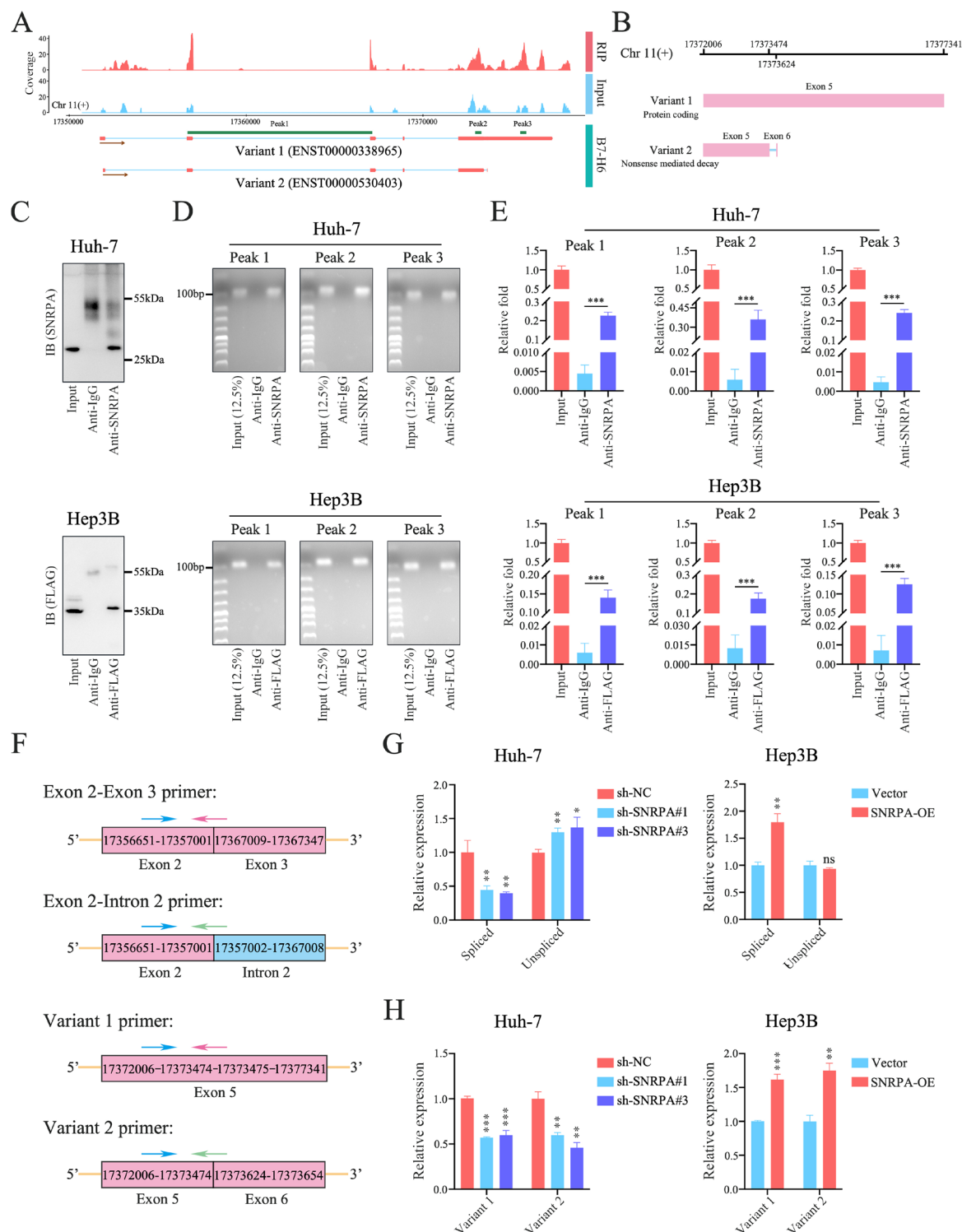


**Figure 4. SNRPA promotes B7-H6 pre-mRNA maturation via its intron 2 normal splicing.** (A) The coverage of SNRPA binding peak reads acquired from RIP-sequencing on B7-H6 transcripts. (B) The schematic representing alternative splicing modes of B7-H6 gene. (C) Western blot to detect the efficiency of SNRPA (upper panel) and FLAG (nether panel) immunoprecipitations. (D) RT-PCR with agarose gel electrophoresis assays to determine combining of endogenous (upper panel) and exogenous (nether panel) SNRPA with Peak 1, Peak 2, and Peak 3 of B7-H6 pre-mRNA. (E) qRT-PCR showing the binding of endogenous (upper panel) and exogenous (nether panel) SNRPA with Peak 1, Peak 2, and Peak 3 of B7-H6 pre-mRNA. (F) The schematic of specific primers to identify B7-H6 pre-mRNA or mature mRNA (upper panel), and B7-H6 variant 1 or variant 2 mRNA (nether panel). Specific primers represented by the two arrows, illustrating their approximate locations. (G) qRT-PCR to detect the B7-H6 pre-mRNA and mature mRNA levels in HCC cells after SNRPA knockdown or overexpression. (H) qRT-PCR to detect the B7-H6 variant 1 and variant 2 expression in HCC cells after SNRPA silencing or upregulating. Continuous data were demonstrated as the mean  $\pm$  SD. <sup>ns</sup>P > 0.05, \*P < 0.05, \*\*P < 0.01, \*\*\*P < 0.001.



response-inhibition test found that SNRPA knockdown significantly declined the IC<sub>50</sub> of SK-Hep-1 cells to lenvatinib, whereas SNRPA overexpression markedly elevated the IC<sub>50</sub> of Hep 3B cells to lenvatinib (Figure 5A). Consistently, colony formation assays showed that SNRPA silencing in SK-Hep-1 cells could enhance the inhibition of proliferation induced by treatment with lenvatinib, whereas SNRPA overexpression had an opposite effect in Hep 3B cells (Figure 5B). Moreover, as shown by flow cytometry assays, SNRPA silencing evidently aggravated the lenvatinib-induced apoptosis of SK-Hep-1 cells; in contrast, SNRPA upregulating in Hep 3B cells significantly relieved the apoptosis caused by treatment with lenvatinib (Figure 5C). Finally, xenograft models with treatment of lenvatinib found that SNRPA silencing could markedly enhance the sensitivity of SK-Hep-1 cells to lenvatinib *in vivo* (Figure 5D and Supplemental Figure S10, <https://www.biosciencetrends.com/supplementaldata/253>). Collectively, these results suggest that SNRPA induces HCC cell resistance to lenvatinib both *in vitro* and *in vivo*.

### 3.6. The effects of SNRPA on HCC cells relies on B7-H6-mediated activation of STAT3 and AKT.

We used RNAi to silence the expression of B7-H6 in Hep 3B cells and verified the silencing efficiency using western blotting (Figure 6A). As shown by CCK-8 and EdU assays, B7-H6 silencing significantly inhibited the proliferation of Hep 3B cells in the empty vector group and could abolish the proliferative ability enhanced by SNRPA overexpression in Hep 3B cells (Figure 6B, C). Similarly, the flow cytometry results demonstrated that B7-H6 silencing suppressed G1-S transition in the cell cycle and promoted apoptosis in the empty vector group Hep 3B cells. In addition, the promotion of G1-S transition in the cell cycle and inhibition of apoptosis in Hep 3B cells caused by SNRPA upregulating were partially offset by B7-H6 silencing (Figure 6D, E). Moreover, western blotting showed that B7-H6 silencing inhibited the phosphorylation of STAT3 and AKT, as well as the expression of CDK4 and CDK6 in empty vector group Hep 3B cells. However, Caspase3 activation in these cells was augmented after B7-H6 silencing. In addition, upregulation of p-STAT3, p-AKT, CDK4, and CDK6, as well as inhibition of Caspase3 activation resulted from SNRPA overexpression depended on B7-H6 expression (Figure 6F). Finally, the dose-response-inhibition test demonstrated that B7-H6 interference reversed lenvatinib resistance acquired by SNRPA overexpression in Hep 3B cells (Supplemental Figure S11, <https://www.biosciencetrends.com/supplementaldata/253>). Taken together, these results indicate that SNRPA promotes the proliferation and resistance to lenvatinib of HCC cells mainly through B7-H6-mediated activation of the STAT3 and AKT signaling pathways.

## 4. Discussion

Thus far, the number of available target therapeutics for HCC has been limited by an accumulative activation of multiple signaling pathways and reactivation of complementary signaling pathways (7,36). Increasing amount of evidence indicates that normal and abnormal pre-mRNA splicing participates in the tumor malignant process and the development of resistance to treatment (11,12,39). In this study, we revealed that the levels of splicing factor SNRPA were frequently elevated in HCC tissues; this increase was predictive of poor survival in patients with HCC. Additionally, SNRPA promoted HCC cell proliferation and resistance to lenvatinib. These findings suggested that SNRPA is an oncogene in HCC, as well as a potential target for therapy and overcoming resistance to lenvatinib in HCC patients.

Previous studies have demonstrated that SNRPA was upregulated in HCC tissues and promoted HCC cell metastasis *via* microvascular invasion (21,22). However, these investigations did not further explore the direct mechanism underlying the promotion of HCC progression by SNRPA through pre-mRNA splicing and the SNRPA resulting in development of resistance to treatment. Additionally, these studies did not employ sequencing to detect the transcript expression profile after SNRPA knockdown or overexpression. In the present study, utilizing nanopore full-length cDNA sequencing and RIP-sequencing assays, we hypothesized that SNRPA promotes HCC proliferation *via* B7-H6 pre-mRNA splicing. According to the sequences of B7-H6 pre-mRNA combined with SNRPA, we designed several pairs of specific exon-intron and exon-exon conjunction primers and performed qRT-PCR. The results revealed that SNRPA upregulated B7-H6 expression by promoting B7-H6 pre-mRNA maturation *via* its intron 2 normal splicing. Reports have shown that SNRPA more often upregulated the expression of transcripts directly bound by SNRPA on the whole-genome level; moreover, SNRPA promoted splicing at the 5' splice site in intron 5 of the mTOR gene to increase its expression (17,40), which further supported our results to a large extent. Additionally, owing to its superiority in detecting transcript levels compared with traditional sequencing (41,42), we utilized nanopore full-length cDNA sequencing to analyze changes in the SNRPA downstream targets. This is the first study exploring the mechanism through which SNRPA aggravates the malignant behaviors of HCC cells at the pre-mRNA splicing level.

Coded by the natural killer cell cytotoxicity receptor 3 ligand 1 (NCR3LG1) gene, B7-H6 protein contributes to tumor progression *via* its two extracellular immunoglobulin domains mediating immune escape (29,30). This was identified as the primary immunological mechanism underlying the involvement of B7-H6 in tumorigenesis. However, at the non-

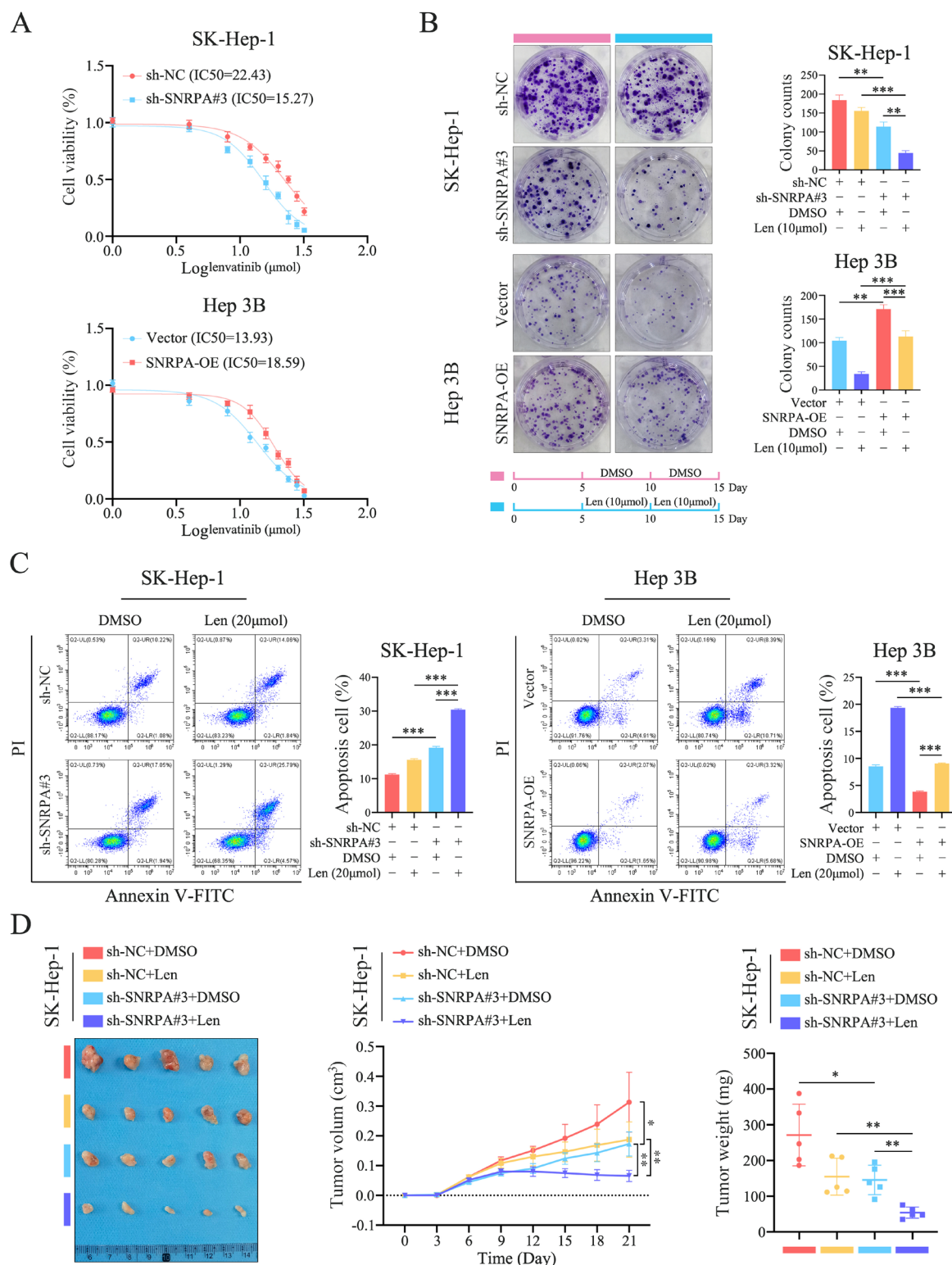


**Figure 5. SNRPA enhances HCC cell resistance to lenvatinib.** (A) The dose-response-inhibition curve of SK-Hep-1 cells after SNRPA knockdown (upper panel) and Hep 3B cells after SNRPA overexpression (nether panel) to lenvatinib. (B) Colony formation assay showing the effect of specific lenvatinib concentration on the proliferation of HCC cells after SNRPA silencing or upregulating. (C) Flow cytometry assay to detect the impact of specific lenvatinib concentration on apoptosis of HCC cells after SNRPA knockdown or overexpression. (D) Subcutaneous xenograft models of SK-Hep-1 cells to assess the affection of lenvatinib on HCC cell growth *in vivo* after SNRPA silencing. Continuous data were shown as the mean  $\pm$  SD. \* $P < 0.05$ , \*\* $P < 0.01$ , \*\*\* $P < 0.001$ .

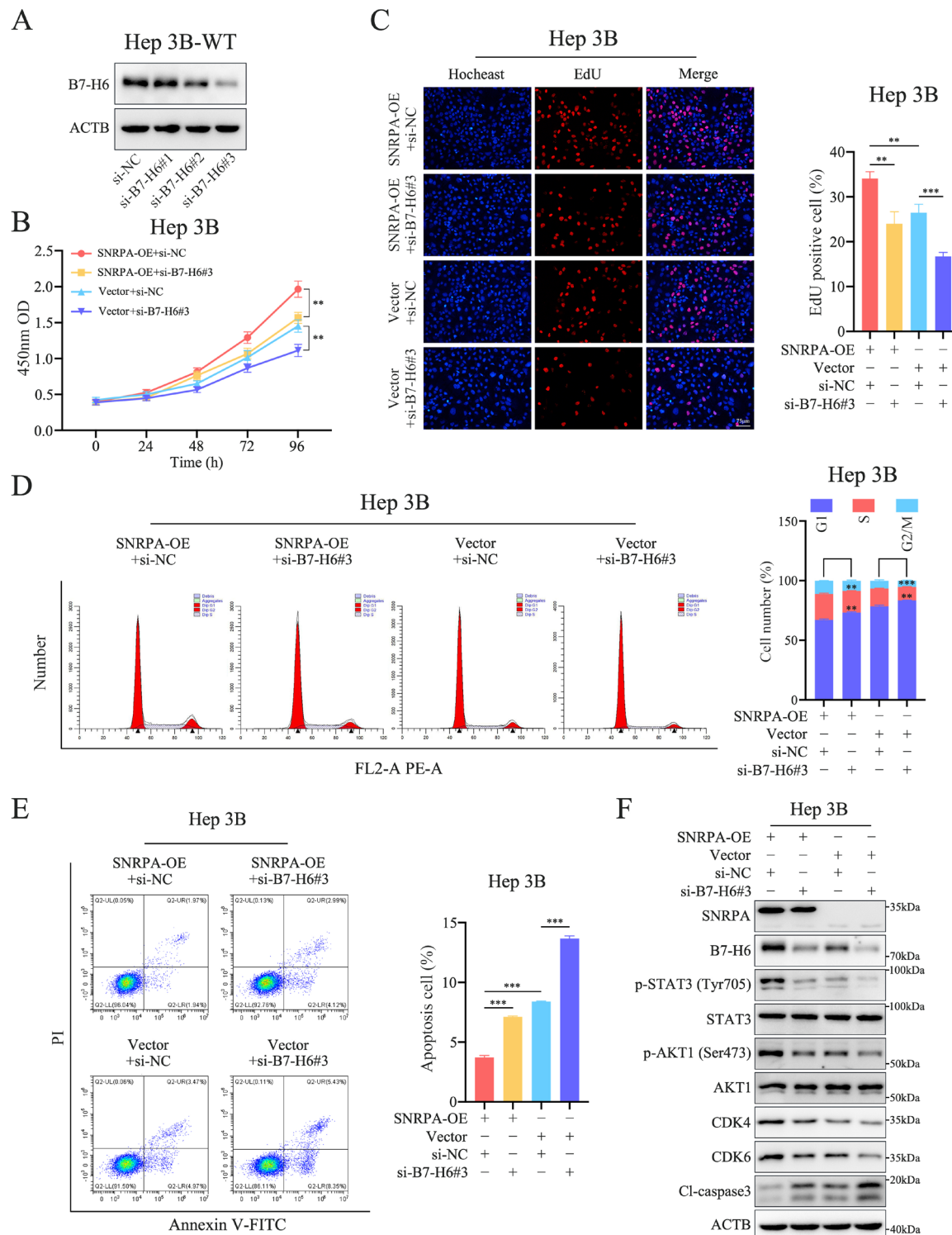


**Figure 6. SNRPA promotes HCC cell proliferation relying on B7-H6 expression.** (A) Western blot to detect the efficiency of B7-H6 interference in Hep 3B cells after treatment of siRNAs. (B) CCK-8 test, (C) EdU assay, (D) flow cytometry analysis for the cell cycle, and (E) flow cytometry analysis for cell apoptosis to determine the effect of SNRPA overexpression on proliferation, cell cycle, and apoptosis of Hep 3B cells in shortage of B7-H6. (F) Western blot to detect the impact of SNRPA upregulating on STAT3/AKT signaling pathway activation, as well as the cell cycle and apoptosis related gene expression of Hep 3B cells in context of B7-H6 interference. Continuous data were shown as the mean  $\pm$  SD. \*\* $P < 0.01$ , \*\*\* $P < 0.001$ .

immunological level, accumulating evidence revealed that B7-H6 activated the STAT3, AKT, and ERK signaling pathways in the development of cancer (27,31). This function may be associated with its ITIM/SH2/SH3

domains, which possess protein tyrosine kinase activity (23,43). Other studies showed that, by accelerating G1-S transition and inhibiting apoptosis, B7-H6 played an important role in the progression of several tumor types

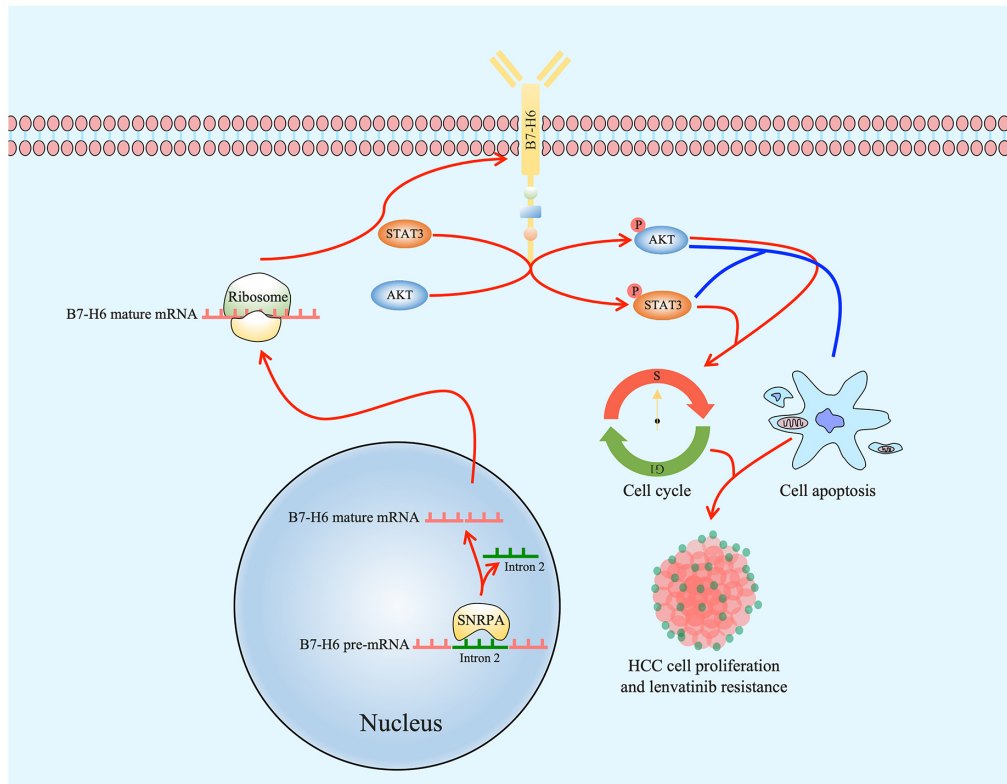


**Figure 7. Schematic depicting the molecular mechanism of SNRPA contributing to HCC progression.**

(32,44,45). In our study, B7-H6 only upregulated the phosphorylation levels of STAT3 and AKT, but not those of ERK, in HCC cells. B7-H6 was abundantly expressed in various tumor tissues, whereas it was rarely detected in normal tissues (23-26). It was previously revealed that, as an oncogene overexpressed in certain tumors, Myc transcriptionally drives B7-H6 expression in tumor cells (30). In addition, it was hypothesized that some post-transcriptional modifications, including ubiquitin or SUMOylation, may block B7-H6 expression in normal tissues by another study (46). Interestingly, our study is the first to demonstrate that B7-H6 pre-mRNA normal splicing is a mechanism involved in maintaining B7-H6 expression in tumor tissues. Notably, there is a lack of the full-length B7-H6 gene sequence and only a short region corresponding to the first exon of human B7-H6 in the mouse genome (23). Consequently, we did not further investigate the relationship of SNRPA with B7-H6 to promote tumorigenesis in a DEN/CCL4-induced mouse HCC model using a gene knockout technique.

Lenvatinib is currently the first-line treatment for patients with advanced HCC (47); however, according to clinical data, only a limited number of patients with HCC benefit from treatment with lenvatinib (48). This was attributed to extensive resistance to lenvatinib in patients with HCC, while the specific factors driving this resistance remain unclear to a large extent. Hu *et al.* revealed that epidermal growth factor receptor (EGFR) induced resistance to lenvatinib in HCC by STAT3-ATP

binding cassette subfamily B member 1 (STAT3-ABCB1) signaling (36). In addition, another study demonstrated that chromobox 1 (CBX1) increased resistance to TKIs (*i.e.*, sorafenib and lenvatinib) in HCC *via* the insulin like growth factor 1 receptor/AKT/SNAIL (IGF-1R/AKT/SNAIL) signaling axis (49). Collectively, the evidence indicated that the complementary reactivation of the STAT3 and AKT signaling pathways plays an essential role in the development of resistance to lenvatinib in patients with HCC. In the present study, we showed that SNRPA activated the STAT3 and AKT signaling pathways in HCC. Furthermore, pre-mRNA splicing has been identified as an important mechanism of resistance to therapy in cancer (50). Thus, we further explored whether SNRPA affected HCC cell resistance to lenvatinib. Based on *in vitro* and *in vivo* functional experiments, we showed that SNRPA induced significant resistance to lenvatinib in HCC cells. Our results suggested that pre-mRNA splicing is also involved in the development of HCC cell resistance to lenvatinib.

In conclusion, the present study revealed that SNRPA promotes HCC cell proliferation and resistance to lenvatinib. This effect is supported through the binding of SNRPA to B7-H6 pre-mRNA; this binding increases B7-H6 expression by facilitating B7-H6 pre-mRNA maturation *via* its intron 2 splicing and thus activating the STAT3 and AKT signaling pathways (Figure 7). These results indicate that SNRPA is a promising target for the treatment of HCC and overcoming resistance to



lenvatinib in patients with this disease.

**Funding:** This work was supported by the grant from Chongqing Natural Science Foundation (CSTB2024NSCQ-MSX0285).

**Conflict of Interest:** The authors have no conflicts of interest to disclose.

**Ethics approval and consent to participate:** This study was approved by Ethics Committee of the Second Affiliated Hospital of Chongqing Medical University (approval number RER2022-637A) and conformed to Helsinki Declaration. Additionally, the patients involved in this study provided their written informed consent. The animal study was approved by the Animal Ethics Committee of the Second Affiliated Hospital of Chongqing Medical University (approval number RER2021-136X).

**Availability of data and materials:** All original data can be available from the corresponding authors based on the reasonable request.

## References

- Sung H, Ferlay J, Siegel RL, Laversanne M, Soerjomataram I, Jemal A, Bray F. Global Cancer Statistics 2020: GLOBOCAN Estimates of Incidence and Mortality Worldwide for 36 Cancers in 185 Countries. *CA Cancer J Clin.* 2021; 71:209-249.
- Luo SY, Qin L, Qiu ZC, Xie F, Zhang Y, Yu Y, Leng SS, Wang ZX, Dai JL, Wen TF, Li C. Comparison of textbook outcomes between laparoscopic and open liver resection for patients with hepatocellular carcinoma: a multicenter study. *Surg Endosc.* 2025; 39:2052-2061.
- Wong LL, Landsittel DP, Kwee SA. Liver Transplantation vs Partial Hepatectomy for Stage T2 Multifocal Hepatocellular Carcinoma < 3 cm Without Vascular Invasion: A Propensity Score-Matched Survival Analysis. *J Am Coll Surg.* 2023; 237:568-577.
- Heumann P, Albert A, Gülow K, Tümen D, Müller M, Kandulski A. Insights in Molecular Therapies for Hepatocellular Carcinoma. *Cancers (Basel).* 2024; 16.
- Wen S, Zeng J, Zhong L, Ye J, Lai X. The efficacy and adverse effects of nivolumab and lenvatinib in the treatment of advanced hepatocellular carcinoma. *Cell Mol Biol (Noisy-le-grand).* 2022; 68:53-57.
- Shen Y, Zheng X, Qian Y, Liu M, Nian Z, Cui Q, Zhou Y, Fu B, Sun R, Tian Z, Wei H. Interactions between driver genes shape the signaling pathway landscape and direct hepatocellular carcinoma therapy. *Cancer Sci.* 2023; 114:2386-2399.
- Wang Y, Deng B. Hepatocellular carcinoma: molecular mechanism, targeted therapy, and biomarkers. *Cancer Metastasis Rev.* 2023; 42:629-652.
- Ghigna C, Paronetto MP. Alternative Splicing: Recent Insights into Mechanisms and Functional Roles. *Cells.* 2020; 9.
- Newman AJ. Pre-mRNA splicing. *Curr Opin Genet Dev.* 1994; 4:298-304.
- Wright CJ, Smith CWJ, Jiggins CD. Alternative splicing as a source of phenotypic diversity. *Nat Rev Genet.* 2022; 23:697-710.
- Li S, Chen Y, Xie Y, *et al.* FBXO7 Confers Mesenchymal Properties and Chemoresistance in Glioblastoma by Controlling Rbfox2-Mediated Alternative Splicing. *Adv Sci (Weinh).* 2023; 10:e2303561.
- Popli P, Richters MM, Chadchan SB, Kim TH, Tycksen E, Griffith O, Thaker PH, Griffith M, Kommagani R. Splicing factor SF3B1 promotes endometrial cancer progression *via* regulating KSR2 RNA maturation. *Cell Death Dis.* 2020; 11:842.
- Wang W, Lei Y, Zhang G, Li X, Yuan J, Li T, Zhong W, Zhang Y, Tan X, Song G. USP39 stabilizes  $\beta$ -catenin by deubiquitination and suppressing E3 ligase TRIM26 pre-mRNA maturation to promote HCC progression. *Cell Death Dis.* 2023; 14:63.
- Zhang W, Cao L, Yang J, *et al.* AEP-cleaved DDX3X induces alternative RNA splicing events to mediate cancer cell adaptation in harsh microenvironments. *J Clin Invest.* 2023; 134.
- Langemeier J, Radtke M, Böhne J. U1 snRNP-mediated poly(A) site suppression: beneficial and deleterious for mRNA fate. *RNA Biol.* 2013; 10:180-184.
- Ran Y, Deng Y, Yao C. U1 snRNP telescripting: molecular mechanisms and beyond. *RNA Biol.* 2021; 18:1512-1523.
- Rovira E, Moreno B, Razquin N, Hjerpe R, Gonzalez-Lopez M, Barrio R, Ruiz de Los Mozos I, Ule J, Pastor F, Blazquez L, Fortes P. U1A is a positive regulator of the expression of heterologous and cellular genes involved in cell proliferation and migration. *Mol Ther Nucleic Acids.* 2022; 28:831-846.
- Bolduc F, Turcotte MA, Perreault JP. The Small Nuclear Ribonucleoprotein Polypeptide A (SNRPA) binds to the G-quadruplex of the BAG-1 5'UTR. *Biochimie.* 2020; 176:122-127.
- Dou N, Yang D, Yu S, Wu B, Gao Y, Li Y. SNRPA enhances tumour cell growth in gastric cancer through modulating NGF expression. *Cell Prolif.* 2018; 51:e12484.
- Liu J, Li J, Su Y, Ma Z, Yu S, He Y. Circ\_0009910 Serves as miR-361-3p Sponge to Promote the Proliferation, Metastasis, and Glycolysis of Gastric Cancer *via* Regulating SNRPA. *Biochem Genet.* 2022; 60:1809-1824.
- Zhang Y, Wang X, Wang H, Jiang Y, Xu Z, Luo L. Elevated Small Nuclear Ribonucleoprotein Polypeptide an Expression Correlated With Poor Prognosis and Immune Infiltrates in Patients With Hepatocellular Carcinoma. *Front Oncol.* 2022; 12:893107.
- Mo Z, Li R, Cao C, Li Y, Zheng S, Wu R, Xue J, Hu J, Meng H, Zhai H, Huang W, Zheng F, Zhou B. Splicing factor SNRPA associated with microvascular invasion promotes hepatocellular carcinoma metastasis through activating NOTCH1/Snail pathway and is mediated by circSEC62/miR-625-5p axis. *Environ Toxicol.* 2023; 38:1022-1037.
- Brandt CS, Baratin M, Yi EC, *et al.* The B7 family member B7-H6 is a tumor cell ligand for the activating natural killer cell receptor NKp30 in humans. *J Exp Med.* 2009; 206:1495-1503.
- Mohammadi A, Najafi S, Amini M, Mansoori B, Baghbanzadeh A, Hoheisel JD, Baradaran B. The potential of B7-H6 as a therapeutic target in cancer immunotherapy. *Life Sci.* 2022; 304:120709.
- Cherif B, Triki H, Charfi S, Bouzidi L, Kridis WB, Khanfir A, Chaabane K, Sellami-Boudawara T, Rebai

- A. Immune checkpoint molecules B7-H6 and PD-L1 co-pattern the tumor inflammatory microenvironment in human breast cancer. *Sci Rep.* 2021; 11:7550.
26. Li D, Xiang S, Shen J, *et al.* Comprehensive understanding of B7 family in gastric cancer: expression profile, association with clinicopathological parameters and downstream targets. *Int J Biol Sci.* 2020; 16:568-582.
27. Li YM, Liu ZY, Li ZC, Wang JC, Yu JM, Yang HJ, Chen ZN, Tang J. Alterations of the Immunologic Co-Stimulator B7 and TNFR Families Correlate with Hepatocellular Carcinoma Prognosis and Metastasis by Inactivating STAT3. *Int J Mol Sci.* 2019; 20.
28. Ni L, Dong C. New B7 Family Checkpoints in Human Cancers. *Mol Cancer Ther.* 2017; 16:1203-1211.
29. Pesce S, Tabellini G, Cantoni C, Patrizi O, Coltrini D, Rampinelli F, Matta J, Vivier E, Moretta A, Parolini S, Marcenaro E. B7-H6-mediated downregulation of Nkp30 in NK cells contributes to ovarian carcinoma immune escape. *Oncoimmunology.* 2015; 4:e1001224.
30. Textor S, Bossler F, Henrich KO, Gartlgruber M, Pollmann J, Fiegler N, Arnold A, Westermann F, Waldburger N, Breuhahn K, Golfier S, Witzens-Harig M, Cerwenka A. The proto-oncogene Myc drives expression of the NK cell-activating Nkp30 ligand B7-H6 in tumor cells. *Oncoimmunology.* 2016; 5:e116674.
31. Chen H, Guo Y, Sun J, Dong J, Bao Q, Zhang X, Fu F. Preferential Expression of B7-H6 in Glioma Stem-Like Cells Enhances Tumor Cell Proliferation *via* the c-Myc/RNMT Axis. *J Immunol Res.* 2020; 2020:2328675.
32. Wu F, Wang J, Ke X. Knockdown of B7-H6 inhibits tumor progression and enhances chemosensitivity in B-cell non-Hodgkin lymphoma. *Int J Oncol.* 2016; 48:1561-1570.
33. Yang S, Yuan L, Wang Y, Zhu M, Wang J, Ke X. B7-H6 Promotes Cell Proliferation, Migration and Invasion of Non-Hodgkin Lymphoma *via* Ras/MEK/ERK Pathway Based on Quantitative Phosphoproteomics Data. *Onco Targets Ther.* 2020; 13:5795-5805.
34. Tellier M, Maudlin I, Murphy S. Transcription and splicing: A two-way street. *Wiley Interdiscip Rev RNA.* 2020; 11:e1593.
35. Izumikawa K, Yoshikawa H, Ishikawa H, Nobe Y, Yamauchi Y, Philipsen S, Simpson RJ, Isobe T, Takahashi N. Chtop (Chromatin target of Prmt1) auto-regulates its expression level *via* intron retention and nonsense-mediated decay of its own mRNA. *Nucleic Acids Res.* 2016; 44:9847-9859.
36. Hu B, Zou T, Qin W, *et al.* Inhibition of EGFR Overcomes Acquired Lenvatinib Resistance Driven by STAT3-ABCB1 Signaling in Hepatocellular Carcinoma. *Cancer Res.* 2022; 82:3845-3857.
37. Miyazaki K, Morine Y, Xu C, Nakasu C, Wada Y, Teraoku H, Yamada S, Saito Y, Ikemoto T, Shimada M, Goel A. Curcumin-Mediated Resistance to Lenvatinib *via* EGFR Signaling Pathway in Hepatocellular Carcinoma. *Cells.* 2023; 12.
38. Tsuchiya H, Shinonaga R, Sakaguchi H, Kitagawa Y, Yoshida K. NEAT1-SOD2 Axis Confers Sorafenib and Lenvatinib Resistance by Activating AKT in Liver Cancer Cell Lines. *Curr Issues Mol Biol.* 2023; 45:1073-1085.
39. Zhou HZ, Li F, Cheng ST, Xu Y, Deng HJ, Gu DY, Wang J, Chen WX, Zhou YJ, Yang ML, Ren JH, Zheng L, Huang AL, Chen J. DDX17-regulated alternative splicing that produced an oncogenic isoform of PXN-AS1 to promote HCC metastasis. *Hepatology.* 2022; 75:847-865.
40. Subramania S, Gagné LM, Campagne S, Fort V, O'Sullivan J, Mocaer K, Feldmüller M, Masson JY, Allain FHT, Hussein SM, Huot M. SAM68 interaction with U1A modulates U1 snRNP recruitment and regulates mTor pre-mRNA splicing. *Nucleic Acids Res.* 2019; 47:4181-4197.
41. Cao J, Routh AL, Kuyumcu-Martinez MN. Nanopore sequencing reveals full-length Tropomyosin 1 isoforms and their regulation by RNA-binding proteins during rat heart development. *J Cell Mol Med.* 2021; 25:8352-8362.
42. Xie S, Leung AW, Zheng Z, Zhang D, Xiao C, Luo R, Luo M, Zhang S. Applications and potentials of nanopore sequencing in the (epi)genome and (epi)transcriptome era. *Innovation (Camb).* 2021; 2:100153.
43. Flajnik MF, Tlapakova T, Criscitiello MF, Krylov V, Ohta Y. Evolution of the B7 family: co-evolution of B7H6 and Nkp30, identification of a new B7 family member, B7H7, and of B7's historical relationship with the MHC. *Immunogenetics.* 2012; 64:571-590.
44. Guo R, Liu G, Li C, Liu X, Xu Y, Yang W, Wang F. B7 homolog 6 promotes the progression of cervical cancer. *Exp Ther Med.* 2021; 22:774.
45. Jiang T, Wu W, Zhang H, Zhang X, Zhang D, Wang Q, Huang L, Wang Y, Hang C. High expression of B7-H6 in human glioma tissues promotes tumor progression. *Oncotarget.* 2017; 8:37435-37447.
46. Hu Y, Zeng T, Xiao Z, Hu Q, Li Y, Tan X, Yue H, Wang W, Tan H, Zou J. Immunological role and underlying mechanisms of B7-H6 in tumorigenesis. *Clin Chim Acta.* 2020; 502:191-198.
47. Vogel A, Martinelli E. Updated treatment recommendations for hepatocellular carcinoma (HCC) from the ESMO Clinical Practice Guidelines. *Ann Oncol.* 2021; 32:801-805.
48. Kudo M, Finn RS, Qin S, *et al.* Lenvatinib versus sorafenib in first-line treatment of patients with unresectable hepatocellular carcinoma: a randomised phase 3 non-inferiority trial. *Lancet.* 2018; 391:1163-1173.
49. Zheng SS, Wu JF, Wu WX, Hu JW, Zhang D, Huang C, Zhang BH. CBX1 is involved in hepatocellular carcinoma progression and resistance to sorafenib and lenvatinib *via* IGF-1R/AKT/SNAI1 signaling pathway. *Hepatol Int.* 2024.
50. Aya F, Lanuza-Gracia P, González-Pérez A, Bonnal S, Mancini E, López-Bigas N, Arance A, Valcárcel J. Genomic deletions explain the generation of alternative BRAF isoforms conferring resistance to MAPK inhibitors in melanoma. *Cell Rep.* 2024; 43:114048.

Received February 5, 2025; Revised March 21, 2025; Accepted April 11, 2025.

§These authors contributed equally to this work.

\*Address correspondence to:

Jianping Gong and Guochao Zhong, Department of Hepatobiliary surgery, The Second Affiliated Hospital of Chongqing Medical University, 74 Linjiang Road, Yuzhong District, Chongqing 400010, China.  
E-mail: 300381@hospital.cqmu.edu.cn (GJ); gczhong1991@hospital.cqmu.edu.cn (GZ)

Released online in J-STAGE as advance publication April 15, 2025.

# Platelet count as a double-edged sword: The impact of thrombocytosis and thrombocytopenia on long-term outcomes after hepatic resection for hepatocellular carcinoma

Xuedong Wang<sup>1,§</sup>, Pengfei Wang<sup>1,§</sup>, Bingjun Tang<sup>1,§</sup>, Jiahao Xu<sup>2,§</sup>, Baidong Wang<sup>2,§</sup>, Lihui Gu<sup>2</sup>, Yingjian Liang<sup>3</sup>, Hongwei Guo<sup>4</sup>, Han Liu<sup>5</sup>, Yifan Wu<sup>6</sup>, Hong Wang<sup>7</sup>, Yahao Zhou<sup>8</sup>, Yongyi Zeng<sup>9</sup>, Yongkang Diao<sup>2</sup>, Lanqing Yao<sup>2</sup>, Mingda Wang<sup>2</sup>, Chao Li<sup>2</sup>, Timothy M. Pawlik<sup>10</sup>, Feng Shen<sup>1</sup>, Lei Cai<sup>11</sup>, Tian Yang<sup>1,2,\*</sup>

<sup>1</sup> Hepatopancreatobiliary Center, Beijing Tsinghua Changgung Hospital, Tsinghua University, Beijing, China;

<sup>2</sup> Department of Hepatobiliary Surgery, Eastern Hepatobiliary Surgery Hospital, Naval Medical University, Shanghai, China;

<sup>3</sup> Department of Hepatobiliary Surgery, First Affiliated Hospital of Harbin Medical University, Harbin, China;

<sup>4</sup> The 2nd Department of General Surgery, The Second People's Hospital of Changzhi, Changzhi, China;

<sup>5</sup> Department of Hepatobiliary and Pancreatic Surgery, General Surgery Center, First Hospital of Jilin University, Changchun, China;

<sup>6</sup> Department of Hepatobiliary Surgery, Affiliated Hospital of Nantong University, Nantong, China;

<sup>7</sup> Department of General Surgery, Liuyang People's Hospital, Liuyang, China;

<sup>8</sup> Department of Hepatobiliary Surgery, Pu'er People's Hospital, Pu'er, China;

<sup>9</sup> Department of Hepatobiliary Surgery, Mengchao Hepatobiliary Hospital of Fujian Medical University, Fuzhou, China;

<sup>10</sup> Department of Surgery, Ohio State University, Wexner Medical Center, Columbus, OH, USA;

<sup>11</sup> Institute of Hepatopancreatobiliary Surgery, Chongqing General Hospital, Chongqing University, Chongqing, China.

**SUMMARY:** The prognostic significance of preoperative platelet counts among patients with hepatocellular carcinoma (HCC) undergoing curative resection remains controversial. The objective of the current study was to investigate the impact of preoperative platelet count on long-term outcomes after HCC resection. Patients who underwent curative-intent resection for HCC between 2000 and 2021 at 10 hepatobiliary centers in China were retrospectively analyzed. Patients were categorized based on platelet count within 2 weeks before surgery: thrombocytopenia ( $< 100 \times 10^9/L$ ), normal platelet count ( $100-299 \times 10^9/L$ ), and thrombocytosis ( $\geq 300 \times 10^9/L$ ). The primary outcomes were overall survival (OS) and recurrence-free survival (RFS). Among 3,116 patients, 655 (21.0%) had thrombocytopenia, 2,374 (76.2%) had normal platelet counts, and 87 (2.8%) had thrombocytosis. The 5-year OS was 52.7%, 56.0%, and 40.2% for thrombocytopenia, normal platelet count, and thrombocytosis groups, respectively ( $p < 0.001$  among the three groups); the corresponding 5-year RFS was 39.3%, 39.3%, and 26.9%, respectively ( $p = 0.001$  among the three groups). Multivariable analysis identified both thrombocytopenia (HR 1.215, 95% CI 1.045-1.413,  $p = 0.011$ ) and thrombocytosis (HR 1.307, 95% CI 1.130-1.511,  $p < 0.001$ ) as independent risk factors for worse OS, and thrombocytosis was independently associated with worse RFS (HR 1.523, 95% CI 1.196-1.939,  $p = 0.001$ ). Both thrombocytopenia and thrombocytosis were associated with worse survival after HCC resection, with thrombocytosis also predicting higher risk of recurrence. Routine preoperative platelet count may serve as a valuable and practical prognostic marker for risk stratification among patients with HCC undergoing resection.

**Keywords:** hepatocellular carcinoma, hepatectomy, platelet, thrombocytosis, thrombocytopenia, recurrence

## 1. Introduction

Hepatocellular carcinoma (HCC) remains a significant global health burden, ranking as the sixth most common cancer and the third leading cause of cancer-related deaths worldwide (1,2). Despite recent advances in diagnostic and therapeutic strategies, the prognosis for HCC remains poor, with a 5-year survival rate of only

18% (3,4). Although curative resection is the primary treatment for patients with localized HCC, long-term outcomes remain unsatisfactory, with 5-year recurrence rates exceeding 50% (5-11). Identifying prognostic factors is crucial to improve patient selection, optimize perioperative management, and guide postoperative surveillance.

The complex interplay between HCC and the

hematologic system, particularly the role of platelets, has gained increasing attention in recent years (12,13). Platelets, traditionally recognized for their crucial role in hemostasis, are now understood to be active participants in tumor biology, influencing processes such as angiogenesis, immune modulation, and metastasis (14-17). Among patients with chronic liver disease, thrombocytopenia is common due to portal hypertension, hypersplenism, and decreased thrombopoietin production (17-20). In contrast, thrombocytosis can occur in various malignancies, including HCC, as a paraneoplastic phenomenon (21,22).

The prognostic significance of platelet count among patients with HCC undergoing curative resection remains controversial. Several studies have reported associations between thrombocytopenia and poor outcomes related to HCC, while the impact of thrombocytosis on HCC prognosis has been less extensively studied (23-26). These conflicting results may be attributed to differences in study populations, sample sizes, and definitions of thrombocytopenia and thrombocytosis. A meta-analysis of 15 studies noted that thrombocytopenia was associated with worse overall and disease-free survival among patients with HCC undergoing various treatments (27). The mechanisms underlying this association may include impaired liver regeneration, compromised immune function, and increased perioperative complications (28). Some reports have suggested that thrombocytosis may be an adverse prognostic factor relative to HCC (29-32), while other studies have failed to demonstrate a significant impact on long-term survival (33,34). These conflicting results may be attributed to differences in study populations, sample sizes, and definitions of thrombocytopenia and thrombocytosis.

To reconcile these conflicting findings and address existing knowledge gaps, this study aims to systematically investigate the impact of preoperative platelet levels on long-term outcomes following curative resection of HCC. It was hypothesized that both thrombocytopenia and thrombocytosis would be associated with worse survival and a higher incidence of recurrence. Considering the routine availability of platelet count as part of standard laboratory testing, our findings could have important clinical implications for preoperative risk stratification, perioperative management, and tailoring postoperative surveillance strategies in HCC patients undergoing curative resection.

## 2. Patients and Methods

### 2.1. Study design and patient population

This retrospective, multicentre cohort study included patients who underwent curative resection for initially diagnosed HCC between January 2000 and December 2021 at 10 hepatobiliary centres in China. The study protocol was approved by the institutional review board

of each participating center, and the requirement for informed consent was waived due to the retrospective nature of the study. Inclusion criteria were: *i*) age  $\geq 18$  years; *ii*) histologically confirmed HCC; *iii*) curative resection with clear surgical margins (R0 resection); and *iv*) available preoperative platelet count data. Exclusion criteria were: *i*) extrahepatic metastasis; *ii*) prior local or systemic HCC treatment; *iii*) history of other malignancies; *iv*) incomplete clinical data or follow-up information; and *v*) perioperative mortality (death within 30 days after surgery).

### 2.2. Data collection and definitions

Demographic, clinical, laboratory, and pathological data were collected from electronic medical records. Preoperative platelet count was defined as the last value obtained within 2 weeks before surgery. As such, patients were categorized into three groups based on platelet count: thrombocytopenia, normal platelet count, and thrombocytosis. In China, almost all of hospitals routinely classify platelet counts  $< 100 \times 10^9/L$  as thrombocytopenia and  $\geq 300 \times 10^9/L$  as thrombocytosis, reflecting local laboratory reference ranges and prior studies in Chinese HCC cohorts (20,29,35,36). Liver function was assessed using the Child-Pugh classification. Tumor characteristics, including size, number, differentiation, and macrovascular and microvascular invasion were determined by pathological examination. Cirrhosis was diagnosed based on histological findings or unequivocal clinical and radiological evidence.

### 2.3. Surgical procedures

All patients underwent curative resection with the goal of complete tumor removal and preservation of adequate future liver remnant. The choice of surgical approach (open or laparoscopic) and extent of resection (anatomical or non-anatomical) was at the discretion of the treating surgeon. Intraoperative ultrasound was routinely used to guide resection. Major hepatectomy was defined as resection of three or more Couinaud segments (37). Perioperative management, including the use of blood products, was performed according to each center's standard protocols.

### 2.4. Follow-up and outcome measures

Postoperative follow-up included physical examination, liver function tests, serum alpha-fetoprotein (AFP), and imaging studies (contrast-enhanced CT or MRI) every 3 months for the first 2 years, and then every 6 months thereafter. Recurrence was diagnosed based on typical imaging findings or histological confirmation when indicated. Treatment for recurrence was determined by a multidisciplinary team, considering tumor characteristics,



liver function, and patient preferences.

The primary outcome measures were overall survival (OS) and recurrence-free survival (RFS). OS was defined as the interval between the date of surgery and the date of death from any cause or last follow-up. RFS was calculated from the date of surgery to the date of first recurrence or last follow-up for recurrence-free patients. Patients who died without documented recurrence were censored at the date of death for RFS analysis.

## 2.5. Statistical analysis

Continuous variables were expressed as median (interquartile range) and compared using the Kruskal-Wallis test. Categorical variables were presented as numbers (percentages) and compared using the chi-square test or Fisher's exact test as appropriate. Survival curves were generated using the Kaplan-Meier method and compared using the log-rank test. Univariable and multivariable Cox proportional hazards models were used to identify factors associated with OS and RFS. Variables with  $p < 0.1$  in univariable analysis were included in the multivariable model. Additionally, preoperative platelet count categories (thrombocytopenia and thrombocytosis) were included in all multivariable models regardless of univariable  $P$  values as they were the primary exposure variables of interest in our study hypothesis, following standard epidemiological practice for analysing pre-specified predictors. Hazard ratios (HRs) with 95% confidence intervals (CIs) were calculated. All statistical analyses were performed using R version 4.1.0 (R Foundation for Statistical Computing, Vienna, Austria) and SPSS version 25.0 (IBM Corp., Armonk, NY, USA). A two-sided  $p < 0.05$  was considered statistically significant.

## 3. Results

### 3.1. Patient characteristics

A total of 3,116 patients were included in the final analysis (Figure 1). None of the included patients had undergone prior splenectomy, received aspirin or other antiplatelet therapy, or had platelet transfusion within two weeks before surgery. Median age was 52 years (IQR 44-60), and 2,728 (87.5%) were male. Hepatitis B virus (HBV) infection was the predominant etiology, which was present in 2,648 (85.0%) patients. Cirrhosis was diagnosed in 2,264 (72.7%) patients. Based on preoperative platelet count, there were 655 (21.0%) patients with thrombocytopenia, 2,374 (76.2%) with normal platelet count, and 87 (2.8%) with thrombocytosis.

The baseline characteristics of the three groups are summarized in Table 1. Patients with thrombocytopenia were more likely to have cirrhosis (92.4% vs. 68.1% vs. 49.4%,  $p < 0.001$ ), worse liver function (Child-Pugh class B: 16.6% vs. 6.1% vs. 10.3%,  $p < 0.001$ ), smaller tumors ( $\leq 5.0$  cm: 66.1% vs. 47.0% vs. 21.4%,  $p < 0.001$ ), and multiple tumors (54.0% vs. 44.0% vs. 36.8%,  $p < 0.001$ ). In contrast, patients with thrombocytosis had larger tumors ( $> 5.0$  cm: 78.6% vs. 53.0% vs. 33.9%,  $p < 0.001$ ), incomplete tumor encapsulation (70.1% vs. 59.7% vs. 54.7%,  $p = 0.007$ ), and were more likely to undergo intraoperative blood transfusion (32.2% vs. 15.2% vs. 19.4%,  $p < 0.001$ ) and major hepatectomy (47.1% vs. 22.6% vs. 11.5%,  $p < 0.001$ ).

### 3.2. Long-term outcomes

The median follow-up time was 50.3 months (IQR 22.0-

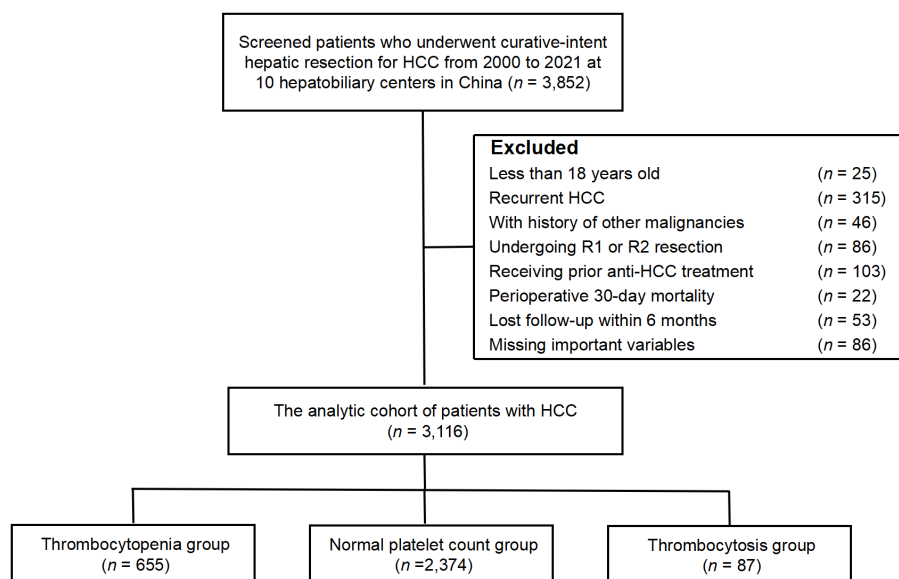


Figure 1. Flow diagram of patient selection. HCC, hepatocellular carcinoma.

65.0). During the study period, 1,565 (50.2%) patients died, and 1,895 (60.8%) experienced recurrence (Table 2). Analysis of mortality causes revealed differences between groups. In the thrombocytopenia group, a higher proportion of non-cancer deaths was observed (11.3%) compared to the normal platelet count (5.7%) and thrombocytosis groups (6.9%), with liver failure and upper gastrointestinal bleeding being the predominant non-cancer causes. The 1-, 3-, and 5-year OS for the entire cohort was 85.0%, 66.1%, and 54.9%, respectively.

Kaplan-Meier analysis demonstrated differences in OS among the three platelet count groups (Figure 2). Meanwhile, 5-year OS was 52.7%, 56.0%, and 40.2% among patients with thrombocytopenia, normal platelet count, and thrombocytosis, respectively ( $p < 0.001$ ).

The 1-, 3-, and 5-year RFS for the entire cohort was 66.1%, 47.9%, and 39.0%, respectively. Of note, RFS differed among the three groups, with 5-year recurrence-free being 39.3%, 39.3%, and 26.9% for the thrombocytopenia, normal platelet count, and

**Table 1. Baseline characteristics of patients according to preoperative platelet count**

| <i>n</i> (%)                       | Normal platelet count group<br>( <i>n</i> = 2,374) | Thrombocytopenia group<br>( <i>n</i> = 655) | Thrombocytosis group<br>( <i>n</i> = 87) | <i>p</i> among three groups |
|------------------------------------|--|---|--|-----------------------------|
| Male sex                           | 2,086 (87.9)                                       | 567 (86.6)                                  | 75 (86.2)                                | 0.622                       |
| Age > 65 years                     | 352 (14.8)   | 76 (11.6)                                   | 13 (14.9)                                | 0.109                       |
| Diabetes mellitus                  | 175 (7.4)  | 68 (10.4)                                   | 6 (6.9)                                  | 0.039                       |
| HBV (+)                            | 1,975 (83.2)                                       | 604 (92.2)                                  | 69 (79.3)                                | < 0.001                     |
| HCV (+)                            | 59 (2.5)   | 23 (3.5)                                    | 0 (0)                                    | 0.104                       |
| ASA score > 2                      | 336 (14.2)   | 83 (12.7)                                   | 18 (20.7)                                | 0.121                       |
| Cirrhosis                          | 1,616 (68.1)                                       | 605 (92.4)                                  | 43 (49.4)                                | < 0.001                     |
| Child-Pugh grade B                 | 144 (6.1)  | 109 (16.6)                                  | 9 (10.3)                                 | < 0.001                     |
| Preoperative AFP > 400 µg/L        | 536 (33.7)   | 162 (36.9)                                  | 19 (33.9)                                | 0.459                       |
| Largest tumor size > 5.0 cm        | 842 (53.0)   | 149 (33.9)                                  | 44 (78.6)                                | < 0.001                     |
| Multiple tumors                    | 1,044 (44.0)                                       | 354 (54.0)                                  | 32 (36.8)                                | < 0.001                     |
| Macrovascular invasion             | 245 (10.3)   | 63 (9.6)                                    | 10 (11.5)                                | 0.803                       |
| Microvascular invasion             | 1,024 (43.1)                                       | 281 (42.9)                                  | 37 (42.5)                                | 0.989                       |
| Incomplete tumor encapsulation     | 1,418 (59.7)                                       | 358 (54.7)                                  | 61 (70.1)                                | 0.007                       |
| Satellite nodules                  | 459 (19.3)   | 116 (17.7)                                  | 20 (23.0)                                | 0.416                       |
| Poor differentiation               | 1,378 (86.7)                                       | 354 (80.6)                                  | 48 (85.7)                                | 0.007                       |
| Laparoscopic approach              | 505 (21.3)   | 165 (25.2)                                  | 16 (18.4)                                | 0.213                       |
| Intraoperative blood loss > 400 mL | 634 (26.7)   | 259 (39.5)                                  | 33 (37.9)                                | < 0.001                     |
| Intraoperative blood transfusion   | 361 (15.2)   | 127 (19.4)                                  | 28 (32.2)                                | < 0.001                     |
| Major hepatectomy                  | 536 (22.6)   | 75 (11.5)                                   | 41 (47.1)                                | < 0.001                     |
| Non-anatomical resection           | 1,830 (77.1)                                       | 549 (83.8)                                  | 54 (62.1)                                | < 0.001                     |
| Narrow resection margin (< 1 cm)   | 1,354 (57.0)                                       | 330 (50.4)                                  | 64 (73.6)                                | < 0.001                     |

AFP,  $\alpha$ -fetoprotein; ASA, American Society of Anesthesiologists; HBV, hepatitis B virus; HCV, hepatitis C virus.

**Table 2. Long-term outcomes of patients according to preoperative platelet count**

| <i>n</i> (%)                    | Normal platelet count group (Group I, <i>n</i> = 2,374) | Thrombocytopenia group (Group II, <i>n</i> = 655) | Thrombocytosis group (Group III, <i>n</i> = 87) | <i>p</i> (II vs. I) | <i>p</i> (III vs. I) | <i>p</i> among three groups |
|---------------------------------|---|---|---|---------------------|----------------------|-----------------------------|
| Duration of follow-up*          | 50.0 ± 33.0   | 50.1 ± 32.1                                       | 40.8 ± 34.1                                     | 0.917               | < 0.001              | < 0.001                     |
| Death                           | 1,153 (48.6)  | 350 (53.4)  | 62 (71.3)                                       | 0.027               | < 0.001              | < 0.001                     |
| Cancer-related                  | 1,017 (42.8)  | 276 (42.1)  | 56 (64.4)                                       | 0.740               | < 0.001              | < 0.001                     |
| Non-cancer-related              | 136 (5.7)   | 74 (11.3)   | 6 (6.9)   | < 0.001             | 0.624                | < 0.001                     |
| Liver failure                   | 65 (2.7)  | 38 (5.8)  | 3 (3.4)   | < 0.001             | 0.705                | < 0.001                     |
| Upper gastrointestinal bleeding | 42 (1.8)  | 29 (4.4)  | 1 (1.1)   | < 0.001             | 0.635                | < 0.001                     |
| Other causes                    | 29 (1.2)  | 7 (1.1)   | 2 (2.3)   | 0.792               | 0.335                | 0.568                       |
| Recurrence                      | 1,444 (60.8)  | 387 (59.1)  | 64 (73.6)                                       | 0.734               | 0.010                | 0.034                       |
| Median OS, months**             | 77.9 (71.4, 84.5)                                       | 68.2 (58.6, 77.9)                                 | 34.6 (18.9, 50.4)                               | 0.131               | < 0.001              | < 0.001                     |
| 1 year, %                       | 84.9  | 86.4  | 78.2  |                     |                      |                             |
| 3 years, %                      | 66.6  | 76.5  | 48.2  |                     |                      |                             |
| 5 years, %                      | 56.0  | 52.7  | 40.2  |                     |                      |                             |
| 8 years, %                      | 43.6  | 39.7  | 24.8  |                     |                      |                             |
| Median RFS, months**            | 32.5 (28.9, 36.2)                                       | 33.3 (25.8, 40.7)                                 | 15.0 (2.0, 28.0)                                | 0.901               | 0.002                | 0.007                       |
| 1 year, %                       | 65.7  | 69.3  | 52.9  |                     |                      |                             |
| 3 years, %                      | 48.2  | 48.5  | 35.5  |                     |                      |                             |
| 5 years, %                      | 39.3  | 39.3  | 26.9  |                     |                      |                             |
| 8 years, %                      | 27.4  | 21.8  | 15.6  |                     |                      |                             |

\*Values are mean ± standard; \*\*Values in parentheses are 95% confidence intervals. OS, overall survival; RFS, recurrence-free survival.

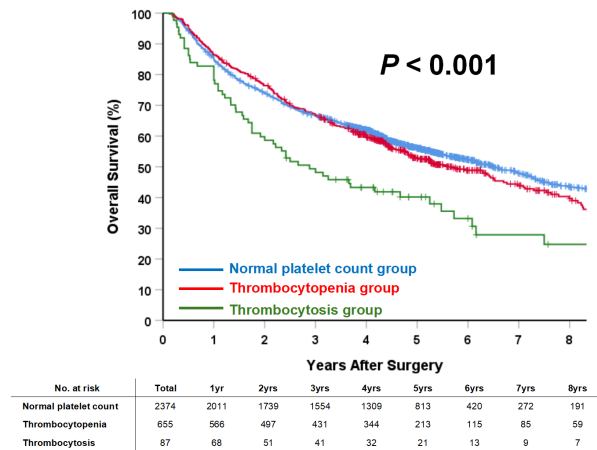


**Figure 2. Kaplan-Meier curves of overall survival according to preoperative platelet count.**  $p = 0.131$  (thrombocytopenia vs. normal platelet count),  $p < 0.001$  (thrombocytosis vs. normal platelet count), and  $p < 0.001$  (thrombocytopenia vs. thrombocytosis).

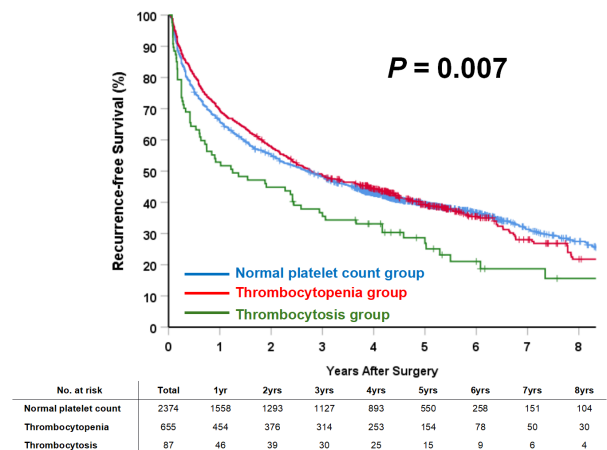


**Figure 3. Kaplan-Meier curves of recurrence-free survival according to preoperative platelet count.**  $p = 0.901$  (thrombocytopenia vs. normal platelet count),  $p = 0.002$  (thrombocytosis vs. normal platelet count), and  $p = 0.003$  (thrombocytopenia vs. thrombocytosis).

**Table 3. Univariable and multivariable Cox-regression analysis for overall survival**

|   | Univariable analysis  |          | Multivariable analysis |          |
|---|-----------------------|----------|------------------------|----------|
|   | Hazard ratio (95% CI) | <i>p</i> | Hazard ratio (95% CI)  | <i>p</i> |
| Sex (male vs. female)                     | 1.068 (0.920-1.239)   | 0.387    |                        |          |
| Age (> 65 vs. ≤ 65 years)                 | 1.001 (0.869-1.152)   | 0.993    |                        |          |
| Diabetes mellitus (yes vs. no)            | 0.965 (0.800-1.163)   | 0.709    |                        |          |
| HBV (positive vs. negative)               | 1.083 (0.939-1.249)   | 0.275    |                        |          |
| HCV (positive vs. negative)               | 1.240 (0.930-1.652)   | 0.143    |                        |          |
| ASA score (> 2 vs. ≤ 2)                   | 1.125 (0.979-1.292)   | 0.096    | NA                     | 0.976    |
| Cirrhosis (yes vs. no)                    | 1.346 (1.198-1.513)   | < 0.001  | 1.238 (1.074-1.427)    | 0.003    |
| Child-Pugh grade (B vs. A)                | 1.869 (1.605-2.177)   | < 0.001  | 1.231 (1.013-1.496)    | 0.036    |
| Preoperative platelet count               |                       |          |                        |          |
| Normal platelet count                     | Reference             |          | Reference              |          |
| Thrombocytopenia                          | 1.097 (0.973-1.236)   | 0.130    | 1.215 (1.045-1.413)    | 0.011    |
| Thrombocytosis                            | 1.762 (1.365-2.276)   | < 0.001  | 1.307 (1.130-1.511)    | < 0.001  |
| Preoperative AFP (> 400 vs. ≤ 400μg/L)    | 1.832 (1.623-2.067)   | < 0.001  | 1.251 (1.101-1.420)    | 0.001    |
| Largest tumor size (> 5 vs. ≤ 5 cm)       | 2.658 (2.347-3.010)   | < 0.001  | 1.753 (1.527-2.013)    | < 0.001  |
| Multiple tumors (yes vs. no)              | 1.242 (1.120-1.377)   | < 0.001  | NA                     | 0.263    |
| Macrovascular invasion (yes vs. no)       | 5.259 (4.609-6.000)   | < 0.001  | 2.832 (2.373-3.379)    | < 0.001  |
| Microvascular invasion (yes vs. no)       | 2.483 (2.245-2.747)   | < 0.001  | 1.313 (1.145-1.505)    | < 0.001  |
| Incomplete encapsulation (yes vs. no)     | 2.434 (2.178-2.720)   | < 0.001  | 1.641 (1.414-1.905)    | < 0.001  |
| Satellite nodules (yes vs. no)            | 2.889 (2.591-3.222)   | < 0.001  | 1.757 (1.531-2.017)    | < 0.001  |
| Tumor differentiation (poor vs. well)     | 1.910 (1.574-2.317)   | < 0.001  | NA                     | 0.351    |
| Surgical approach (open vs. laparoscopic) | 1.004 (0.907-1.111)   | 0.943    |                        |          |
| Blood loss (> 400 vs. ≤ 400 mL)           | 1.991 (1.762-2.250)   | < 0.001  | NA                     | 0.983    |
| Blood transfusion (yes vs. no)            | 2.370 (2.110-2.662)   | < 0.001  | 1.429 (1.223-1.670)    | < 0.001  |
| Extent of hepatectomy (major vs. minor)   | 2.153 (1.929-2.402)   | < 0.001  | NA                     | 0.602    |
| Anatomical resection (no vs. yes)         | 0.942 (0.837-1.059)   | 0.318    |                        |          |
| Resection margin (narrow vs. wide)        | 2.492 (2.235-2.778)   | < 0.001  | 1.906 (1.682-2.159)    | < 0.001  |

AFP,  $\alpha$ -fetoprotein; ASA, American Society of Anesthesiologists; HBV, hepatitis B virus; HCV, hepatitis C virus; CI, confidence interval; NA, not available.

thrombocytosis groups, respectively ( $p = 0.007$ ) (Figure 3).

### 3.3 Univariable and multivariable analyses for OS and RFS

In univariable and multivariable Cox regression analysis,

both thrombocytopenia (HR 1.215, 95% CI 1.045-1.413,  $p = 0.011$ ) and thrombocytosis (HR 1.307, 95% CI 1.130-1.511,  $p < 0.001$ ) were independent risk factors for poor OS, along with other established prognostic factors (Table 3). In univariable and multivariable analysis regarding RFS, thrombocytosis remained an independent predictor (HR 1.523, 95% CI 1.196-1.939,  $p = 0.001$ ),

**Table 4. Univariable and multivariable Cox-regression analysis for recurrence-free survival**

|   | Univariable analysis  |          | Multivariable analysis |          |
|---|-----------------------|----------|------------------------|----------|
|   | Hazard ratio (95% CI) | <i>p</i> | Hazard ratio (95% CI)  | <i>p</i> |
| Sex (male vs. female)                     | 0.984 (0.860-1.125)   | 0.808    | NA                     | 0.972    |
| Age (> 65 vs. ≤ 65 years)                 | 0.926 (0.816-1.050)   | 0.230    |                        |          |
| Diabetes mellitus (yes vs. no)            | 1.051 (0.897-1.232)   | 0.538    |                        |          |
| HBV (positive vs. negative)               | 1.790 (0.994-1.398)   | 0.058    |                        |          |
| HCV (positive vs. negative)               | 1.216 (0.944-1.565)   | 0.130    |                        |          |
| ASA score (> 2 vs. ≤ 2)                   | 1.083 (0.957-1.225)   | 0.206    | 1.323 (1.174-1.491)    | < 0.001  |
| Cirrhosis (yes vs. no)                    | 1.350 (1.218-1.495)   | < 0.001  |                        |          |
| Child-Pugh grade (B vs. A)                | 1.736 (1.509-1.999)   | < 0.001  |                        |          |
| Preoperative platelet count               |                       |          |                        |          |
| Normal platelet count                     | <i>Reference</i>      |          | <i>Reference</i>       |          |
| Thrombocytopenia                          | 0.993 (0.892-1.105)   | 0.901    | 0.941 (0.843-1.050)    | 0.278    |
| Thrombocytosis                            | 1.463 (1.149-1.862)   | 0.002    | 1.523 (1.196-1.939)    | 0.001    |
| Preoperative AFP (> 400 vs. ≤ 400µg/L)    | 1.568 (1.407-1.748)   | < 0.001  | 1.127 (1.004-1.265)    | 0.042    |
| Largest tumor size (> 5 vs. ≤ 5 cm)       | 2.190 (1.967-2.438)   | < 0.001  | 1.511 (1.343-1.699)    | < 0.001  |
| Multiple tumors (yes vs. no)              | 1.193 (1.091-1.304)   | < 0.001  | NA                     | 0.495    |
| Macrovascular invasion (yes vs. no)       | 4.746 (4.184-5.385)   | < 0.001  | 3.078 (2.597-3.649)    | < 0.001  |
| Microvascular invasion (yes vs. no)       | 2.123 (1.944-2.318)   | < 0.001  | 1.134 (1.007-1.278)    | 0.039    |
| Incomplete encapsulation (yes vs. no)     | 2.161 (1.966-2.374)   | < 0.001  | 1.497 (1.320-1.699)    | < 0.001  |
| Satellite nodules (yes vs. no)            | 2.611 (2.361-2.888)   | < 0.001  | 1.748 (1.539-1.986)    | < 0.001  |
| Tumor differentiation (poor vs. well)     | 1.834 (1.557-2.159)   | < 0.001  | 1.198 (1.009-1.421)    | 0.039    |
| Surgical approach (open vs. laparoscopic) | 1.027 (0.887-1.190)   | 0.722    | NA                     | 0.932    |
| Blood loss (> 400 vs. ≤ 400 mL)           | 1.695 (1.518-1.894)   | < 0.001  |                        |          |
| Blood transfusion (yes vs. no)            | 2.005 (1.800-2.233)   | < 0.001  | 1.341 (1.162-1.549)    | < 0.001  |
| Extent of hepatectomy (major vs. minor)   | 1.918 (1.735-2.120)   | < 0.001  | NA                     | 0.258    |
| Anatomical resection (no vs. yes)         | 0.993 (0.893-1.104)   | 0.900    | 1.834 (1.644-2.047)    | < 0.001  |
| Resection margin (narrow vs. wide)        | 2.122 (1.934-2.329)   | < 0.001  |                        |          |

AFP,  $\alpha$ -fetoprotein; ASA, American Society of Anesthesiologists; HBV, hepatitis B virus; HCV, hepatitis C virus; CI, confidence interval; NA, not available.

while thrombocytopenia did not (HR 0.941, 95% CI 0.843-1.050,  $p = 0.278$ ) (Table 4).

#### 4. Discussion

This multicenter study demonstrated that preoperative platelet count was an independent predictor of long-term outcomes after curative resection for HCC. The findings of the present study demonstrated that both thrombocytopenia ( $< 100 \times 10^9/L$ ) and thrombocytosis ( $\geq 300 \times 10^9/L$ ) were independent predictors of worse OS, a "double-edged sword" phenomenon not previously established in HCC literature. Furthermore, thrombocytosis was an independent risk factor for postoperative recurrence, a finding not previously reported in the context of HCC resection. These results underscore the complex interplay among platelets, liver function, and tumor biology in HCC. By establishing preoperative platelet count levels as a robust and clinically accessible prognostic marker, this work provides a framework for refining risk stratification protocols, informing personalized treatment algorithms, and potentially improving outcomes in HCC patients selected for curative-intent resection. The "sweet spot" of normal platelet count identified in this study opens new avenues for preoperative optimization and targeted interventions in the management of HCC.

The adverse impact of thrombocytopenia on

postoperative outcomes among patients with HCC has been reported in several previous studies (23-26). The results of the current study confirmed and extended these observations in a larger cohort. The mechanisms underlying this association were likely multifactorial. First, thrombocytopenia often reflects the presence of portal hypertension and advanced liver fibrosis or cirrhosis, which are known risk factors for poor outcomes after HCC resection (38). Indeed, in the present cohort, patients with thrombocytopenia had a higher prevalence of cirrhosis and worse liver function. Platelets also play important roles in liver regeneration and repair (39). Thrombocytopenia may impair liver regeneration capacity, leading to increased postoperative liver dysfunction and complications. In addition, platelets are involved in various aspects of the immune response against cancer (40). Thrombocytopenia may compromise antitumor immunity and promote tumor progression.

The prognostic significance of thrombocytosis in HCC has not been well-established, with conflicting results in the literature (13,29,31). The present study provided strong evidence that thrombocytosis was an independent predictor of both decreased OS and RFS. This finding is consistent with reports related to other malignancies, in which elevated platelet counts had been associated with advanced disease and poor prognosis (41). The mechanisms by which thrombocytosis may promote HCC progression include: *i*) production of



growth factors and cytokines that stimulate tumor growth and angiogenesis (42); *ii*) formation of platelet-tumor cell aggregates that facilitate metastasis (43); and *iii*) induction of epithelial-mesenchymal transition in tumor cells (44). In the present study, patients with thrombocytosis had larger tumors and were more likely to undergo major hepatectomy, suggesting a more advanced disease stage.

The discrepancy in our findings - where thrombocytopenia independently predicted worse OS but not RFS - provides important insights into the mechanisms through which low platelet counts affect outcomes. To further investigate this pattern, we performed additional analyses of mortality causes and conducted competing risk modeling. These analyses revealed that patients with thrombocytopenia had a higher proportion of non-cancer deaths (11.3%) compared to those with normal platelet counts (5.7%) or thrombocytosis (6.9%), with liver failure and upper gastrointestinal bleeding being the predominant non-cancer causes. When accounting for the competing risk of non-cancer mortality in our statistical models, thrombocytopenia was not significantly associated with cancer-specific mortality (subhazard ratio 1.108, 95% CI 0.952-1.289,  $p = 0.186$ ), while thrombocytosis remained a significant predictor (subhazard ratio 1.401, 95% CI 1.172-1.674,  $p < 0.001$ ). These findings suggest that thrombocytopenia primarily affects OS through liver-related complications rather than through direct effects on tumor biology. In contrast, thrombocytosis appears to have a more direct relationship with cancer progression, reflected in its significance across all outcome measures.

A notable methodological consideration in our study is the discrepancy between unadjusted Kaplan-Meier curves and multivariable analysis results for thrombocytopenia. While unadjusted survival curves showed similar patterns between thrombocytopenia and normal platelet count groups, multivariable analysis revealed thrombocytopenia as an independent risk factor after controlling for confounding variables (HR 1.215,  $p = 0.011$ ). This highlights the importance of statistical adjustment when analyzing groups with substantial differences in baseline characteristics, as was the case in our cohort where patients with thrombocytopenia had significantly higher rates of cirrhosis (92.4% vs. 68.1%), worse liver function (Child-Pugh B: 16.6% vs. 6.1%), and smaller tumors ( $\leq 5$  cm: 66.1% vs. 47.0%) compared to those with normal platelet counts. These confounding variables, if not properly adjusted for, can mask the true independent effect of thrombocytopenia on survival outcomes.

Interestingly, while both thrombocytopenia and thrombocytosis were associated with worse OS, only thrombocytosis independently predicted RFS. This discrepancy is further explained by our analysis of mortality causes, which revealed a higher proportion of non-cancer deaths in the thrombocytopenia group

(11.3%) compared to other groups (5.7% and 6.9%). The mechanisms underlying this association likely reflect the role of thrombocytopenia as a marker of advanced liver dysfunction and portal hypertension, leading to increased risk of liver failure and variceal bleeding.

The findings of the current study have several important clinical implications. First, preoperative platelet count should be considered in the risk assessment of HCC patients being evaluated for curative resection. Patients with either thrombocytopenia or thrombocytosis may require more intensive preoperative optimization and closer postoperative surveillance. Second, the underlying causes of abnormal platelet counts should be thoroughly investigated and addressed when possible. For patients with thrombocytopenia due to hypersplenism, splenectomy or splenic artery embolization might be considered to improve platelet counts and potential outcomes (45,46). In cases of thrombocytosis, ruling out chronic inflammation or occult infection is crucial.

These results also raise the question of whether modulating platelet counts may improve outcomes in HCC patients. For patients with thrombocytopenia, platelet transfusion or thrombopoietin receptor agonists may be beneficial (47). However, the optimal timing and target platelet count for such interventions remain to be determined. Among patients with thrombocytosis, antiplatelet therapy could potentially mitigate the negative impact on prognosis. Preclinical studies have demonstrated promising results with aspirin and other antiplatelet agents in HCC models (48), but clinical evidence is still limited (49,50).

Several limitations of the present study should be considered. First, the retrospective nature of the study introduces the potential for selection bias and unmeasured confounding. Second, a single preoperative platelet count measurement was used, which may not fully capture the dynamic changes in platelet levels over time. Platelet counts can fluctuate daily in individual patients due to various physiological and pathological factors, adding uncertainty to the captured readings. This study did not account for post-operative platelet counts, which may differ significantly after hepatectomy due to increased liver stiffness, elevated portal pressure, and other surgical sequelae. Prospective studies incorporating serial platelet measurements throughout the perioperative period are warranted to elucidate the temporal dynamics of platelet fluctuations and their impact on longitudinal outcomes. Third, despite efforts to adjust for known prognostic factors, residual confounding cannot be completely ruled out. Fourth, the platelet count cutoffs in this study were tailored to regional clinical standards ( $100-300 \times 10^9/L$ ), which differ from international reference ranges ( $150-450 \times 10^9/L$ ). While this enhances the relevance of our findings to Chinese clinical practice, it may limit direct comparisons with studies from other regions. Fifth, we acknowledge that platelets interact with various components of the immune system, which may

influence HCC outcomes. However, our retrospective design spanning two decades and multiple centers precluded comprehensive immune cell profiling. Future studies should explore the relationship between platelet counts, immune cell populations (including neutrophils, lymphocytes, and regulatory T cells), and inflammatory markers to develop more integrated prognostic models. While we recognize the limitations of using a single biomarker for prognostic assessment, we believe identifying readily available, low-cost parameters with strong prognostic value has significant clinical utility, especially in resource-limited settings. Finally, the cohort consisted predominantly of HBV-related HCC patients from China, potentially limiting the generalizability of the findings to other populations.

In conclusion, this large multicentre study demonstrated that preoperative platelet count was an independent predictor of long-term outcomes after curative resection for HCC. Both thrombocytopenia and thrombocytosis were associated with worse OS, while thrombocytosis additionally predicts higher recurrence risk. These findings highlight the potential of platelet count as a simple yet valuable prognostic marker for risk stratification in HCC patients undergoing resection. Future studies should focus on validating these results in diverse populations and exploring potential therapeutic strategies targeting platelet-related pathways in HCC.

**Funding:** This study was supported by the National Natural Science Foundation of China (No. 82425049 and 82273074 for Yang T; 82241223 for Wang M; 92359301 for Wang X), Dawn Project Foundation of Shanghai (No. 21SG36 for Yang T), Shanghai Health and Hygiene Discipline Leader Project (No. 2022XD001 for Yang T), Shanghai Outstanding Academic Leader Program (No. 23XD1424900 for Yang T), and the Natural Science Foundation of Shanghai (No. 22ZR1477900 for Wang M).

**Conflict of Interest:** The authors have no conflicts of interest to disclose.

## References

- Bray F, Ferlay J, Soerjomataram I, Siegel RL, Torre LA, Jemal A. Global cancer statistics 2018: GLOBOCAN estimates of incidence and mortality worldwide for 36 cancers in 185 countries. *CA Cancer J Clin.* 2018; 68:394-424.
- Wang MD, Diao YK, Yao LQ, Fan ZQ, Wang KC, Wu H, Gu HL, Xu JH, Li C, Lv GY, Yang T. Emerging role of molecular diagnosis and personalized therapy for hepatocellular carcinoma. *iLIVER.* 2024; 3:100083.
- Vogel A, Meyer T, Sapisochin G, Salem R, Saborowski A. Hepatocellular carcinoma. *Lancet.* 2022; 400:1345-1362.
- Vitale A, Cabibbo G, Iavarone M, *et al.* Personalised management of patients with hepatocellular carcinoma: a multiparametric therapeutic hierarchy concept. *Lancet Oncol.* 2023; 24:e312-e322.
- Pinna AD, Yang T, Mazzaferro V, De Carlis L, Zhou J, Roayaie S, Shen F, Sposito C, Cescon M, Di Sandro S, Yi-Feng H, Johnson P, Cucchetti A. Liver Transplantation and Hepatic Resection can Achieve Cure for Hepatocellular Carcinoma. *Ann Surg.* 2018; 268:868-875.
- Yao LQ, Chen ZL, Feng ZH, *et al.* Clinical Features of Recurrence After Hepatic Resection for Early-Stage Hepatocellular Carcinoma and Long-Term Survival Outcomes of Patients with Recurrence: A Multi-institutional Analysis. *Ann Surg Oncol.* 2022; 29:4291-4303.
- Yao LQ, Li C, Diao YK, *et al.* Grading severity of microscopic vascular invasion was independently associated with recurrence and survival following hepatectomy for solitary hepatocellular carcinoma. *Hepatobiliary Surg Nutr.* 2024; 13:16-28.
- Diao YK, Sun L, Wang MD, *et al.* Development and validation of nomograms to predict survival and recurrence after hepatectomy for intermediate/advanced (BCLC stage B/C) hepatocellular carcinoma. *Surgery.* 2024; 176:137-147.
- Tang SC, Diao YK, Lin KY, *et al.* Association of Pringle maneuver with postoperative recurrence and survival following hepatectomy for hepatocellular carcinoma: a multicenter propensity score and competing-risks regression analysis. *Hepatobiliary Surg Nutr.* 2024; 13:412-424.
- Yan WT, Li C, Yao LQ, *et al.* Predictors and long-term prognosis of early and late recurrence for patients undergoing hepatic resection of hepatocellular carcinoma: a large-scale multicenter study. *Hepatobiliary Surg Nutr.* 2023; 12:155-168.
- Chen WY, Li C, Liu ZP, *et al.* Novel online calculator to predict reduced risk of early recurrence from adjuvant transarterial chemoembolisation for patients with hepatocellular carcinoma. *eGastroenterology.* 2023; 1:e100008.
- Kurokawa T, Ohkohchi N. Platelets in liver disease, cancer and regeneration. *World J Gastroenterol.* 2017; 23:3228-3239.
- Carr BI, Guerra V. Thrombocytosis and hepatocellular carcinoma. *Dig Dis Sci.* 2013; 58:1790-1796.
- Gay LJ, Felding-Habermann B. Contribution of platelets to tumour metastasis. *Nat Rev Cancer.* 2011; 11:123-134.
- Zhao J, Huang A, Zeller J, Peter K, McFadyen JD. Decoding the role of platelets in tumour metastasis: enigmatic accomplices and intricate targets for anticancer treatments. *Front Immunol.* 2023; 14:1256129.
- Pavlovic N, Rani B, Gerwins P, Heindryckx F. Platelets as Key Factors in Hepatocellular Carcinoma. *Cancers (Basel).* 2019; 11:1022.
- Mammadova-Bach E, Mangin P, Lanza F, Gachet C. Platelets in cancer. From basic research to therapeutic implications. *Hamostaseologie.* 2015; 35:325-336.
- Maan R, de Kneegt RJ, Veldt BJ. Management of Thrombocytopenia in Chronic Liver Disease: Focus on Pharmacotherapeutic Strategies. *Drugs.* 2015; 75:1981-1992.
- Gallo P, Terracciani F, Di Pasquale G, Esposito M, Picardi A, Vespasiani-Gentilucci U. Thrombocytopenia in chronic liver disease: Physiopathology and new therapeutic strategies before invasive procedures. *World J Gastroenterol.* 2022; 28:4061-4074.
- Peck-Radosavljevic M. Thrombocytopenia in chronic

- liver disease. *Liver Int.* 2017; 37:778-793.
21. Stone RL, Nick AM, McNeish IA, *et al.* Paraneoplastic thrombocytosis in ovarian cancer. *N Engl J Med.* 2012; 366:610-618.
22. Hwang SJ, Luo JC, Li CP, Chu CW, Wu JC, Lai CR, Chiang JH, Chau GY, Lui WY, Lee CC, Chang FY, Lee SD. Thrombocytosis: a paraneoplastic syndrome in patients with hepatocellular carcinoma. *World J Gastroenterol.* 2004; 10:2472-2477.
23. Kaneko K, Shirai Y, Wakai T, Yokoyama N, Akazawa K, Hatakeyama K. Low preoperative platelet counts predict a high mortality after partial hepatectomy in patients with hepatocellular carcinoma. *World J Gastroenterol.* 2005; 11:5888-5892.
24. Amano H, Tashiro H, Oshita A, Kobayashi T, Tanimoto Y, Kuroda S, Tazawa H, Itamoto T, Asahara T, Ohdan H. Significance of platelet count in the outcomes of hepatectomized patients with hepatocellular carcinoma exceeding the Milan criteria. *J Gastrointest Surg.* 2011; 15:1173-1181.
25. Llovet JM, Bruix J. Novel advancements in the management of hepatocellular carcinoma in 2008. *J Hepatol.* 2008; 48 Suppl 1:S20-37.
26. Maithel SK, Kneuer PJ, Kooby DA, Scoggins CR, Weber SM, Martin RC 2nd, McMasters KM, Cho CS, Winslow ER, Wood WC, Staley CA 3rd. Importance of low preoperative platelet count in selecting patients for resection of hepatocellular carcinoma: a multi-institutional analysis. *J Am Coll Surg.* 2011; 212:638-648; discussion 648-650.
27. Pang Q, Qu K, Zhang JY, Song SD, Liu SS, Tai MH, Liu HC, Liu C. The Prognostic Value of Platelet Count in Patients With Hepatocellular Carcinoma: A Systematic Review and Meta-Analysis. *Medicine (Baltimore).* 2015; 94:e1431.
28. Lesurtel M, Graf R, Aleil B, Walther DJ, Tian Y, Jochum W, Gachet C, Bader M, Clavien PA. Platelet-derived serotonin mediates liver regeneration. *Science.* 2006; 312:104-107.
29. Lee CH, Lin YJ, Lin CC, Yen CL, Shen CH, Chang CJ, Hsieh SY. Pretreatment platelet count early predicts extrahepatic metastasis of human hepatoma. *Liver Int.* 2015; 35:2327-2336.
30. Scheiner B, Kirstein M, Popp S, Hücke F, Bota S, Rohr-Udilova N, Reiberger T, Müller C, Trauner M, Peck-Radosavljevic M, Vogel A, Sieghart W, Pinter M. Association of Platelet Count and Mean Platelet Volume with Overall Survival in Patients with Cirrhosis and Unresectable Hepatocellular Carcinoma. *Liver Cancer.* 2019; 8:203-217.
31. Shen SL, Fu SJ, Chen B, Kuang M, Li SQ, Hua YP, Liang LJ, Guo P, Hao Y, Peng BG. Preoperative Aspartate Aminotransferase to Platelet Ratio is an Independent Prognostic Factor for Hepatitis B-Induced Hepatocellular Carcinoma After Hepatic Resection. *Ann Surg Oncol.* 2014;21:3802-3809.
32. Pang Q, Zhang JY, Xu XS, Song SD, Qu K, Chen W, Zhou YY, Miao RC, Liu SS, Dong YF, Liu C. Significance of platelet count and platelet-based models for hepatocellular carcinoma recurrence. *World J Gastroenterol.* 2015; 21:5607-5621.
33. Shim JH, Jun MJ, Han S, Lee YJ, Lee SG, Kim KM, Lim YS, Lee HC. Prognostic nomograms for prediction of recurrence and survival after curative liver resection for hepatocellular carcinoma. *Ann Surg.* 2015; 261:939-946.
34. Pawlik TM, Delman KA, Vauthey JN, Nagorney DM, Ng IO, Ikai I, Yamaoka Y, Belghiti J, Lauwers GY, Poon RT, Abdalla EK. Tumor size predicts vascular invasion and histologic grade: Implications for selection of surgical treatment for hepatocellular carcinoma. *Liver Transpl.* 2005; 11:1086-1092.
35. Kuter DJ. Milestones in understanding platelet production: a historical overview. *Br J Haematol.* 2014; 165:248-258.
36. Nilles KM, Flamm SL. Thrombocytopenia in Chronic Liver Disease: New Management Strategies. *Clin Liver Dis.* 2020; 24:437-451.
37. Strasberg SM. Nomenclature of hepatic anatomy and resections: a review of the Brisbane 2000 system. *J Hepatobiliary Pancreat Surg.* 2005; 12:351-355.
38. D'Amico G, Garcia-Tsao G, Pagliaro L. Natural history and prognostic indicators of survival in cirrhosis: a systematic review of 118 studies. *J Hepatol.* 2006; 44:217-231.
39. Lesurtel M, Clavien PA. Platelet-derived serotonin: translational implications for liver regeneration. *Hepatology.* 2014; 60:30-33.
40. Rachidi S, Metelli A, Riesenberger B, Wu BX, Nelson MH, Wallace C, Paulos CM, Rubinstein MP, Garrett-Mayer E, Hennig M, Bearden DW, Yang Y, Liu B, Li Z. Platelets subvert T cell immunity against cancer *via* GARP-TGFβ axis. *Sci Immunol.* 2017; 2:eaa17911.
41. Buerge D, Wenz F, Groden C, Brockmann MA. Tumor-platelet interaction in solid tumors. *Int J Cancer.* 2012; 130:2747-2760.
42. Yan M, Jurasz P. The role of platelets in the tumor microenvironment: From solid tumors to leukemia. *Biochim Biophys Acta.* 2016; 1863:392-400.
43. Labelle M, Begum S, Hynes RO. Direct signaling between platelets and cancer cells induces an epithelial-mesenchymal-like transition and promotes metastasis. *Cancer Cell.* 2011; 20:576-590.
44. Haemmerle M, Stone RL, Menter DG, Afshar-Kharghan V, Sood AK. The Platelet Lifeline to Cancer: Challenges and Opportunities. *Cancer Cell.* 2018; 33:965-983.
45. Chen ZL, Yao LQ, Pu JL, *et al.* Impact of concurrent splenectomy and esophagogastric devascularization on surgical outcomes of partial hepatectomy for hepatocellular carcinoma in patients with clinically significant portal hypertension: A multicenter propensity score matching analysis. *Eur J Surg Oncol.* 2022; 48:1078-1086.
46. Miyoshi A, Ide T, Kitahara K, Noshiro H. Appraisal of simultaneous laparoscopic splenectomy and hepatic resection in the treatment of hepatocellular carcinoma with hypersplenic thrombocytopenia. *Hepatogastroenterology.* 2013; 60:1689-1692.
47. Terrault N, Chen YC, Izumi N, Kayali Z, Mitrut P, Tak WY, Allen LF, Hassanein T. Avatrombopag Before Procedures Reduces Need for Platelet Transfusion in Patients With Chronic Liver Disease and Thrombocytopenia. *Gastroenterology.* 2018; 155:705-718.
48. Sitia G, Aiolfi R, Di Lucia P, Mainetti M, Fiocchi A, Mingozzi F, Esposito A, Ruggeri ZM, Chisari FV, Iannaccone M, Guidotti LG. Antiplatelet therapy prevents hepatocellular carcinoma and improves survival in a mouse model of chronic hepatitis B. *Proc Natl Acad Sci U S A.* 2012; 109:E2165-2172.
49. Ricciotti E, Wangenstein KJ, FitzGerald GA. Aspirin in Hepatocellular Carcinoma. *Cancer Res.* 2021; 81:3751-3761.

50. Sitia G, Iannacone M, Guidotti LG. Anti-platelet therapy in the prevention of hepatitis B virus-associated hepatocellular carcinoma. J Hepatol. 2013; 59:1135-1138.

Received March 5, 2025; Revised April 15, 2025; Accepted April 18, 2025.

<sup>§</sup> These authors contributed equally to this work.

\*Address correspondence to:

Tian Yang, Department of Hepatobiliary Surgery, Eastern Hepatobiliary Surgery Hospital, Naval Medical University, No. 225, Changhai Road, Shanghai 200438, China, or Hepatopancreatobiliary Center, Beijing Tsinghua Changgung Hospital, Tsinghua University, Beijing, China.  
E-mail: yangtianchbh@smmu.edu.cn

Released online in J-STAGE as advance publication April 22, 2025.



# Liver exposure during laparoscopic right-sided hepatectomy *via* stretching of the ligamentum teres hepatis: A propensity score matching analysis

Keda Song<sup>1,2</sup>, Yang Xu<sup>1,3</sup>, Zhongyu Li<sup>1</sup>, Mingyuan Wang<sup>1</sup>, Dong Chen<sup>1,4</sup>, Yongzhi Zhou<sup>1</sup>, Guangchao Yang<sup>1</sup>, Yong Ma<sup>1,5,\*</sup>

<sup>1</sup> Department of Minimally Invasive Hepatic Surgery, the First Affiliated Hospital of Harbin Medical University, Harbin, Heilongjiang, China;

<sup>2</sup> Department of General Surgery, Linyi Central Hospital, Linyi, Shandong, China;

<sup>3</sup> Department of Hepatobiliary Surgery, Aerospace Center Hospital, Beijing, China;

<sup>4</sup> National Clinical Research Center for Cancer/Cancer Hospital of Shenzhen Hospital, Chinese Academy of Medical Sciences and Peking Union Medical College, Shenzhen, Guangdong, China;

<sup>5</sup> Key Laboratory of Hepatosplenic Surgery, Ministry of Education, the First Affiliated Hospital of Harbin Medical University, Harbin, Heilongjiang, China.

**SUMMARY:** One of the challenges of laparoscopic liver resection (LLR) is the exposure of the surgical field. We propose a new surgical approach to better expose the right liver, stretching of the ligamentum teres hepatis (SLTH), and we evaluated its clinical feasibility and limitations through a study analyzing relevant cases. Clinicopathologic data on patients who underwent laparoscopic right partial hepatectomy (LRPH) at our center were retrospectively collected, and subjects were 276 patients with liver space-occupying lesions who met the selection criteria and who underwent the new surgical approach (SLTH) or the conventional surgical approach (no stretching of the ligamentum teres hepatis, or NSLTH). After 1:1 propensity score matching (PSM), 102 patients in each cohort were selected for further analysis. There were no significant differences in the operating time or the duration of postoperative hospitalization between the SLTH cohort and the NSLTH cohort. The duration of detachment of the hepatic parenchyma and the duration of hepatic portal occlusion were significantly shorter in the SLTH cohort than in the NSLTH cohort. The intraoperative blood loss in the SLTH cohort was significantly less than that in the NSLTH cohort. Alanine aminotransferase (ALT) and aspartate aminotransferase (AST) levels were significantly lower in the SLTH cohort than in the NSLTH cohort on day 5 postoperatively. Results confirmed that SLTH is a simple, safe, effective, and highly reproducible technique for the treatment of LRPH. SLTH may help to perform LRPH by increasing the level of laparoscopic exposure of the right liver and reducing bleeding and operating time.

**Keywords:** laparoscopic right hepatectomy, stretching of the ligamentum teres hepatis, surgical approach

## 1. Introduction

Improvements in laparoscopic technology and equipment have facilitated an increasing number of complex laparoscopic surgeries (1). Laparoscopic techniques have gradually replaced conventional open approaches because of several advantages, such as smaller incisions, less pain, and quick postoperative recovery (2-3). Moreover, laparoscopic approaches provide the necessary precision for anatomic liver resection in terms of reducing tissue damage and intraoperative bleeding in an effort to reduce systemic trauma (4). In hepatobiliary surgery, sufficient attention has been paid to laparoscopic techniques and their use has been encouraged (5). The complexity and difficulty of laparoscopic liver surgery

vary. Laparoscopic hepatectomy on the right side faces many challenges, including a poor surgical field, limited intraoperative movement of the liver, difficulty in selecting the surgical section, and hemorrhage control (6). These challenges often require more effort on the part of the assistant and surgeon to expose the liver, and relying solely on laparoscopic instruments to expose the liver is consequently more fatiguing and unstable (7). Exposure during laparoscopic right hepatectomy needs to be urgently addressed.

Many techniques for surgical field exposure have been used in clinical practice during laparoscopic right hepatectomy, such as changing the patient's position (8-9), adjusting the laparoscopic trocar layout (10-11), the liver hanging maneuver (12-13), and sterile glove

pouching (14-15). However, these techniques all have certain limitations. For instance, a change in position, adjustment of the laparoscopic trocar layout, and the liver hanging maneuver cannot be performed at will. Sterile glove pouching is usually performed to a limited extent in laparoscopic surgery. Therefore, further screening is required for clinical use. Through continuous exploration and the practice of laparoscopic liver resection (LLR), the current authors explored an innovative procedure to expose the right side of the liver which they designated stretching of the ligamentum teres hepatis (SLTH). This procedure is performed as follows. After the right liver is dissected, the ligamentum teres hepatis is severed, and a traction thread is sutured at the stump. Then, tissue clamps are used to fix the traction suture, a hook needle is used to guide the traction suture outside of the body, and the suture can be fixed outside the abdominal wall. The right liver can be better exposed and rotated with the SLTH. As the authors' team gained proficiency and increasingly used hepatic ligament retraction, results indicated that the technique was very helpful for LRPH exposure, largely increasing the surgeon's space to maneuver and reducing the difficulty of exposure for the assistant. The aim of the current study was to introduce the SLTH and to evaluate its clinical feasibility and limitations.

## 2. Materials and Methods

### 2.1. General information

Data on all patients who underwent LRPH at the First Affiliated Hospital of Harbin Medical University from January 2015 to July 2022 were analyzed. The research ethics committee of Harbin Medical University approved this study in accordance with the Declaration of Helsinki (as revised in 2013). Clinical information and written informed consent were collected from all participants. Subjects were a total of 276 patients who underwent LRPH, including patients who underwent SLTH ( $n = 135$ , SLTH cohort) or not ( $n = 141$ , NSLTH cohort) during LRPH. All surgeries were performed by the same surgical team, and there were no differences in the learning curve between the two cohorts.

### 2.2. Selection criteria

Subjects were a total of 276 patients who met the following selection criteria: (1) patients with a single tumor located in the right lobe of the liver (segments 5-8); (2) patients who were Child-Pugh grade A or B and whose liver function was restored to grade A after short-term liver protection treatment; (3) patients with a retention rate of indocyanine green for 15 minutes of less than 20%; (4) patients free of tumor infiltration or metastasis; and (5) patients who had not previously undergone abdominal surgery (16-17).

### 2.3. Surgical procedure

All surgeries were performed by the same surgical team following surgical and oncological principles. Following general anesthesia with tracheal intubation, invasive arterial blood pressure and central venous pressure were monitored during the procedure. Patients were placed in the supine or semilateral position. The position was further adjusted with the operating table as needed. CO<sub>2</sub> pneumoperitoneum was performed to maintain intra-abdominal pressure at 14 mmHg (1 mmHg = 0.133 kPa). Five trocars were typically placed in the abdomen, and a 30-degree rigid laparoscope was used. Laparoscopic ultrasonography was used to locate the lesion and identify the important pipeline structures around the lesion. The round ligament and the falciform ligament were dissected until the secondary porta hepatis was revealed. The liver was completely mobilized by dissecting the ligaments around the liver. The appropriate fixation angle was selected by pulling the falciform ligament. The free ligamentum teres hepatis was reattached to the abdominal wall with a Hem-o-lok clip or endoscopic suture. The extent of removal was evaluated to determine whether the gallbladder could be preserved. The first hepatic hilar blood flow occlusion device was pre-placed through the foramen of Winslow to perform the Pringle operation. The liver parenchyma was transected with a harmonic scalpel (Ethicon Endo-Surgery, USA). After transection, the stump was clipped with a Hem-o-lok clip or titanium clip. Laparoscopically, the thick stump was closed with a linear cutting closure and sutured with Prolene 5.0 for hemostasis. The specimen was removed from the bag endoscopically. Bleeding from the incision was carefully stopped by bipolar coagulation, and the incision was repeatedly rinsed. After confirming that the section was free of bleeding or biliary fistulae, fibrin glue was uniformly sprayed on the liver wound. The traction clamp or suture line was incised with the harmonic scalpel and then removed *via* the port. A drainage tube was inserted, and the wound was closed in layers. The operating time, hepatic portal occlusion time, parenchymal resection time, and intraoperative blood loss were recorded. Preoperative and postoperative blood biochemical indices and the duration of postoperative hospitalization were recorded.

To eliminate confounding variables between the two cohorts, propensity score matching (PSM) analysis was performed. This analysis was used to match variables of baseline characteristics that differed significantly between the two cohorts. A matching caliper of 0.02 and 1:1 nearest neighbor matching were used.

### 2.4. Statistical analysis

Statistical analyses were performed using SPSS 24.0 (IBM SPSS, USA). The distribution of measurements

was analyzed in each cohort. Normally distributed data were expressed as the mean  $\pm$  standard deviation, and the two-sample independent *t*-test was used for intercohort comparisons; if the data did not follow a normal distribution, data were expressed using the median (interquartile range), and nonparametric tests (*Mann–Whitney U* test) were used for intercohort comparisons. Numerical data are expressed as frequencies (percentages), and the differences between the two cohorts were compared using the chi-square test. A *P* value  $< 0.05$  was considered to indicate statistical significance.

### 3. Results

#### 3.1. Baseline characteristics

First, the baseline characteristics of patients were compared, and significant differences between the two cohorts were noted in terms of BMI, Child–Pugh classification, and preoperative AST level (Table 1). The differences in these three indicators may affect the evaluation of the effectiveness of SLTH in surgery. Therefore, PSM analysis was used to select patients from the two cohorts at a 1:1 ratio. Ultimately, through PSM analysis, 102 patients were selected from each cohort and their baseline characteristics were compared. There were no significant differences in any indicator

between the two cohorts of patients, thus eliminating the influence of baseline characteristics in the current study (Table 2).

Moreover, no major complications (Clavien–Dindo IIIa or worse) occurred in either cohort perioperatively, and no patients were transferred to the ICU or died perioperatively.

#### 3.2. Perioperative surgical outcomes

Next, surgical indicators in the aforementioned patients were compared. Results indicated that the duration of hepatic parenchymal detachment and the hepatic portal occlusion time were significantly shorter in the SLTH cohort than in the NSLTH cohort, while intraoperative blood loss was significantly less in the SLTH cohort than in the NSLTH cohort. In addition, data revealed that there were no significant differences in the operating time or the duration of postoperative hospitalization between the SLTH cohort and the NSLTH cohort (Table 3).

#### 3.3. Postoperative liver function

In addition, postoperative liver function in patients in both cohorts was compared. The alanine aminotransferase (ALT) and aspartate aminotransferase (AST) levels peaked on day 1 postoperatively and

**Table 1. Comparison of patients' baseline characteristics**

|                           | SLTH cohort ( <i>n</i> = 135) | NSLTH cohort ( <i>n</i> = 141) | <i>P</i> values |
|---------------------------|-------------------------------|--------------------------------|-----------------|
| Age (years)               | 49.42 $\pm$ 11.06             | 48.53 $\pm$ 11.06              | 0.504           |
| Sex                       |                               |                                |                 |
| Male                      | 64                            | 66                             | 0.921           |
| Female                    | 71                            | 75                             |                 |
| Child–Pugh class          |                               |                                |                 |
| A                         | 124                           | 138                            | 0.045           |
| B                         | 11                            | 3                              |                 |
| BMI (kg/m <sup>2</sup> )  | 22.03 $\pm$ 2.37              | 21.42 $\pm$ 2.27               | 0.030           |
| Pathological diagnosis    |                               |                                |                 |
| Hepatocellular carcinoma  | 62                            | 68                             | 0.702           |
| Hepatic hemangioma        | 73                            | 73                             |                 |
| Alpha-fetoprotein (ng/mL) |                               |                                |                 |
| 0–400                     | 90                            | 89                             | 0.537           |
| > 400                     | 45                            | 52                             |                 |
| Cirrhosis                 |                               |                                |                 |
| Yes                       | 55                            | 61                             | 0.671           |
| No                        | 80                            | 80                             |                 |
| Tumor location            |                               |                                |                 |
| Segment 5                 | 27                            | 23                             | 0.991           |
| Segment 6                 | 26                            | 24                             |                 |
| Segment 7                 | 34                            | 36                             |                 |
| Segment 8                 | 26                            | 34                             |                 |
| Junction of segments 5–6  | 4                             | 4                              |                 |
| Junction of segments 5–8  | 8                             | 10                             |                 |
| Junction of segments 6–7  | 6                             | 6                              |                 |
| Junction of segments 7–8  | 2                             | 2                              |                 |
| Other                     | 2                             | 2                              |                 |
| Preoperative ALT          | 16.22 $\pm$ 4.67              | 16.29 $\pm$ 4.43               | 0.904           |
| Preoperative AST          | 19.29 (3.78)                  | 18.85 (3.31)                   | 0.049           |

**Table 2. Comparison of patients' baseline characteristics after PSM**

|                           | SLTH cohort (n = 102) | NSLTH cohort (n = 102) | P values |
|---------------------------|-----------------------|------------------------|----------|
| Age (years)               | 49.40 ± 11.48         | 48.33 ± 11.15          | 0.501    |
| Sex                       |                       |                        |          |
| Male                      | 47                    | 49                     | 0.779    |
| Female                    | 55                    | 53                     |          |
| Child-Pugh class          |                       |                        |          |
| A                         | 100                   | 99                     | 1.000    |
| B                         | 2                     | 3                      |          |
| BMI (kg/m <sup>2</sup> )  | 21.67 ± 2.01          | 21.91 ± 2.20           | 0.405    |
| Pathological diagnosis    |                       |                        |          |
| Hepatocellular carcinoma  | 45                    | 44                     | 0.888    |
| Hepatic hemangioma        | 57                    | 58                     |          |
| Alpha-fetoprotein (ng/mL) |                       |                        |          |
| 0-400                     | 69                    | 68                     | 0.881    |
| > 400                     | 33                    | 34                     |          |
| Cirrhosis                 |                       |                        |          |
| Yes                       | 40                    | 38                     | 0.773    |
| No                        | 62                    | 64                     |          |
| Tumor location            |                       |                        |          |
| Segment 5                 | 23                    | 18                     | 0.964    |
| Segment 6                 | 22                    | 20                     |          |
| Segment 7                 | 25                    | 22                     |          |
| Segment 8                 | 19                    | 25                     |          |
| Junction of segments 5-6  | 3                     | 4                      |          |
| Junction of segments 5-8  | 4                     | 5                      |          |
| Junction of segments 6-7  | 3                     | 4                      |          |
| Junction of segments 7-8  | 2                     | 2                      |          |
| Other                     | 1                     | 2                      |          |
| Preoperative ALT U/L      | 15.60 (6.60)          | 16.70 (4.70)           | 0.378    |
| Preoperative AST U/L      | 19.34 (3.82)          | 19.17 (3.55)           | 0.360    |

**Table 3. Comparison of perioperative surgical outcomes between the two cohorts after PSM**

|                                     | SLTH cohort (n = 102) | NSLTH cohort (n = 102) | P       |
|-------------------------------------|-----------------------|------------------------|---------|
| Operating time (min)                | 226.00 (130.00)       | 238.00 (114.00)        | 0.391   |
| Parenchymal transection time (min)  | 102.00 (76.00)        | 148.00 (122.00)        | < 0.001 |
| Blood loss (mL)                     | 100.00 (64.00)        | 120.00 (70.00)         | 0.006   |
| Hospitalization (day)               | 10.00 (3.00)          | 10.00 (2.00)           | 0.783   |
| Hepatic portal occlusion time (min) | 25.00 (27.00)         | 40.50 (31.00)          | < 0.001 |

**Table 4. Comparison of postoperative liver function in the two cohorts after PSM**

|                       | SLTH cohort (n = 102) | NSLTH cohort (n = 102) | P       |
|-----------------------|-----------------------|------------------------|---------|
| ALT (U/L)             |                       |                        |         |
| Day 1 postoperatively | 277.9 (64.70)         | 289.40 (59.1)          | 0.076   |
| Day 5 postoperatively | 49.70 (4.80)          | 65.50 (4.60)           | < 0.001 |
| Day 7 postoperatively | 16.05 (6.20)          | 17.50 (4.70)           | 0.057   |
| AST (U/L)             |                       |                        |         |
| Day 1 postoperatively | 302.19 ± 76.49        | 297.7 ± 67.53          | 0.714   |
| Day 5 postoperatively | 51.98 ± 17.22         | 60.77 ± 18.21          | 0.045   |
| Day 7 postoperatively | 15.97 ± 4.39          | 16.94 ± 4.52           | 0.203   |

did not differ significantly between the two cohorts. The ALT and AST levels in both cohorts gradually decreased. Notably, the ALT and AST levels were significantly lower in the SLTH cohort than in the NSLTH cohort on day 5 postoperatively. Seven days postoperatively, the ALT and AST levels in both cohorts had decreased to normal levels (Table 4).

#### 4. Discussion

In LRPH, several methods, such as intraoperative position changes (8), adjustment of the trocar layout (10-11), and liver suspension and surgical glove techniques (12,14), have been widely used in clinical practice to expand the surgical field and reduce the difficulty of



surgery. The liver hanging maneuver was first used in open right hepatectomy by Belghiti *et al.* (18). The specific procedure consisted of establishing a channel between the inferior vena cava and the liver parenchyma and then passing a pulling sling through, which was perforated between the right hepatic vein and the middle hepatic vein. By pulling the sling to help expose the deep portion of liver, compressing the intrahepatic vessels and guiding the direction of resection, the hanging liver maneuver can effectively shorten the operating time and reduce intraoperative bleeding. However, this technique involves certain surgical difficulties and risks. First, the anterior inferior vena cava is not visible, so surgical skill is required (19). Additionally, short hepatic veins are at risk of rupture. Second, this procedure is associated with considerable anatomic risk at the second hepatic hilum. Finally, the blind establishment of channels for tumors near the diaphragm may lead to tumor rupture (20). Thus, the conventional liver hanging maneuver is difficult to perform laparoscopically.

Therefore, an improved liver hanging maneuver was proposed (12). Instead of dissecting the hepatic vein at the second portal, the pulling sling is placed on the right side of the right hepatic vein after dissection of the deltoid ligament is completed. Moreover, the right adrenal gland and inferior vena cava were selected to avoid injury to the short hepatic vein. This technique significantly reduces the risk of surgery. These string-based techniques help to expose the liver, reduce bleeding, and shorten the operating time (21). However, many of the drawbacks of the liver hanging maneuver remain unavoidable during laparoscopic procedures. For example, the pulled sling occupies an already limited space and blocks the surgeon's instruments. The direction of the sling is limited by port positioning

during laparoscopy and cannot meet the surgeon's requirements. In addition, applying sufficient pressure to the vasculature to occlude some of the blood flow, as is done in open surgery, is difficult.

More recently, surgical glove techniques have been used in laparoscopic right hepatectomy (14,18). This procedure consists of the following steps. After transection of the right deltoid ligament and the coronal ligament, water-injected gloves are placed behind the right liver. The pressure of the water capsule pushes the right liver forward and to the left, leading to the exposure of deep liver tissue. The advantages of this technique are the relative ease with which it is performed, the low level of risk, and the short preparation time. As the water capsule pushes the liver forward and to the left, it narrows the distance between the surgeon and the liver. This technique increases the exposure of the posterior hepatic field and the angle of operation. This technique is considered to reduce the duration of hepatic amputation and blood loss. The surgical glove technique seems to be more beneficial than conventional LRPH. When treating large tumors on the right side of the liver, however, the water capsule may further reduce the surgical field. Additionally, the liver is deformed by compression from the water capsule, which may lead to a change in the section surface after the removal of the water capsule.

Compared to the aforementioned techniques to increase the exposure of the right liver during laparoscopic surgery, the most striking features of SLTH are that it is simple and virtually risk-free. In LRPH, the space to manipulate the diaphragmatic surface of the liver is usually adequate due to the establishment of pneumoperitoneum, while the exposure of the hidden surface is difficult and unstable. This technique increases the space for the hidden surface of the right side of the

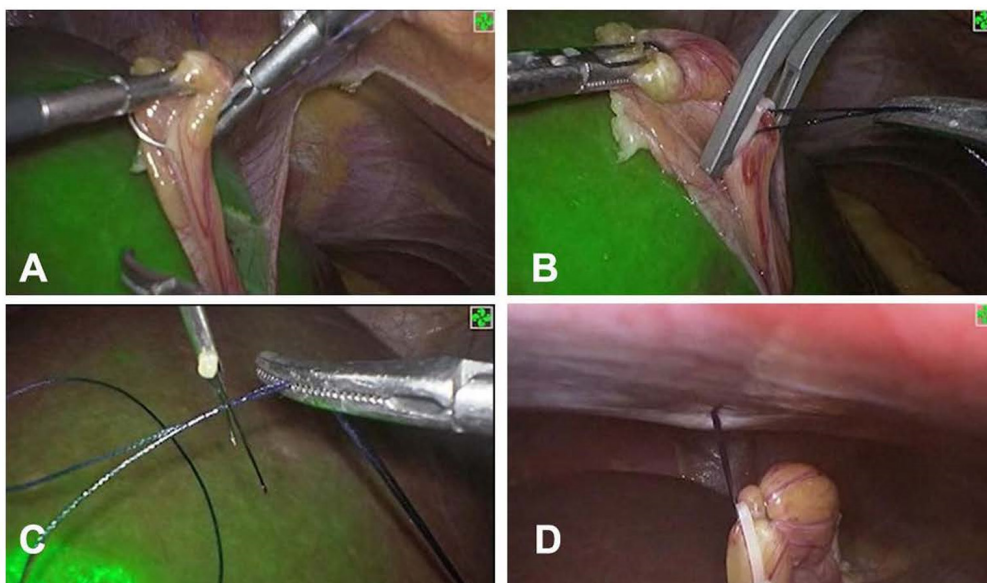


**Figure 1. Stretching of the ligamentum teres hepatis. (A)** A traction thread was sutured at the stump of the ligamentum teres hepatis. **(B)** Tissue clamps with fixed traction sutures. **(C)** A hook needle is used to guide the traction suture outside of the body. **(D)** External traction and fixation.

liver through suspension of the ligamentum teres hepatis so that the right side of the liver hangs in the abdominal cavity. Therefore, the assistant can more easily and stably assist the surgeon in exposing and transecting the right side of the liver. After liver dissection is complete, the right liver can be optionally rotated by pulling the ligamentum teres hepatis to select a more convenient surgical section. In addition, the sutured ligamentum teres hepatis is more solid than the sutured liver parenchyma, so the pulling strength is ideal and bleeding is rare.

Moreover, fixation of the ligamentum teres hepatis can better expose the hidden surface of the liver and facilitate observation of and surgery on deeper portions. As methods of detecting liver-related diseases improve, we will be able to detect smaller liver tumors earlier. Due to its lower risk and the ease with which it is performed, SLTH seems to be more suitable for small areas of liver resection.

The current study successfully used SLTH to increase the exposure of the liver in LLR. SLTH was feasible in all patients after screening. Compared to the NSLTH cohort, the SLTH cohort had a shorter duration of liver parenchymal detachment, a shorter hepatic portal occlusion time, and less intraoperative blood loss. Results indicated that the SLTH is a simple, safe, and effective surgical approach. This approach could increase the exposure of the right liver and reduce surgical difficulty, which may accelerate the early restoration of postoperative liver function.

This study had several limitations. First, identifying the ligamentum teres hepatis is difficult in patients who have undergone prior abdominal surgery. In these patients, the upper abdomen, and especially the liver, is strongly attached to the abdominal wall. Second, the liver has to be fixed multiple times in the event of multiple tumors. Third, the sample size was relatively small, and the follow-up was too short. Therefore, a larger sample size is needed and follow-up needs to be longer for further verification.

**Funding:** This work was funded by grants from the National Nature Science Foundation of China (grant nos. 81100305, 81470876, and 82370643), the Key Research and Development Program of Heilongjiang Province (grant no. 2024ZX12C28), the Natural Science Foundation of Heilongjiang Province (grant no. LC2018037), and the Postdoctoral Scientific Research Development Fund of Heilongjiang Province (grant no. LBH-Q17097).

**Conflict of Interest:** The authors have no conflicts of interest to disclose.

## References

- Alkhalili E, Berber E. Laparoscopic liver resection for malignancy: A review of the literature. *World J Gastroenterol.* 2014; 20:13599-13606.
- van der Heijde N, Ratti F, Aldrighetti L, Benedetti Cacciaguerra A, Can MF, D'Hondt M, Di Benedetto F, Ivanecz A, Magistri P, Menon K, Papoulas M, Vivarelli M, Besselink MG, Abu Hilal M.. Laparoscopic versus open right posterior sectionectomy: An international, multicenter, propensity score-matched evaluation. *Surg Endosc.* 2021; 35:6139-6149.
- Makki K, Chorasaya VK, Sood G, Srivastava PK, Dargan P, Vij V. Laparoscopy-assisted hepatectomy versus conventional (open) hepatectomy for living donors: When you know better, you do better. *Liver Transpl.* 2014; 20:1229-1236.
- Gotohda N, Cherqui D, Geller DA, *et al.* Expert Consensus Guidelines: How to safely perform minimally invasive anatomic liver resection. *J Hepatobiliary Pancreat Sci.* 2022; 29:16-32.
- Han HS, Yoon YS, Cho JY, Hwang DW. Laparoscopic liver resection for hepatocellular carcinoma: Korean experiences. *Liver Cancer.* 2013; 2:25-30.
- Inoue Y, Suzuki Y, Fujii K, Kawaguchi N, Ishii M, Masubuchi S, Yamamoto M, Hirokawa F, Hayashi M, Uchiyama K. Laparoscopic liver resection using the lateral approach from intercostal ports in segments VI, VII, and VIII. *J Gastrointest Surg.* 2017; 21:2135-2143.
- Tarantino G, Magistri P, Serra V, Berardi G, Assirati G, Ballarin R, Di Benedetto F. Laparoscopic liver resection of right posterior segments for hepatocellular carcinoma on cirrhosis. *J Laparoendosc Adv Surg Tech A.* 2017; 27:559-563.
- Belli G, Fantini C, D'Agostino A, Cioffi L, Limongelli P, Russo G, Belli A. Laparoscopic segment VI liver resection using a left lateral decubitus position: A personal modified technique. *J Gastrointest Surg.* 2008; 12:2221-2226.
- Chen JC, Zhang RX, Chen MS, Xu L, Chen JB, Yang KL, Zhang YJ, Zhou ZG. Left jackknife position: A novel position for laparoscopic hepatectomy. *Chin J Cancer.* 2017; 36:31.
- Chiw AK, Lewin J, Manoharan B, Cavallucci D, Bryant R, O'Rourke N. Intercostal and transthoracic trocars enable easier laparoscopic resection of dome liver lesions. *HPB (Oxford).* 2015; 17:299-303.
- Lee W, Han HS, Yoon YS, Cho JY, Choi Y, Shin HK. Role of intercostal trocars on laparoscopic liver resection for tumors in segments 7 and 8. *J Hepatobiliary Pancreat Sci.* 2014; 21:E65-68.
- Kim JH, Ryu DH, Jang LC, Choi JW. Lateral approach liver hanging maneuver in laparoscopic anatomical liver resections. *Surg Endosc.* 2016; 30:3611-3617.
- Chu H, Cao G, Tang Y, Du X, Min X, Wan C. Laparoscopic liver hanging maneuver through the retrohepatic tunnel on the right side of the inferior vena cava combined with a simple vascular occlusion technique for laparoscopic right hemihepatectomy. *Surg Endosc.* 2018; 32:2932-2938.
- Bin J, Binghai Z, Sanyuan H. Liver exposure using sterile glove pouch during laparoscopic right liver surgery in hepatocellular carcinoma patients. *World J Surg.* 2016; 40:946-950.
- Tabath M, Lim C, Goumard C, Scatton O. Surgical glove technique for laparoscopic liver resection. *J Gastrointest Surg.* 2020; 24:1912-1919.
- D'Hondt M, Ovaere S, Knol J, Vandeputte M, Parmentier I, De Meyere C, Vansteenkiste F, Besselink M, Pottel H,

- Verslype C. Laparoscopic right posterior sectionectomy: Single-center experience and technical aspects. *Langenbecks Arch Surg.* 2019; 404:21-29.
17. Jin H, Yin Z, Zhou Y, Ma T, Jian Z. Safety and feasibility of a laparoscopy-assisted non-anatomic resection technique for hepatocellular carcinoma located at right posterior segments in cirrhotic patients: A case-controlled study with propensity score matching. *Dig Surg.* 2018; 35:411-418.
  18. Belghiti J, Guevara OA, Noun R, Saldinger PF, Kianmanesh R. Liver hanging maneuver: A safe approach to right hepatectomy without liver mobilization. *J Am Coll Surg.* 2001; 193:109-111.
  19. Liddo G, Buc E, Nagarajan G, Hidaka M, Dokmak S, Belghiti J. The liver hanging manoeuvre. *HPB (Oxford).* 2009; 11:296-305.
  20. Dokmak S, Aussilhou B, Rebai W, Cauchy F, Belghiti J, Soubrane O. Up-to-down open and laparoscopic liver hanging maneuver: An overview. *Langenbecks Arch Surg.* 2021; 406:19-24.
  21. Troisi RI, Montalti R. Modified hanging maneuver using the Goldfinger dissector in laparoscopic right and left hepatectomy. *Dig Surg.* 2012; 29:463-467.
- Received February 10, 2025; Revised March 27, 2025; Accepted April 3, 2025.
- \*Address correspondence to:*  
 Yong Ma, Department of Minimally Invasive Hepatic Surgery, the First Affiliated Hospital of Harbin Medical University, 23rd Youzheng Street, Nangang District, Harbin, Heilongjiang, China 150001.  
 E-mail: mayong@ems.hrbmu.edu.cn
- Released online in J-STAGE as advance publication April 9, 2025.



## Guide for Authors

### 1. Scope of Articles

*BioScience Trends* (Print ISSN 1881-7815, Online ISSN 1881-7823) is an international peer-reviewed journal. *BioScience Trends* devotes to publishing the latest and most exciting advances in scientific research. Articles cover fields of life science such as biochemistry, molecular biology, clinical research, public health, medical care system, and social science in order to encourage cooperation and exchange among scientists and clinical researchers.

### 2. Submission Types

**Original Articles** should be well-documented, novel, and significant to the field as a whole. An Original Article should be arranged into the following sections: Title page, Abstract, Introduction, Materials and Methods, Results, Discussion, Acknowledgments, and References. Original articles should not exceed 5,000 words in length (excluding references) and should be limited to a maximum of 50 references. Articles may contain a maximum of 10 figures and/or tables. Supplementary Data are permitted but should be limited to information that is not essential to the general understanding of the research presented in the main text, such as unaltered blots and source data as well as other file types.

**Brief Reports** definitively documenting either experimental results or informative clinical observations will be considered for publication in this category. Brief Reports are not intended for publication of incomplete or preliminary findings. Brief Reports should not exceed 3,000 words in length (excluding references) and should be limited to a maximum of 4 figures and/or tables and 30 references. A Brief Report contains the same sections as an Original Article, but the Results and Discussion sections should be combined.

**Reviews** should present a full and up-to-date account of recent developments within an area of research. Normally, reviews should not exceed 8,000 words in length (excluding references) and should be limited to a maximum of 10 figures and/or tables and 100 references. Mini reviews are also accepted, which should not exceed 4,000 words in length (excluding references) and should be limited to a maximum of 5 figures and/or tables and 50 references.

**Policy Forum** articles discuss research and policy issues in areas related to life science such as public health, the medical care system, and social science and may address governmental issues at district, national, and international levels of discourse. Policy Forum articles should not exceed 3,000 words in length (excluding references) and should be limited to a maximum of 5 figures and/or tables and 30 references.

**Communications** are short, timely pieces that spotlight new research findings or policy issues of interest to the field of global health and medical practice that are of immediate importance. Depending on their content, Communications will be published as "Comments" or "Correspondence". Communications should not exceed 1,500 words in length (excluding references) and should be limited to a maximum of 2 figures and/or tables and 20 references.

**Editorials** are short, invited opinion pieces that discuss an issue of immediate importance to the fields of global health, medical practice, and basic science oriented for clinical application. Editorials should not exceed 1,000 words in length (excluding references) and should be limited to a maximum of 10 references. Editorials may contain one figure or table.

**News** articles should report the latest events in health sciences and medical research from around the world. News should not exceed 500 words in length.

**Letters** should present considered opinions in response to articles published in *BioScience Trends* in the last 6 months or issues of general interest. Letters should not exceed 800 words in length and may contain a maximum of 10 references. Letters may contain one figure or table.

### 3. Editorial Policies

For publishing and ethical standards, *BioScience Trends* follows the Recommendations for the Conduct, Reporting, Editing, and Publication of Scholarly Work in Medical Journals issued by the International Committee of Medical Journal Editors (ICMJE, <https://icmje.org/recommendations>), and the Principles of Transparency and Best Practice in Scholarly Publishing jointly issued by the Committee on Publication Ethics (COPE, <https://publicationethics.org/resources/guidelines-new/principles-transparency-and-best-practice-scholarly-publishing>), the Directory of Open Access Journals (DOAJ, <https://doaj.org/apply/transparency>), the Open Access Scholarly Publishers Association (OASPA, <https://oaspa.org/principles-of-transparency-and-best-practice-in-scholarly-publishing-4>), and the World Association of Medical Editors (WAME, <https://wame.org/principles-of-transparency-and-best-practice-in-scholarly-publishing>).

*BioScience Trends* will perform an especially prompt review to encourage innovative work. All original research will be subjected to a rigorous standard of peer review and will be edited by experienced copy editors to the highest standards.

**Ethical Approval of Studies and Informed Consent:** For all manuscripts reporting data from studies involving human participants or animals, formal review and approval, or formal review and waiver, by an appropriate institutional review board or ethics committee is required and should be described in the Methods section. When your manuscript contains any case details, personal information and/or images of patients or other individuals, authors must obtain appropriate written consent, permission and release in order to comply with all applicable laws and regulations concerning privacy and/or security of personal information. The consent form needs to comply with the relevant legal requirements of your particular jurisdiction, and please do not send signed consent form to *BioScience Trends* to respect your patient's and any other individual's privacy. Please instead describe the information clearly in the Methods (patient consent) section of your manuscript while retaining copies of the signed forms in the event they should be needed. Authors should also state that the study conformed to the provisions of the Declaration of Helsinki (as revised in 2013, <https://wma.net/what-we-do/medical-ethics/declaration-of-helsinki>). When reporting experiments on animals, authors should indicate whether the institutional and national guide for the care and use of laboratory animals was followed.

**Reporting Clinical Trials:** The ICMJE (<https://icmje.org/recommendations/browse/publishing-and-editorial-issues/clinical-trial-registration.html>) defines a clinical trial as any research project that prospectively assigns people or a group of people to an intervention, with or without concurrent comparison or control groups, to study the relationship between a health-related intervention and a health outcome. Registration of clinical trials in a public trial registry at or before the time of first patient enrollment is a condition of consideration for publication in *BioScience Trends*, and the trial registration number will be published at the end of the Abstract. The registry must be independent of for-profit interest and publicly accessible. Reports of trials must conform to CONSORT 2010 guidelines (<https://consort-statement.org/consort-2010>). Articles reporting the results of randomized trials must include the CONSORT flow diagram showing the progress of patients throughout the trial.

**Conflict of Interest:** All authors are required to disclose any actual or potential conflict of interest including financial interests or relationships with other people or organizations that might raise questions of bias



in the work reported. If no conflict of interest exists for each author, please state "There is no conflict of interest to disclose".

**Submission Declaration:** When a manuscript is considered for submission to *BioScience Trends*, the authors should confirm that 1) no part of this manuscript is currently under consideration for publication elsewhere; 2) this manuscript does not contain the same information in whole or in part as manuscripts that have been published, accepted, or are under review elsewhere, except in the form of an abstract, a letter to the editor, or part of a published lecture or academic thesis; 3) authorization for publication has been obtained from the authors' employer or institution; and 4) all contributing authors have agreed to submit this manuscript.

**Initial Editorial Check:** Immediately after submission, the journal's managing editor will perform an initial check of the manuscript. A suitable academic editor will be notified of the submission and invited to check the manuscript and recommend reviewers. Academic editors will check for plagiarism and duplicate publication at this stage. The journal has a formal recusal process in place to help manage potential conflicts of interest of editors. In the event that an editor has a conflict of interest with a submitted manuscript or with the authors, the manuscript, review, and editorial decisions are managed by another designated editor without a conflict of interest related to the manuscript.

**Peer Review:** *BioScience Trends* operates a single-anonymized review process, which means that reviewers know the names of the authors, but the authors do not know who reviewed their manuscript. All articles are evaluated objectively based on academic content. External peer review of research articles is performed by at least two reviewers, and sometimes the opinions of more reviewers are sought. Peer reviewers are selected based on their expertise and ability to provide quality, constructive, and fair reviews. For research manuscripts, the editors may, in addition, seek the opinion of a statistical reviewer. Every reviewer is expected to evaluate the manuscript in a timely, transparent, and ethical manner, following the COPE guidelines ([https://publicationethics.org/files/cope-ethical-guidelines-peer-reviewers-v2\\_0.pdf](https://publicationethics.org/files/cope-ethical-guidelines-peer-reviewers-v2_0.pdf)). We ask authors for sufficient revisions (with a second round of peer review, when necessary) before a final decision is made. Consideration for publication is based on the article's originality, novelty, and scientific soundness, and the appropriateness of its analysis.

**Suggested Reviewers:** A list of up to 3 reviewers who are qualified to assess the scientific merit of the study is welcomed. Reviewer information including names, affiliations, addresses, and e-mail should be provided at the same time the manuscript is submitted online. Please do not suggest reviewers with known conflicts of interest, including participants or anyone with a stake in the proposed research; anyone from the same institution; former students, advisors, or research collaborators (within the last three years); or close personal contacts. Please note that the Editor-in-Chief may accept one or more of the proposed reviewers or may request a review by other qualified persons.

**Language Editing:** Manuscripts prepared by authors whose native language is not English should have their work proofread by a native English speaker before submission. If not, this might delay the publication of your manuscript in *BioScience Trends*.

The Editing Support Organization can provide English proofreading, Japanese-English translation, and Chinese-English translation services to authors who want to publish in *BioScience Trends* and need assistance before submitting a manuscript. Authors can visit this organization directly at <https://www.iacmhr.com/iac-eso/support.php?lang=en>. IAC-ESO was established to facilitate manuscript preparation by researchers whose native language is not English and to help edit works intended for international academic journals.

**Copyright and Reuse:** Before a manuscript is accepted for publication in *BioScience Trends*, authors will be asked to sign a transfer of copyright agreement, which recognizes the common

interest that both the journal and author(s) have in the protection of copyright. We accept that some authors (e.g., government employees in some countries) are unable to transfer copyright. A JOURNAL PUBLISHING AGREEMENT (JPA) form will be e-mailed to the authors by the Editorial Office and must be returned by the authors by mail, fax, or as a scan. Only forms with a hand-written signature from the corresponding author are accepted. This copyright will ensure the widest possible dissemination of information. Please note that the manuscript will not proceed to the next step in publication until the JPA Form is received. In addition, if excerpts from other copyrighted works are included, the author(s) must obtain written permission from the copyright owners and credit the source(s) in the article.

#### 4. Cover Letter

The manuscript must be accompanied by a cover letter prepared by the corresponding author on behalf of all authors. The letter should indicate the basic findings of the work and their significance. The letter should also include a statement affirming that all authors concur with the submission and that the material submitted for publication has not been published previously or is not under consideration for publication elsewhere. The cover letter should be submitted in PDF format. For an example of Cover Letter, please visit: <https://www.biosciencetrends.com/downloadcentre> (Download Centre).

#### 5. Submission Checklist

The Submission Checklist should be submitted when submitting a manuscript through the Online Submission System. Please visit Download Centre (<https://www.biosciencetrends.com/downloadcentre>) and download the Submission Checklist file. We recommend that authors use this checklist when preparing your manuscript to check that all the necessary information is included in your article (if applicable), especially with regard to Ethics Statements.

#### 6. Manuscript Preparation

Manuscripts are suggested to be prepared in accordance with the "Recommendations for the Conduct, Reporting, Editing, and Publication of Scholarly Work in Medical Journals", as presented at <https://www.ICMJE.org>.

Manuscripts should be written in clear, grammatically correct English and submitted as a Microsoft Word file in a single-column format. Manuscripts must be paginated and typed in 12-point Times New Roman font with 24-point line spacing. Please do not embed figures in the text. Abbreviations should be used as little as possible and should be explained at first mention unless the term is a well-known abbreviation (e.g. DNA). Single words should not be abbreviated.

**Title page:** The title page must include 1) the title of the paper (Please note the title should be short, informative, and contain the major key words); 2) full name(s) and affiliation(s) of the author(s), 3) abbreviated names of the author(s), 4) full name, mailing address, telephone/fax numbers, and e-mail address of the corresponding author; 5) author contribution statements to specify the individual contributions of all authors to this manuscript, and 6) conflicts of interest (if you have an actual or potential conflict of interest to disclose, it must be included as a footnote on the title page of the manuscript; if no conflict of interest exists for each author, please state "There is no conflict of interest to disclose").

**Abstract:** The abstract should briefly state the purpose of the study, methods, main findings, and conclusions. For articles that are Original Articles, Brief Reports, Reviews, or Policy Forum articles, a one-paragraph abstract consisting of no more than 250 words must be included in the manuscript. For Communications, Editorials, News, or Letters, a brief summary of main content in 150 words or fewer should be included in the manuscript. For articles reporting clinical trials, the trial registration number should be stated at the end of the Abstract. Abbreviations must be kept to a minimum and non-standard

abbreviations explained in brackets at first mention. References should be avoided in the abstract. Three to six key words or phrases that do not occur in the title should be included in the Abstract page.

**Introduction:** The introduction should provide sufficient background information to make the article intelligible to readers in other disciplines and sufficient context clarifying the significance of the experimental findings

**Materials/Patients and Methods:** The description should be brief but with sufficient detail to enable others to reproduce the experiments. Procedures that have been published previously should not be described in detail but appropriate references should simply be cited. Only new and significant modifications of previously published procedures require complete description. Names of products and manufacturers with their locations (city and state/country) should be given and sources of animals and cell lines should always be indicated. All clinical investigations must have been conducted in accordance Materials/Patients and Methods.

**Results:** The description of the experimental results should be succinct but in sufficient detail to allow the experiments to be analyzed and interpreted by an independent reader. If necessary, subheadings may be used for an orderly presentation. All Figures and Tables should be referred to in the text in order, including those in the Supplementary Data.

**Discussion:** The data should be interpreted concisely without repeating material already presented in the Results section. Speculation is permissible, but it must be well-founded, and discussion of the wider implications of the findings is encouraged. Conclusions derived from the study should be included in this section.

**Acknowledgments:** All funding sources (including grant identification) should be credited in the Acknowledgments section. Authors should also describe the role of the study sponsor(s), if any, in study design; in the collection, analysis, and interpretation of data; in the writing of the report; and in the decision to submit the paper for publication. If the funding source had no such involvement, the authors should so state.

In addition, people who contributed to the work but who do not meet the criteria for authors should be listed along with their contributions.

**References:** References should be numbered in the order in which they appear in the text. Citing of unpublished results, personal communications, conference abstracts, and theses in the reference list is not recommended but these sources may be mentioned in the text. In the reference list, cite the names of all authors when there are fifteen or fewer authors; if there are sixteen or more authors, list the first three followed by *et al.* Names of journals should be abbreviated in the style used in PubMed. Authors are responsible for the accuracy of the references. The EndNote Style of *BioScience Trends* could be downloaded at **EndNote** ([https://ircabssagroup.com/examples/BioScience\\_Trends.ens](https://ircabssagroup.com/examples/BioScience_Trends.ens)).

Examples are given below:

*Example 1 (Sample journal reference):*

Inagaki Y, Tang W, Zhang L, Du GH, Xu WF, Kokudo N. Novel aminopeptidase N (APN/CD13) inhibitor 24F can suppress invasion of hepatocellular carcinoma cells as well as angiogenesis. *Biosci Trends*. 2010; 4:56-60.

*Example 2 (Sample journal reference with more than 15 authors):*

Darby S, Hill D, Auvinen A, *et al.* Radon in homes and risk of lung cancer: Collaborative analysis of individual data from 13 European case-control studies. *BMJ*. 2005; 330:223.

*Example 3 (Sample book reference):*

Shalev AY. Post-traumatic stress disorder: Diagnosis, history and life course. In: *Post-traumatic Stress Disorder, Diagnosis, Management and Treatment* (Nutt DJ, Davidson JR, Zohar J, eds.). Martin Dunitz, London, UK, 2000; pp. 1-15.

*Example 4 (Sample web page reference):*

World Health Organization. The World Health Report 2008 – primary health care: Now more than ever. [http://www.who.int/whr/2008/whr08\\_en.pdf](http://www.who.int/whr/2008/whr08_en.pdf) (accessed September 23, 2022).

**Tables:** All tables should be prepared in Microsoft Word or Excel and should be arranged at the end of the manuscript after the References section. Please note that tables should not in image format. All tables should have a concise title and should be numbered consecutively with Arabic numerals. If necessary, additional information should be given below the table.

**Figure Legend:** The figure legend should be typed on a separate page of the main manuscript and should include a short title and explanation. The legend should be concise but comprehensive and should be understood without referring to the text. Symbols used in figures must be explained. Any individually labeled figure parts or panels (A, B, *etc.*) should be specifically described by part name within the legend.

**Figure Preparation:** All figures should be clear and cited in numerical order in the text. Figures must fit a one- or two-column format on the journal page: 8.3 cm (3.3 in.) wide for a single column, 17.3 cm (6.8 in.) wide for a double column; maximum height: 24.0 cm (9.5 in.). Please make sure that the symbols and numbers appeared in the figures should be clear. Please make sure that artwork files are in an acceptable format (TIFF or JPEG) at minimum resolution (600 dpi for illustrations, graphs, and annotated artwork, and 300 dpi for micrographs and photographs). Please provide all figures as separate files. Please note that low-resolution images are one of the leading causes of article resubmission and schedule delays.

**Units and Symbols:** Units and symbols conforming to the International System of Units (SI) should be used for physicochemical quantities. Solidus notation (*e.g.* mg/kg, mg/mL, mol/mm<sup>2</sup>/min) should be used. Please refer to the SI Guide [www.bipm.org/en/si/](http://www.bipm.org/en/si/) for standard units.

**Supplemental data:** Supplemental data might be useful for supporting and enhancing your scientific research and *BioScience Trends* accepts the submission of these materials which will be only published online alongside the electronic version of your article. Supplemental files (figures, tables, and other text materials) should be prepared according to the above guidelines, numbered in Arabic numerals (*e.g.*, Figure S1, Figure S2, and Table S1, Table S2) and referred to in the text. All figures and tables should have titles and legends. All figure legends, tables and supplemental text materials should be placed at the end of the paper. Please note all of these supplemental data should be provided at the time of initial submission and note that the editors reserve the right to limit the size and length of Supplemental Data.

## 5. Submission Checklist

The Submission Checklist will be useful during the final checking of a manuscript prior to sending it to *BioScience Trends* for review. Please visit Download Centre and download the Submission Checklist file.

## 6. Online Submission

Manuscripts should be submitted to *BioScience Trends* online at <https://www.biosciencetrends.com/login>. Receipt of your manuscripts submitted online will be acknowledged by an e-mail from Editorial Office containing a reference number, which should be used in all future communications. If for any reason you are unable to submit a file online, please contact the Editorial Office by e-mail at [office@biosciencetrends.com](mailto:office@biosciencetrends.com)

## 8. Accepted Manuscripts

**Page Charge:** Page charges will be levied on all manuscripts accepted for publication in *BioScience Trends* (Original Articles / Brief Reports / Reviews / Policy Forum / Communications: \$140 per page for black white pages, \$340 per page for color pages; News / Letters: a total cost of \$600). Under exceptional circumstances, the author(s) may apply to the editorial office for a waiver of the publication charges by stating the reason in the Cover Letter when the manuscript online.

**Misconduct:** *BioScience Trends* takes seriously all allegations of potential misconduct and adhere to the ICMJE Guideline (<https://icmje.org/recommendations>) and COPE Guideline ([https://publicationethics.org/files/Code\\_of\\_conduct\\_for\\_journal\\_editors.pdf](https://publicationethics.org/files/Code_of_conduct_for_journal_editors.pdf)). In cases of

suspected research or publication misconduct, it may be necessary for the Editor or Publisher to contact and share submission details with third parties including authors' institutions and ethics committees. The corrections, retractions, or editorial expressions of concern will be performed in line with above guidelines.

(As of December 2022)

**BioScience Trends**  
Editorial and Head Office  
Pearl City Koishikawa 603,  
2-4-5 Kasuga, Bunkyo-ku,  
Tokyo 112-0003, Japan.  
E-mail: [office@biosciencetrends.com](mailto:office@biosciencetrends.com)





